Département de Géosciences – Sciences de la Terre
Université de Fribourg (Suisse)

High-frequency palaeoenvironmental changes in mixed carbonate-siliciclastic sedimentary systems (Late Oxfordian, Switzerland, France, and southern Germany)

Thèse

présentée à la Faculté des Sciences de l'Université de Fribourg (Suisse)
pour l'obtention du grade de *Doctor rerum naturalium*

Stéphanie VÉDRINE

de Paris, France

Thèse N° 1579

Multiprint SA, Fribourg, 2007

Acceptée par la Faculté des Sciences de l'Université de Fribourg (Suisse)
sur la proposition de :

Prof. André STRASSER	Université de Fribourg (Suisse)	Directeur
Dr. Bernard PITTET	Université de Lyon 1 (France)	Expert
Prof. John REIJMER	Université Libre d'Amsterdam (Pays-Bas)	Expert
Prof. Bernard GROBETY	Université de Fribourg (Suisse)	Président du jury

Fribourg, le 5 octobre 2007

Le Doyen: Prof. Titus Jenny

Directeur de thèse: Prof. André Strasser

“En science, la phrase la plus excitante à entendre, celle qui annonce de nouvelles découvertes, n’est pas «Eureka» mais «c’est drôle...».”

Isaac Asimov

TABLE OF CONTENTS

ABSTRACT

The main goal of this study is to monitor the high-frequency palaeoenvironmental changes occurring during a marine transgression in mixed carbonate-siliciclastic sedimentary systems. Based on a well-established bio- and sequence-stratigraphic framework, a narrow time window in the Bimammatum Zone of the Late Oxfordian is investigated. Seven shallow platform sections (Swiss Jura, Lorraine), two deep platform sections (Haute-Marne, Swabian Jura), and one basin section (SE France) have been logged and analysed in detail. Then, the deposits have been interpreted in terms of palaeoenvironments and sequence- and cyclostratigraphy with a high time resolution. Facies and microfacies analysis allows to propose depositional models for the Swiss Jura platform and the other studied areas. The high-resolution sequence- and cyclostratigraphic analysis permits defining hierarchically stacked depositional sequences: medium-scale, small-scale, and elementary sequences, formed through orbitally controlled sea-level changes with periodicities of 400, 100, and 20 kyr, respectively.

This study investigates deposits comprised in the first half of a medium-scale sequence, corresponding to two small-scale sequences, each composed of five elementary sequences. In the shallow platform sections, an elementary sequence generally consists of one to four beds including more or less developed marl intervals. In the deep platform sections, an elementary sequence generally consists of one or two limestone beds with a more or less developed marl interval. In the basin section, an elementary sequence is defined by one marl-limestone couplet.

The good correlation of depositional sequences over long distances between the seven shallow platform sections and the similar number of elementary sequences in all sections are valuable arguments that allocyclic processes must have been involved in the formation of these depositional sequences. Additional factors such as the position on the platform and the pre-existing morphology have to be considered in the formation of depositional sequences on a shallow platform. The presence of thickness variations at the scale of small-scale and elementary sequences reveals variable sediment accumulation rates, interpreted as resulting mainly from differential subsidence due to the activity of tectonic blocks. The relief created by tectonics therefore contributed significantly to the general facies distribution. Furthermore, the irregular distribution of siliciclastics can be explained by localized depressions, which were created by differential subsidence and served as depocenters.

The vertical and lateral distribution of facies, oncoids, and benthic foraminifera is investigated within the narrow high-resolution time framework established (20-kyr time resolution). Significant lateral facies changes are evidenced by comparison of time-equivalent small-scale and elementary sequences between the Swiss Jura sections. They reflect the dynamics and complexity of sedimentary systems where juxtaposed sub-environments evolved and shifted through space and time.

Four types of oncoids are defined based on surface morphology, configuration and composition of the cortex, and the encasing sediment. Micrite-dominated oncoids (types 1 and 2) have a smooth surface and *Bacinella-Lithocodium* oncoids (types 3 and 4) display a lobate surface. The stratigraphic and spatial distribution of these oncoid types shows a correlation with the sequence-stratigraphic evolution, and thus with relative sea-level fluctuations. At the scale of 100-kyr and 20-kyr sequences, type 1 and 2 oncoids are

preferentially found around sequence boundaries and in transgressive deposits, while type 3 and 4 oncoids are preferentially found around maximum floodings and in highstand deposits. This implies that changes of water energy and water depth were direct controlling factors. Discrepancies in oncoid distribution point to additional controlling factors. Platform morphology defines the distribution and type of the lagoon where the oncoids flourished. A low accumulation rate is required for oncoid growth. Additionally, humidity changes in the hinterland act on the terrigenous influx, which modifies water transparency and trophic level and thus plays a role in the biotic composition and diversity in the oncoid cortex. This study demonstrates that oncoids are valuable proxies for high-resolution palaeoenvironmental and palaeoecological studies.

The benthic foraminifer assemblages of the Swiss Jura sections include agglutinated forms (Textularids), in a lower amount porcelaneous forms (Miliolids), and locally hyaline foraminifera (only *Lenticulina*). The distribution of porcelaneous and hyaline foraminifera shows a correlation with the sequence-stratigraphic evolution. Miliolids are preferentially found in the highstand deposits of the elementary and/or small-scale sequences. The hyaline foraminifera, rare in the studied sections, are preferentially found in the transgressive deposits of elementary sequences. Consequently, the benthic foraminifera are indirectly linked to relative sea-level (accommodation changes) and indirectly to climate changes (sediment and nutrient input).

The distribution of the benthic foraminifer *Mohlerina basiliensis* and *Bacinella-Lithocodium* oncoids shows a strong correlation. The co-occurrence of these two components suggests that they require similar ecological conditions. In addition, the successively later occurrence of *M. basiliensis* from "distal" to "proximal" sections illustrates the stepwise flooding of the platform and thus implies a dependence on normal-marine conditions.

Clay-mineral assemblages and stable isotopes give palaeoenvironmental information on the scale of 400 kyr and 100 kyr but a higher time resolution is difficult to obtain probably due to time averaging by sedimentological and/or diagenetic processes. The medium-scale trends of the kaolinite content and K/I ratio between all sections from shallow platform to basin show a correlation, particularly around the medium-scale SB Ox6+ and MF Ox6+. Clay mineral distribution was not only controlled by climate changes but also by relative sea-level changes and platform morphology. Carbon and oxygen isotope analysis shows minor fluctuations (±1‰) that probably reflect variations of local environmental conditions (e.g., salinity, temperature, trophic level).

* * *

RÉSUMÉ

Le but principal de cette étude est d'examiner les changements paléoenvironnementaux de haute fréquence survenant durant une transgression marine dans des systèmes sédimentaires mixtes silico-carbonatés. Basée sur un cadre biostratigraphique et séquentiel bien établi, une fenêtre de temps précise dans la zone à Bimammatum de l'Oxfordien supérieur est étudiée. Sept coupes de plate-forme peu profonde (Jura suisse, Lorraine), deux coupes de plate-forme profonde (Haute-Marne, Jura souabe) et une coupe de bassin (SE France) ont été levées et analysées en détail. Les dépôts ont ensuite été interprétés en terme de paléoenvironnments et de stratigraphie séquentielle et cyclostratigraphie avec une haute résolution dans le temps. L'analyse des faciès et microfaciès permet de proposer des modèles de dépôt pour la plate-forme du Jura Suisse et les autres zones d'étude. L'analyse séquentielle et cyclostratigraphique de haute résolution permet de définir l'empilement hiérarchique des séquences de dépôt (séquences à moyen terme, à court terme et élémentaires) formées par les fluctuations du niveau marin avec des périodicités de 400, 100, et 20 ka respectivement, contrôlées par les cycles orbitaux.

Cette étude examine les dépôts situés dans la première moitié d'une séquence à moyen terme, correspondant à deux séquences à court terme, chacune composée de cinq séquences élémentaires. Dans les coupes de plate-forme peu profonde, une séquence élémentaire consiste généralement en un à quatre bancs incluant des intervalles marneux plus ou moins développés. Dans les coupes de plate-forme profonde, une séquence élémentaire consiste généralement en un à deux bancs calcaires avec un intervalle marneux plus ou moins développé. Dans la coupe de bassin, une séquence élémentaire est définie par un banc calcaire et un intervalle marneux.

La bonne corrélation des séquences de dépôt sur de longues distances entre les sept coupes de plate-forme peu profonde ainsi que le nombre similaire de séquences élémentaires dans toutes les coupes sont des arguments valables pour montrer que des processus allocycliques doivent avoir joué un rôle dans la formation de ces séquences de dépôt. Des facteurs additionnels tels que la position sur la plate-forme et la morphologie pré-existante doivent être considérées dans la formation des séquences sur une plate-forme peu profonde. La présence de variations d'épaisseurs à l'échelle des séquences élémentaires et à court terme révèle des taux d'accumulation sédimentaire variables, interprétés comme résultant principalement de la subsidence différentielle due à l'activité tectonique de blocs. Le relief créé par la tectonique contribue aussi significativement à la distribution générale des faciès. De plus, la distribution irrégulière des siliciclastiques peut être expliquée par des dépressions locales, créées par la subsidence différentielle, et servant de depôt-centres.

La distribution verticale et horizontale des faciès, des oncoïdes et des foraminifères benthiques est étudiée dans le cadre de temps haute résolution établi dans ce travail (résolution temporelle de 20 ka). Des changements de faciès latéraux sont mis en évidence par comparaison des séquences élémentaires et à court terme entre les coupes du Jura suisse. Ils reflètent la dynamique et complexité des systèmes sédimentaires où des environnements juxtaposés évoluent et se modifient dans le temps et dans l'espace.

Quatre types d'oncoïdes sont définis à partir de la morphologie de surface, la configuration et composition du cortex et le sédiment encaissant. Les oncoïdes dont le cortex est dominé par la micrite (types 1 et 2) ont une surface lisse tandis que les oncoïdes

riches en *Bacinella-Lithocodium* (types 3 et 4) ont une surface lobée. La distribution stratigraphique et spatiale de ces types d'oncoïdes montre une corrélation avec l'évolution séquentielle et donc les fluctuations du niveau marin relatif. A l'échelle des séquences élémentaires et à court terme, les oncoïdes de type 1 et 2 sont préférentiellement trouvées autour des limites de séquence et dans les cortèges de dépôt transgressifs tandis que les oncoïdes de type 3 et 4 sont préférentiellement trouvés autour des maxima d'inondation et dans les cortèges de haut niveau marin. Cela implique que des changements d'énergie et de profondeur d'eau ont été des facteurs contrôlant directs. Des disparités dans la distribution des oncoïdes suggèrent des facteurs contrôlant additionnels. La morphologie de la plate-forme définit la distribution et le type de lagon où les oncoïdes se développent. Un faible taux d'accumulation sédimentaire est requis pour la croissance des oncoïdes. Des changements d'humidité dans l'arrière-pays agissent sur l'influx terrigène ce qui modifie la transparence et le niveau trophique de l'eau et joue donc un rôle dans la composition et la diversité biotique dans le cortex des oncoïdes. Cette étude démontre que les oncoïdes sont des indicateurs valables pour des études paléoenvironnementales et paléoécologiques de haute résolution.

Les assemblages de foraminifères benthiques des coupes du Jura suisse comprennent des formes agglutinées (Textularidés), dans une plus faible proportion des formes porcelanées (Miliolidés) et localement des foraminifères hyalins (seulement *Lenticulina*). La distribution des foraminifères porcelanés et hyalins montre une corrélation avec l'évolution séquentielle. Les Miliolidés sont préférentiellement trouvés dans les cortèges de dépôt de haut niveau marin de certaines séquences élémentaires et/ou à court terme. Les foraminifères hyalins, rare dans les coupes étudiées, sont préférentiellement trouvés dans les dépôts transgressifs de certaines séquences élémentaires. Par conséquence, les foraminifères benthiques sont indirectement liés aux changements du niveau marin relatif (changements d'accommodation) ainsi qu'aux changements climatiques (apports sédimentaires et de nutriments).

La distribution du foraminifère benthique *Mohlerina basiliensis* et des oncoïdes riches en *Bacinella-Lithocodium* montre une forte corrélation. La co-existence de ces deux composants suggère qu'ils requièrent des conditions écologiques similaires. De plus, l'apparition de plus en plus tardive des *M. basiliensis* des coupes distales aux coupes proximales illustre l'inondation par étape de la plate-forme et implique alors une dépendance aux conditions marines.

Les assemblages des minéraux argileux et les isotopes stables donnent des informations paléoenvironnementales à l'échelle des séquences de 400 ka et 100 ka; une plus haute résolution est difficile à obtenir probablement à cause de l'homogénéisation du temps par des processus sédimentologiques et/ou diagénétiques. Les tendances à moyen terme du contenu en kaolinite et du rapport kaolinite/illite entre toutes les coupes, de la plate-forme peu profonde au bassin, montre une corrélation particulièrement autour de la limite de séquence SB Ox6+ et du maximum d'inondation à moyen terme MF Ox6+. La distribution des minéraux argileux n'était pas seulement contrôlée par des changements climatiques mais aussi par des changements du niveau marin relatif et de la morphologie de la plate-forme. L'analyse des isotopes de l'oxygène et du carbone montre des fluctuations mineures (± 1 ‰) qui reflètent probablement des variations de conditions environnementales locales (par exemple, la salinité, la température et/ou le niveau trophique).

* * *

ZUSAMMENFASSUNG

Das Ziel dieser Studie ist es, hochfrequente Umweltveränderungen nachzuzeichnen, welche ein gemischt siliziklastisch-karbonatisches Sedimentsystem während einer marinen Transgression beeinflussten. Basierend auf einem gut etablierten bio- und sequenzstratigraphischen Rahmen wird ein enges Zeitfenster in der Bimammatum Zone des Späten Oxfordians untersucht. Sieben Profile der flachen Plattform (Schweizer Jura, Lorraine), zwei Profile der tiefen Plattform (Haute-Marne, Schwäbischer Jura) und ein Beckenprofil (Südost-Frankreich) wurden im Detail aufgenommen und analysiert. Dann wurden die Sedimente hinsichtlich Ablagerungsräume sowie Sequenz- und Zyklostratigraphie mit einer hohen Zeitauflösung interpretiert. Die Fazies- und Mikrofaziesanalysen erlauben es, Ablagerungsmodelle für die Schweizer Jura Plattform und die anderen untersuchten Gebiete vorzuschlagen. Die hochauflösende sequenz- und zyklostratigraphische Analyse führt zur Definition hierarchisch gestapelter Ablagerungssequenzen (medium-scale, small-scale und Elementarsequenzen), welche orbital kontrollierten Meeresspiegelschwankungen mit Periodizitäten von jeweils 400, 100 und 20 ka entsprechen.

Diese Studie untersucht Ablagerungen, welche die ersten Hälfte einer medium-scale Sequenz aufbauen und zwei small-scale Sequenzen entsprechen, die jeweils aus fünf Elementarsequenzen bestehen. In den Profilen der flachen Plattform bestehen die Elementarsequenzen generell aus ein bis vier Bänken einschliesslich mehr oder weniger entwickelter Mergelintervalle. In den Profilen der tiefen Plattform bestehen Elementarsequenzen aus ein oder zwei Kalkbänken mit einem mehr oder weniger ausgebildeten Mergelhorizont. Im Beckenprofil ist die Elementarsequenz durch ein Kalk-Mergel-Paar definiert.

Die gute Korrelation der Ablagerungssequenzen über grosse Distanzen zwischen den sieben Profilen der flachen Plattform und der ähnlichen Anzahl elementarer Sequenzen in allen Profilen sind gute Argumente dafür, dass allozyklische Prozesse bei der Bildung dieser Sequenzen beteiligt gewesen sein müssen. Andere Faktoren wie die Position auf der Plattform und die vorgegebene Plattform-Morphologie müssen jedoch ebenfalls in Betracht gezogen werden. Mächtigkeitsschwankungen innerhalb der small-scale und Elementarsequenzen deuten auf variable Sedimentationsraten hin. Diese werden hauptsächlich als das Resultat der differenziellen Subsidenz tektonisch aktiver Blöcke interpretiert. Das durch die Tektonik entstandene Relief hat demnach signifikant zur generellen Faziesverteilung beigetragen. Ebenso kann die unregelmässige Verteilung der Siliziklastika durch lokale Depressionen erklärt werden, die durch differentielle Subsidenz entstanden sind und als Sedimentationszentren dienten.

Die vertikale und laterale Verteilung von Fazies, Onkoiden und benthischen Foraminiferen wird innerhalb des etablierten hochauflösenden Zeitrahmens untersucht (20 ka Zeitauflösung). Signifikante laterale Fazieswechsel können im Vergleich mit zeitäquivalenten small-scale und Elementarsequenzen zwischen den Profilen im Schweizer Jura nachgewiesen werden. Sie reflektieren die Dynamik und Komplexität von sedimentären Systemen, wo sich verschiedene Ablagerungsräume nebeneinander entwickelten und sich in Zeit und Raum verlagerten.

Vier Typen von Onkoiden werden definiert, basierend auf Oberflächenmorphologie, Konfiguration und Zusammensetzung des Kortex und dem umgebenden Sediment. Mikrit-dominierte Onkoide (Typen 1 und 2) haben eine glatte Oberfläche, *Bacinella-*

Lithocodium Onkoide (Typen 3 und 4) zeigen eine lappige Oberfläche. Die stratigraphische und räumliche Verteilung dieser Onkoidtypen zeigt eine Korrelation mit der sequenzstratigraphischen Entwicklung und somit mit relativen Meeresspiegelschwankungen. Bei den 100 ka und 20 ka Sequenzen werden Onkoide der Typen 1 und 2 vorzugsweise an Sequenzgrenzen und in transgressiven Ablagerungen gefunden, während Onkoide der Typen 3 und 4 den schnellsten Meeresspiegelanstieg und Hochstandsablagerungen charakterisieren. Dies impliziert dass Änderungen der Wasserenergie und Wassertiefe direkt kontrollierende Faktoren waren. Diskrepanzen in der Onkoidverteilung weisen auf zusätzliche kontrollierende Faktoren hin. Die Plattformmorphologie definiert die Verteilung und die Art der Lagunen, wo Onkoide gedeihen. Eine langsame Sedimentationsrate ist für die Onkoidbildung erforderlich. Zusätzlich beeinflussen Änderungen der Niederschlags im Hinterland den Terrigeneintrag, der die Wassertransparenz und das trophische Niveau modifiziert und so für die biotische Zusammensetzung und Diversität im Onkoidkortex eine Rolle spielt. Diese Arbeit zeigt, dass Onkoide wertvolle Indikatoren für hochauflösende Paläoumwelt- und Paläoökologiestudien sind.

Die Foraminiferen-Vergesellschaftungen in den Profilen des Schweizer Jura umfassen agglutinierte Formen (Textulariden), weniger häufig porzellanschalige Formen (Milioliden) und lokal hyaline Foraminiferen (ausschliesslich *Lenticulina*). Die Verteilung der porzellanschaligen und hyalinen Foraminiferen zeigt eine Korrelation mit der sequenzstratigraphischen Entwicklung. Milioliden werden vorzugsweise in Hochstandsablagerungen der elementaren und small-scale Sequenzen gefunden. Die hyalinen Foraminiferen, die in den untersuchten Profilen selten sind, werden bevorzugt in den transgressiven Ablagerungen von Elementarsequenzen gefunden. Folglich besteht ein indirekter Zusammenhang zwischen den benthischen Foraminiferen und den relativen Meeresspiegelschwankungen sowie den Klimawechseln (Sediment- und Nährstoffeintrag).

Die Verteilungen der benthischen Foraminifere *Mohlerina basiliensis* und der *Bacinella-Lithocodium* Onkoide zeigen eine starke Korrelation. Das gemeinsame Auftreten dieser zwei Komponenten deutet darauf hin, dass sie ähnliche ökologische Bedingungen brauchten. Zusätzlich illustriert das sukzessiv spätere Auftreten von *M. basiliensis* von „distal“ nach „proximal“ die schrittweise Überflutung der Plattform und impliziert so eine Abhängigkeit von normal-marinen Bedingungen.

Tonmineral-Vergesellschaftungen und stabile Isotope informieren über die Umweltbedingungen für die 400 ka und 100 ka Sequenzen; eine höhere Auflösung ist auf Grund von Zeitmittlung durch sedimentologische und/oder diagenetische Prozesse schwierig zu erreichen. Die medium-scale Trends des Gehalts an Kaolinit und des K/I Verhältnisses zwischen allen Profilen von der seichten Plattform bis ins Becken zeigen eine Korrelation, vor allem an der medium-scale Sequenzgrenze SB Ox6+ und beim schnellsten Meeresspiegelanstieg MF Ox6+. Die Tonmineralverteilung wurde demnach nicht nur durch Klimaänderungen sondern auch durch relative Meeresspiegelschwankungen und Plattformmorphologie kontrolliert. Kohlenstoff- und Sauerstoffisotopenanalysen zeigen geringfügige Schwankungen (±1%), welche wahrscheinlich Variationen in den lokalen Umweltbedingungen reflektieren (Salinität, Temperatur, Nährstoffeintrag).

* * *

ACKNOWLEDGEMENTS

This work would not have been possible without the support of many colleagues, friends, and family to whom I am truly thankful.

First of all, I would like to thank my thesis director (my "Doktorvater"), Prof. André STRASSER, for his exceptional human and professional qualities. As he warned me the first day, a thesis is an adventure. However, his kindness, his unbelievable availability, his eternal good mood, and his (Swiss German) rigor without a bit of stress made of this Swiss "adventure" the best experience of my life. He offered me the unique opportunity to participate in scientific congresses all around the world and to discover some modern carbonate platforms by plane, boat, kayak, swim, and/or dive. I thank him very much for his confidence from the start until now. Thank you very very much André!

I further thank the experts, Bernard PITTET (University of Lyon 1) and John REIJMER (Free University Amsterdam) for taking time to read the manuscript and having accepted to participate in the jury. Thank you, Bernard PITTET, who gave me the location of the Balingen-Tieringen section in southern Germany.

I would like to thank Prof. Christian CARON, the institute's director, and his wife, Prof. Michèle CARON, micropalaeontologist, who continuously have taken care of me, as one of their grand-daughters, since my first day in Fribourg. I will never forget their extraordinary kindness and hospitality as well as their confidence when they lent me their private car for my fieldwork in the Swiss Jura Mountains, only one month after I passed my driving licence. Thanks to their enthusiasm and generosity, I also could take advantage of the winter pleasures (skiing) in the Préalpes ski stations. Christian and Michèle also took care of my working conditions: first class office (high-tech computer, optical and binocular microscopes…), equality with the other PhD students and with some flowers from Michele's garden. I will never forget all the things that you did and still do for me. Thank you very very much Michèle and Christian!

Many thanks go to Jonas TRESCH, my office neighbour. He supported me during the different steps of the thesis. I thank him very much for his kindness, his peaceful attitude, his sense of humour, his help in the field, and his availability for answering my various questions and for having helped to put a name on strange things. I could never have dreamed of a better colleague! Thank you very much Jonas!

I would also like to thank Elias SAMANKASSOU for his kindness, his listening, and his patience during all these years. His confidence during the practical and block courses allowed me to better appreciate the teaching but still not enough for... Thanks to Silvia SPEZZAFERRI for all the lunch discussions on life and science as well as for having given me the opportunity to participate in the EGU 2007. I hope that in few months we can reveal to the entire world the phylogeny of *Mohlerina basiliensis*. Thanks to Jon MOSAR, for his dynamic attitude that always impressed me. Thanks to Jean-Pierre BERGER for his continuous good humour.

Thanks to Wolfgang HUG, who highlighted the opening questions and found a new section to investigate, and Neils RAMEIL, who advised me a lot at the beginning on how to manage and finish a thesis.

Without the technical staff, Patrick DIETSCHE, Daniel CUENNET, and Jean-Paul BOURQUI, no scientific results would have been possible. I really thank them for their patience and precision. Thanks also

to Christophe Neururer for the sample preparation for SEM analyses on the Swiss Jura oncoids, some benthic foraminifera, and green grains as well as his thirst of "why doing this", which clarified my ideas. Thank you also to Nicole Bruegger, for her help with the administrative tasks.

I would like to thank Thierry Adatte and his collaborators (University of Neuchâtel) for the measurements, determinations and interpretations of the clay minerals, and Laszlo Kocsis and Torsten Vennemann (University of Lausanne) for the measurements of the stable isotopes.

Thanks to M. Van Troost, director of the Révoi quarry (Pagny-sur-Meuse), exploited by the NOVACARB society, who gave me permission to work in the quarry and who took care of our security.

I also thank Bernard Grobéty for having accepted to be the president of the jury and for his good humour.

Thanks to all the scientific staff as well as the PhD and master students: Vincent Serneels, Luc, Pierre, Noémie, Daniel (Marty), Richard, Claudius, Katja, Martin, Thibault, Giordana, Stephan, Laureline, Pia, Maëlle, Sophie, Elie, Paola, Reto… and good luck for the future!

Special thanks to Noémie Stienne, for her dynamic style, her good humour, and her help for the re-rent of my flat and other services. I wish you all the best for the future. Thanks to Richard Waite for the translation of the abstract into the German Zusammenfassung. The Belize trip with André, Daniel, Noémie, and Richard was an unforgettable scientific and human experience…Keep the planet clean! Lands and oceans!

The financial support by the Swiss National Science Foundation (grants 20-67736.02 and 20-109214.05) is gratefully acknowledged.

I would like to thank my good friends: Annabel, Millena, Marie, Joseph, Caroline, François, who over the distance and with the help of the msn messenger are still here!

I deeply thank my family: my parents, Yves and Eliane, my brother, Eric, and his wife, Valérie, for having accepted my choices and having endlessly supported me during all my studies.

And last but not least, thank you, Hugo, for your help and advises that were very precious for me. You always supported and encouraged me in spite of the distance. Thank you with all my heart.

* * *

1 - INTRODUCTION

Modern shallow-water carbonate systems commonly display a highly complex pattern of juxtaposed depositional environments with a patchy facies distribution (facies mosaics: GISCHLER & LOMANDO 1999; RIEGL & PILLER 1999; RANKEY 2002). Considering the complexity of today's shallow-water carbonate systems it must be expected that also the sedimentary record of such systems is complex. There is no reason to believe that Phanerozoic carbonate systems were less complex than modern ones, although plate-tectonic configuration, climatic conditions, amplitude of sea-level changes, sea-water geochemistry, and the evolution of the participating organisms certainly preclude a direct comparison. Complexity is added by the fact that only a part of the history is recorded. Information is missing due to non-deposition and/or erosion, only a part of the organisms participating in the ecosystems is fossilized, and diagenesis may create a preservational bias. On ancient carbonate platforms, the reconstruction of lateral facies distribution is often hampered not only by discontinuous outcrop but also by lack of sufficiently high time resolution. This case study proposes a way to improve the temporal and spatial resolution for the interpretation of carbonate rocks. To obtain a sedimentary record as complete as possible, a period of transgression was studied where the sediment preservation potential is best because of a high accommodation gain.

A marine transgression is the flooding of land by the sea and is caused by subsidence and/or sea-level rise. Today many coasts experience transgression due to sea-level rise resulting from thermal expansion of the ocean water and from melting of continental ice (ICCP 2001). It is therefore appropriate to study transgressions in the geological past and to evaluate the effects they can have on depositional environments and ecosystems. Shallow carbonate platform deposits were chosen for investigation due to their high sensitivity to sea-level and climate changes.

In the last 10 years, the Fribourg research group investigated the Jura platform and other regions with high-resolution sequence- and cyclostratigraphy (e.g., STRASSER et al. 1999). A time interval of about 20 myr from the Oxfordian to the Valanginian has been investigated by several PhD studies (PASQUIER 1995; PITTET 1996; HILLGÄRTNER 1999; DUPRAZ 1999; COLOMBIÉ 2002; HUG 2003; RAMEIL 2005; TRESCH 2007). This study uses the well-defined biostratigraphic and sequence-stratigraphic framework established by PITTET (1996), GYGI et al. (1998), DUPRAZ (1999), and HUG (2003) for the Oxfordian interval and focuses on a narrow time window (Fig. 1.1).

1.1 OBJECTIVES AND APPROACH

This study aims to identify, within a narrow and high-resolution time framework (20-kyr time resolution), high-frequency palaeoenvironmental changes occurring on the shallow carbonate platform of the northern margin of the Tethys Ocean during the early Late Oxfordian. The methodology is based on (1) a facies and microfacies analysis that allows for the interpretation of depositional environments and (2) a high-resolution sequence-stratigraphic and cyclostratigraphic analysis that allows defining depositional sequences, which formed through sea-level changes that were induced by the 400-, 100-, and 20-kyr orbital cycles. Comparisons of sections from the shallow platform with deeper-marine sections will help to evaluate the expression and importance of controlling factors (e.g., sea level, climate, tectonics).

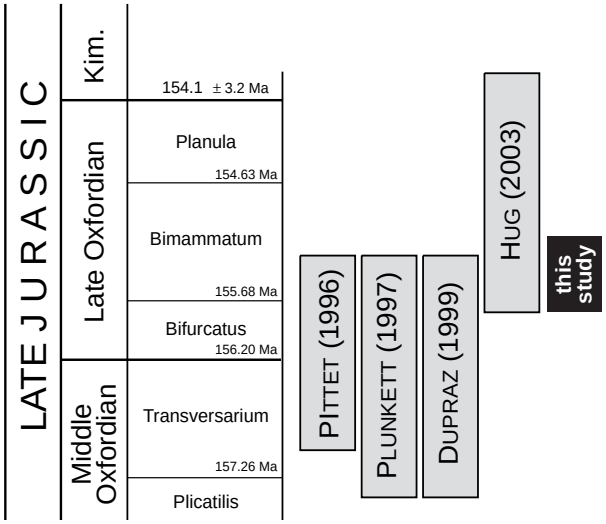

Fig. 1.1 - Stratigraphic ranges of studies carried out by the Fribourg sequence- and cyclostratigraphic working group in the Jura Mountains. Numerical ages from GRADSTEIN et al. (1995).

The main objective is to investigate the evolution of the Late Oxfordian transgression from shallow platform to basin environments with high time resolution. To reach this goal, the following steps are realized:

- Logging the field outcrops at a cm-scale and performing facies and microfacies analysis in order to interpret them in terms of depositional environments and to develop a facies model for the different palaeogeographic settings (Chapter 2).
- Interpretation of the hierarchical stacking pattern and facies evolution in terms of sequence stratigraphy (Chaps 3 and 4).
- High-resolution correlations of all sections based on biostratigraphy and sequence stratigraphy (Chap. 5).
- Identifying the controlling factors of sea-level changes and establishing a cyclostratigraphic framework (Chap. 6).
- Interpreting high-frequency palaeoenvironmental and palaeoecological changes with a 20-kyr time resolution (Chap. 7). Improving the understanding of the platform dynamics and the marine transgression by evaluating the importance of the controlling factors (Chaps 7, 8 and 9).

1.2 GENERAL CONTEXT

1.2.1 Geography and palaeogeography

The studied outcrops are located in northern Switzerland, in the east and southeast of France, and in southern Germany (Fig.1.2a). Six carbonate platform sections were analysed in the Swiss Jura Mountains (Fig. 1.2b). Two supplementary platform sections were investigated in France; in Lorraine west of Nancy, and in Haute-Marne north of Dijon (Fig. 1.2c). One deep-shelf section was analysed in the Swabian Jura south of Balingen (Germany), and one basin section was studied in SE France near Castellane (France; Fig. 1.2d).

During the Late Oxfordian, the study area consisted of a patchwork of low-relief islands in a shallow epicontinental sea at the northern (passive) margin of the Alpine Tethys (THIERRY et al. 2000). Erosion of crystalline massifs to the north (i.e. Bohemian Massif, Rhenish Massif, Massif Central, London-Brabant Massif; Fig. 1.3) furnished siliciclastics to the Paris Basin and to the northern Tethyan platform. The study area ranged from 24°N to 35°N palaeolatitude (DERCOURT et al. 1993; THIERRY et al. 2000).

The **Swiss Jura platform** corresponded to a shallow-water carbonate platform with tidal flats, oncoid-rich lagoons, oolitic bars, and coral patch-reefs. Synsedimentary tectonics structured the platform into highs and depressions that shifted their position through time (ALLENBACH 2001).

The **Lorraine carbonate platform** was probably connected to the SE to the Jura platform, to the NW to the Paris Basin, and sloped from the London-Brabant landmass located about 100 km to the north (ZIEGLER 1990; CECCA et al. 1993). It was bounded by the Vittel fault to the south (HUMBERT 1971; MARCHAND & MENOT 1980; GEISTER & LATHUILIÈRE 1991; COLLIN & COURVILLE 2000). A tectonic tilt of the platform to the north is observed in the Late Oxfordian (CARPENTIER 2004). The platform evolved from a shallow marine carbonate-dominated platform in the Middle Oxfordian to a mixed siliciclastic-carbonate platform in the Late Oxfordian (OLIVIER et al. 2004a; CARPENTIER 2004).

The **Haute-Marne** was located between the Burgundy platform and the Lorraine platform. This area corresponded to a deeper-water platform ("distal platform"; LORIN et al. 2004) sloping to the Paris Basin. In the Late Oxfordian, sedimentation

was characterized by thick marl deposits (Marnes de Latrecey) and limestones (Calcaires de Latrecey; COURVILLE & VILLIER 2003).

The Swabian Jura deep shelf was located about 50 km to the east of the Jura platform (MEYER & SCHMIDT-KALER 1989, 1990; GYGI 1990). Located in the deeper part (estimated palaeobathymetry of 100-200 m; PITTET & MATTIOLI 2002; OLIVIER et al. 2004b) of a gently inclined carbonate ramp marginal to the Tethys Ocean, this deep platform was characterized by hemipelagic sedimentation with siliceous-sponge and microbialite bioherms (Swabian facies; e.g., WAGENPLAST 1972; GWINNER 1976; KEUPP et al. 1990;

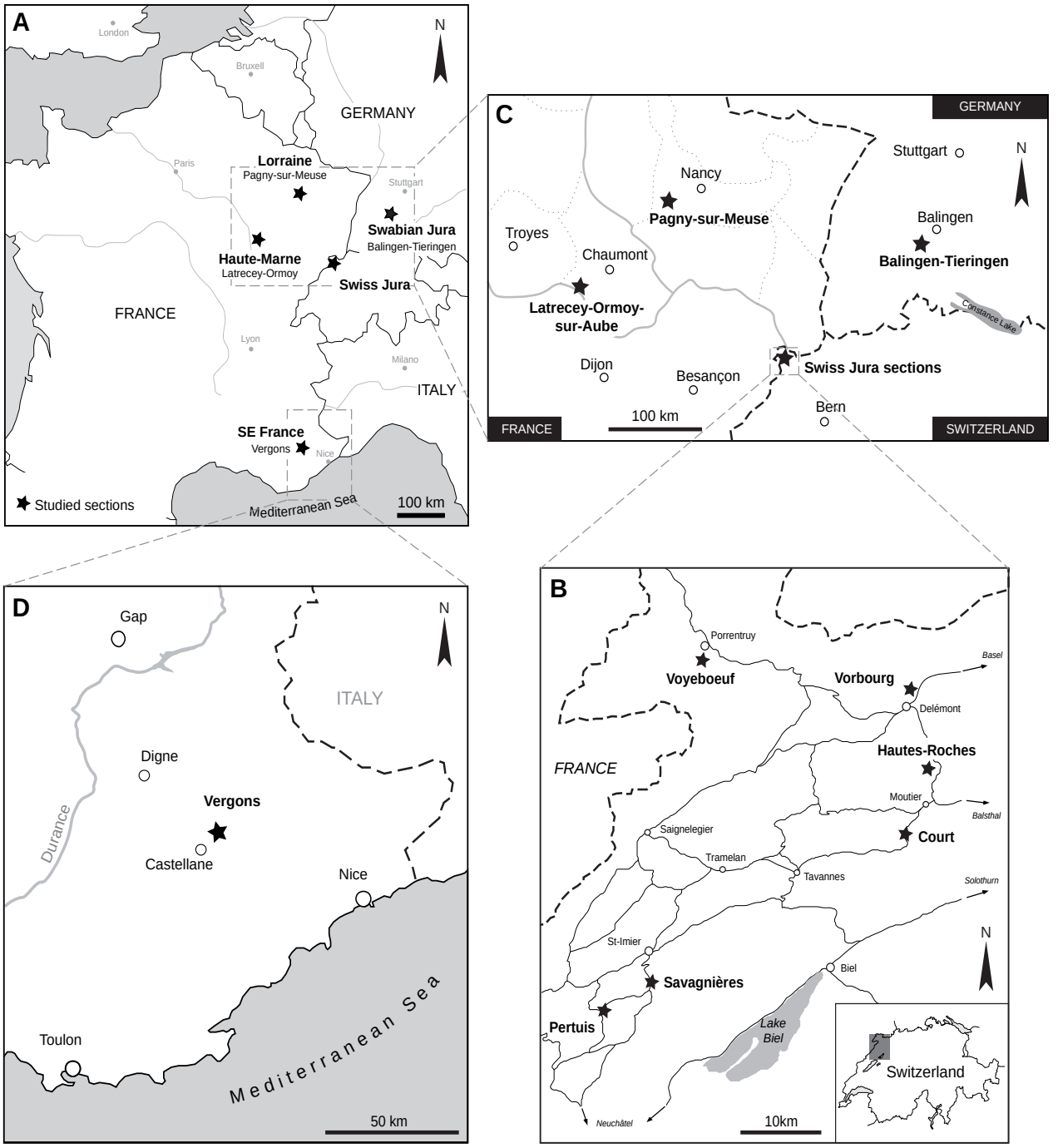

Fig. 1.2 - Geographical location of the studied sections (a) in central Europe; (b) in the Swiss Jura Mountains; (c) in eastern France and southern Germany; (d) in the southeast of France.

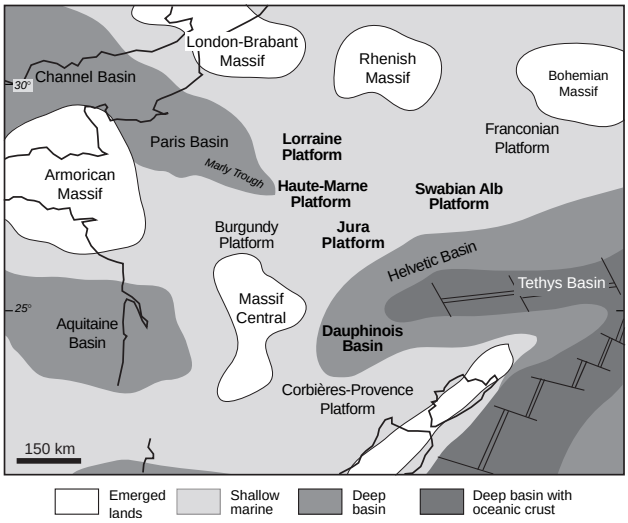

Fig. 1.3 - Palaeogeography of the northern margin of the Alpine Tethys during the Late Oxfordian (modified from MEYER & SCHMIDT-KALER 1989; ZIEGLER 1988; THIERRY et al. 2000). The studied areas are in bold.

LEINFELDER et al. 1994; OLIVIER et al. 2004b). Also considered as an intraplatform basin, the Swabian Jura is confined by the Swiss Jura platform to the SW and by the Franconian (Bohemian) platform to the NE. It opened southwards towards the "deep" Helvetic basin.

The **SE France basin** (or Dauphinois Basin) and the Helvetic rim basins represent a branch of the Alpine Tethys, which was bordered to the north by the Jura platform and to the south and southwest by the Corbières-Provence platform. During the Late Jurassic, the SE France Basin was a passive margin basin characterized by synsedimentary tectonics and horst and graben structures (DEBRAND-PASSARD et al. 1984). Throughout the Late Jurassic and Early Cretaceous, this area was characterized by hemipelagic to pelagic sedimentation with instability phases generating gravity deposits with biodetrital influx from the surrounding platforms.

1.2.2 Stratigraphy

The studied interval comprises platform and basin deposits of the beginning of the Bimammatum zone (Semimammatum and Berrense ammonite subzones) in the Late Oxfordian (Figs 1.4 and 1.5).

Lithostratigraphy and biostratigraphy

Facies and lithostratigraphy of the Middle and Late Oxfordian deposits from **northern Switzerland** have been investigated extensively by, e.g., ZIEGLER (1962), BOLLIGER & BURRI (1967, 1970), GYGI (1969, 1992, 1995), and GYGI & PERSOZ (1986). GYGI (2000a, b) gives an excellent summary of the history of lithostratigraphic classification of northern Switzerland. In the Swiss Jura Mountains, the studied interval concerns the very top of the Röschenz Member and most of the Hauptmumienbank Member and its lateral equivalent, the Steinebach Member, which all belong to the middle part of the Vellerat Formation (Fig. 1.4). The Röschenz Member is composed of marls and thin limestone beds whereas the Hauptmumienbank and Steinebach members consist of relatively massive limestone beds. The Hauptmumienbank ("main mummy bed", STEINMANN 1880) Member has a typical oncolitic facies while the Steinebach Member features oolites and coral boundstones.

The biostratigraphic framework for the Oxfordian and Kimmeridgian in the Jura Mountains was established using ammonites from platform and basin deposits (ENAY et al. 1988; GYGI 1995). Dating of the platform deposits was improved by mineralostratigraphic correlations (PERSOZ & REMANE 1976; GYGI & PERSOZ 1986). These authors used the vertical distribution of kaolinite and detrital quartz to correlate ammonite-rich basin sections with biostratigraphically less well constrained sections on the platform. The Hauptmumienbank and Steinebach members are dated of the Hypselum subzone, equivalent to the Semimammatum and Berrense subzones placed at the beginning of the Bimammatum zone (GYGI & PERSOZ 1986, GYGI 2000b; Fig. 1.4).

In **Lorraine**, the lithostratigraphy of Middle to Late Oxfordian deposits has been studied by HUMBERT (1971), MARCHAND & MENOT (1980), and CARPENTIER (2004). In this study, the *Calcaires à polypiers de Pagny* (CPP), the *Oolithe de Saucourt inférieure* (OSI), and the *Marnes à huîtres de Pagny* (MHP) members are examined (Fig. 1.4). The *Calcaires à polypiers de Pagny* are characterized by grey limestones (mudstones-wackestones to oyster lumachella packstones-grainstones) intercalated with dark marls. Laterally and locally, these limestones pass into coral and/or bivalve patch-reefs. The total thickness of this member varies between 3 and 10 metres. The *Oolithe de Saucourt* comprises all the

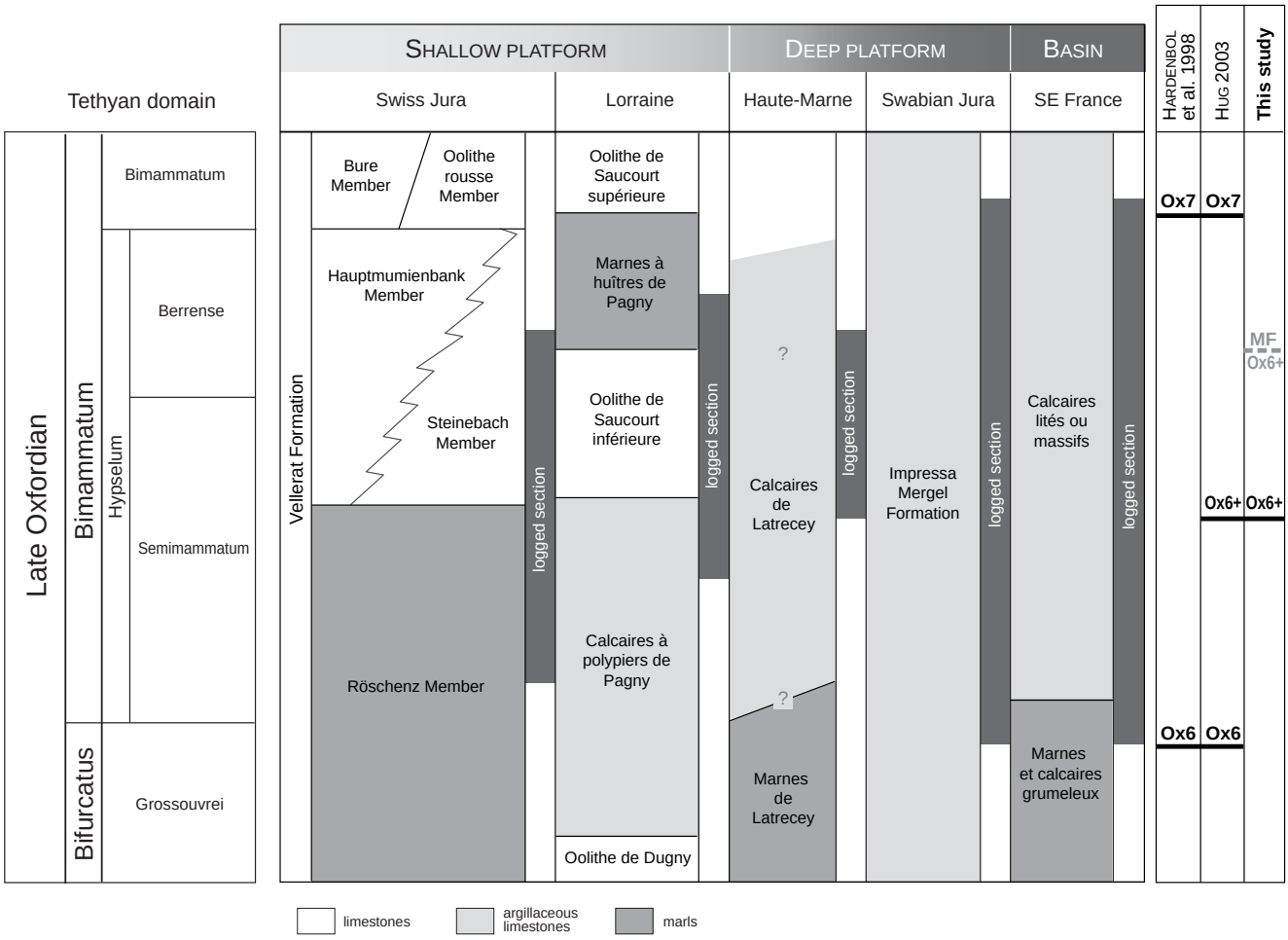

Fig. 1.4 - Bio- and lithostratigraphy for the studied interval of all the sections from shallow platform to basin. Ammonite biostratigraphy and sequence stratigraphy from HARDENBOL et al. (1998). Lithostratigraphy of the Swiss Jura after GYGI (1995), Lorraine after CARPENTIER (2004) and CARPENTIER et al. (2006), Haute-Marne after COURVILLE & VILLIER (2003), Swabian Jura after SCHWEIGERT (1995a), and SE France according to ENAY et al. (1984).

oolitic facies intercalated between the different marly facies at the base of the Late Oxfordian present in the Marne Valley area. This formation can be subdivided into three members, which are laterally continuous over most of the Lorraine platform. The *Oolithe de Saucourt inférieure* designates the first oolitic and oncolitic facies, which cover the *Calcaires à polypiers de Pagny*. The *Marnes à huîtres de Pagny* correspond to dark marly facies (slightly silty), which overlie the *Oolithe de Saucourt inférieure*. They pass laterally into more or less argillaceous carbonate facies (more or less rich in oysters or lumachella). The third member is the *Oolithe de Saucourt supérieure*, which is rich in ooids and oncoids.

The biostratigraphy of the studied deposits is based on the recent discovery of two ammonites, one at the base and the other at the top of the *Calcaires à polypiers de Pagny* (CARPENTIER 2004). They correspond, respectively, to the species *Perisphinctes (Dichotomoceras) bifurcatoïdes* and *Perisphinctes (Perisphinctes) hallatus* (determination of R. Enay) and indicate the Bifurcatus and the Bimammatum zones. Consequently, the Bifurcatus-Bimammatum limit is positioned within the *Calcaires à polypiers de Pagny*.

In **Haute-Marne**, the studied interval concerns the member of the *Calcaires de Latrecey*. This member is characterized by homogeneous carbonate facies with quite poor and poorly diversified benthic macrofauna and corresponds to outer, deep-water platform environments (Fig. 1.4; COURVILLE & VILLIER 2003). Ammonites indicate that the *Calcaires de Latrecey* belong to the Semimammatum subzone and probably reach into the Berrense subzone (COURVILLE & VILLIER 2003).

The **western Swabian Jura** (Swabian Alb, southern Germany) exposes deeper-water carbonate facies (i.e., marl-limestone alternations and siliceous

sponges) of the upper part of the Impressa-Mergel Formation (Fig. 1.4; SCHWEIGERT 1995a), also described as the Malm-alpha Formation (QUENSTEDT 1843). Ammonite biostratigraphy indicates the Bifurcatus and Bimammatum ammonite zones (SCHWEIGERT 1995a, b; SCHWEIGERT & CALLOMON 1997).

In the **SE France basin**, the studied interval displays marl-limestone alternations belonging to the *Marnes et calcaires grumeleux* and the *Calcaires lités ou massifs* (ENAY et al. 1984), which are dated by ammonites and dinocysts of the Bifurcatus and Bimammatum zones (ATROPS 1982, 1984; Fig. 1.4).

Sequence- and cyclostratigraphy

This study examines platform and basin deposits that lie between the third-order sequence boundaries (SB) Ox6 and Ox7 defined by HARDENBOL et al. (1998) in European basins. Between Ox6 and Ox7, an additional major sequence boundary (SB Ox6+ of HUG 2003) was identified in the Hypselum subzone (Fig. 1.4; HUG 2003; STRASSER et al. 2005). This sequence boundary coincides with the 2nd-order maximum regression according to HARDENBOL et al. (1998).

Based on the absolute ages given by GRADSTEIN et al. (1995), HARDENBOL et al. (1998) date SB Ox6 at 155.81 Ma and SB Ox7 at 155.15 Ma (Fig. 1.5). This implies a time span of 600 to 700 kyr between these two large-scale (3rd-order) sequence boundaries. In the corresponding interval, PITTET (1996), HUG (2003), and STRASSER et al. (2000) counted 8 small-scale sequences, each composed of five elementary sequences. This suggests that a small-scale sequence formed within 75 to 87.5 kyr, and an elementary sequence within 15 to 17.5 kyr. These values approach those of the first orbital eccentricity cycle (100 kyr) and of the precession cycle (between 18 and 22 kyr in the Oxfordian; BERGER et al. 1989). Furthermore, the systematic stacking of 5 elementary sequences into one small-scale sequence over the entire Middle Oxfordian to Early Tithonian interval investigated in the Swiss Jura points to an orbital control on the formation of the depositional sequences (STRASSER 2008). It is implied that these orbital cycles induced climate changes that translated into sea-level fluctuations, which in turn controlled the formation of the observed depositional sequences.

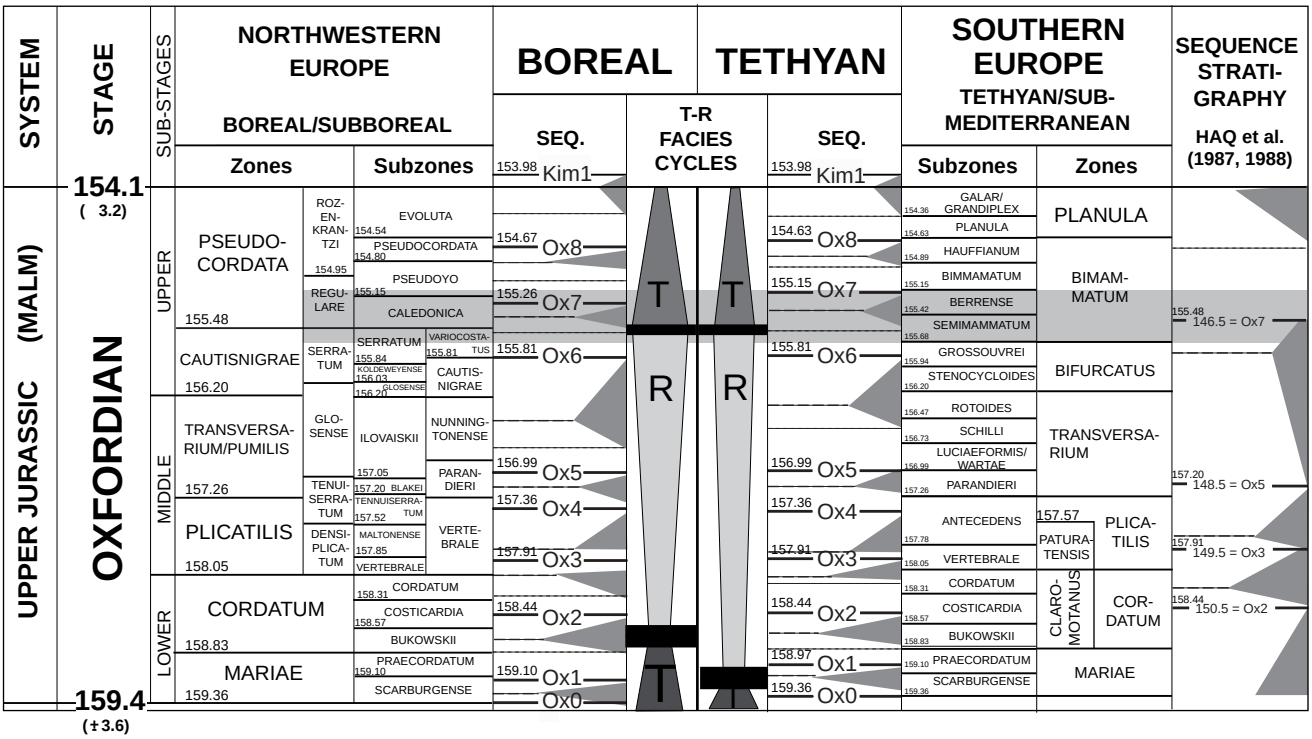

Fig. 1.5 - Bio-, chrono-, and sequence-stratigraphic framework of the Oxfordian, according to HARDENBOL et al. (1998) and compared with the HAQ et al. (1987, 1988) eustatic charts. The studied time interval is shaded. For this study, the sequence-boundary positions of the Tethyan realm are used.

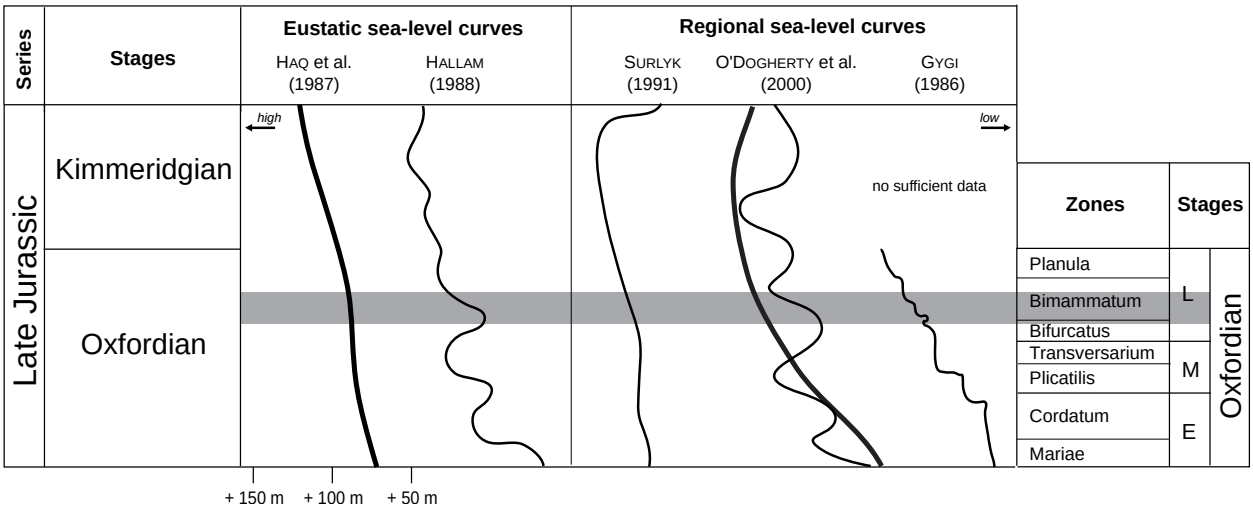

Fig. 1.6 - Comparisons of several eustatic and regional sea-level curves for the Oxfordian/Kimmeridgian. The studied time interval is shaded.

1.2.3 Eustatic sea-level changes

The Oxfordian and Kimmeridgian stages are characterized by a long-term transgressive trend. During the Oxfordian, a T-R facies cycle is recognized (e.g., HAQ et al. 1987; HARDENBOL et al. 1998; JACQUIN et al. 1998; HALLAM 2001; Fig. 1.6). A long-term eustatic sea-level curve for the Jurassic has been published by HAQ et al. (1987) and HALLAM (1988). Regional long-term sea-level curves have been published for the Oxfordian by, e.g., GYGI (1986), SURLYK (1991), and O'DOGHERTY et al. (2000); they all indicate a transgression at the Late Oxfordian (Fig. 1.6).

High-frequency eustatic sea-level fluctuations with low amplitudes, related to insolation changes in the Milankovitch-frequency band, were superimposed on this long-term sea-level trend. A reconstruction of high-frequency eustatic sea-level fluctuations has been attempted for the studied interval (VÉDRINE 2005; VÉDRINE & STRASSER 2005).

1.2.4 Palaeoclimate

Late Jurassic climate was characterized by a greenhouse period with high atmospheric CO_2 levels (e.g., MOORE et al. 1992), a monsoonal rainfall pattern (PARRISH 1993), warm and humid conditions and markedly reduced latitudinal temperature gradients with respect to the present day (HALLAM 1984, 1985; WIGNALL & RUFFELL 1990). However, superimposed on this record of warmth is mounting evidence for cooler climate periods with high-latitude seasonal ice ("cool mode", FRAKES et al. 1992).

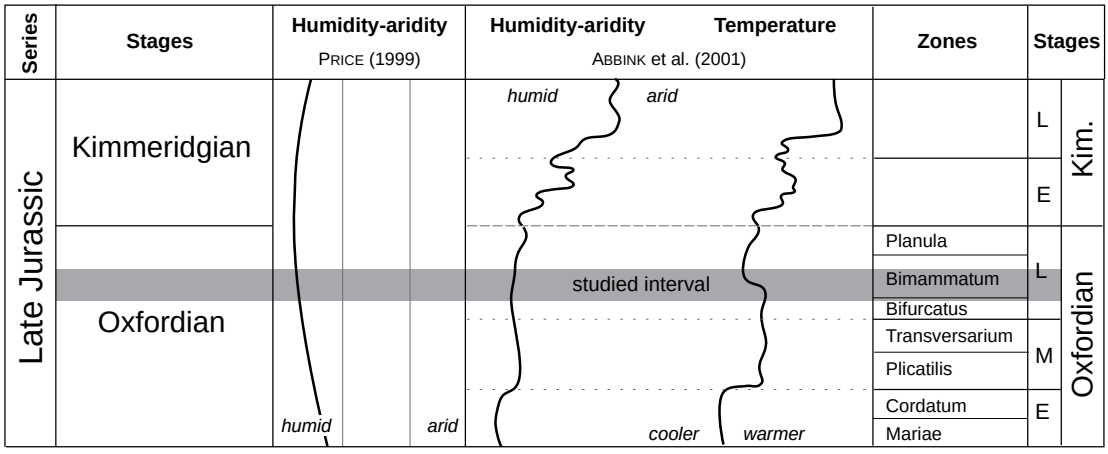

Fig. 1.7 - Evolution of humidity-aridity and temperature for the Oxfordian/Kimmeridgian. The studied time interval is shaded.

In the Middle and Late Oxfordian, abundant rainfall in the hinterland allowed vegetation growth and continental run-off of siliciclastics into the study area (Gygi 1986; Pittet 1996). Associated nutrient input periodically led to eutrophication and to crises of coral reefs (Dupraz & Strasser 1999). Towards the Late Oxfordian and Kimmeridgian, climate became more arid, as indicated by generally less siliciclastics and by evaporite pseudomorphs (Hug 2003; Rameil 2005; cf. Fig. 1.7 and Chap. 8)). Frakes et al. (1992) indicate up to 27°C for the Late Oxfordian ocean surface temperatures according to oxygen isotopes measured on planktonic foraminifera and belemnites. Based on $\delta^{18}O$ analyses of Middle Oxfordian samples (modified bulk) from the Swiss Jura platform, Plunkett (1997) calculated palaeotemperatures of 26-27°C.

This general climatic evolution was controlled by high-frequency climate changes related to orbital (Milankovitch) cycles (Pittet 1996). These not only controlled siliciclastic input through periodically increased rainfall but also periodic evaporite formation (Hug 2003). Furthermore, they were responsible for low-amplitude sea-level fluctuations that led to the formation of hierarchically stacked depositional sequences (Strasser et al. 1999, 2000).

1.2.5 Global and regional tectonics

At a global scale, increased tectonic subsidence rates during Oxfordian-Kimmeridgian times correlate with intensified rifting and wrench activity within the Arctic-North Atlantic rift system and along the northern Tethyan margin ("Oxfordian crisis"; Arnaud 1988). In Late Jurassic times, the Swiss Jura was part of the passive northern margin of the Tethys Ocean (e.g., Wetzel et al. 2003). The tectonic regime was extensional and pre-existing tectonic structures in the basement were reactivated (Burkhalter 1996; Wetzel & Allia 2000; Allenbach 2001; Wetzel et al. 2003). This caused differential subsidence and/or rotation of fault-bounded blocks, which morphologically differentiated the depositional area into swells and depressions. The relief created by tectonics contributed significantly to the general facies distribution on the shallow platform.

1.3 Methods

Based on facies and microfacies analyses, this study concentrates on the transgressive part of sequence Ox6+. Three domains of sedimentation are investigated: shallow platform, deep platform, and basin. Seven shallow platform sections, two deep platform sections, and one basin section have been logged at a cm scale and densely sampled for a detailed sedimentological analysis. Samples were taken at the base, in the middle, and at the top of beds. In total, 505 polished slabs and thin sections, plus 60 washing residues of marls were examined. Field observation, texture analysis, and semi-quantification of skeletal and non-skeletal elements were performed in order to interpret the depositional environments (cf. Chap. 2).

Based on the hierarchical stacking pattern, bed surfaces, facies, and microfacies, a high-resolution sequence- and cyclostratigraphic analysis was carried out for this transgressive interval. Sequence analysis is based on the comprehensive sedimentological analysis of sections and is first made separately for each section. In a second step, the sections are correlated and a best-fit solution is sought for. This methodology is summarized in Strasser et al. (1999). The terminology follows that of the sequence-stratigraphic model of Vail et al. (1977, 1991). A depositional sequence is defined as a succession of genetically related sediments. Different orders of depositional sequence are identified in the studied sections: medium-scale, small-scale, and elementary sequences (cf. Chap. 3). These depositional sequences were caused by sea-level fluctuations, which were related to climate changes, themselves controlled by the astronomical parameters of the Earth's orbit. Consequently, the observed depositional sequences are the sedimentological expression of orbital cycles and are attributed to the precession cycle (20 kyr) for the elementary sequences, and to the short- and long-eccentricity cycles (100 kyr and 400 kyr) for the small- and medium-scale sequences, respectively.

This methodology provides a precise sequential and chronological framework, in which palaeoenvironmental and palaeoecological changes on the shallow platform can be monitored through time and space. In addition, platform-basin relationships (i.e., carbonate mud and clay exportation) can be discussed based on a best-fit sequence-stratigraphic platform-to-basin correlation of all sections.

* * *

2 - FACIES AND MICROFACIES ANALYSIS

2.1 INTRODUCTION

Facies is the sum of all organic and inorganic characteristics of sedimentary rocks including color, texture, grain size, mineralogical composition, fossil content, and sedimentary structures (FLÜGEL 2004; TUCKER & WRIGHT 1990). *Microfacies* describes an association of all sedimentological and palaeontological criteria observable in thin section or on polished slab (FLÜGEL 2004). Facies and microfacies assist in interpreting environmental parameters that control deposition and the distribution of organisms and grains. Facies and microfacies analyses also allow for the interpretation of depositional sequences, i.e. the recognition of shallowing/deepening trends.

The *depositional environment* is the area in which organisms live and sediments are deposited. Fossils are the most important indicators of ancient environments because strong interactions exist between organisms and their environment. From the facies and microfacies analyses, and from the study of floral and faunal associations, the physical, chemical, and ecological parameters influencing the depositional environment can be deduced.

2.2 METHODOLOGY

The facies and microfacies analyses are based on very detailed field, macroscopic, and microscopic observations. First, sections were logged at a cm-scale and densely sampled. The hierarchical stacking pattern of beds and bed surfaces was examined. Thin sections and the respective polished slabs, and the marl washings were examined under the binocular and optical microscope. The Dunham classification is used for the description of texture. The abundance of skeletal and non-skeletal grains was evaluated semi-quantitatively (cf. Chaps 4 and 7). Matrix and cements were also examined. These informations are then integrated to interpret the depositional environment.

In the following paragraphs, the elements of platform and basinal facies and microfacies are described. The interpretation is based on comparison with the literature (e.g., FLÜGEL 2004) and on the sedimentological context within which the elements occur.

2.3 SHALLOW PLATFORM FACIES

2.3.1 Non-skeletal carbonate elements

Peloids

The peloids occurring in the studied samples are spherical to elliptical micritic grains without any internal structures (Pl. 5/6). They are commonly smaller than 1 mm of diameter. Several modes of formation are possible: fecal, microbial, reworked cohesive mud, internal molds of fossils, complete micritization of bioclasts or other carbonate grains (TUCKER & WRIGHT 1990; FLÜGEL 2004; SAMANKASSOU et al. 2006). Peloids are abundant in lagoons and are preserved in low-energy subtidal and intertidal zones.

Oncoids

Oncoids (from the Greek ονκοσ, "lump"; HEIM 1916) are irregularly formed calcareous components with non-concentric micritic laminae, round or lobate shapes, dense texture with or without inclusions, and in some cases with indistinct boundaries. They are mainly due to biogenic accretion around a nucleus.

		Micrite-dominated oncoids		*Bacinella-Lithocodium* oncoids	
		type 1 	**type 2** 	**type 3** 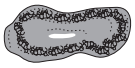	**type 4** 
Morphological criteria	Prevailing size	few millimeters	few mm to 1 cm	few cm to 5 cm	few mm to 10 cm
	Shape and surface	elliptical to spherical smooth	elliptical smooth	elliptical lobate	elliptical lobate
	Nucleus	bioclastic or lithoclastic nucleus		bioclasts or without nucleus	no nucleus recognizable
Cortex configuration and composition	Lamination type	concentric and continuous but barely visible	irregular and truncated	rarely continuous	no lamination
	Microfabric	micritic laminations or homogeneous	micritic laminations and organism-bearing laminations	organism-bearing laminations and few micritic laminations	microbial meshwork
	Bioclasts	rare	common bioclasts		rare
	Microencrusters	no fauna associated	serpulid worms, *Bullopora*	abundant microencrusters: *Bacinella, Lithocodium*	
Surrounding sediment	Classification	mudstone - wackestone	packstone and locally wackestone	mudstone - wackestone and locally packstone	
	Associated fauna and grains	mainly benthic foraminifera, peloids, and ooids		brachiopods, commonly *Mohlerina basiliensis*, bivalves	echinoderms, commonly *Mohlerina basiliensis*
Depositional environment	Relative energy	moderate and intermittent	high and intermittent	low and intermittent	very low
	Bathymetry	subtidal			
	Sedimentation rate	low			
	Environment	protected lagoon	fully marine lagoon		

Fig. 2.1 - Classification of the oncoids found in the Hauptmumienbank Member. Morphological criteria, cortex configuration and composition, surrounding sediment, and depositional environmental conditions are indicated.

Peryt (1983) defined them as "a group of algally (red algae excepted), cyanobacterially and bacterially coated grains, which are initiated in marine and freshwater phreatic environments".

The oncoids found in the Hauptmumienbank Member display a wide variability in size, shape, and composition (Védrine et al. 2007). Observed oncoid sizes vary between a few millimetres to a few centimetres. The oncoids have a well-defined rounded or irregular shape and smooth, wavy, or lobate contours. The final shape follows in many cases that of the nucleus, although a higher sphericity is obtained. If a nucleus is present, it is of bio- or lithoclastic nature and the envelope has a variable thickness. The cortex is characterized by micritic and/or organism-bearing laminations, which are continuous or discontinuous when the oncoid surface was eroded (Pl. 4).

Types of oncoids are mainly defined and differentiated by the surface morphology, the cortex structure and by the presence, the nature, and the abundance of microencrusters in their cortex. Microfacies analysis of the encasing sediment furnishes the environmental context within which the oncoids were formed. In the Hauptmumienbank Member, oncoids are mainly found in wackestones, locally floatstones or rudstones, with bioclasts, ooids, and peloids. Transported micrite-dominated oncoids are also observed in ooid-rich grainstones. Texture, faunal composition, and sedimentary structures suggest a deposition in shallow-water lagoons. Based on more than 300 thin sections and macroscopic samples from the Hauptmumienbank Member, four types of oncoids can be distinguished (Fig. 2.1). Transitions between types also exist, suggesting a continuum.

Type 1 oncoids have diameters of a few millimetres and correspond to elliptical or spherical particles with relatively smooth contours. The cortex is micritic, homogeneous, and without microencruster inclusions (Pl. 4/1). This pattern probably results from the trapping of fine-grained sediment on the oncoid surface by microorganisms. Laminations are difficult to distinguish. Type 1 oncoids are preferentially found in peloidal and bioclastic (foraminifera, bivalves, echinoderms) mudstones-wackestones of protected and moderate-energy lagoonal environments. This type of oncoid is relatively rare in the studied interval (cf. Chap. 7 and Fig. 7.5).

Type 2 oncoids have diameters of a few millimetres (up to 1 cm) and present elliptical shapes with smooth contours. The cortex has irregular and locally truncated micritic laminae, and different growth phases can be distinguished in many cases (Pl. 4/2-5). This suggests relatively high-energy conditions with intermittent periods of wave agitation leading to a partial erosion of the cortex. The cortex of the micrite-dominated oncoids presents a relatively low-diversity fauna such as serpulid worms and *Bullopora*. Occasionally, ooids are incorporated in the cortex (Pl. 4/3). These oncoids are found in packstones with normal-marine or semi-restricted fauna (brachiopods, oysters, foraminifera, echinoderms, bivalves, serpulids, ostracodes) and also in marls. Type 2 oncoids are common in all studied sections (Fig. 7.5).

Type 3 oncoids have diameters of a few millimetres to a few centimetres (up to 5 cm) and sub-elliptical shapes with wavy contours. The cortex is made of alternating organism-bearing and thin micritic laminations (Pl. 4/6-7). The organism-bearing laminations are formed by two microencrustres: *Bacinella irregularis* (Radoicic 1959; Pl. 10/1) and *Lithocodium aggregatum* (Elliott 1956; Pl. 10/2). *Bacinella irregularis* is an enigmatic microencruster with an irregular micritic meshwork and interspaces filled with calcite spar. This is assumed to represent a cyanobacterial structure (e.g., Schmid 1996; Dupraz 1999; Shiraishi & Kano 2004). *Lithocodium*, originally interpreted as a codiacean alga by Elliott (1956), is characterized by inner cavities and an aggregated outer wall with numerous alveoli (complex wall structure) probably containing symbiotic and photosynthetic algae (Schmid & Leinfelder 1996). These authors thus attributed it to a loftusiacean foraminifer with an encrusting life habit. Recently, Cherchi & Schroeder (2006) interpreted *Lithocodium* as colonies of calcified cyanobacteria because of the absence of apertures connecting neighbouring cavities, and because of the very irregular form and arrangement of these hollows. These *Bacinella-Lithocodium* oncoids can be compared to the porostromate oncoids of Peryt (1981) because of the presence of cyanobacteria in their cortex. The alternation of micrite laminae and organism-bearing laminae suggests calm periods, during which *Bacinella-Lithocodium* could grow, and more agitated periods, when micrite laminae were formed by the rolling on the lagoon floor. Type 3 oncoids are preferentially found in wackestones with normal-marine fauna (brachiopods, oysters, foraminifera, echinoderms, bivalves) indicating relatively low-energy conditions. The *Bacinella-Lithocodium* association characterizes lagoonal environments with oligotrophic conditions, low accumulation rate, clear, oxygenated, shallow, and normal-marine waters (e.g., Leinfelder et al. 1993; Dupraz & Strasser 1999; Immenhauser et al. 2005). Dupraz & Strasser (1999), who examined the encrustations of Oxfordian coral reefs in the Swiss Jura, correlated the *Bacinella-Lithocodium* association with episodes of relatively high coral diversity. *Bacinella* and *Lithocodium* have also been identified in the microbial crusts associated with other coral and sponge reefs of the Late Jurassic (e.g., Helm & Schülke 1998; Schmid & Leinfelder 1996; Shiraishi & Kano 2004). This may suggest that palaeoecological conditions for *Bacinella-Lithocodium* bearing oncoids were analogous. The presence of the benthic foraminifer *Mohlerina basiliensis* (Mohler 1938; Schlagintweit & Ebli 1999; Schlagintweit et al. 2005), preferentially in wackestones with type 3 and/or 4 oncoids, suggests that oncoids and benthic foraminifera were, at least partly, controlled by similar environmental parameters.

Type 4 oncoids have diameters of a few millimetres to several centimetres (up to 10 cm) and display irregular shapes with lobate contours. Exclusively composed of *Bacinella* and/or *Lithocodium* meshwork, they have no nucleus nor laminations (Pl. 4/8). Type 4 oncoids are found in bioclastic wackestones, commonly associated with type 3 oncoids. Low-energy conditions with no or only rare agitation are suggested. Locally, type 4 oncoids develop into carpet-like structures and build-ups of *Bacinella* (e.g., Hug 2003; Immenhauser et al. 2005).

Oncoids are considered as good proxies for palaeoenvironmental studies (Dahanayake 1977, 1978, 1983; Kuss 1990; Hug 2003). Based on this study, water energy, water depth, trophic level, and sediment accumulation rate appear as the main direct environmental controlling parameters (Védrine et al. 2007; cf. Chap. 7 for more discussion on the controlling factors).

Ooids

In the shallow platform deposits examined, three types of ooids have been observed. Ooids with thinly laminated fine-radial cortices (type 3 of Strasser 1986; Pl. 5/1) are very common and imply high-energy marine environments (Davies et al. 1978). The ooids can also be transported into quiet-water environments and be incorporated into packstones and wackestones.

These radial ooids commonly display a partial or complete micritization (micritized type 3 ooids; Pl. 5/2-3).

Some oo-oncoids (type 2 of STRASSER 1986) are occasionally found in the studied deposits. They consist of a radial ooid, which is enveloped by an oncoid cortex, characterized by irregular micritic thin laminae (Pl. 5/4-5). This points to a change from higher energy, where the radial ooids (type 3 of STRASSER 1986) formed to quiet waters in a protected lagoonal environment, where microbial activity was favoured.

Lithoclasts

Lithoclasts are common in the studied Oxfordian shallow marine sediments. They consist of slightly rounded mudclasts or consolidated sediment fragments with bioclasts and/or ooids (Pl. 5/7-8). These clasts indicate erosion and redeposition of material derived from pre-existing carbonate sediments.

2.3.2 Skeletal carbonate elements

Skeletal grains comprise complete and fragmented fossils. None of the observed organisms has biostratigraphic significance.

Calcareous algae

Calcareous algae are relatively rare in the studied deposits. Charophytes are macrophytic green algae that grow predominantly in oligotrophic freshwater environments. Oogons and stems have been found only at the base of the Hautes-Roches section. The microencrusting green alga *Thaumatoporella* is locally present in the microbial encrustations of corals. Dasycladacean algae are rarely observed in thin sections (Pl. 6/6). Their absence may be caused by bad preservation conditions due to an original aragonite skeleton mineralogy. No red alga fragments were identified in the studied thin sections.

Ostracodes

In this study, ostracodes are mostly seen in thin section and have therefore not been determined. They have been found in the shallow platform as well as in the basin sections (Pl. 6/3). Ostracodes can be useful in the biostratigraphic analysis of marine and non-marine sediments, particularly in freshwater environments where other fossils are lacking.

Serpulids

Small reworked tube-clusters of serpulids (suspension-feeding polychaete worms) are observed in the Savagnières section (Pl. 1/2, Pl. 6/7). Furthermore, they commonly occur as encrusters on shell debris (Pl. 11/5) or in oncoids (Pl. 4/4).

Serpulids are relatively tolerant of changes in salinity, water temperature, substrate, and water depth (MILLIMAN 1974).

Bivalves

In the studied shallow-water deposits, bivalves are common. In addition to undetermined bivalves, three groups of bivalves could be identified: oysters, inocerams, and lithophages. Oysters are common on firm- and hardgrounds (Pl. 6/1, Pl. 3). The accumulation of (monospecific) oyster shells may indicate environments with brackish conditions. Inocerams have a very coarse ostracum composed of vertically oriented calcite prisms (honeycomb pattern; Pl. 6/2). They tolerate fluctuations in bathymetry, types of sediment, and oxygenation (MACLEOD & HOPPE 1992). Lithophages chemically and mechanically perforate hard substrates. They are commonly observed in corals (Pl. 6/8).

Gastropods

In the studied sections, gastropods are locally present (Pl. 5/3). Some large gastropods of the species *Bourgetia striata* (grazers, herbivores and detritus feeders) abound with in-situ echinoids, brachiopods, and crinoids in the marly interval at the base of the Hautes-Roches section (DUPRAZ 1999). This association indicates open-marine conditions.

Benthic foraminifera

In the studied shallow-water carbonates, a variety of benthic foraminifera is observed. Most of them belong to the suborders Textulariina, Lagenina and Miliolina.

Textulariids are common in the studied deposits.

Code	Texture Folk	Texture Dumham	Major components	Other components	Sedimentary features	Interpretation
SHALLOW PLATFORM						
Clays and marls						
si1	Clays		coal debris			argillaceous lagoon
si2	Argillaceous marls		unifossiliferous or with restricted fauna (charophytes, gastropods, ostracodes)	foraminifera, serpulids, coal debris		protected lagoon
si3	Bioclastic marls		normal-marine fauna (echinoderms, bivalves, foraminifera)	oncoids, serpulids, ostracodes		protected to semi-open lagoon
si4			normal-marine fauna (brachiopods, echinoderms)	corals, ooids	nodular aspect	open lagoon
si5	Sandy marls		normal-marine fauna (oysters, echinoderms, foraminifera, ostracodes, gastropods)	quartz		argillaceous lagoon with siliciclastic input
Tidal mudflat						
tf1	Marls - biomicrite	m - P	oysters, peloids, quartz, glauconite	type 3 ooids, mudclasts	lenticular bedding, ripples	bidirectional current in tidal mudflat
tf2	Micrite	M	undifferentiated bioclasts		birdseyes	emersion on tidal flat
Inner lagoon - Protected						
prl1	Biomicrite	M	-	echinoderms, foraminifera (*Lenticulina, Spirillina*), bivalves	bioturbation	muddy lagoon
prl2	Biomicrite	M-W-P	dominated by semi-restricted to normal-marine fauna (ostracodes, inocerams), foraminifera (Textularids, Miliolids, *Lenticulina*), quartz	echinoderms, organic matter debris, chamosite		protected lagoon with low-diversity fauna (probably tidal channels or bioclastic bars)
prl3	Pelmicrite	W-P	peloids	semi-restricted to normal-marine fauna (ostracodes, inocerams, echinoderms, oysters, brachiopods), foraminifera (Textularids, *Lenticulina*, Miliolids), quartz, organic matter		tidal channels in protected to semi-open lagoon
Outer lagoon - Semi-Open						
sol1	Biomicrite	W - M	foraminifera (Textularids, *Lenticulina*), brachiopods, bivalves, serpulids, fine quartz	peloids, organic matter debris	black facies	bioclastic lagoon with siliciclastic input
sol2	Biomicrite	W	normal-marine fauna (brachiopods, serpulids, echinoderms, coral rubble), quartz	organic matter		bioclastic lagoon with siliciclastic input
sol3	Onco-biomicrite	W - P	type 2 oncoids, foraminifera (Textularids, Lenticulina, Miliolids), quartz	normal-marine fauna (bivalves, echinoderms, ostracodes, serpulids), peloids, grapestones, organic matter, chamosite		oncolitic and bioclastic lagoon with siliciclastic input
sol4	Onco-oomicrite	W - P	type 2 oncoids, type 3 ooids	type 2 ooids, peloids, foraminifera (Textularids), little quartz		oncolitic lagoon
sol5	Oncomicrite	W-P-Rud	type 2 oncoids	normal-marine fauna (ostracodes, inocerams, oysters, serpulids, echinoderms), foraminifera (Textularids, *Lenticulina*, Miliolids), type 3 oncoids, peloids, quartz		oncolitic lagoon
sol6	Pel-oomicrite	P	peloids, micritized type 3 ooids, type 2 oncoids, little quartz	foraminifera (Textularids, *Lenticulina,* Miliolids), corals, brachiopods, echinoderms, bivalves, sometimes type 2 ooids		tidal bar or channel? in oncolitic lagoon
sol7	Pel-biomicrite	M-W-P	peloids, foraminifera (Textularids, *Lenticulina*), normal-marine fauna (dasycladaceans, ostracodes, bryozoans, bivalves, serpulids, echinoderms, corals, brachiopods, oysters), quartz	type 2 and 1 oncoids		tidal bar or channel? in bioclastic lagoon
Outer lagoon - Open						
ol1	Biomicrite	W - P	dominated by normal-marine fauna (echinoderms, oysters, brachiopods), foraminifera (*Lenticulina*, Textularids, Miliolids), peloids	type 2 and 3 oncoids, serpulids, gastropods, ostracodes, lithoclasts, peloids (old type 3 ooids)		bioclastic lagoon
ol2	Biomicrite	W-P-G	dominated by normal-marine fauna (brachiopods, oysters, echinoderms, calcareous sponges, serpulids, corals)	foraminifera (Textularids, Miliolids), peloids, type 2 oncoids		bioclastic lagoon - locally bars
ol3	Onco-oomicrite	W-P-Rud	type 3 and 2 oncoids, type 3 ooids	foraminifera (Textularids, *Mohlerina,* Miliolids), peloids, type 2 ooids, normal-marine fauna (brachiopods, echinoderms)		oncolitic lagoon
ol4	Oncomicrite	W-F (Rud)	type 3 oncoids	open-marine fauna (serpulids, oysters, brachiopods, echinoderms, inocerams), foraminifera (Textularids, Lenticulina, Mohlerina, Miliolids), type 2 oncoids, peloids, micritized type 3 ooids		oncolitic lagoon
ol5	Oncomicrite	M-W-F	type 3 and 4 oncoids	foraminifera (Textularids, *Lenticulina, Mohlerina*, Miliolids), normal-marine fauna (echinoderms, oysters, brachiopods, gastropods), type 2 oncoids, micritized type 3 ooids, peloids		oncolitic lagoon
ol6	Pel-biomicrite	W	peloids, foraminifera (Miliolids, Textularids, *Mohlerina, Lenticulina*), normal-marine fauna (echinoderms, brachiopods)	type 3 oncoids		tidal channel in oncolitic lagoon

Tab. 2.1 - Main microfacies occurring in the Swiss Jura and Lorraine sections classified according to the depositional environments that they represent.

These agglutinating foraminifera have a labyrinthic or alveolar (complex) internal microstructure (*Pseudocyclammina* sp., Pl. 8/2 and 8/4; *Alveosepta* sp.; *Everticyclammina* sp.) or a simple internal microstructure (*Nautiloculina* sp., Pl. 8/5; *Ammobaculites* sp.; *Tolypammina* sp., Pl. 13/3). Textulariids are ubiquitous ranging from transitional environments with brackish and marsh conditions to bathyal and abyssal depths (FLÜGEL 2004).

Among the Lagenid foraminifera, *Lenticulina* sp. is the most common hyaline foraminifer (Pl. 8/8-9). It occurs from platform to basin and may be found reworked in lagoons.

Code	Texture Folk	Texture Dumham	Major components	Other components	Sedimentary features	Interpretation
High-energy deposits						
bar1	Oosparite	G	micritized type 3 ooids	type 3 ooids, type 2 oncoids, lithoclasts, grapestones		(active) ooid bar
bar2	Oomicrite	W-P	micritized type 3 ooids, foraminifera (Textularids, Miliolids, *Lenticulina*)	type 2 ooids, type 2 oncoids, normal-marine fauna (brachiopods, serpulids), peloids, litho-oncoids		(inactive) ooid bar
bar3	Oomicrite	W - P	micritized type 3 and 2 ooids, quartz	few type 2 oncoids	iron color	abandoned ooid bar - channel?
bar4	Oo-pelmicrite	W	type 2 ooids, peloids, quartz	foraminifera (*Lenticulina*), micritized type 3 ooids, type 2 oncoids		abandoned ooid bar - channel?
bar5	Oosparite/micrite	G - P	type 3 ooids	echinoderms, oysters, lithoclasts, grapestones	isopaque cement	(active) ooid bar in subtidal lagoon
bar6	Oomicrite	W-P-G	type 3 ooids	type 2 oncoids, foraminifera (Textularids, *Lenticulina*), normal-marine fauna (bryozoans, ostracodes, bivalves, serpulids, brachiopods, echinoderms, corals), peloids, quartz, grapestones		(active to inactive) oo-bioclastic bar in subtidal lagoon, washover deposit?
bar7	Oo-Onco-biomicrite /sparite	W-P-G	type 3 ooids (sometimes micritized), type 2 oncoids, normal-marine fauna (brachiopods, echinoderms, corals)	peloids, foraminifera (Textularids, *Lenticulina,* Miliolids, *Mohlerina*), type 2 ooids	cross stratification	(active to inactive) oo-bioclastic bar in subtidal lagoon
bar8	Oo-biomicrite	P - G	oysters, type 3 ooids	echinoderms, peloids, agglutinated foraminifera, gastropods, lithoclasts, grapestones, quartz	locally herringbone cross stratifications	oo-bioclastic bar with siliciclastics in sandtidal flat
bar9	Biomicrite	G	oysters, ostracodes, echinoderms	quartz, lithoclasts	vertical and horizontal burrows	bioclastic bar in tidal sandflat
bar10	Biomicrite	P	oysters, quartz	type 3 ooids, gastropods, quartz	ferrug. color	bioclastic bar with siliciclastic input
bar11	Biomicrite	P	oysters	type 3 ooids, echinoderms	large shells	bioclastic bar - lumachella
Coral reefs						
c1	Biolithite	B (P)	microencrusted corals (*in situ*)	sponges, serpulids, type 3 ooids, bivalves		coral patch-reef
c2	Biolithite	B (M-W-P)	microencrusted corals (*in situ* and in rubble)	peloids, type 3 and 1 ooids, type 2 and 1 oncoids, brachiopods, serpulids, sponges, foraminifera (*Placopsilina, Bullopora*), lithoclasts, quartz		coral patch-reef
c3	Biolithite	B (P)	microencrusted corals rubble	type 3 ooids, peloids, bioclasts (bivalves, echinoderms, brachiopods, serpulids), type 2 oncoids		close to coral patch-reef
c4	Biolithite	B (P)	microencrusted corals rubble	brachiopods, sponges, peloids, serpulids, gastropods, echinoderms		close to coral patch-reef

Tab. 2.1 (continued) - Main microfacies occurring in the Swiss Jura and Lorraine sections classified according to the depositional environments that they represent.

Miliolids are commonly found in the studied deposits (Pl. 8/7). They are made of a porcelaneous wall without pores, characterized by a shiny and smooth appearance. They usually characterize protected environments when they are abundant.

Mohlerina basiliensis (Mohler 1938) has been found in the Swiss Jura deposits. This foraminifer occurs from the Middle-Late Bathonian to the Valanginian and displays a double-layered wall microstructure with a thick outer hyaline radial-fibrous calcite layer and a thin inner micritic layer (Pl. 9). Its taxonomy is still in debate (cf. Annex 1; Védrine in press). It was previously attributed to the suborder Spirillina (e.g., Darga & Schlagintweit 1991), then to the suborder Involutinina, family Ventrolaminidae, and genus *Archaeosepta* (Tasli 1993), and more recently to the suborder Rotaliina and the family Discorbidae (e.g., Bernier 1984; Bucur et al. 1996). However, the double-layered structure of *Mohlerina basiliensis* does not match with the perforated hyaline test, which characterizes the suborders Spirillina, Involutinina, and Rotaliina. The most probable attribution is given by Septfontaine (1981) who placed *Mohlerina basiliensis* with the suborder Fusulinina, which has a similar double-layered microstructure. As the suborder Fusulinina occurs only in the Late Palaeozoic. Septfontaine (1981) called them "Mesozoic Fusulinina". *Mohlerina basiliensis* preferentially occurs in low-energy facies and is always associated with *Bacinella-Lithocodium* oncoids. As the *Bacinella-Lithocodium* association indicates oligotrophic, clear, oxygenated, and normal-marine waters (e.g., Dupraz & Strasser 1999), it is suggested that *Mohlerina basiliensis* requires similar ecological conditions (cf. Chap. 7; Védrine 2008).

In the studied deposits, Textulariids, *Lenticulina*, and Miliolids are commonly associated (Tab. 2.1). Low-diversity fauna suggests more restricted conditions whereas maximum diversity indicates open-marine environments. The spatial and stratigraphic distribution of agglutinated, hyaline, and porcelaneous foraminifera of the Swiss Jura sections is analysed in Chap. 7 and their main controlling factors are discussed.

Encrusting foraminifera

Bullopora (Quenstedt 1856) is abundant in the studied deposits. Different species exist but *Bullopora tuberculata* (Sollas), characterized by spines on the test, is easily recognizable (Pl. 10/3; Schmid 1996). *Bullopora* is composed of small chambers linked by tubes and presents a perforated calcareous test. This foraminifer is attached to the substratum or can colonize dead corals.

Placopsilina (d'Orbigny 1850) is an encrusting foraminifer, which particularly agglutinates quartz grains (Pl. 10/5 and 10/8). *Placopsilina* is abundant in the studied bioherms and in oncoid levels. *Placopsilina* is found together with microbial crusts, suggesting a simultaneous growth in a same environment, especially in columnar forms (Pl. 10/8).

Troglotella incrustans (Wernli & Fookes 1992; Pl. 10/2 and 10/4) is a cryptic encrusting foraminifer, which can perforate calcareous substrate (Schmid & Leinfelder 1996; Cherchi & Schroeder 2006). *Troglotella* is commonly associated with the cyanobacterium *Lithocodium aggregatum* (Pl. 10/2). This suggests that *Troglotella* probably fed on the photoautotrophic symbionts of *Lithocodium* (Schmid & Leinfelder 1996).

Echinoderms

Echinoderms are mainly represented by spines and plates of sea urchins (Pl. 6/5). These strictly stenohaline organisms, i.e. very intolerant to salinity changes, indicate open-marine environments with normal salinity. However, echinoderm fragments are easily transported by currents, which explains their occasionally great abundance in internal lagoons, associated with euryhaline organisms.

Brachiopods

In the studied deposits, two groups of articulate brachiopods are observed: Terebratulids and Rhynchonellids. Terebratulids (Pl. 6/4 and Pl. 11/6) are bulbous in shape, commonly circular or ovoid in outline. They are distinguished by a very short hinge line, a punctuated shell, and smooth or ribbed shells. Rhynchonellids are easily recognized by their strongly ribbed wedge-shaped or nut-like shells and their zigzagged frontal commisure. Rhynchonellids appear to be more sensitive to bad environmental conditions (high turbidity) and to the lack of hard substrate than Terebratulids (Gaillard 1983). Brachiopods are stenohaline organisms and imply normal-marine conditions.

Corals

Corals appear commonly in the Oxfordian deposits (Pl. 6/8-10). They mainly form patch-reefs (e.g., Court section) and carpets (e.g., Hautes-Roches section) in lagoons and indicate open-marine environments. Coral rubble frequently occurs, indicating wave or storm current transport on the platform.

Input of siliciclastics and associated nutrients as well as water chemistry were the major controlling factors for reef development (Dupraz 1999; Dupraz & Strasser 1999). Bathymetry played a subordinate role on the shallow Jura platform, but opening and closing of lagoons linked to low-amplitude sea-level fluctuations as well as fluctuating terrigenous run-off created periodic changes in trophic conditions (Dupraz & Strasser 1999). Demise of corals generally coincides with low sea level and humid climate (Dupraz & Strasser 1999).

2.3.3 Carbonate mud

In the studied sections, the majority of rocks is formed by mud-supported sediments that reflect low-energy settings. Detailed geochemical investigations of the micrite matrix have not been undertaken in this study. The origin of lime mud is still discussed in the scientific community (a compilation is given in Flügel 2004). For the Vellerat Formation in the Swiss Jura Mountains, Dupraz (1999) proposes two sources of micrite: bacterial activity (automicrite) and bioerosion (allomicrite). Carbonate mud produced on shallow-marine platforms is also a major source for periplatform sediments deposited on slopes and in basins (Pittet et al. 2000).

2.3.4 Other constituents

Siliciclastics

Siliciclastics commonly derive from continental areas and are transported onto the platform by rivers, currents and/or wind. The main components are clay

minerals, quartz, feldspars, and heavy minerals. Based on clay mineral analyses of Oxfordian deposits in the Swiss Jura, GYGI & PERSOZ (1986) and PITTET (1996) have observed that: (1) kaolinite and illite have a negative correlation, (2) the mineralogy is independent of facies, (3) there is a low smectite content. In this study, clay mineral analyses have been performed with a high time resolution (cf. Chap. 8).

Subangular quartz grains, ranging from 0.02 to 0.1 mm in diameter (average size 0.08 mm) are locally abundant. Quantities of up to 40% can be reached locally, but 10% are rarely exceeded.

It is admitted that most siliciclastics were brought onto the platform by rivers (GYGI & PERSOZ 1986) probably from northern crystalline massifs (Fig. 1.3). The study of nature and distribution of siliciclastics is thus important for the palaeoclimatic and palaeohydrological conditions in the source area (cf. Chap. 7).

Organic matter

In siliciclastic intervals, small fragments of plant matter are locally present in the Court and Pagny-sur-Meuse sections. However, most of the organic matter is finely dispersed in the matrix (cf. Chap. 2.3.6).

Pyrite

Pyrite is commonly present in most sections as framboids and cubic crystals. In sedimentary systems, pyrite formation results from bacterial degradation of organic matter in reducing conditions.

Chamosite/glauconite

In the studied shallow platform deposits, a low amount of dispersed small green grains is observed in oyster-rich packstones of the Pagny-sur-Meuse section. Geochemical analysis (EDX analysis) indicates a glauconite composition: hydrous silicate of iron and potassium (cf. Annex 2). According to VAN HOUTEN & PURUCKER (1984), glauconite typically occurs in deeper, open-marine settings, whereas chamosite forms preferentially in lagoons. Recently, EL ALBANI et al. (2005) identified glauconite in the Purbeckian facies, characteristic of shallow lagoonal environments, and showed that the glauconite composition changes with the chemical conditions imposed by the local environment.

2.3.5 Sedimentary structures

Birdseyes

Only the Court section presents a level of birdseyes (Pl. 11/1). Birdseyes are mm-scale cavities in carbonate mud that are created by active algal/microbial growth and decomposition, and/or by trapping of gas released during the decomposition of organic matter (FLÜGEL 2004; SHINN & ROBBIN 1983). They occur in the upper intertidal and supratidal zones and are typical sedimentary structures of tidal flat facies.

Bioturbation and perforations

Bioturbation is frequent in the studied interval and indicated by differences of color and texture or differential dolomitization (Pl. 1/1, probably *Thalassinoides*). Nodular limestones are common and result from intense bioturbation. Bioturbation is characteristic of soft sediments while perforations are representative of indurated sediments. Levels of intense bioturbation and/or bioperforation indicate low sedimentation rates or omission phases (HILLGÄRTNER 1999).

In the Vorbourg section, at the top of an oolite bar, a perforated and oyster-encrusted hardground is exposed (Pl. 3/1-3). In the Pagny-sur-Meuse section, a similar hardground is observed (Pl. 3/4-6). These surfaces are interpreted as subtidal hardgrounds.

Herringbone cross beddings

Herringbone cross bedding is observed at the base of the “Oolithe de Saucourt inférieure” (Pagny-sur-Meuse section, Fig. 4.17a). These structures form when current periodically flows in opposing directions (bi-directional currents) such as on a sandflat or in a tidal channel. Such structures are thus interpreted as resulting from tidal currrents.

Lenticular bedding

In the examined sediments, lenticular bedding is observed in the marly deposits at the base of the Pagny-sur-Meuse (Pl. 15/2, Fig. 4.17a). Lenticular bedding is a diagnostic feature for bi-directional currents. Such structures point to low-energy environments such as tidal mudflats (REINECK & SINGH 1975).

Washover deposits

Washover deposits are observed at the base of the Vorbourg and Court sections in the marly Röschenz Member (cf. Chap. 4). They consist of centimetric beds rich in ooids, peloids, bioclasts, and detrital quartz.

Washover deposits result from storm waves that transport and deposit the sediment in a protected (e.g., marly and/or muddy lagoon) behind a barrier island.

2.3.6 Early diagenesis

Micritization

Micritization of grains is common in the Oxfordian deposits of the Swiss Jura. It is a major early diagenetic process in protected and shallow-water environments (Tucker & Barthurst 1990). Bioclastic grains may entirely loose their primary structure and become peloids.

Cementation

Cementation is the initial process leading to sediment lithification. Composition of pore fluids (e.g., freshwater, marine and/or a mixture of them) and depositional environment (e.g., vadose or phreatic cementation) induce precipitation of characteristic cement types (Flügel 2004). However, caution is required because identical cement types may be formed in different diagenetic environments.

In the studied shallow platform deposits, bladed isopachous calcite cements followed by a blocky calcite cement, and syntaxial echinoderm overgrowth cements are commonly observed. Such features are characteristic of phreatic environments. Marine phreatic cements may have existed but were then replaced by calcite in the freshwater zone. Vadose features such as gravitational and meniscus cements were not observed in the studied deposits. The detailed study of Plunkett (1997) on the early diagenesis of the Middle to Late Oxfordian platform sediments shows the predominance of the cementation within a fresh-water phreatic regime. Marine phreatic and vadose regimes were identified only locally.

Dolomitization

In the studied limestones, two varieties of dolomite (sucrosic and isolated euhedral, described by Plunkett 1997) are commonly dispersed in the matrix or locally abundant and filling burrows. Pittet (1996) suggests an early dolomitization and then a dedolomitization (replacement by calcite).

In platform environments, dolomite formation is relatively common and mainly explained by precipitation from modified seawater (Tucker & Wright 1990; Rameil 2005). However, other factors can play a role (e.g., groundwater circulation, presence of organic matter, or influence of sulphates). In general, marine diagenetic features would be expected to develop during the transgressive part of depositional sequences while meteoric diagenetic textures are expected to develop during the regressive part (Tucker 1993). However, for the Middle to Late Oxfordian platform deposits from the Swiss Jura, Plunkett (1997) did not find any correlation of dolomite crystals with the sequence-stratigraphic interpretations.

Silicification

In the deposits of the Pagny-sur-Meuse section, silicification is frequently observed. It takes the form of selective replacement of bioclasts. Like dolomitization, silicification can take place during early or late diagenesis.

Black facies

Black facies are frequently observed in the Swiss Jura deposits within intervals rich in siliciclastics. In shallow carbonate environments, blackening is essentially caused by finely disseminated pyrite or by organic matter. Blackening typically takes place in anoxic bottom waters or anoxic sediment in stagnant bays, lakes, ponds or channels (Strasser 1984; Berner 1989).

2.4 Deep platform and basin facies

The following description is based on three sections of different facies. The Latrecey section (Haute-Marne) presents homogeneous facies with a very low fauna content. The Balingen-Tieringen section (Swabian Jura) is characterized by marl-limestone alternations that pass laterally into sponge bioherms. The Vergons section (SE France basin) is dominated by marl-limestone alternations, with calcarenites and breccias occurring locally.

Code	Texture Folk	Texture Dumham	Major components	Other components	Sedimentary features	Interpretation
DEEP PLATFORM						
Marl-limestone alternations (para- to autochtonous)						
dp1	Marls	m	Miliolids, ostracodes, *Spirillina*, echinoderms	sponges, *Tolypammina,* belemnites	pyrite, glauconite	hemi-pelagic sedimentation
dp2	Marls	m	sponges, tuberoids, echinoderms, foraminifera (*Lenticulina*, *Spirillina*), belemnites	ammonites	glauconite	hemi-pelagic sedimentation
dp3	Micrite	M	undifferentiated bioclasts		birdseyes	distal platform sedimentation
dp4	Biomicrite	M	echinoderms, *Spirillina*, calcispheres, encrusting foraminifera, *Lenticulina*	quartz	intense bioturbation	hemi-pelagic sedimentation
dp5	Biomicrite	W	undifferentiated bioclasts	ostracodes, tuberoids, lithoclasts, encrusting foraminifera, Protoglobigerinids	bioturbation	hemi-pelagic sedimentation
Siliceous sponge reefs						
dp6	Biomicrite	B - M	siliceous sponges/microbialites	brachiopods, bivalves, tuberoids, peloids		siliceous sponge-microbialites bioherms
dp7	Biomicrite	W	reworked siliceous sponges	tuberoids	nodular aspect	reworked sponges - close to sponge reefs
dp8	Biomicrite	B (P)	siliceous sponges/microbialites	serpulids, echinoderms, peloids, glauconite	nodular aspect	in marly intervals - sponge reefs
dp9	Biomicrite	W - P	tuberoids, echinoderms, encrusting foraminifera	peloids, bivalves, brachiopods, serpulids, gastropods, *Lenticulina*, sponges fragments, glauconite		around sponge reefs
dp10	Pel-biomicrite	P	peloids, tuberoids	encrusting foraminifera, echinoderms, brachiopods, undifferentiated bioclasts		around sponge reefs

Tab. 2.2 - Main microfacies occurring in the Haute-Marne and Swabian Jura sections representing deep platform environments.

Code	Texture Folk	Texture Dumham	Major components	Other components	Sedimentary features	Interpretation
BASIN						
Marl-limestone alternations (para- to autochtonous)						
b1	Marls	m	-	foraminifera, bivalve fragments		hemi-pelagic sedimentation
b2	Marls	m	-	ooids	pyrite	hemi-pelagic sedimentation
b3	Biomicrite	M	*Globocahaete*, echinoderms, *Spirillina*, *Lenticulina*, ostracodes, encrusting foraminifera, calcispheres	pyrite, quartz	bioturbation	hemi-pelagic sedimentation
b4	Biomicrite	W	ostracodes, bivalves, echinoderms, *Lenticulina*	radiolarians, Protoglobigerinids, encrusting foraminifera		hemi-pelagic sedimentation
b5	Biomicrite	W	radiolarians, Protoglobigerinids	ammonites, G*lobochaete*, ostracodes, echinoderms, *Lenticulina*, calcispheres, *Spirillina,* encrusting foraminifera	bioturbation	hemi-pelagic sedimentation
Resediments sediments (allochtonous to para-autochtonous)						
b6	Intramicrite	P - Rud	lithoclasts, calcareous sponges fragments, radiolarians, Protoglobigerinids	echinoderms, bivalves, encrusting foraminifera, type 3 ooids,		breccia - probably debris flows
b7	Intramicrite	P - G	lithoclasts	type 3 ooids, *Lenticulina*, echinoderms, undifferentiated bioclasts, tuberoids?	slump, grading	calcarenites - probably turbidites reworked by contour currents or tempestites?

Tab. 2.3 - Main microfacies occurring in the SE France section representing basin environment.

2.4.1 Non-skeletal elements

In Balingen-Tieringen, lithoclasts and peloids are commonly observed (Tab. 2.2). Lithoclasts are sub-rounded particles, mainly composed of sponge fragments, foraminifera, and peloids embedded in a micritic matrix. In the resediments of the Vergons section, lithoclasts and ooids occur locally.

2.4.2 Skeletal elements

Sponges and tuberoids

Sponges and tuberoids commonly occur in the Balingen-Tieringen section (Tab. 2.2; Pl. 7/5 and Pl. 13/3). Siliceous sponges are typical dwellers of deep platform and basinal environments, forming sponge reefs. These sponge boundstones pass laterally to marl-limestone alternations more or less rich in tuberoids. This term was suggested for irregularly shaped, dark calcareous lumps of varied size (0.1 mm to several millimetres), which show various internal microstructures (dense or peloidal micrite, locally still visible sponge microstructure) corresponding to transported sponge fragments that are in decomposition (Fritz 1958; Flügel & Steiger 1981; Pl. 7/7-9 and Pl. 13/3-4). Some tuberoids are encrusted by nubeculariids and other microencrusting foraminifera (Pl. 7/10), and/or perforated by lithophages. This indicates that these particles stayed a certain time on the sediment surface in a semi-lithified state before being buried in carbonate mud.

The distribution of siliceous sponges in deep-marine environments is mainly controlled by trophic level, substrate, and sedimentation rate (Olivier et al. 2004b). The abundance of tuberoids and lithoclasts in some beds implies the proximity of sponge reefs (Flügel & Steiger 1981) and strong bottom currents (Brachert 1992; Pawellek & Aigner 2003).

Radiolarians

In the studied limestones, radiolarians are locally abundant, particularly in the carbonate-dominated part of the Vergons section (Pl. 7/4, 6; Tab. 2.3). The preservation of radiolarian tests is relatively poor; they are generally calcitized.

Planktonic foraminifera

Protoglobigerinids are observed in the Balingen-Tieringen and Vergons sections, where they are commonly associated with ammonites and radiolarians (Pl. 8/10-12). These planktonic foraminifera are known from the Liassic to the Early Cretaceous and their abundance is essentially linked to increased nutrient supply (Hemleben et al. 1988).

Cephalopods

Cephalopods are common in the Vergons section and occur locally in the Balingen-Tieringen deep-platform section. They are represented by ammonites, aptychi, and belemnites. Ammonites usually are seen at the surfaces of limestone beds or in marly intervals whereas belemnites have a more widespread distribution.

Filaments

Filaments, interpreted as juvenile shells of pelagic bivalves, locally occur in the Vergons section (Pl. 7/3).

Globochaete

Globochaete (Lombard 1945) are common constituents of the Vergons section. They are fibro-radial calcite spheres with a diameter of 10 to 100 µm and show a characteristic cross under polarized light. They occur in clusters, isolated, or serially arranged (Pl. 7/3). They are interpreted as calcified cysts of unicellular planktonic green algae. *Globochaete* are abundant in open-marine pelagic carbonates but also occur in shallow-marine environments (Tomasovych 2004).

Calcispheres

Calcispheres are commonly present in the Vergons section and locally in the Latrecey section. They consist of small globules with diameters of 20 to 100 µm. Their test is made of calcite, commonly displaying several layers with different texture (hyaline, microgranular, and/or fibro-radial). In pelagic sediments, calcispheres are generally interpreted as cysts of dinoflagellates (Keup 1991).

Benthic foraminifera

In the Balingen-Tieringen section, the most common benthic foraminifera are *Lenticulina* and Miliolids (Tab. 2.2). Encrusting foraminifera such as *Bullopora tuberculata*, *Tolypammina* sp., and Nubeculariids are common (Pl. 10). In the Latrecey and Vergons sections, *Spirillina* and *Lenticulina* occur (Tabs 2.2 and 2.3). Compared to shallow platform environments, benthic foraminifera are relatively rare. Most of the specimens have probably been exported from the platform and thus cannot be used for palaeoecological interpretations.

2.4.3 Others constituents

Millimetric green grains are observed at the base of the Balingen-Tieringen section (cf. Annex 2). EDX analyses have shown that they are glauconite, corroborating the deeper, open-marine setting (van Houten & Purucker (1984).

2.4.4 Carbonate mud

A source of micrite in basinal settings is nannofossils; degradation of foraminiferal tests is considered to be only a minor contribution (Flügel 2004). However, for the Late Oxfordian deep-shelf deposits, the relative scarcity of nannofossils and insignificant bioerosion in autochtonous sponge reefs that could have produced fine-grained carbonate suggest that carbonate mud exportation from the shallow platform was important (Pittet & Strasser

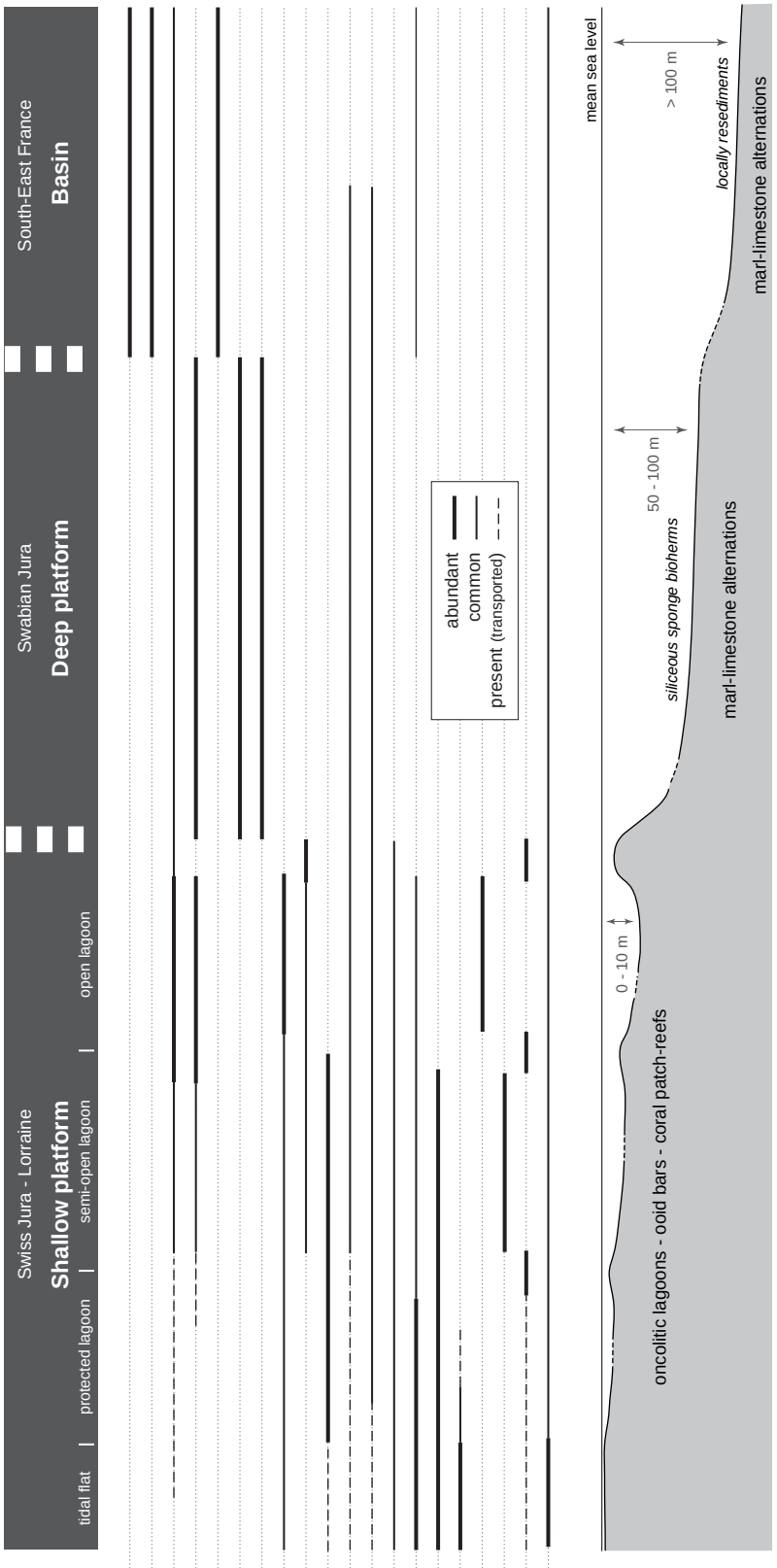

Fig. 2.2 - Distribution of main components in the studied sedimentary systems from shallow platform (Swiss Jura and Lorraine) to basin (SE France).

1998a, b; c.f. Chap. 5). PITTET et al. (2000) observed that the marly intervals are richer in nannofossils than the limestone beds. The higher the sediment accumulation rate, the lower is the nannofossil record. This suggests that the main factor responsible for the generally low nannofossil content is dilution by allochthonous carbonate mud.

2.4.5 Reworked sediments

Episodically, resediments interrupt the "normal" sedimentation in the Vergons section. Calcarenites occur at several levels (beds 48, 50, and 71; Fig. 4.23; Pl. 13/7-8) and have a packstone-grainstone texture with allochthonous particles (microfacies b7, Tab. 2.3). They are interpreted as turbidites reworked by contour currents (PELLATON & ULLRICH 1997). A level of breccia is also identified (bed 53; Pl. 2/3). The matrix of this bed has a packstone texture with autochthonous and allochthonous particles (microfacies b6, Tab. 2.3) and is interpreted as a debris flow (PELLATON & ULLRICH 1997).

2.4.6 Sedimentary structures

Bioturbation

Bioturbation is very common in deep-water marine environments. In the Vergons section, bioturbation is common within limestones and locally marked by nodular bed surfaces (Pl. 17/6). In the Latrecey section, trace fossils such as *Zoophycos* locally occur. *Chondrites* are locally present in the Balingen-Tieringen section.

2.5 MICROFACIES CLASSIFICATION

Based on 505 polished slabs and thin sections as well as on 60 washing residues of marls, a microfacies classification has been established for the three studied sedimentary domains (Tabs 2.1, 2.2 and 2.3; Annex 3). According to the microfacies and the associated sedimentary features, the depositional environments are interpreted.

For the platform, discriminating criteria are components, fauna association and diversity, Dunham classification, and terrigenous particles. Environmental conditions such as energy, salinity, oxygenation, and trophic level are also evaluated (Fig. 2.3). For example, the co-occurrence of stenohaline organisms such as corals, brachiopods, and echinoderms indicates normal salinity in open-marine environments, whereas charophytes, ostracodes, and gastropods imply restricted environments. High-diversity fauna indicates normal salinity and open-marine conditions whereas low-diversity fauna indicates protected environments with variable salinity. Siliciclastics are generally more abundant in proximal environments (protected lagoon to semi-open lagoon) but can be transported by currents onto the platform and deposited in depressions (PITTET 1996).

Contrary to platform facies, deeper marine facies are less diversified and classified according to their lithology and the abundance of para-autochthonous and/or allochthonous particles. Marl-limestone alternations are common in deep platform and basin environments. Sponge reefs occur only in the Swabian Jura, resediments only in SE France.

Environments	Protected	Semi-open	Open
Environmental conditions	**Semi-restricted**	**Normal-marine**	
Fauna association	euryhaline fauna (charophytes, ostracodes, gastropods)	stenohaline fauna (echinoderms, brachiopods, corals)	
Fauna diversity	low	moderate	high
Energy	low	low to high	
Salinity	low, variable	normal, constant	
Trophic level	eutrophic	mesotrophic	oligotrophic

Fig. 2.3 - Characterization of depositional environments and environmental conditions of lagoonal deposits investigated in the Swiss Jura Mountains. Water energy, salinity, oxygenation, and trophic level are used as discriminating factors.

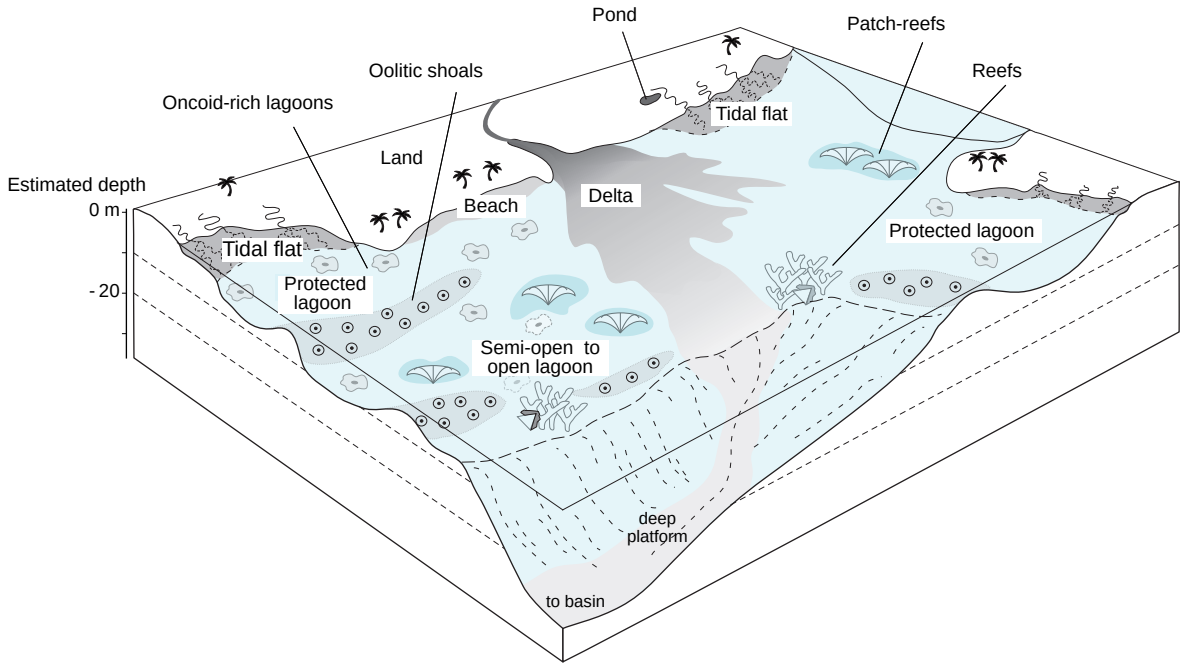

Fig. 2.4 - Block diagram showing the spatial relations (not to scale) between the studied environments. Modified from PITTET (1996).

The major organic and inorganic components of these domains are schematically positioned along a platform-basin transect (Fig. 2.2), and the major microfacies types are presented in Pl. 11 to Pl. 13.

2.6 DEPOSITIONAL ENVIRONMENTS

Based on facies and microfacies analyses, depositional environments can be interpreted. A three-dimensional block-diagram is used to better illustrate the lateral coexistence of the interpreted depositional environments, particularly on the shallow platform (Fig. 2.4).

2.6.1 Shallow platform

In the Late Oxfordian, the Swiss Jura region corresponded to a shallow carbonate platform (Fig. 1.3). The presence of tidal structures implies tidal (sand or mud) flat environments (Tab. 2.1). Tidal flats consist of areas regularly to rarely cover by water, dominated by weak current and wave action due to their position behind beach-barriers and around lagoons. Three types of shallow lagoon are considered in this study. The protected lagoon consists of marls and limestones with semi-restricted fauna (e.g., bivalves, gastropods, ostracodes, inocerams, serpulids, Miliolids), a relatively low-diversity fauna, and intense bioturbation (Tab. 2.1). Due to its proximity to the hinterland, the terrigenous input is important in protected lagoons. The semi-open and open lagoons are mainly characterized by carbonate-dominated facies, from mudstone to grainstone, with a higher diversity fauna, normal salinity conditions and a relatively low turbidity (Tab. 2.1). Coral patch-reefs and/or coral carpets commonly occur in open lagoons (Tab. 2.1). Coral reefs and ooid bars exist on the platform edge or within the platform, probably depending on the tectonically induced morphology (Fig. 2.4). Siliciclastics are common but heterogeneously distributed. They concentrate in depressions, formed by differential subsidence, or in-between ooid shoals and coral reefs.

2.6.2 Deep platform and basin

Deep platform and basin environments are mainly dominated by hemipelagic to pelagic sedimentation. In the deep platform facies of the Swabian Jura, marl-limestone alternations pass laterally into sponge reefs (Tabs 2.2 and 2.3). The limestone facies are commonly sponge boundstones and wackestones-packstones with bioclasts and tuberoids. Marls contain sponges, tuberoids, echinoderms, benthic foraminifera (*Lenticulina*, *Spirillina*, Miliolids),

ostracodes, *Tolypammina*, ammonites, and belemnites. The abundance of tuberoids and lithoclasts in some beds implies variations in water-energy conditions (bottom currents) probably related to relative sea-level changes (BRACHERT 1992; PAWELLEK & AIGNER 2003). In basin environments, sedimentation is much more monotonous than on shallow-water platform environments (Tabs 2.2 and 2.3). Marl-limestone alternations are episodically interrupted by reworked sediments mainly generated by slope instabilities.

* * *

3 - SEQUENCE ANALYSIS

3.1 INTRODUCTION

Sequence stratigraphy is a conceptual model that explains stratigraphic patterns and the evolution of sedimentary basins mainly as the effects of large-scale eustatic sea-level changes and tectonics (e.g., VAIL et al. 1977; POSAMENTIER et al. 1988, 1992; POSAMENTIER & JAMES 1993; HUNT & TUCKER 1992, 1995; KOLLA et al. 1995; MIALL 1986, 1991, 1997; NYSTUEN 1998). Sequence stratigraphy is a relatively new methodology, introduced by the research group of EXXON (VAIL et al. 1977) for documenting and interpreting the sedimentary record.

Originally, the sequence-stratigraphic model was developed on the basis of seismic studies on passive continental margins and mostly in siliciclastic systems, which had a low vertical resolution, and which only allowed to identify major lithological changes and stratigraphic geometries. Even with the technical advance in seismics, coring, and downhole logging, outcrop-based studies offer a higher level of detail and the advantage of working with real rocks and surfaces. Yet, a disadvantage is the common lack of information on geometries of large-scale sediment bodies in outcrop. The methods based on identification of remarkable surfaces interpreted as time lines (e.g., subaerial unconformities, transgressive and maximum-flooding surfaces calibrated by other stratigraphical methods) and therefore places sequence stratigraphy in a chronostratigraphic framework.

Over the years, the initial concepts of sequence stratigraphy were refined by integrating the results of numerous case studies. This led to a continuous questioning and redefining of the principles and terminology and ever finer stratigraphic subdivisions for different sedimentary environments. Different schools of thought and different models developed, depending on how sequences are identified and subdivided and on the interpretation of which kinds of processes have controlled the genesis of depositional sequences. In addition, the evolution of concepts and theories has been studied by MIALL & MIALL (2001) from a sociological point of view. The main models are the original EXXON model of VAIL et al. (1977), the genetic sequences of GALLOWAY (1989), the T-R sequences of EMBRY (1993, 1995), the base-level cycles of CROSS (1991) and CROSS & LESSENGER (1998), and the regime theory of THORNE & SWIFT (1991a, b) that led to the accommodation-supply model of SCHLAGER (1993) (for a detailed review see NYSTUEN 1998).

Eventually, it has been realized that eustatic variations are not necessarily the dominant factor controlling the formation of depositional sequences in tectonically unstable settings or in carbonate systems (e.g., CLOETINGH 1988; HUBBARD 1988; SCHLAGER 1989, 1991, 1993). Also the validity of global correlations of apparently eustatic events as presented in global cycle charts (HAQ et al. 1988) was questioned (MIALL 1991, 1992).

3.2 DEPOSITIONAL SEQUENCES

3.2.1 Definition

A depositional sequence is a succession of genetically related sediments whose facies evolution and/or stacking pattern is repetitive within a section. Depositional sequences are commonly delimited by discontinuity surfaces or intervals of well-marked (facies) change, indicating an inversion in the trend of environmental change. They are the stratigraphic expression of recurring environmental changes, independent of scale and time. This is the original

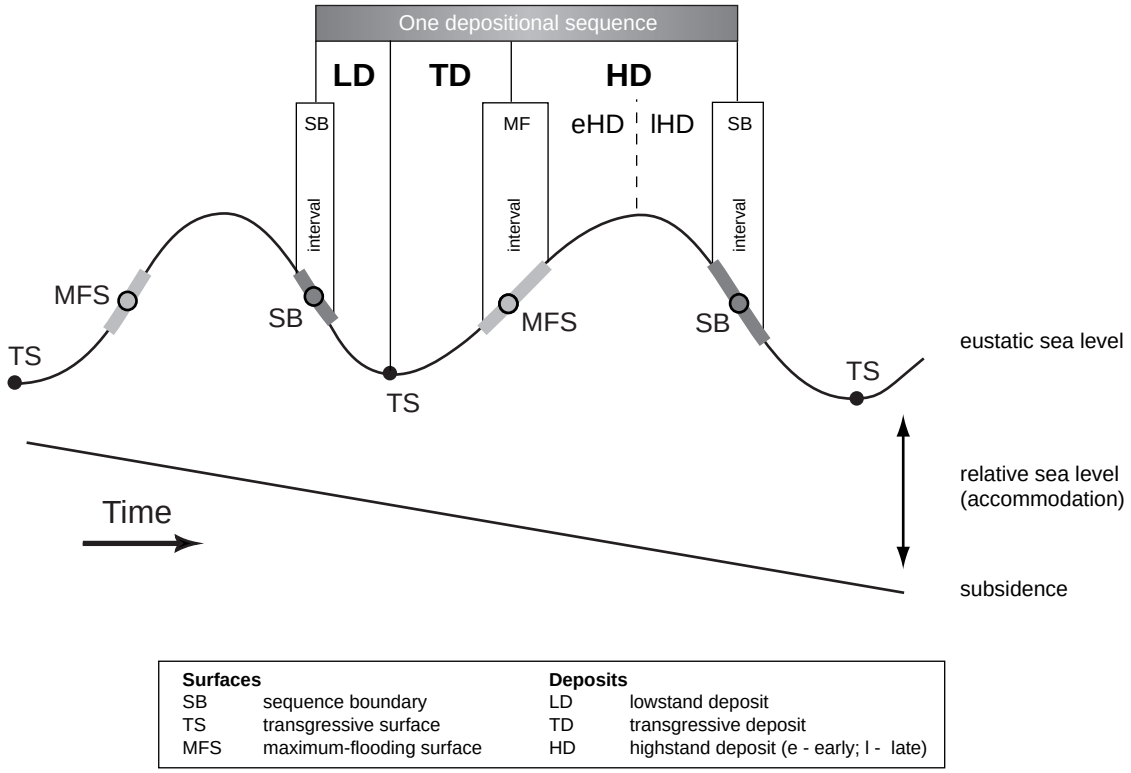

Fig. 3.1 - Theoretical model of depositional sequences controlled by relative sea-level fluctuations (accommodation). Sequences are subdivided into deposits, which correspond to the system tracts of VAIL et al. (1977). For discussion refer to text.

definition of VAIL et al. (1977) and will be used in our case study. For simplicity, the terms "cycle" and "cyclic" will be used for such changes, although recurrences in natural systems are at the most quasi-periodic (SCHWARZACHER 2000). In this study, the term "sequence" is used synonymously with "depositional sequence".

3.2.2 Formation of depositional sequences

The term "eustasy" describes a global sea level with reference to a fixed datum (e.g., centre of the Earth; POSAMENTIER et al. 1988). Because it is generally not clear whether investigated sedimentary records have primarily been controlled by eustatic sea-level changes, by tectonic movements and/or by sedimentary processes, the term "relative sea level" has been introduced. Relative sea level includes eustasy (i.e., net sea-level change) and local subsidence and/or uplift by referring to the position of a datum (e.g., basement) or the sea floor (POSAMENTIER et al. 1988). A depositional sequence results from one cycle of relative sea level.

The combination of changing eustatic sea level and vertical crustal movements (subsidence) creates accommodation space, which can be filled with sediment over time (Fig. 3.1). On shallow carbonate platforms, accommodation variations through time are generally represented by thickness variations of depositional sequences (or beds) and facies evolution. However, the stacking pattern depends not only on variations of accommodation space but also on variations of sediment accumulation (POSAMENTIER et al. 1992; SCHLAGER 1993). Accommodation loss or gain does not always result from a decrease or increase of relative sea level but can also come from more or less sediment supply or *in situ* production. KENDALL & SCHLAGER (1981) stated that "stratigraphic sequences of shallow-water deposits and their facies patterns are primarily controlled by the rates and types of sedimentation, local crustal movements, and eustatic sea level".

3.2.3 Criteria for sequence identification and interpretation

Criteria to identify and interpret depositional sequences are multiple. Sedimentological analysis provides various parameters such as deepening-up and shallowing-up trends in general facies evolution,

variations of fauna and flora composition, interpretation of beds and discontinuities, and vertical variations in bed thickness and stacking patterns. Specific analyses of diagenetic features or geochemical signatures (e.g., stable isotopes), the study of clay-mineral abundance and composition, and palynofacies can give supporting evidence (e.g., Blondel et al. 1993; Joachimski 1994; Budd et al. 1995; Pasquier 1995; Pittet & Gorin 1997; Plunkett 1997; Hillgärtner 1999; Rameil et al. 2000; Colombié 2002; d'Argenio et al. 2004).

Facies evolution

Facies evolution is the sedimentary expression of environmental changes, which can be the result of intrinsic cycles within the depositional system (autocycles), or which follow cyclic or quasi-linear external forcing mechanisms (allocycles; Strasser 1991). Lateral and vertical facies evolution is the main tool for sequence-stratigraphic analysis. In this study, the examination of lateral facies variations is limited by the outcrop extension. Vertical facies variations marked as deepening-up and shallowing-up trends are commonly linked to bathymetric changes on the shallow platform. However, migrating sediment bodies can produce a shallowing-up sequence also at constant relative sea level (e.g., Pratt & James 1986).

Discontinuity surfaces, bedding and stacking pattern

Discontinuity surfaces on shallow-marine carbonate platforms are characterized by a wide variety of diagnostic features (Hillgärtner 1999). All surfaces reflect reactions of the sedimentary system to rapid and drastic environmental changes. Changes in energy regime, relative sea level, accumulation rate, and sediment type are expressed, in the sedimentary record, by subaqueous erosion, subaerial exposure (including erosion), or subaqueous omission. Discontinuity surfaces may correspond to sequence boundaries, transgressive surfaces, maximum-flooding surfaces, or else they may result from an autocyclic process. Single beds are always delimited by discontinuity surfaces of various types (Hillgärtner 1999). One bed may represent an entire depositional sequence, but in many cases a depositional sequence includes several beds. If facies contrast is low, several sequences may be amalgamated in one bed. Stacking pattern and thickness variations of all depositional sequences reflect environmental changes through time that caused variations in accommodation and/or accumulation rate (Strasser et al. 1999). For example, on carbonate platforms, a thickening-up trend of beds commonly points to increasing accommodation space while a thinning-up trend may reflect a loss of accommodation. However, thinning-up can also be created by rapid deepening that reduces the carbonate production.

Bioturbation

The degree of bioturbation is closely related to specific environmental conditions. Hence, it can be an excellent tool to interpret depositional sequences (Pemberton et al. 1992). The intensity of bioturbation is a function of sediment accumulation rate, oxygenation, and nutrient availability (e.g., Wetzel 1991; Wignall 1993). In platform environments, terrigeneous input can significantly increase nutrient levels, which may result in major overturns of benthic communities and consequently in a drop of carbonate production and accumulation rate (e.g., Hallock & Schlager 1986; Dupraz & Strasser 1999). The intensity of bioturbation seems to be independent of substrate type (e.g., muddy vs. grainy) but is particularly high below firm- and hardgrounds (Hillgärtner 1999). This implies that sediment accumulation rate is the most important controlling factor on bioturbation intensity in these environments.

Clay content

Variation of clay content in platform carbonates is commonly expressed by differential weathering of the outcrop strata. This accentuates the stacking pattern of beds and depositional sequences. However, even marly intervals may, once excavated, reveal additional limestone beds (cf. Chap. 4). Most clay minerals in marly sediments are of detritic origin and result from erosion of crystalline bedrock and/or palaeosols. Clays are generally transported by rivers to the coastal plain and to marine depositional settings. Marl deposits (clay minerals and carbonate mud) commonly accumulate in low-energy conditions in supratidal to subtidal environments and thus can be reworked by currents and waves (cf. Chap. 7). In marginal-marine settings, they are deposited in shallow protected lagoons and in deeper, open-marine environments below the action of waves.

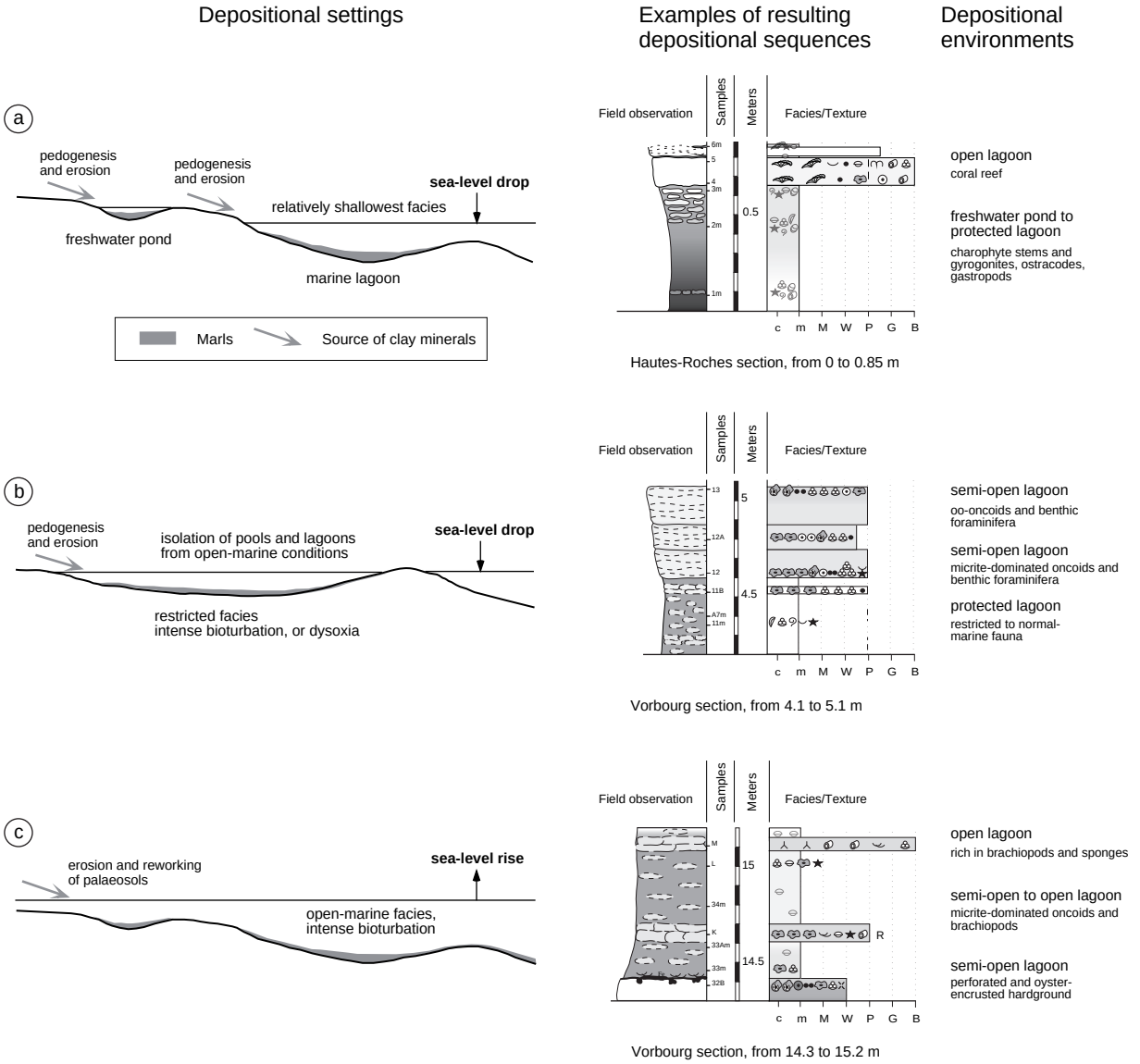

Fig. 3.2 - Different models for clay occurrence in marginal-marine environments caused by relative sea-level changes and climate (modified from STRASSER & HILLGÄRTNER 1998). Examples of depositional sequences are taken from the studied sections. For legend of symbols, refer to Fig. 4.1.

The relative abundance of clay minerals in carbonates is the result of two phenomena (EINSELE & RICKEN 1991): (1) variations of terrigeneous input with a constant rate of carbonate production (dilution cycle) or (2) variations in carbonate production with constant terrigeneous influx (productivity cycle). Both phenomena are closely connected on shallow carbonate platforms (HILLGÄRTNER 1999) as well as in hemipelagic settings (EINSELE & RICKEN 1991). The occurrence and distribution of clay minerals on shallow carbonate platforms can be related to three main types of environmental changes caused by relative sea-level fluctuations and climate changes (STRASSER & HILLGÄRTNER 1998; Fig. 3.2):

(a) A relative sea-level fall enlarges the emersion area in coastal settings. Consequently, an increase of continental erosion, pedogenesis and subsequent clay input to shallow-marine environments can be postulated. Accordingly, the clays are associated with the shallowest facies. The occurrence of charophytes (cf. Chap. 2) points to the formation of freshwater ponds on the partly emergent platform.

(b) A relative sea-level fall and low sea level can lead to isolation of pools and shallow lagoons decreasing and/or cutting off open-marine influence. Such environmental isolation reduces water energy, enabling the settling out of clay minerals. In this

case, marly intervals are characterized by relatively restricted fauna, increased bioturbation (lowered accumulation rates) or dysoxic facies due to reduced water circulation.

(c) A relative sea-level rise and high sea level can also provoke low-energy conditions by rising wave base. Marls deposited under such conditions are characterized by open-marine constituents, indicating a relatively deep facies. Bioturbation intensity may be high, due to lower carbonate production. A sea-level rise can also lead to an additional input of clay minerals by the erosion and reworking of previously exposed palaeosols during transgression.

Furthermore, an elevation of rainfall in the hinterland increases the surface run-off and may increase the clay input into the marine depositional system. Clay minerals in marginal-marine environments, therefore, can be interpreted as a climate signal depending mainly on palaeolatitude and on atmospheric circulation patterns (e.g., PERLMUTTER & MATTHEWS 1989, 1992; KINDLER et al. 1997; PITTET & STRASSER 1998a). In certain palaeogeographic positions and palaeoclimatic regimes, climate may be more humid at high sea-level stands, in other contexts more rain occurs at low sea levels (PITTET 1996). The kaolinite/illite ratio can furnish information on the climatic conditions (cf. Chap. 8).

Other criteria

Stable isotope analyses ($\delta^{13}C$, $\delta^{18}O$) are commonly used to interpret depositional and diagenetic histories of shallow carbonate limestones (e.g., ALLAN & MATTHEWS 1982; JOACHIMSKI 1991, 1994; cf. Chap. 8). For example, subaerial exposure may be identified by isotopic signatures even if sedimentary evidence is lacking (PLUNKETT 1997). However, particularly in shallow-marine carbonates, diagenetic overprinting of the original isotopic signals must be considered when using stable isotopes for the interpretation of depositional sequences. Palynofacies analyses investigate particulate and amorphous organic matter in order to determine the ratio of terrestrial and marine influences. Such ratios then have been used to interpret depositional sequences in different environments (e.g., PITTET & GORIN 1997). Geochemical analyses of trace elements have been used to investigate environmental conditions and to relate trace element evolution to depositional sequences (COLOMBIÉ 2002; VINCENT et al. 2006).

3.3 SEQUENCE MODEL AND TERMINOLOGY APPLIED

The Fribourg approach is a combination of sequence- and cyclostratigraphic aspects developed for studying depositional sequences on shallow-water carbonate platforms, but its principles are generally applicable (cf. Chap. 6). Methodology and reasoning for interpretation are summarized in STRASSER et al. (1999) and STRASSER et al. (2000). Over more than a decade, the approach for interpreting successions of carbonate rock in outcrops have been improved and refined by high-resolution outcrop studies in Mesozoic carbonate platform environments in the French and Swiss Jura Mountains (STRASSER 1994; PASQUIER 1995; PITTET 1996; PASQUIER & STRASSER 1997; PITTET & STRASSER 1998a, b; STRASSER & HILLGÄRTNER 1998; HILLGÄRTNER 1999; COLOMBIÉ 2002; COLOMBIÉ & STRASSER 2003, 2005; HUG 2003). The nomenclature and terminology are partly based on the sequence-stratigraphic model of VAIL et al. (1991). However, the stacked depositional sequences of different sizes are not attributed to different orders that have a predefined connotation of time (STRASSER et al. 1999). Consequently, the applied nomenclature has the advantage of being purely descriptive at the beginning. The time attribution is only given after a thorough sequence- and cyclostratigraphic analysis. The Fribourg approach avoids the term "systems tract" because large-scale geometries are mostly not visible in outcrop. Accordingly, this study speaks of lowstand, transgressive, and highstand "deposits" instead of "system tracts" (Fig. 3.1).

3.3.1 Discontinuity surfaces and deposits

Discontinuity surfaces and deposits of a sequence are independent of the temporal scale of relative sea-level change. A sequence boundary (**SB**) forms during the fastest relative sea-level fall (Fig. 3.1). It causes decrease of accommodation space creating the highest possibility for subaerial exposure (i.e., birdseyes, desiccation cracks, karst dissolution). It can be a surface or interval marked by exposure structures, restricted facies, subaerial erosion or pedogenesis. In platform settings, lowstand deposits are very thin, missing, or reworked in the transgressive sediments. They are commonly represented by low-energy facies with low-sedimentation rate. It is very difficult to distinguish, in terms of facies, deposits that correspond to a lowstand of relative sea level ("lowstand deposits", **LD**) from deposits that

formed during the initial phase of the subsequent transgression ("early transgressive deposits", **eTD**). In the traditional sequence stratigraphic model, the sediments of the lowstand systems tract are located below the platform edge on the slope (VAIL et al. 1991). Thus, in order to avoid confusion, all deposits that are located between well-developed SB and TS, corresponding to a low sea level and/or the beginning of the subsequent transgression, are labelled early transgressive deposits (eTD). These deposits have the lowest preservation potential and tend to be eroded and reworked during the subsequent transgression (WALKER 1995). Consequently, transgressive surfaces in many cases directly overlie the sequence-bounding exposure surfaces (SB/TS).

The transgressive surface (**TS)** corresponds to the first flooding, permitting the restoration of sedimentation (Fig. 3.1). It is marked by rapid facies changes from the relatively shallowest facies to deeper sedimentary environments. Just after the initial flooding, carbonate production is still in "start up" mode (KENDALL & SCHLAGER 1981) and thus the TS is commonly characterized by reworked clasts ("lag deposit") and an abrupt increase in mean grain diameter. Because of rapid cementation of carbonates during subaerial exposure, erosion during transgression is less important than in siliciclastic systems ("transgressive surface of erosion (TSE)", NUMMEDAL & SWIFT 1987; "ravinement surface", SWIFT 1968). The "start up" phase is equivalent to the "lag time" of STRASSER (1991). Deposits that indicate relative deepening and/or opening of the system are called "transgressive deposits" (**TD**) (Fig. 3.1). They correspond to the phase when accommodation increases during relative sea-level rise, after an initial flooding. At the beginning of a sea-level rise, accommodation is created on the shallow platform, but carbonate production is still low ("start-up" phase). Carbonate export from the platform is still limited, and the deep shelf records only little carbonate (PITTET & STRASSER 1998a).

With increasing water depth and the recovery of the carbonate factory, conditions become ideal for maximum carbonate production and thus the previously created accommodation space begins to fill up ("catch up" phase, KENDALL & SCHLAGER 1981). A maximum-flooding surface or interval indicates the fastest relative sea-level rise and matches with the most important bathymetry (Fig. 3.1). Intensively bioturbated and/or marly intervals or distinct omission surfaces testify to reduced sedimentation rate. If a distinct single surface is developed, this is denoted as "maximum flooding surface" (**MFS**) generally displaying hardgrounds, intensely bioturbated surfaces, or ferruginous crusts. In the case of repeated maximum-flooding surfaces or an interval that lacks distinct surfaces but clearly shows the most open-marine conditions, the term "maximum flooding" (**MF**) is used. If the sea floor drops below the photic zone during maximum flooding, carbonate production and accumulation will be reduced ("give-up" phase). However, in shallow-water, maximum flooding may also be indicated by the thickest beds because accommodation gain is highest. In basinal setting, the maximum flooding corresponds to a condensed section (**CS**) characterized by low accumulation rates (LOUTIT et al. 1988; BASSANT 1999).

After the maximum flooding, facies indicate a shallowing trend that correspond to a slow-down in relative sea-level rise and an initial fall: these are the "highstand deposits" (**HD**) (Fig. 3.1). In some cases, facies permit to distinguish early highstand deposits (**eHD**) that still correspond to relatively open or deep environments, and late highstand deposit (**lHD**) that show shallowing up. During the highstand, the carbonate platform is usually in "keep-up" mode (KENDALL & SCHLAGER 1981). If the carbonate production matches the creation of accommodation space, the platform will grow predominantly vertically (aggradation). However, when carbonate production is higher than the creation of accommodation space (especially in the late highstand phase), sediment fills up to sea level and the platform progrades towards the basin. Therefore, during highstand conditions, the carbonate export from the platform to the basin increases.

3.4 TYPES OF DEPOSITIONAL SEQUENCES IN THE STUDIED SECTIONS

On the shallow platform, three types of depositional sequence are distinguished. They are defined by their characteristic facies evolution and the enhancement or attenuation of characteristic surfaces, which indicate bathymetric changes (Fig. 3.3). Rather than shallowing or deepening trends, facies evolution may also indicate changes from more open-marine to more restricted conditions and vice versa. In deeper marine environments, one type of depositional sequence exists: the marl-limestone alternation (or couplet) (Fig. 3.4). These types of sequences are observed at the scale of elementary and small-scale sequences (cf. Chap. 3.5).

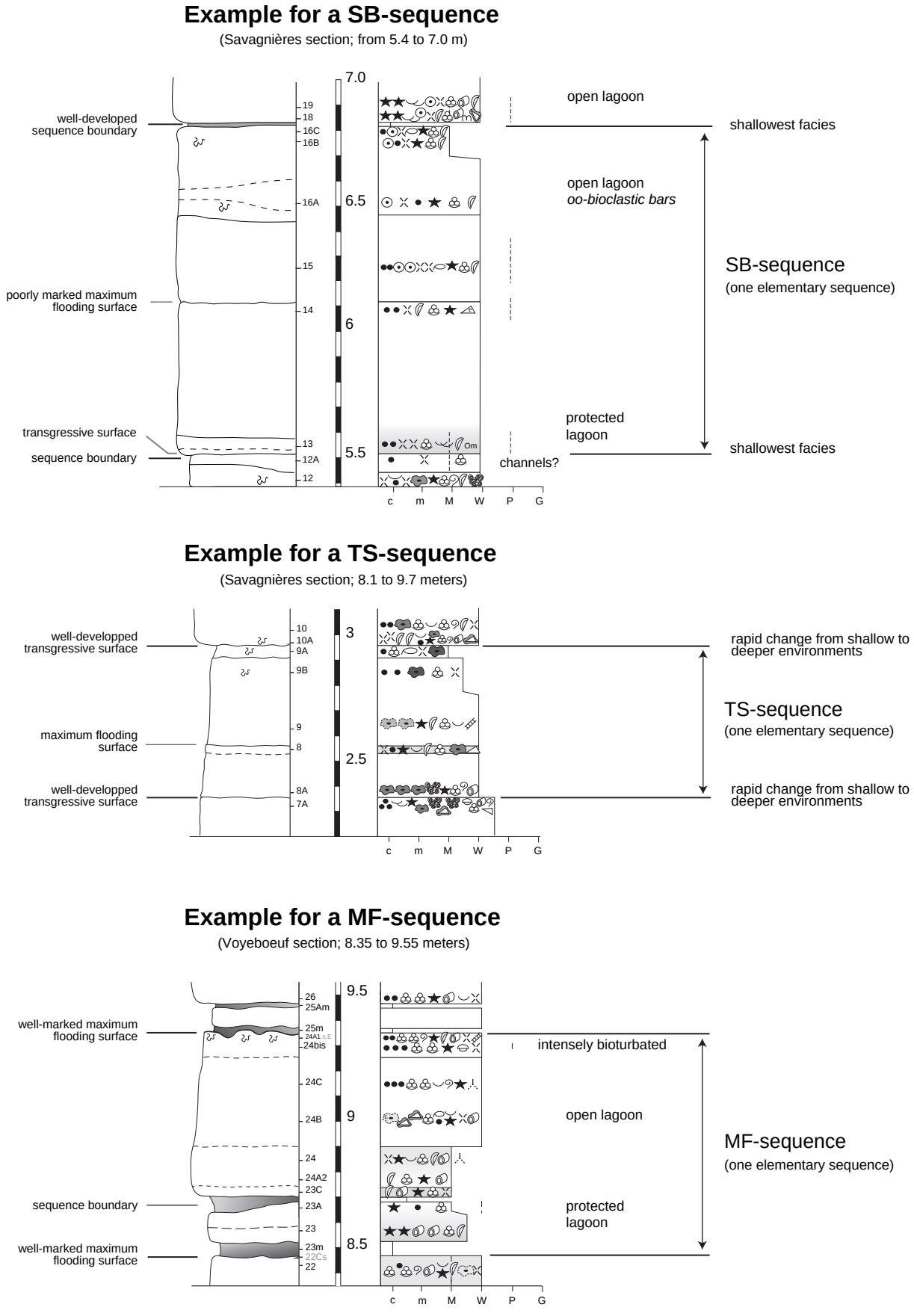

Fig. 3.3 - Examples of SB-, TS-, MF-sequences from the studied sections (see text for discussion). For symbols, refer to Fig.4.1.

Deepening-shallowing sequences defined by sequence boundaries (SB-sequences)

In SB-sequences, facies evolution through time indicates that water depth first increased, then decreased. In shallow-water carbonate-dominated environments, their evolution is commonly asymmetric, i.e., many depositional sequences are composed of a thin deepening-up and a thick shallowing-up part (e.g., Strasser 1988; Jones & Desrochers 1992; Pratt et al. 1992). The shallowing-up trend is due to the high production and accumulation rates of carbonate platform systems, which — as long as environmental conditions are favourable — easily outpace relative sea-level rise ("catch-up phase", Kendall & Schlager 1981). The shallowing-up trend may additionally be enhanced by the deceleration of sea-level rise and a subsequent fall. Prolonged emersion can lead to vadose cementation. If the climate is humid enough, a prolonged emersion may also produce chemical dissolution of carbonate grains (leaching), (incipient) pedogenesis, and karstification.

This type of depositional sequence corresponds to the definition of classical sequence stratigraphy where the sequence boundaries form during relative sea-level fall. However, the boundaries of such sequences may also be generated in subtidal or intertidal environments that reflect the relatively shallowest conditions within the sequence. Deepening–shallowing sequences that never reach intertidal or supratidal facies have been termed "subtidal cycles" by Osleger (1991). Shallowing-up sequences can also be created by progradation or migration of sedimentary systems (e.g., Ginsburg 1971; Pratt & James 1986) without being related to sea-level fall. However, if supratidal facies and/or vadose diagenesis are directly superimposed on subtidal sediments, or if regressive surfaces of erosion can be correlated over large distances, relative sea-level fall must have been involved (Strasser 1991).

Deepening-shallowing sequences defined by flooding surfaces (TS-sequences)

These sequences display a facies evolution comparable to the sequences described above. The main difference is that the bounding discontinuities mark a rapid facies change from the relatively shallowest (or most restricted) to deeper (or more marine) sedimentary environments, which is attributed to transgressive surfaces. As these surfaces are the most visible in the field and as evidence of subaerial exposure may lack or may not be well expressed, they define the depositional sequence (Fig. 3.3). Facies changes related to sea-level fall or maximum flooding may be identifiable but are commonly too subtle to be developed as well-expressed diagnostic surfaces or intervals. Such sequences are usually strongly asymmetric and can be compared to the "parasequences" of Van Wagoner et al. (1990), which are defined as being bounded by marine flooding surfaces.

Shallowing-deepening sequences defined by maximum flooding and/or condensation (MF-sequences)

In such sequences, facies evolution shows an inverse trend (shallowing to deepening). Depositional sequences are bounded by maximum-flooding surfaces, which are the best marked diagnostic surfaces seen in the field (Fig. 3.3). Some maximum-flooding surfaces are intensely bioturbated, suggesting low sedimentation rates; others are developed as firm- or hardgrounds, partly with fossil or mineral encrustations, suggesting strongly reduced sedimentation rates. This type of sequences can be compared to the "genetic sequences" defined by Galloway (1989).

These three types of platform sequences have to be regarded as models or end members in a continuous spectrum of sequence architectures. In reality, any given sequence can combine features of the above-mentioned type-sequences to a different extent. For example, in transitional zones where the long-term trend of relative sea-level changes from rise to fall, all types of discontinuities can be well expressed. It may occur that a MF-sequence overlaps with a subsequent SB-sequence. SB-sequences generally form when the general, long-term sea-level trend is falling. TS- and MF-sequences tend to form when long-term sea level is rising.

Basinal sequences

This type of depositional sequence consists of one marl-limestone alternation (Fig. 3.4). In some, but specifically in larger-scale depositional sequences, lowstand deposits consist of relatively thick packages of resedimented carbonates (Strohmenger & Strasser 1993). Major maximum floodings can be expressed

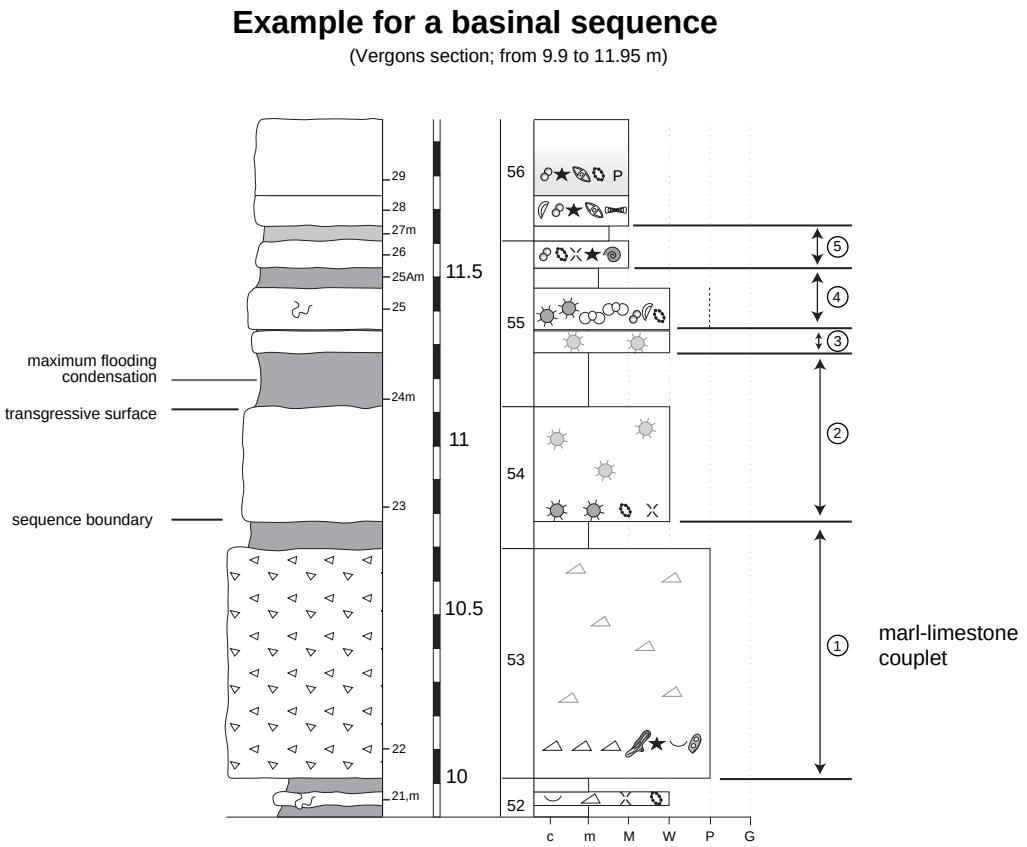

Fig. 3.4 - Examples of basinal sequence (see text for discussion). For symbols, refer to Fig.4.1.

through sediment starvation, i.e. condensed sections and/or discontinuity surfaces that display evidence for condensation (e.g., iron/manganese crusts, glauconite, fossil concentrations, and bioturbation). In terms of sea-level variations, quantitative analysis of ammonite faunas in marl and limestone facies may define bathymetric increase and decrease (REBOULET & ATROPS 1997). In the present study, however, such analyses have not been performed.

The formation of marl-limestone alternations is subject of debate (e.g., EINSELE & RICKEN 1991; BÖHM 2003; WESTPHAL et al. 2004b). Their origin may be explained in part by periodic changes in: **(1) pelagic carbonate productivity** (EINSELE & RICKEN 1991; CLAPS et al. 1995; MATTIOLI 1997); **(2) import of carbonate mud from shallow platforms** (e.g., DAVAUD & LOMBARD 1973; GAILLARD 1983; BOARDMAN & NEUMANN 1984; BRACHERT 1992; MILLIMAN et al. 1993; PASQUIER & STRASSER 1997; PITTET & STRASSER 1998a; BETZLER et al. 1999; PITTET et al. 2000; COLOMBIÉ & STRASSER 2003); **(3) clay input from the hinterland**, and/or **(4) post-depositional processes** like differential diagenesis affecting carbonates during burial (e.g., EDER 1982; HALLAM 1986; MUNNECKE & STAMTLEBEN 1996; MUNNECKE et al. 1997; BÖHM 2003; WESTPHAL et al. 2004a, b). However, it has been demonstrated in many cases that marl-limestone alternations were deposited with Milankovitch periodicities (e.g., COTILLON 1991): orbitally forced insolation variations caused climatic and sea-level changes that acted on carbonate production and deposition, and/or on clay input. Differential diagenesis may subsequently have accentuated the contrast between limestones and marls.

3.5 HIERARCHY AND STACKING OF DEPOSITIONAL SEQUENCES

In all the studied sections, the depositional sequences are commonly stacked in a hierarchical pattern. In this high-resolution study, three hierarchies of sequences are recognized and described: elementary, small-scale, and medium-scale sequences. A part of this study is dedicated to the identification and correlation of the smallest depositional sequences (elementary sequences) and to their interpretation.

Elementary sequences

These sequences are the smallest units recognizable in the sedimentary record and are defined as having formed through one cycle of environmental change (Strasser et al. 1999). In the studied sections, they commonly consist of two to three beds, bounded by discontinuity surfaces. The thickness of elementary sequences usually ranges from a few centimeters to a few tens of centimeters. Deepening-shallowing trends or shallowing-up trends of facies evolution can be identified in many cases (SB- or TS-sequences). When accommodation is low, elementary sequences may not be deposited or eroded ("missed beats" of Goldhammer et al. 1990). Consequently, the best chance of recording elementary sequences on the platform is during long-term transgression when accommodation space is created while carbonate production keeps up. Beds that can be clearly attributed to event deposits (e.g., tempestites, turbidites) are not considered as elementary sequences.

In basinal settings, elementary sequences consist of one marl-limestone couplet, interpreted as being related to change in planktonic carbonate productivity and/or input of clays, and/or carbonate mud export from the platform. In some cases, however, one cycle of sea-level change can produce two couplets because carbonate mud may be exported during transgression as well as during regression (Pittet & Strasser 1998a).

Small-scale sequences

Small-scale sequences in the studied sections are composed of five elementary sequences and measure from a few tens of centimeters to a few meters. They commonly show a well-defined deepening-shallowing facies evolution (SB- or TS-sequences), but shallowing-deepening trends also occur (MF-sequences). Asymmetry in the facies evolution (shallowing vs. deepening) is present (Strasser 1991).

In basinal settings, small-scale sequences are commonly defined by thickening-upwards or thinning-upwards trends of a set of five limestone beds (cf. Fig. 3.4). These trends are often subtle and observable only in parts of the studied sections.

Medium-scale sequences

Medium-scale sequences generally are composed of four small-scale sequences. If a smaller number of small-scale sequences builds up the medium-scale sequence, this is always accompanied by evident features of erosion or non-deposition. Facies evolution is comparable to that of the small-scale sequences but usually shows a higher degree of complexity. Additionally, medium-scale sequences are delimited by well-developed discontinuity surfaces, testifying to exposure or condensation. Commonly, they display a rather symmetric deepening-shallowing facies evolution and a well-developed MF. Thickening-up of beds and small-scale sequences may appear in the lower part, thinning-up in the upper part, indicating overall increasing then decreasing accommodation. In addition, dolomitization is a common phenomenon at the base and top of medium-scale sequences; to a lesser degree in the early transgressive deposits at the base and well developed in the highstand deposits (Rameil 2005).

In the basin, medium-scale sequences can only be detected on the basis of abrupt changes in the stacking pattern of the small-scale sequences. This is expressed by changes in thickness of limestone and/or marl layers, which mirror general changes in sedimentation rate and changes in the ratio of lime *versus* clay sedimentation. More abundant gravity deposits (e.g., slumps, turbidites) indicate slope instability during sea-level lowstand. A gradual increase of marls towards the center of the sequence can be present implying maximum flooding. In many cases, however, changes in colour and weathering aspect due to changing contents of iron or clay are the only elements that permit to delimit the medium-scale sequences. The thickness of medium-scale sequences on the platform and in the basin varies from a few meters to a few tens of meters.

3.5.1 Superposition of relative sea-level changes

The observed hierarchical stacking of elementary, small-scale and medium-scale sequences cannot be explained by a simple sinusoidal curve of sea-level change. For the studied interval, the three orders of sequences described above are attributed to superimposed relative sea-level fluctuations with three different amplitudes and frequencies (e.g., Goldhammer et al. 1990; Mitchum & Van Wagoner 1991; Osleger & Read 1991; Strasser 1994; Lehrmann & Goldhammer 1999; Fig. 3.5). This superimposition of relative sea-level changes not only creates depositional sequences at different scales, but also leads to multiplication of their characteristic

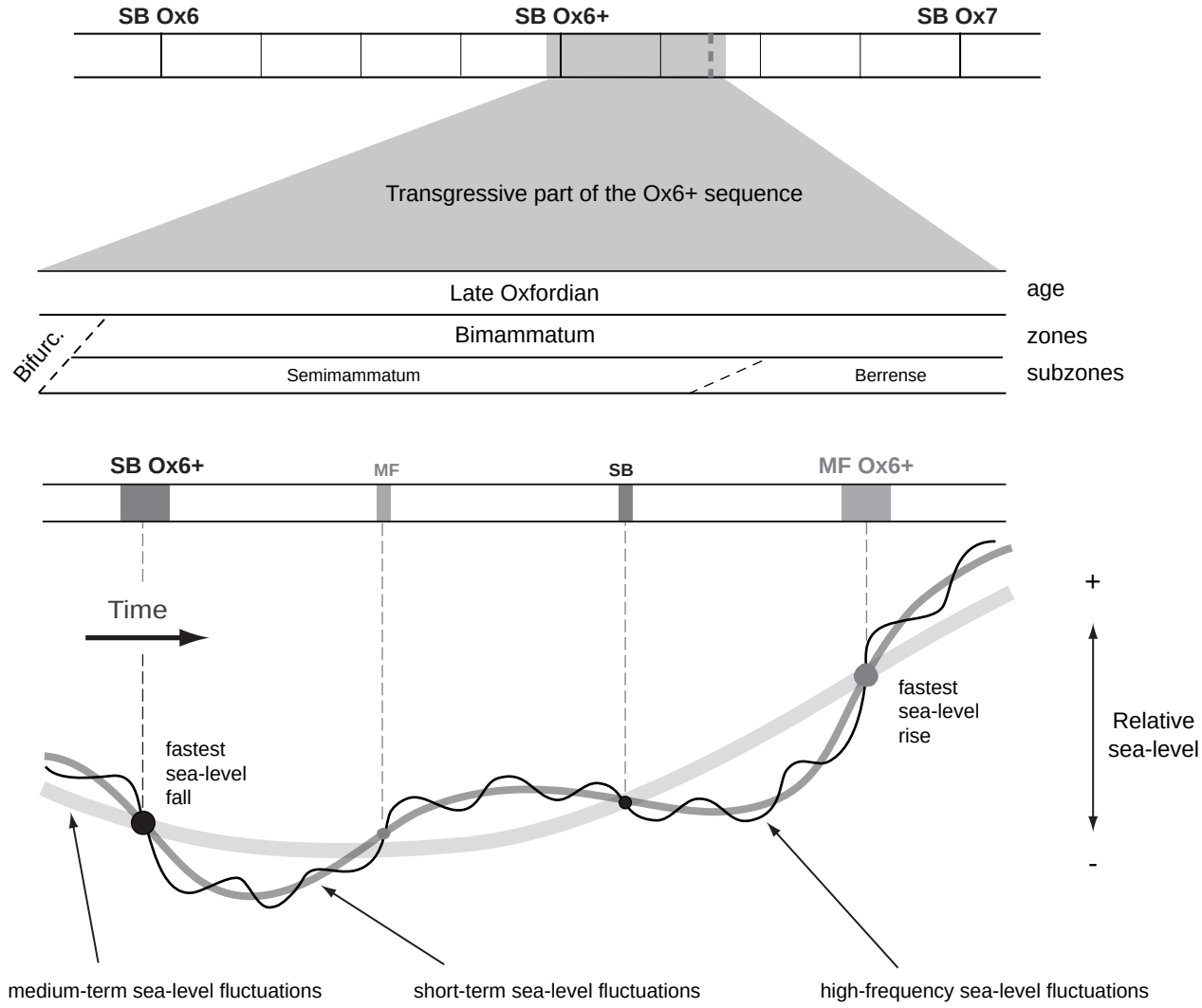

Fig. 3.5 - Superposition of medium-term, short-term, and high-frequency sea-level fluctuations can explain the stacking of sequences observed in the studied interval.

discontinuity surfaces. Thus, a sequence boundary of a large-scale sequence will in many cases not consist of one well-marked surface but of a group of regressive discontinuity surfaces, each of them bounding small-scale or elementary sequences (MONTAÑEZ & OSLEGER 1993; PASQUIER & STRASSER 1997).

3.6 ALLOCYCLIC AND AUTOCYCLIC PROCESSES

Commonly, it is not straightforward to distinguish whether extrinsic (eustatic sea level, tectonics, climate change) and/or intrinsic processes have been involved in the deposition of the observed sedimentary succession (e.g., migration of sediment bodies; STRASSER 1991). At the scale of elementary sequences, auto- and allocyclic processes have to be considered when interpreting the sedimentary record. However, autocyclic processes are less important in the formation of larger-scale sequences.

Different autocyclic models have been developed to explain the stacking pattern and/or the facies evolution of shallow-marine sedimentary successions. Shallowing-up sequences in peritidal carbonate systems have been explained by the combination of vertical aggradation and lateral progradation of tidal flats during a stable relative sea level ("tidal-flat model" according to GINSBURG 1971; in LEHRMANN & GOLDHAMMER 1999). Other models relate the deposition of shallowing-up sequences to the migration of islands and coeval subtidal areas and channels ("tidal flat - island model"; PRATT & JAMES 1986; SATTERLEY 1996).

These models, however, convince only for laterally discontinuous shallowing-up sequences (SCHLAGER 2005). Also shoal and tidal channel deposits are strongly controlled by autocyclic processes. However, they are of limited lateral extension, displaying rather a local depositional geometry.

Allocyclic forcing of sedimentary systems can be imposed by large-scale tectonics or climate changes. However, sea-level fluctuations have the most direct influence in shallow-marine depositional settings (e.g., ANDERSON & GOODWIN 1990). Allocyclic processes affect the sedimentation over a much larger area than autocyclic processes (HILLGÄRTNER 1999). Depositional sequences, which can be correlated between widely-spaced sections, therefore have mainly been controlled by allocyclic processes. Different studies made by the Fribourg working group showed that small- and medium-scale sequences can be traced between measured sections for distances of up to 100 km (e.g., PASQUIER 1995; PASQUIER & STRASSER 1997; PITTET & STRASSER 1998b; HILLGÄRTNER 1999; COLOMBIÉ 2002; COLOMBIÉ & STRASSER 2003; RAMEIL 2005; TRESCH 2007). Therefore, it is possible to establish a sequence-stratigraphical framework at least on the level of small- and medium-scale sequences. The interpretation and correlation of elementary sequences remains a challenge. An attempt to push the limits of high-resolution sequence-stratigraphical interpretations by correlating elementary sequences over short and long distances is presented in Chapter 5.

* * *

4 - STUDIED SECTIONS

Sections have been investigated and sampled in great detail. For each section, a sedimentological description and facies interpretation and then a sequence- and cyclostratigraphic interpretation are given. Where sedimentological data are not sufficient to propose an unequivocal sequence-stratigraphical interpretation, a best-fit solution is used based on comparison and correlation of the section with other sections. For methods and procedure of correlation refer to Chap. 5. The sections are presented in the following way (Fig. 4.1):

Column 1 indicates biostratigraphy.

Column 2 indicates lithostratigraphy.

Column 3 displays the sequence-stratigraphic interpretation. Small-scale and elementary sequences are numbered for the studied interval and are counted from SB/TS to SB/TS, even when they are not well delimited.

Column 4 shows the logged section with the weathering profile and sedimentary structures (on the left side), and texture, relative abundance of constituents and quartz content (on the right side). The relative abundance of each constituent in a thin section is indicated by the number of symbols (cf. Fig. 4.1; Chap. 2): one symbol: present; two symbols: common; three symbols: abundant.

Column 5 indicates the relative abundance of non-skeletal grains such as peloids, oncoids (four types), and ooids (three types). The width of the bars indicates the degree of relative abundance.

Column 6 gives the interpretation of the depositional environments. On the left side, facies type is indicated for each thin setion (cf. Tabs 2.1, 2.2, 2.3). Additionally, the relative bathymetric trend between supratidal and shallow subtidal is illustrated on the right side for the platform sections.

The location of each section is indicated on a geographical map (legend in Fig. 4.2). The first section (Voyeboeuf) is described in more detail to clearly demonstrate the methodological approach.

4.1 PLATFORM SECTIONS

4.1.1 Swiss Jura

Six sections were investigated in the Swiss Jura Mountains (Fig. 4.3). The sections correspond to shallow-water carbonate platform environments from tidal flat to open-marine lagoon. This study investigates the deposits of the top part of the marly Röschenz Member and of the oncoid-rich Hauptmumienbank and/or ooid-rich Steinebach members belonging to the Vellerat Formation. Biostratigraphic data are based on ammonites from platform and basin sections (GYGI 1995; cf. Chap. 1). The Röschenz Member is attributed to the lower part of the Hypselum subzone and the Hauptmumienbank and Steinebach members to the upper part of the Hypselum subzone (Fig. 1.4).

Most of the studied sections were first described by R. GYGI through the 1980's (sedimentological logs in GYGI 2000b). PITTET (1996) and HUG (2003) presented a sedimentological and sequence-stratigraphic interpretation of several sections. PITTET (1996) labeled long-term sequence boundaries and transgressive surfaces. HUG (2003) placed sequence boundary Ox6+ between Ox6 and Ox7 of HARDENBOL et al. (1998) and identified medium-scale, small-scale, and elementary sequences. Differences in location of sequence boundaries and transgressive surfaces between these authors and my own study are mainly explained by additional sedimentological evidences. PITTET (1996)

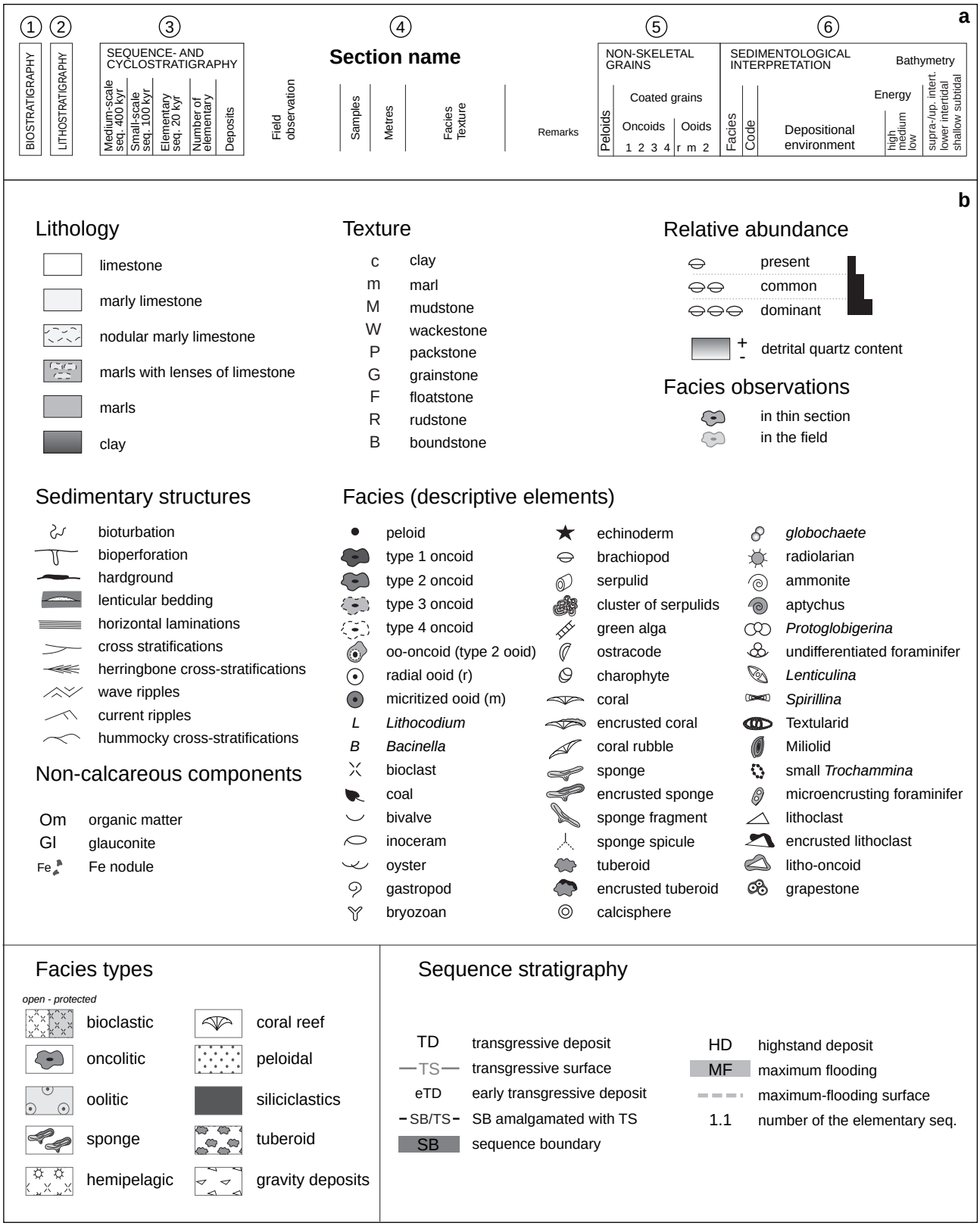

Fig. 4.1 - Legend for all the studied sections.

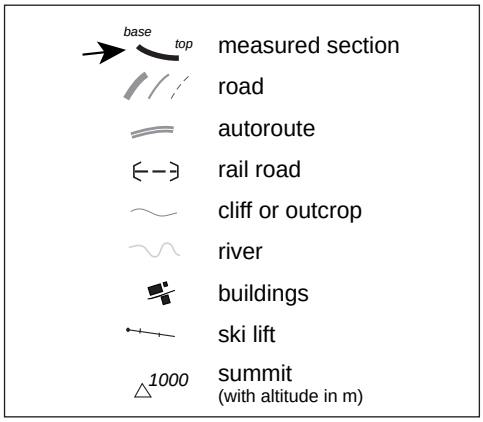

Fig. 4.2 - Legend for all maps describing geographical positions of the measured sections.

also presented clay-mineral and palynofacies analyses and DUPRAZ (1999) improved the palaeoenvironmental and palaeoecological interpretations of coral-reef ecosystems from the Hautes-Roches, Savagnières, and Pertuis sections.

Voyeboeuf (Figs 4.4 and 4.5a-b; Pl. 14/1)

Geography and stratigraphy

The Voyeboeuf section is located on the south side of the Banné anticline south of Porrentruy, on the east side of the road linking Porrentruy to Courgenay. The

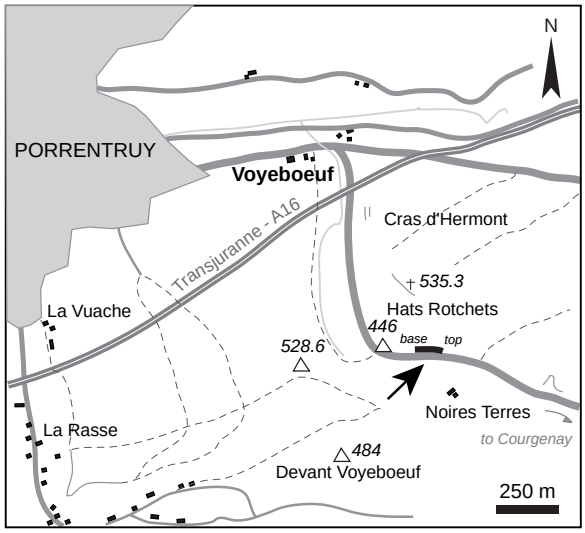

Fig. 4.4 - Location of the Voyeboeuf section. Based on topographic map of St-Ursanne (1085), Carte nationale de la Suisse, 1:25 000.

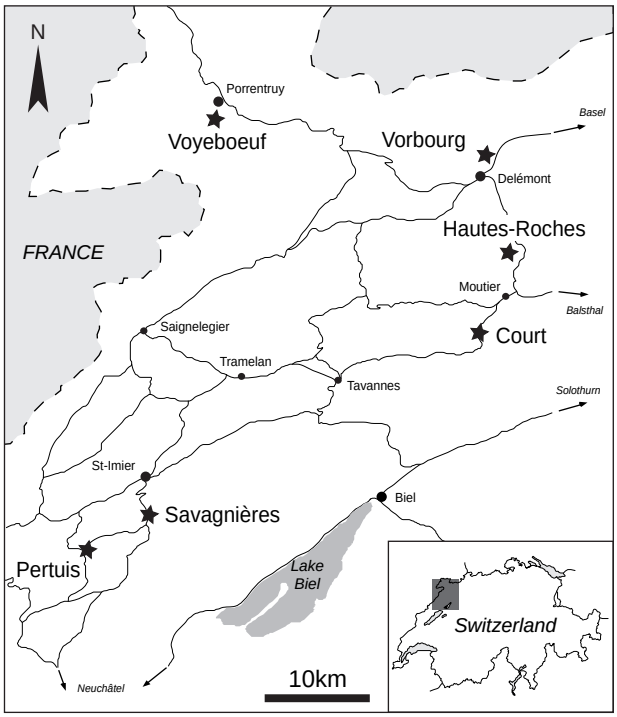

Fig. 4.3 - Location of the six sections studied in the Swiss Jura Mountains.

Voyeboeuf section covers about 11.5 m of lagoonal deposits from sandy bioclastic limestones attributed to the top part of the Röschenz Member, dated of the lower Hypselum subzone (GYGI 1995; cf. Chap. 1) to massive oncoid-rich beds belonging to the Hauptmumienbank Member, dated of the upper Hypselum subzone.

Sedimentological interpretation

The base of the section is characterized by nodular bioclastic mudstones-wackestones rich in ostracodes and quartz (from base to 0.85 m) interpreted as protected lagoon deposits. More massive oncoid-rich wackestones-packstones with a relatively high-diversity fauna (from 0.85 to 1.1 m) are interpreted as semi-open lagoon deposits and mark a slight opening of the depositional environment. The following nodular ostracode-rich mudstones (from 1.1 to 1.4 m) suggest a slight protection of the depositional environment.

The first massive limestone beds (from 1.4 to 2.2 m) consist of inoceram-rich mudstones-wackestones. The increase of inoceram abundance and the gradual decrease of quartz content point to an opening of the depositional environment. The following beds consist of oncoid-rich wackestones (from 2.35 to 2.8 m) interpreted as semi-open lagoon deposits and peloid-rich wackestones-mudstones (from 2.8 to 2.95 m)

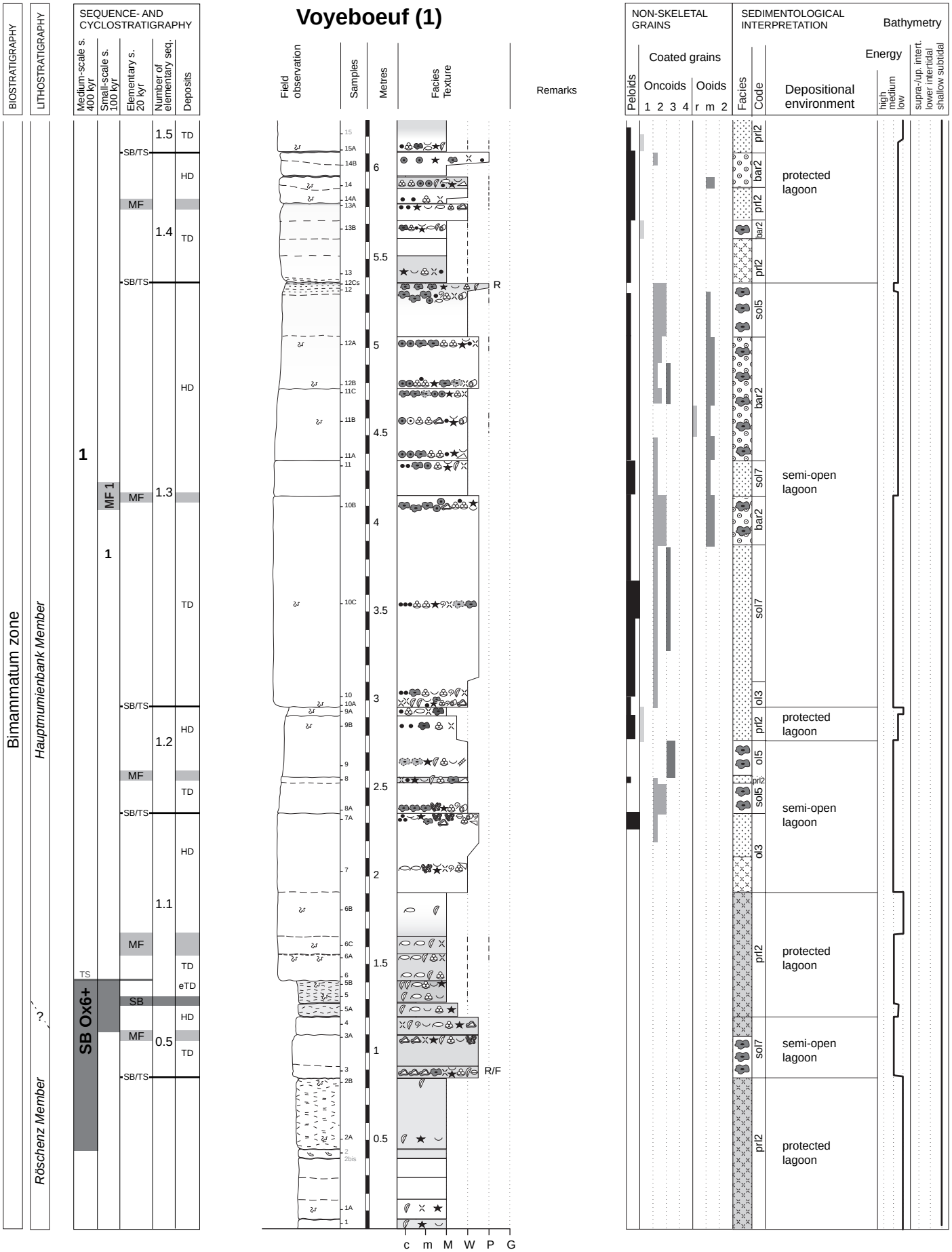

Fig. 4.5a - Voyeboeuf section (1).

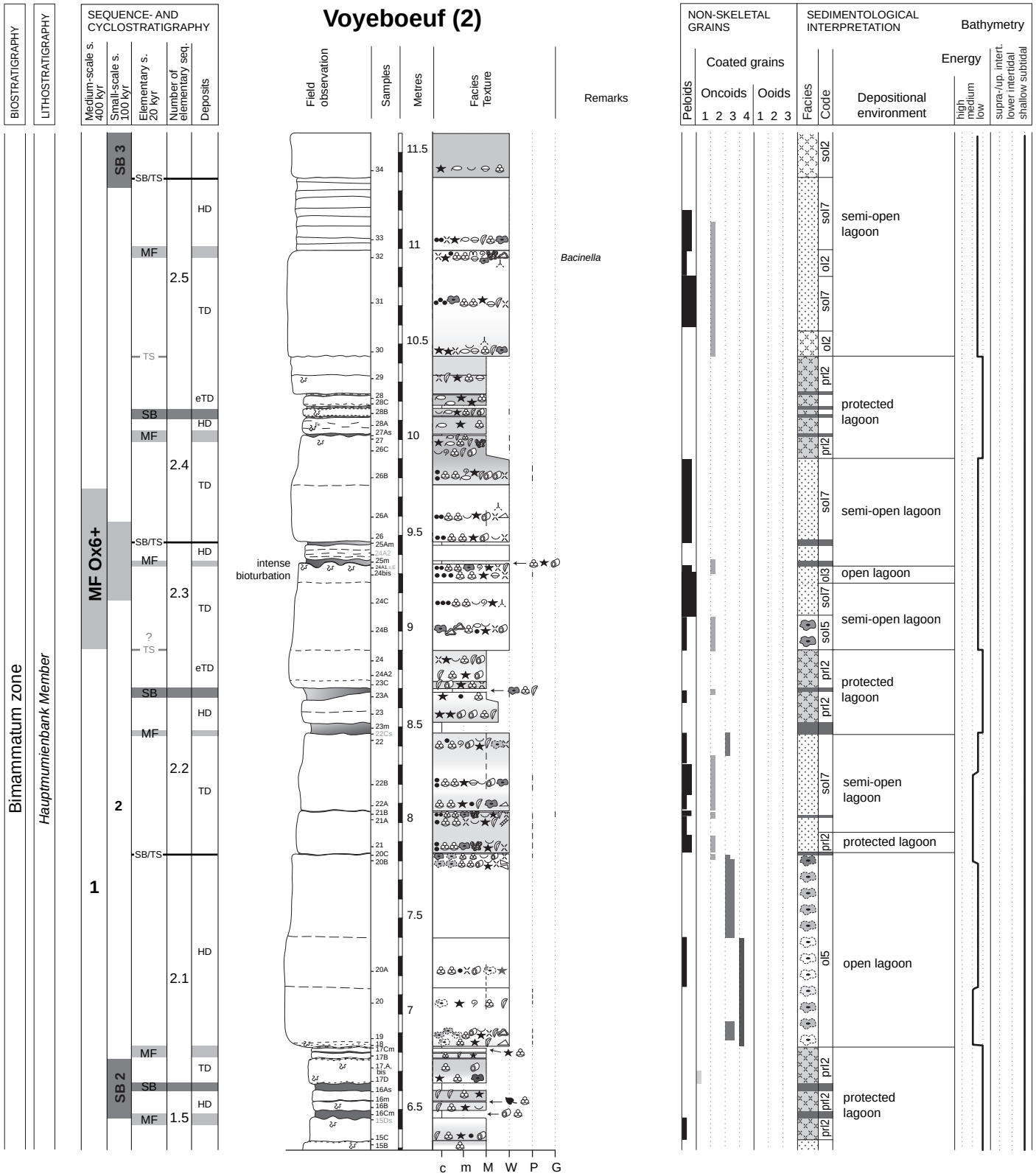

Fig. 4.5b - Voyeboeuf section (2).

interpreted as protected lagoon deposits. This suggests a slight shallowing of the depositional environment. An important increase of accommodation space is indicated by the deposition of a thick peloid-oncoid-ooid wackestone-packstone bed (from 2.95 to 4.15 m). The following beds (from 4.15 to 6.8 m) become thinner (i.e., thinning-up trend) suggesting a general decrease of the accommodation space. Clay-rich intervals are more common, suggesting a more humid climate or local remobilization of siliciclastics. The marls and the thin undulated mudstone beds (from 6.45 to 6.85 m) consist of shallow facies with coal debris in the marls and a low diversity fauna (i.e., ostracodes, benthic foraminifera, echinoderms) in the limestones. This interval corresponds to an important shallowing of the depositional environment.

Then, an increase of accommodation space and a deepening phase is marked by the deposition of a massive and thick wackestone bed (from 6.85 to 7.85 m). This bed rich in *Bacinella-Lithocodium* oncoids suggests low-energy conditions in an open lagoon. The following beds (from 7.85 to 8.45 m) are peloid and foraminifer (miliolid) packstones-wackestones with a small amount of quartz and are interpreted as a more protected lagoonal environment. The deposition of marls rich in oncoids, foraminifera and ostracodes (at 8.7 m) probably reflects a shallowing of the depositional environment. The following beds are ostracode and serpulid mudstones, also interpreted as protected lagoon deposits. Then follow peloid and foraminifer (textulariid) wackestones, interpreted as semi-open to open lagoon deposits. This facies evolution points to a slight opening of the depositional environment. The wavy bed surface (9.35 m) probably results from an intense bioturbation, suggesting a lower sedimentation rate. This bed surface is overlain by a clay-rich interval (from 9.35 to 9.45 m) that may reflect a climate change in the hinterland or a remobilization of siliciclastics formerly stored on the proximal platform. The evolution from peloid-foraminifer wackestone to inoceram-echinoderm mudstone (from 9.45 to 10.25 m) associated with an increase in quartz content points to lower-energy conditions probably due to protection of the depositional environment behind a shoal field. The surface of this bed is also wavy, characterizing bioturbation, and covered by a thin marl-limestone interval. The interval from 10 to 10.25 m consists of thin clay levels intercalated with three bioturbated mudstones rich in inocerams and echinoderms. These deposits are interpreted as more protected lagoonal environments. More massive and thicker wackestone beds (from 10.45 m) with a normal-marine and relatively diversified fauna but no quartz content suggest a slight opening of the system until a relative sea-level drop is implied by the increase of quartz content (11.4 m).

Sequence-stratigraphic interpretation

The relatively sandy facies, the thin beds implying low accommodation, and the protected-lagoonal fauna at the transition between the Röschenz and Hauptmumienbank members all point to an important sequence boundary. The nodular sandy limestones (1.3-1.4 m) are interpreted as the corresponding medium-scale SB Ox6+. The following massive limestone beds (from 1.4 m) represent an important relative sea-level rise. The base of these limestones (at 1.4 m) is interpreted as the medium-scale TS Ox6+. The depositional sequences of this section present commonly sequence boundaries amalgamated with transgressive surfaces (SB/TS) due to very thin or absent lowstand or early transgressive deposits.

The small-scale sequence 1 consists of five elementary sequences. The transgressive deposit of the first elementary sequence (1.1) consists of inoceram-ostracode mudstones with a small amount of quartz while the highstand deposit contains more diversified bioclast wackestones without quartz. The second elementary sequence is relatively thin and composed of three beds. The first bed is characterized by type 2 oncoids and serpulids and is interpreted as the transgressive deposit. The following beds, interpreted as the highstand deposit, begin with *Bacinella-Lithocodium* oncoids and end with peloids and type 2 oncoids. This evolution probably reflects an energy change and a relative sea-level drop. The third elementary sequence is the thickest sequence of the section. It suggests maximum accommodation gain. The maximum flooding of this elementary sequence is assumed to be located at the top of the first bed where type 2 oncoids abund. This MF is interpreted as being also the MF of small-scale sequence 1 (MF 1). The fourth elementary sequence is composed of three beds. The transgressive deposit corresponds to the first relatively thick bed, which is bioclastic and peloidal while the highstand deposit is richer in micritized ooids. The fifth elementary sequence is thin, pointing to a decrease of accommodation space. The first two beds are interpreted as the transgressive deposit. The maximum flooding is positioned at the wavy surface (6.45 m) at the top of the second bed. The clay level and two thin wavy beds are interpreted as the highstand deposit.

The clay level at 6.62 m with the coal debris found just below reflects a relative sea-level drop and is thus interpreted as the small-scale sequence boundary SB 2. The first elementary sequence (2.1) is relatively thick. Bioclastic mudstones with a small amount of quartz are interpreted as protected lagoon deposits that formed during transgression. The thick oncoid-rich bed showing an evolution from *Bacinella-Lithocodium* oncoids (type 3 and 4) to micrite-dominated oncoids (type 2) is interpreted as the highstand deposit. The facies at the base of this massive bed are interpreted as the deepest and most open marine and are thus attributed to a maximum flooding. The second, third and fourth elementary sequences have the same pattern and consist of a more or less thin clay level, one or two massive, thick limestone beds, another clay level, and one limestone bed. For each sequence, the sequence-stratigraphic interpretation is the following: the sequence boundary is placed in the clay interval below the massive limestone bed, which is interpreted as the transgressive deposit; the wavy surface at the top of this massive bed is considered as the maximum flooding, and the highstand deposit corresponds to the second clay level and to the limestone bed. The highly bioturbated surface (9.35 m) of the third elementary sequence is considered to represent the maximum flooding of the medium-scale sequence (MF Ox6+). In the fifth elementary sequence, clay levels and quartz gradually disappear, indicating a slight opening of the depositional environment. In the following bed, the quartz content significantly increases, suggesting a terrigenous input probably caused by a relative sea-level drop. This limit at 11.38 m is interpreted as the small-scale SB 3.

Vorbourg (Figs 4.6 and 4.7a-c; Pl. 14/4-5)

Geography and stratigraphy

The Vorbourg section is located in northwestern Switzerland north of Delémont (canton Jura) (Fig. 4.6). The studied section crops out in a parking lot along the small road that cuts through the Béridier anticline, close to the Vorbourg chapel. This section represents a good reference section for the Hauptmumienbank Member (cf. section RG 366 in Gygi 2000b). Along the parking area, marly deposits, which are partly covered by vegetation, constitute the Röschenz Member dated of the lower Hypselum subzone (Gygi 1995; cf. Chap. 1). The massive limestones of the Hauptmumienbank and Steinebach members, dated of the upper Hypselum subzone, are exposed in the southern extremity of

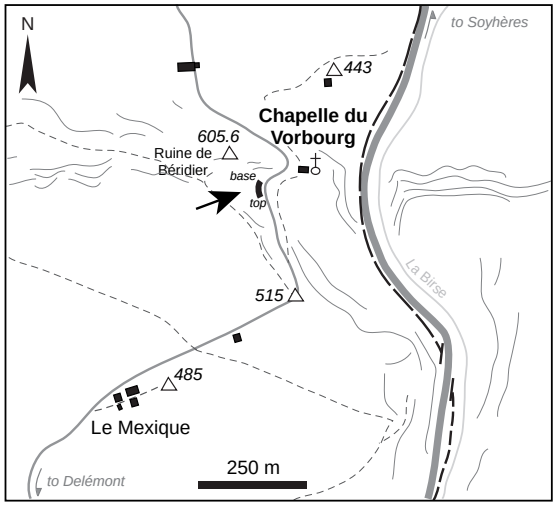

Fig. 4.6 - Location of the Vorbourg section. Based on topographic map of Delémont (1086), Carte nationale de la Suisse, 1:25 000.

the parking. The Vorbourg section consists of 12.5 m lagoonal deposits, covering the top part of the marly Röschenz Member and most of the oncoid-rich Hauptmumienbank Member.

Sedimentological interpretation

The base of the section (from 0 to 4.6 m) consists of fossiliferous yellowish marls, pointing to relatively low-energy environments, and higher energy deposits (ooid-peloid-foraminifer packstones) interpreted as washover deposits. This succession was probably deposited in a marly, semi-open lagoon. The marly level (from 4.1 to 4.6 m) presents a relatively semi-restricted faunal association with ostracodes, gastropods, and type 2 oncoids suggesting a more protected lagoonal environment.

Then the sedimentation style changes: marly deposits disappear and are replaced by massive and thick limestones rich in oncoids. This well-marked facies change (at 4.6 m) also marks the beginning of an increase of accommodation space. The following beds (from 4.6 to 5.55 m) consist of (a few tens of centimetres) thick packstone beds rich in type 2 oncoids, in foraminifera, and radial ooids. These oncoid beds are interpreted as semi-open lagoonal deposits. The following bed (from 5.55 to 5.75 m), dominated by brachiopods, echinoderms and coral rubble, marks an important opening and deepening of the depositional environment. Radial ooid grainstone bars, formed by autocyclic processus, migrated over this bioclastic deposit and momentarily interrupted

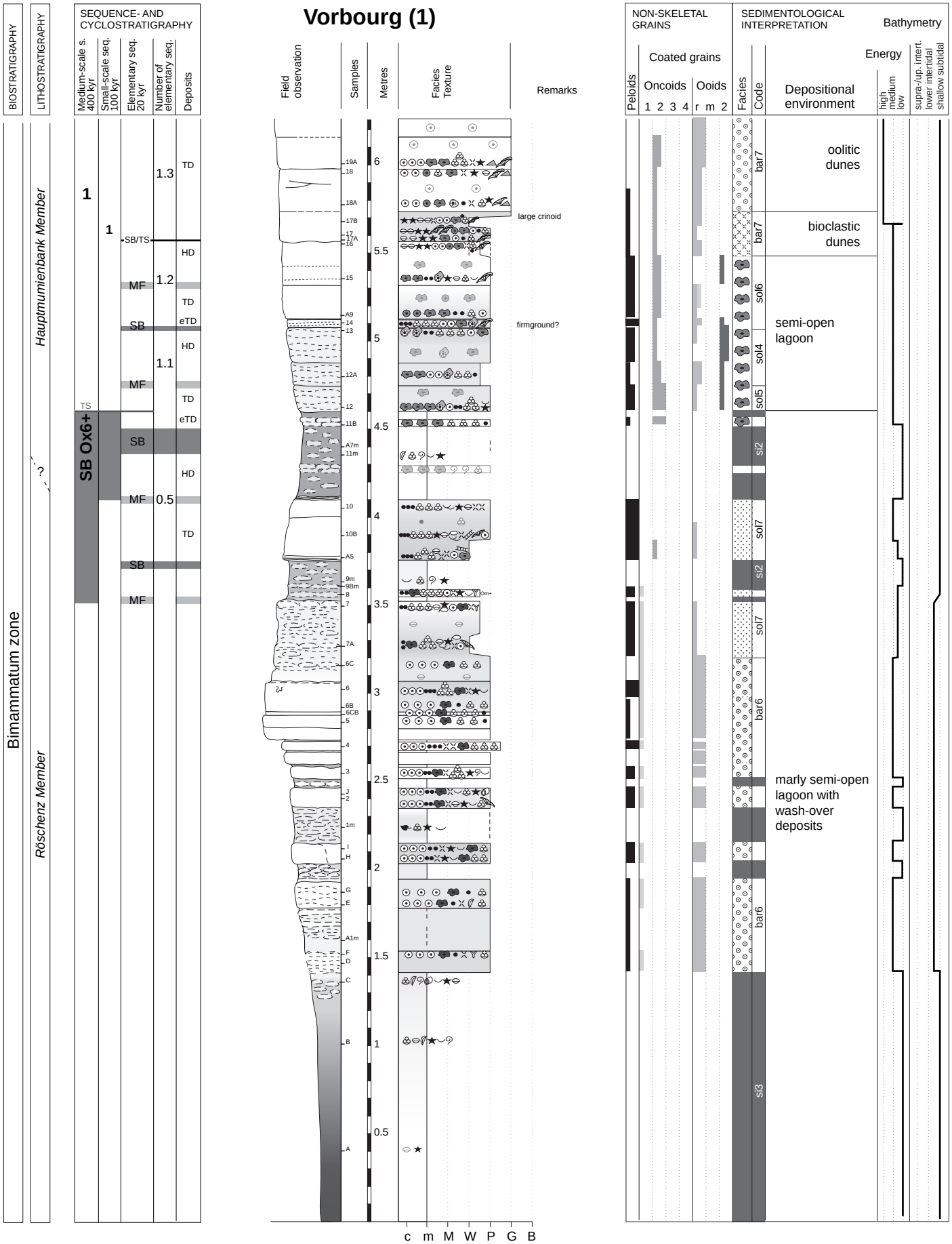

Fig. 4.7a - Vorbourg section (1).

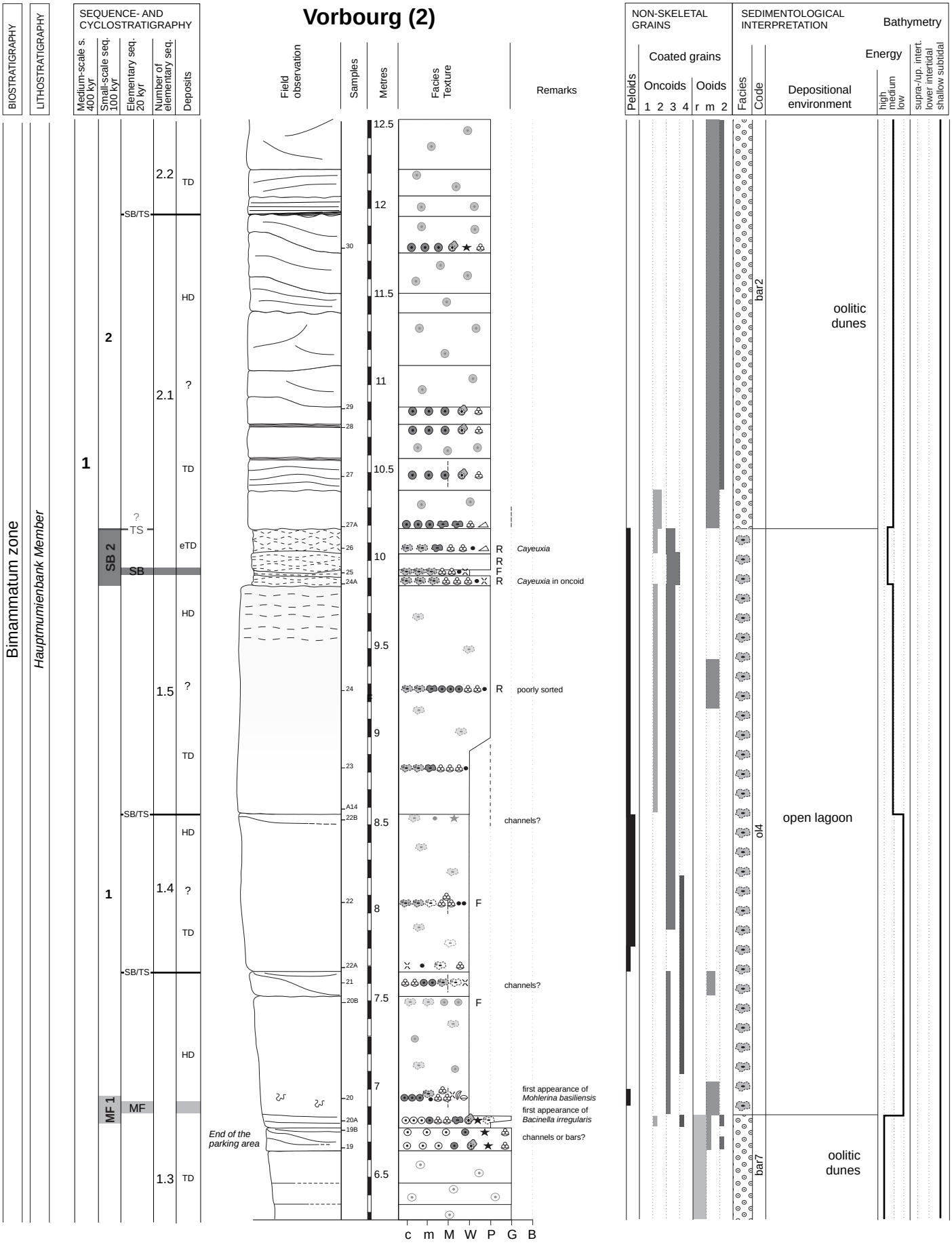

Fig. 4.7b - Vorbourg section (2).

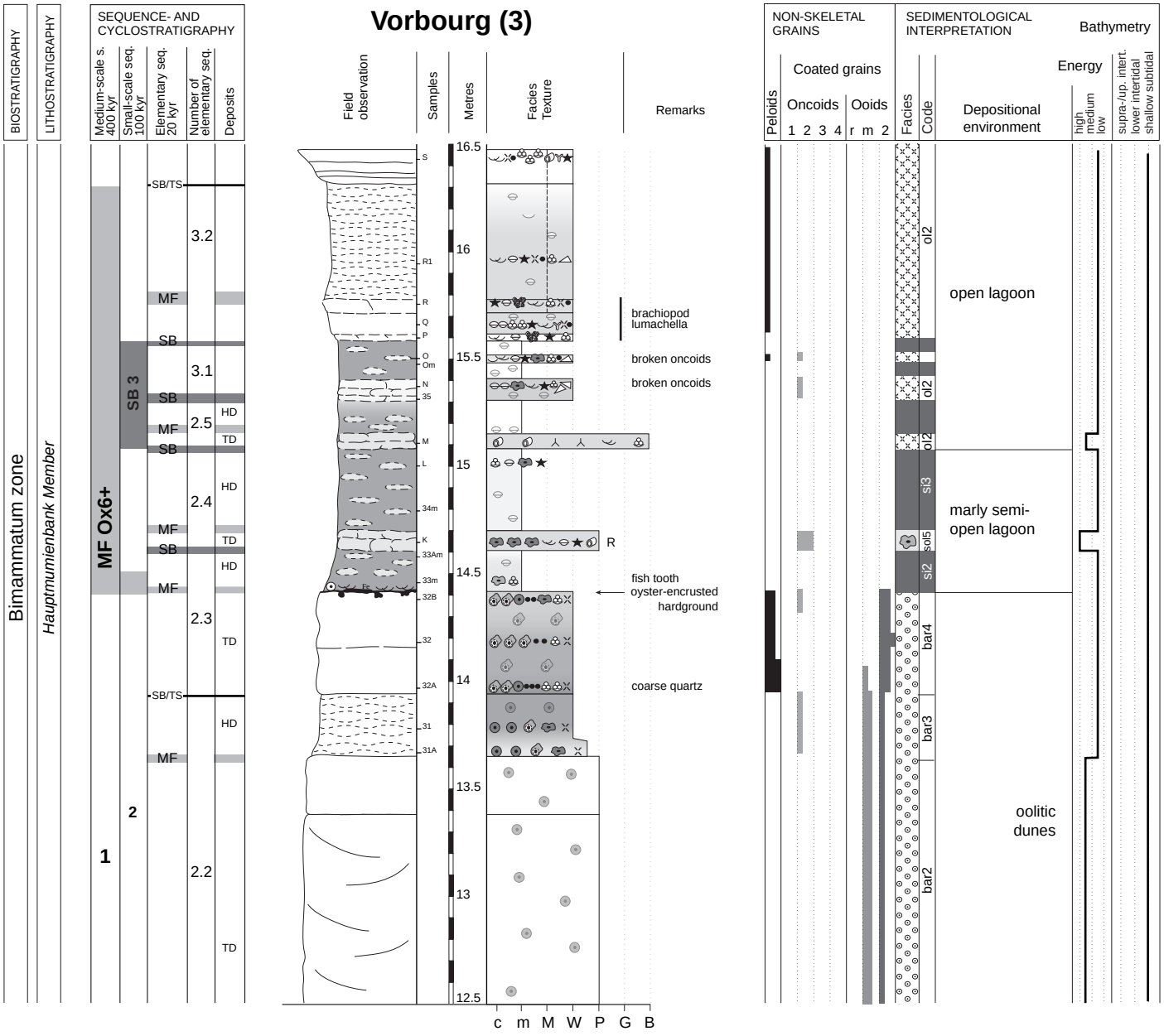

Fig. 4.7c - Vorbourg section (3).

the oncolitic sedimentation (from 5.75 to 6.55 m). Ooid bars become thinner and show a facies change (at 6.85 m) to a thick bioturbated wackestone bed with micritized ooids, *Bacinella-Lithocodium* (type 3) oncoids, foraminifera, and brachiopods. This evolution suggests lower energy conditions in an open lagoonal environment and probably reflects the migration and/or desactivation of ooid bars. This massive and thick bed is followed by a thinner bed (from 7.5 to 7.7 m) interpreted as a channel deposit and probably indicating a decrease of accommodation. The following massive and thick bed (from 7.7 to 8.55 m) consisting of *Bacinella-Lithocodium* (type 3) oncoid wackestones-floatstones is interpreted as open lagoonal deposit. At its top, a small channel occurs, pointing to a decrease of accommodation. The following massive and thick bed (from 8.55 to 9.85 m) is a packstone (locally rudstone) with *Bacinella-Lithocodium* (type 3) oncoids, foraminifera, and micritized ooids.

This bed is followed by thin nodular rudstone beds (from 9.85 to 10.2 m) rich in *Bacinella-Lithocodium* (type 3) oncoids and benthic foraminifera. These rudstone beds point to higher energy conditions probably due to a decrease of water depth. This interval is overlain (from 10.2 to 13.65 m) by packstone bars containing micritized ooids. The thickness of these

deposits points to an increase of accommodation space. From 13.65 to 14.4 m, a nodular wackestone bed rich in micritized ooids and then a second wackestone bed rich in oo-oncoids, peloids, and foraminfera suggest lower energy conditions. At 14.4 m, a perforated and oyster-encrusted hardground caps these beds and probably reflects a sediment starvation (lower accumulation rate) during a rapid deepening of the depositional environment. This hardground is covered by an important marl interval. This abrupt lithological change marks the turnover of the system towards a siliciclastic-dominated sedimentary system probably caused by a climatic change to more humid conditions. The marly level (from 14.4 to 15.6 m) consists of yellowish marls rich in terebratulid brachiopods, benthic foraminifera, and type 2 oncoids. This interval includes three thin nodular limestone beds: one type 2 oncoid rudstone at 14.65 m, one boundstone of serpulids with sponge spicules at 15.1 m, and one wackestone rich in brachiopods and broken oncoids at 15.3 m. In the final part of the section, limestone beds with brachiopods (from 15.6 to 16.3 m) dominate and represent open-marine conditions.

Sequence-stratigraphic interpretation

The marly interval at the top of the Röschenz Member represents the shallowest facies and is interpreted as the medium-scale sequence boundary SB Ox6+. The following rapid lithological change (from marl to limestone), recognized all over the Swiss Jura, is interpreted as the major transgressive surface TS Ox6+ corresponding to the beginning of the early Bimammatum transgression. This transgressive surface is the equivalent of the long-term TS 2 of Pittet (1996).

Sequence boundaries, transgressive surfaces, and maximum floodings of elementary sequences are precisely defined from facies and microfacies analyses and stacking pattern. The sequence boundaries are commonly amalgamated with the well-marked transgressive surfaces because of very thin or not developed lowstand and early transgressive deposits. In small-scale sequence 1, five elementary sequences have been identified. The first and second elementary sequences are rich in type 2 oncoids and interpreted as semi-open lagoonal deposits. In the first elementary sequence (1.1), the first nodular oncoid packstone bed is considered as the transgressive deposit and the two following beds as the highstand deposit. The maximum flooding is placed at the slight texture change from packstone to wackstone/packstone (at 4.75 m). The second elementary sequence is the smallest sequence and shows a gradual decrease of quartz content. The peloid-foraminifer packstone (at 5.1 m) is interpreted as an early transgressive deposit and the two following beds as the transgressive and highstand deposits, respectively. The maximum flooding of this sequence is assumed to be located between the two massive and thick beds (at 5.3 m), where type 2 oncoids are abundant and brachiopods and corals are present. The third elementary (1.3) is the thickest sequence of this section, suggesting maximum gain of accommodation. The bioclastic (i.e., brachiopods, echinoderms, corals) wackestone/packstone bed (from 5.55 to 5.75 m) and the radial ooid grainstone beds (from 5.75 to 6.85 m) are interpreted as transgressive deposits. High sediment accumulation rate kept water depth low and allowed for the formation of channel just below the maximum flooding. The facies evolution to micritized ooid and type 3 oncoid bioturbated wackestone then points to more open-marine conditions in a deeper depositional environment. This facies change (at 6.9 m) is interpreted as the maximum flooding of the third elementary sequence. This well-expressed maximum flooding is also the maximum flooding of small-scale 1, which is confirmed by lateral correlation. The wackestone-floatstone bed (from 6.85 to 7.7 m) rich in micritized ooids *Bacinella-Lithocodium* oncoids, and foraminifera is interpreted as the highstand deposit in an open lagoon. Channels at the end of this highstand deposit probably indicate a slight decrease of accommodation space and thus a relative sea-level fall. The fourth elementary sequence mainly consists of one massive and thick wackestone-floatstone bed rich in *Bacinella-Lithocodium* oncoids and foraminifera. A small channel occurs in the highstand deposit and suggests a slight sea-level fall. In the fifth elementary sequence, mainly composed of one massive and thick bed, a texture evolution from wackestone to packstone-rudstone suggests higher energy conditions in the second part of this bed, thus interpreted as the highstand deposit.

The rudstone interval (from 9.85 to 10.2 m) suggests higher energy conditions and probably reflects a relative sea-level drop. This interval is thus interpreted as small-scale SB 2. The small-scale sequence 2 consists of five elementary sequences. The first elementary sequence (2.1) begins with thin nodular oncoid rudstones, interpreted as early transgressive deposits. The following oolitic packstones were controlled by autocyclic processus, which makes the identification of elementary sequences difficult. However, fine laminations and thinner beds at 11.95 m

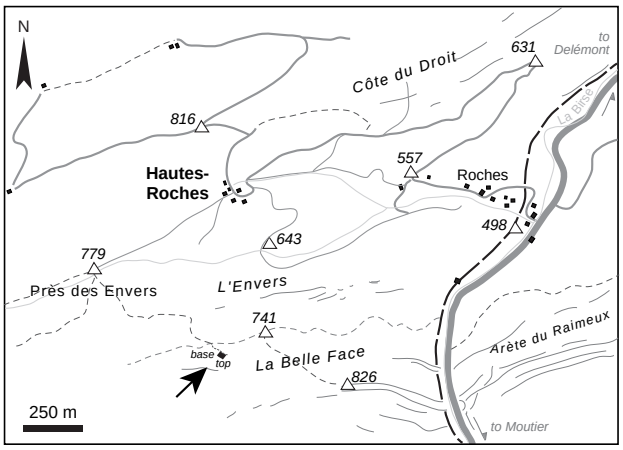

Fig. 4.8 - Location of the Hautes-Roches section. Based on topographic map of Moutier (1106), Carte nationale de la Suisse, 1:25 000.

suggest a hydrodynamic change, which is interpreted as corresponding to the sequence boundary of the second elementary sequence. The following sequence boundary is placed at the transition from nodular to more massive oolitic beds rich in coarse quartz (at 13.95 m). The oyster-encrusted hardground (at 14.4 m), which caps the top of the carbonate-dominated part, is interpreted as the maximum-flooding surface of the third elementary sequence. This maximum-flooding surface is interpreted as belonging to the medium-scale MF Ox6+. The fourth and fifth elementary sequences are defined within the marly interval and are composed of a thin nodular limestone bed, interpreted as the transgressive deposit, and marls rich in brachiopods, interpreted as the highstand deposit.

Hautes-Roches (Figs 4.8 and 4.9a-b)

Geography and stratigraphy

The Hautes-Roches section is situated on the southern flank of the Mont Raimeux. This section is along a forest path to the south of the hamlet of Hautes-Roches (Fig. 4.8). The Hautes-Roches section is dominated by ooid bars belonging to the Steinebach Member. Locally there are some coral patch-reefs and clays are abundant at the base and top of the section. This section is only about 7 m thick.

Sedimentological interpretation

At the base of the section, the marly interval presents charophyte oogones and stems, gastropods (i.e., large *Bourgetia striata*), *in situ* urchins and benthic foraminifera. This restricted fauna indicates protected marly lagoonal environment.

The deposition of limestone beds points to an opening of the system and a stop of the siliciclastic input. The first two beds (from 0.6 to 0.95 m) are coral boundstones with a bioclastic matrix. The development of coral patch-reefs marks an important opening of the depositional environment associated to an increase of accommodation space. The third bed is a packstone rich in coral rubble and ooids interpreted as a peri-reefal bar. The presence of ooids since the first bed announces the ooid grainstones from 1.1 m onwards. The beds from 1.1 to 4.3 m consist of high-energy ooid bars. A subtidal sandwave occurs at 1.4 m. These ooid bars are topped at 4.3 m by a bioperforated hardground. This surface is assumed to have formed in a subtidal high-energy environment and represents an omission period due to a rapid decrease of accommodation.

This hardground is overlain by a thin marly interval containing a level of coral carpet indicating an increase of the accommodation space. The following limestone beds (from 4.4 to 5.4 m) consist of ooid-rich packstones to grainstones with local coral rubble, type 2 oncoids, echinoderms, and grapestones. These beds are interpreted as ooid bars. They are covered by a thin marl level, which is followed by a thick nodular wackestone bed rich in normal-marine fauna (i.e., corals, sponges, brachiopods). This facies evolution probably reflects a slight deepening and opening of the depositional environment. The top part of the section consists of marly deposits (from 5.8 m) with two relatively thick nodular limestone beds (at 5.9 m and 6.4 m). The marls contain a normal-marine fauna (i.e., brachiopods, echinoderms, foraminifera) and the nodular limestones are mainly composed of corals, sponges, and serpulids. This marly interval displays low energy conditions probably due to the deepening of the system and/or protection of the depositional area by a shoal field.

Sequence-stratigraphic interpretation

The marly interval rich in charophytes and gastropods at the base of the section represents the shallowest facies and is thus interpreted as the medium-scale SB Ox6+. The base of the first limestone bed (at 0.65 m) represents the medium-scale TS Ox6+, previously identified by Pittet (1996) as a long-term transgressive surface. Indeed, this rapid facies change from clay-dominated to limestone-dominated and the

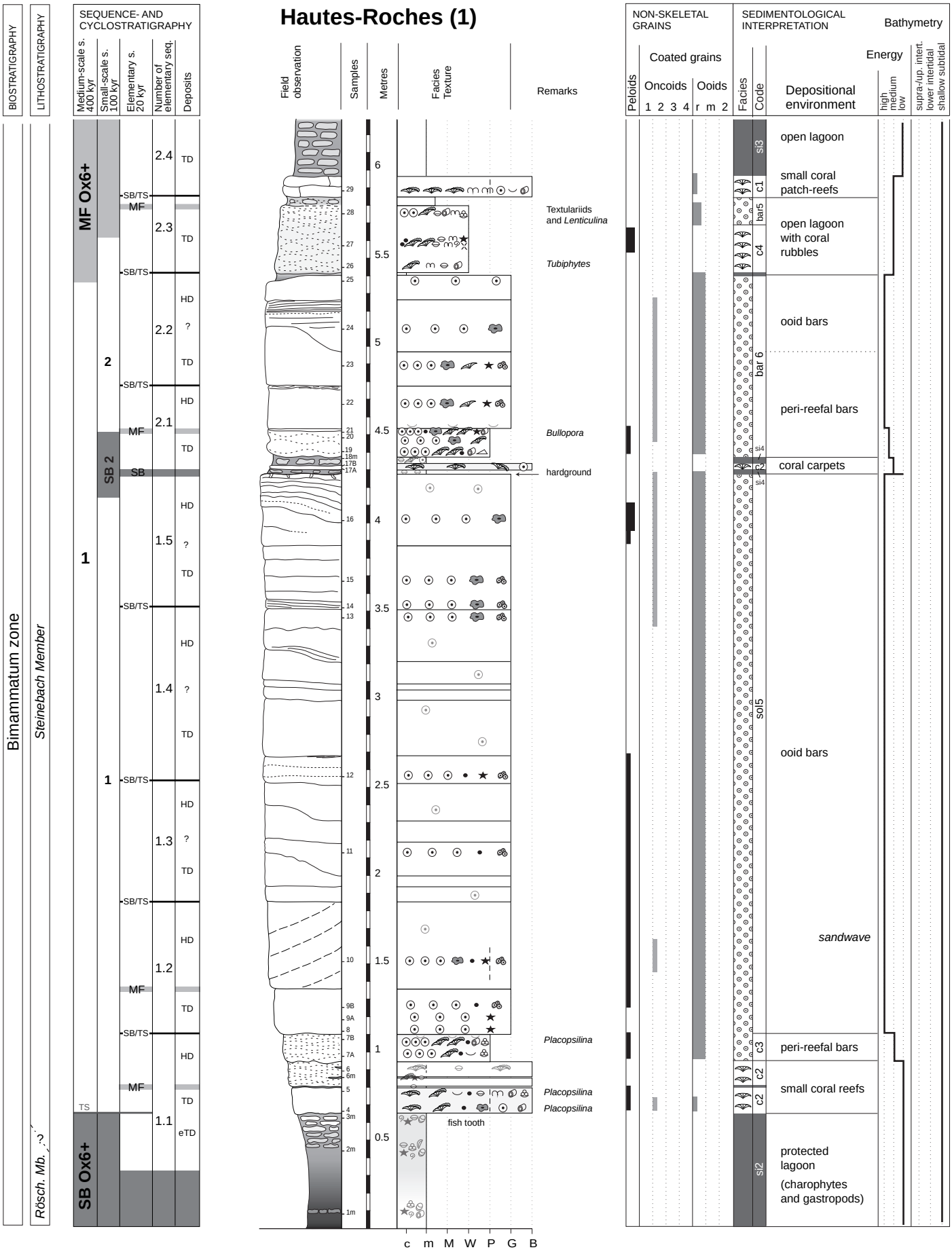

Fig. 4.9a - Hautes-Roches section (1).

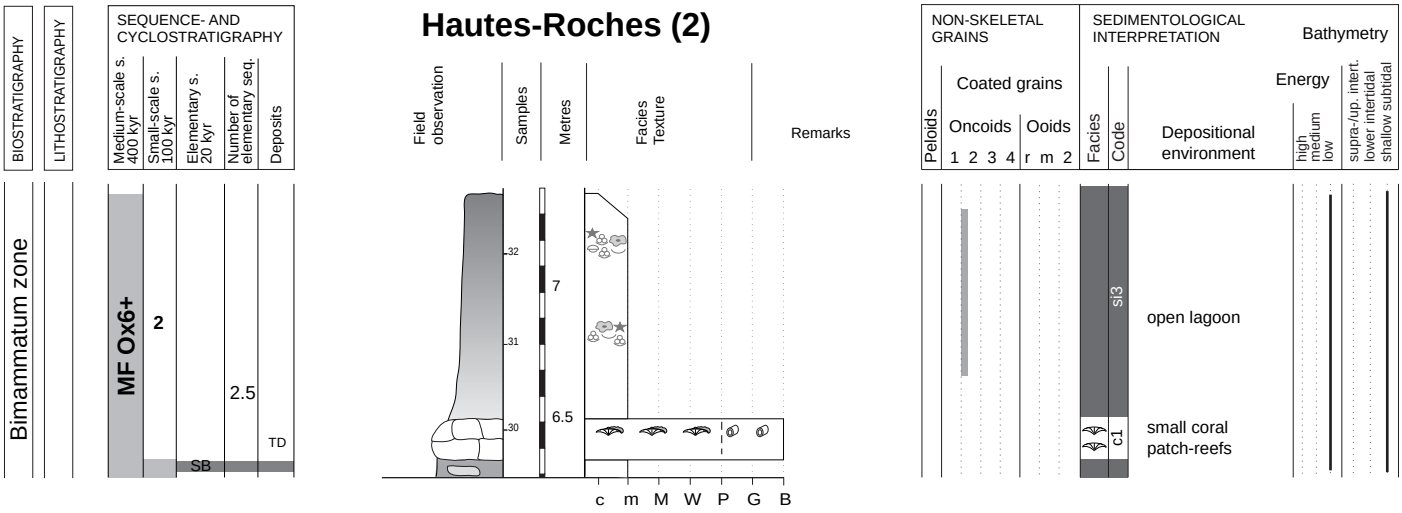

Fig. 4.9b - Hautes-Roches section (2).

evolution from charophytes to sponges and brachiopods reflect an important relative sea-level rise.

Small-scale sequence 1 is almost entirely composed of high-energy deposits, which makes the sequence-stratigraphic interpretation difficult because the bars are subject to autocyclic processes. However, with the help of sedimentary structures and bedding changes, sequence boundaries may be proposed. Five elementary sequences have been identified in this small-scale sequence. The first elementary sequence mainly consists of a marly interval and three limestone beds. The first two beds, composed of bioconstruction levels, are interpreted as the transgressive deposits and the third bed, composed of ooids, is interpreted as the highstand deposit. The facies change from an open-marine environment with a small reef installation to higher-energy deposits dominated by ooids and coral rubble is interpreted as the maximum-flooding surface. The next four elementary sequences consist of high-energy deposits. In the top part of these ooid bars, beds are thinner and point to a decrease of the accommodation space. The hardground, followed by a marl level, probably reflects a rapid sea-level drop and is interpreted as small-scale SB 2.

In small-scale sequence 2, only the first three elementary sequences have been investigated. The first elementary sequence consists of a thin marl level with limestone nodules and two thicker limestone beds. The maximum flooding of this sequence is placed at a texture change (at 4.5 m) between the two limestone beds. The second elementary sequence consists entirely of ooid grainstones making the identification of the maximum flooding difficult. The third elementary sequence consists of a nodular bioclastic (brachiopods, corals, sponges) wackestone bed followed by a thin marly interval. The maximum-flooding surface is assumed to be located at the top of the nodular limestone bed (5.8 m). Based on lateral correlation, this maximum flooding is interpreted as the medium-scale MF Ox6+.

Court (Figs 4.10 and 4.11a-c)

Geography and stratigraphy

The Court section is located on the northern flank of the Graitery anticlinal near “La Bâme” along the road leading from Court to Moutier (Fig. 4.10). The

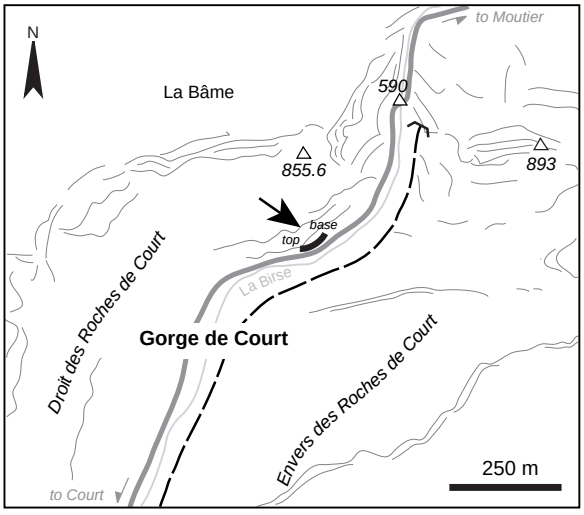

Fig. 4.10 - Location of the Court section. Based on topographic map of Moutier (1106), Carte nationale de la Suisse, 1:25 000.

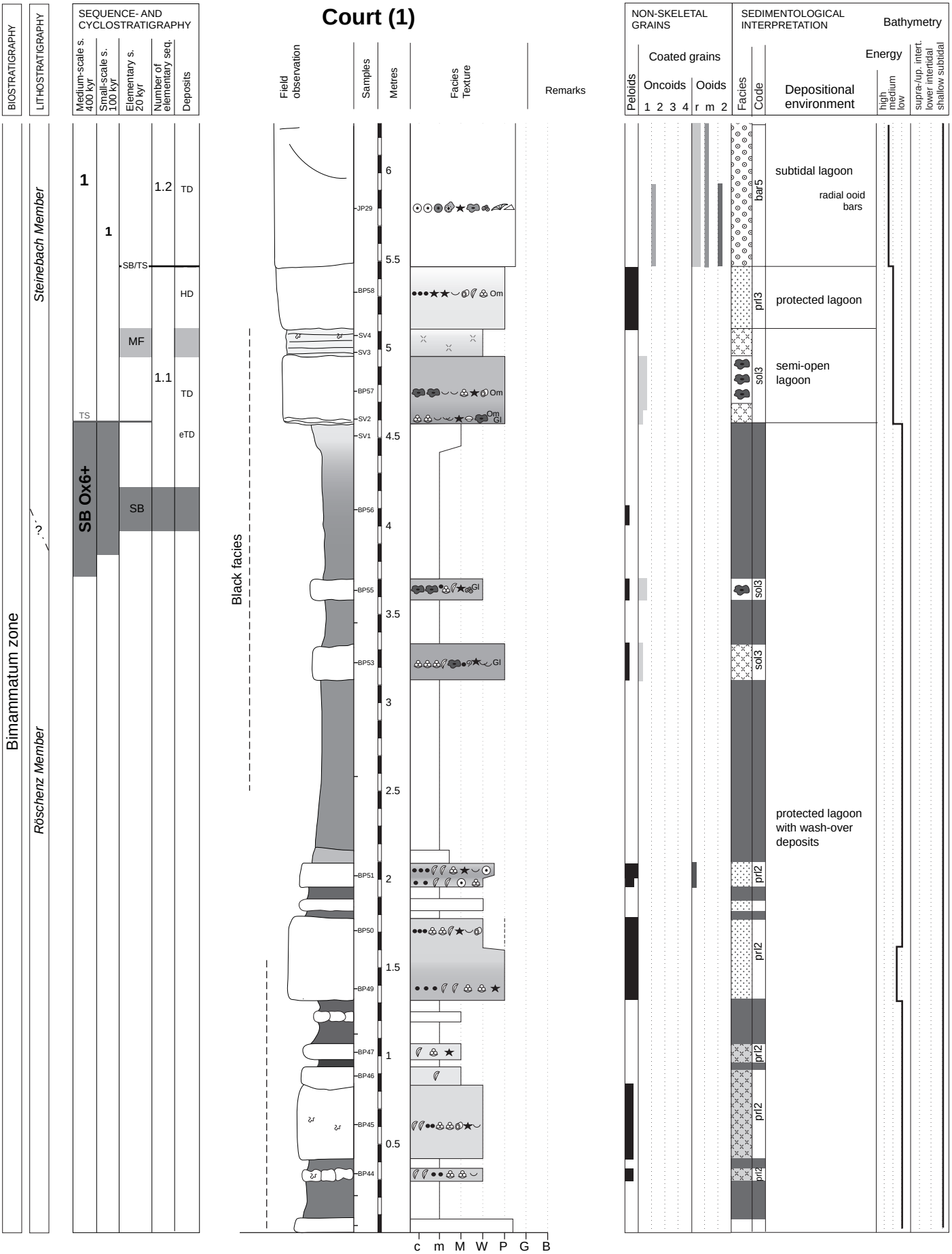

Fig. 4.11a - Court section (1).

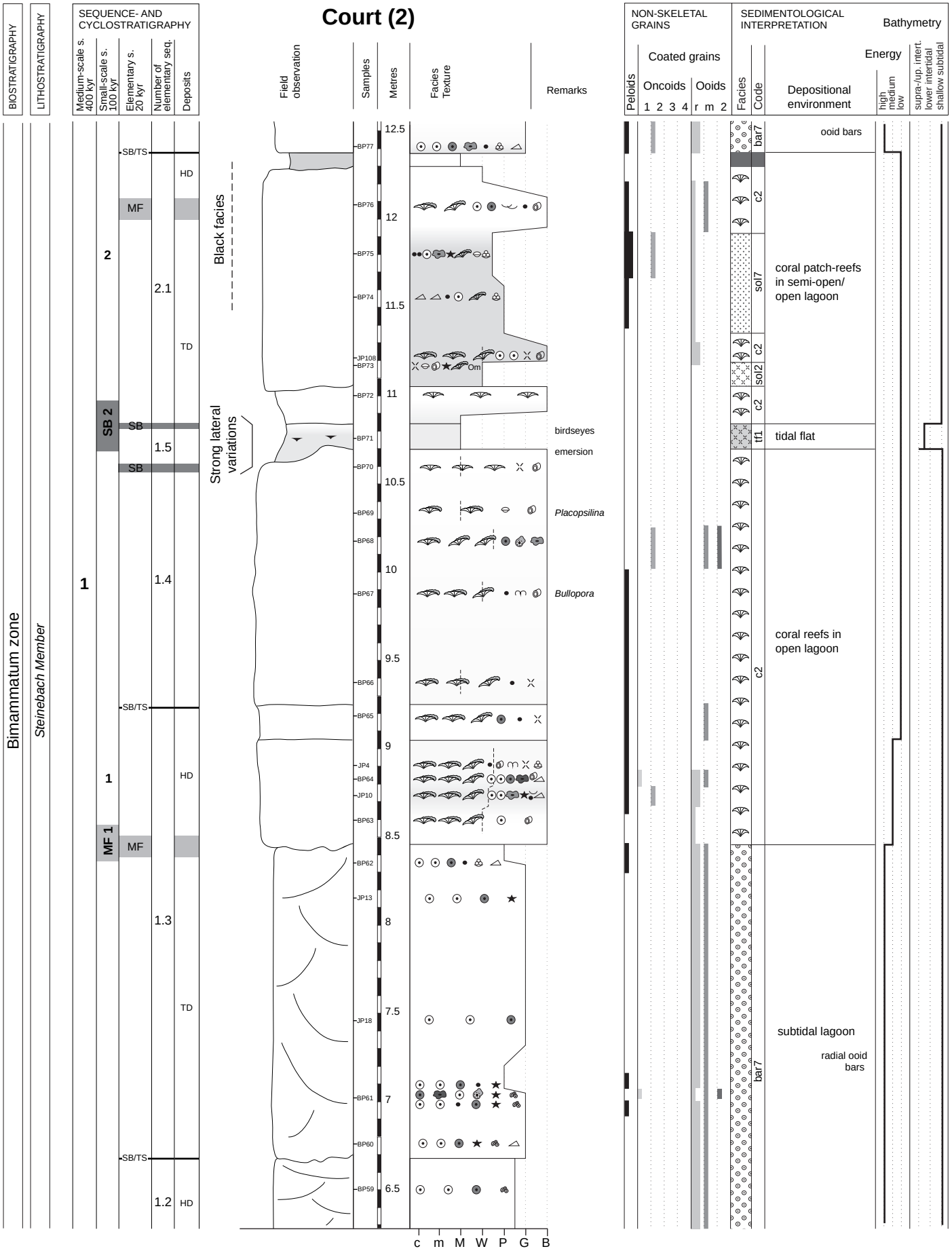

Fig. 4.11b - Court section (2).

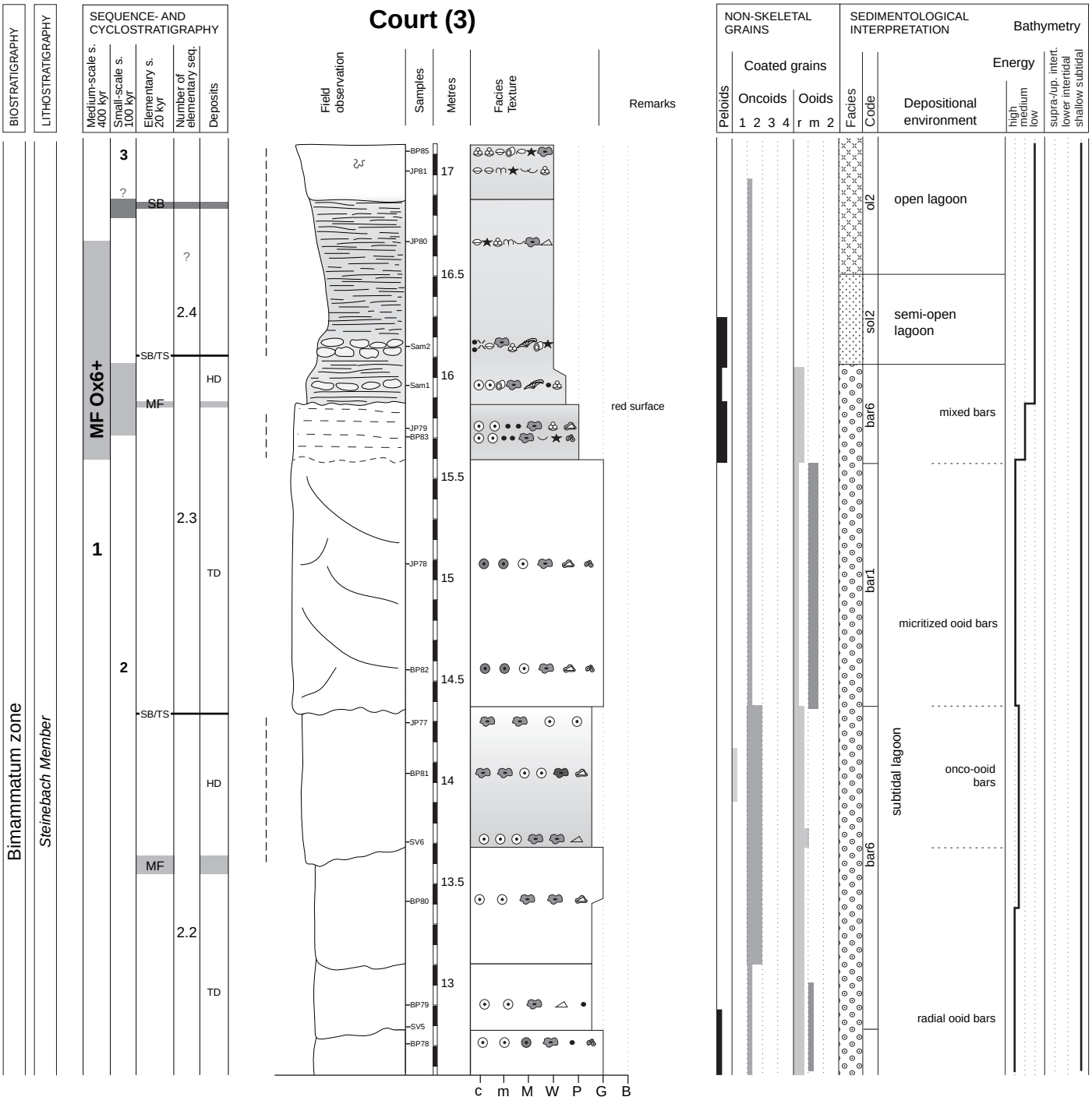

Fig. 4.11c - Court section (3).

studied section is about 17 m thick and exposes the top part of the marly Röschenz Member and the ooid-rich Steinebach Member.

Sedimentological interpretation

The base of the section is characterized by marls with local wash-over deposits (packstones-wackestones) rich in quartz, peloids, ostracodes, and benthic foraminifera (Fig. 4.11). This suggests protected conditions with storm influence (Pittet 1996). Then, massive packstone beds appear (at 4.6 m) associated with a gradual decrease in quartz content and organic matter debris. These beds are interpreted as semi-open to protected lagoon deposits influenced by siliciclastic input. From 5.5 to 8.5 m, thick high-

energy (radial) ooid bars appear, which are interpreted as subtidal deposits. Then coral reefs develop in an open lagoon. The top part of these bioconstructions is very irregular and covered by tidal facies with birdseyes and undifferentiated bioclasts. The presence of birdseyes indicates a decrease of accommodation space and a shallowing of the depositional environment up to the intertidal zone.

Some coral patch-reefs again develop from 10.9 to 12.4 m in association with normal-marine fauna (e.g., brachiopods). High-energy deposits (from 12.4 m to 15.9 m), still deposited in the subtidal zone, then follow. From 13.7 to 14.35 m, detrital quartz, more type 2 oncoids and even some type 1 oncoids are noticed and suggest a hydrodynamic change to lower energy associated with a minor siliciclastic input. These thick deposits are overlain (from 15.6 to 15.85 m) by an ooid-peloid packstone bed with horizontal laminations and a small amount of quartz. This bed indicates lower energy conditions. Its wavy surface (at 15.9 m), probably bioturbated, and the red coloration point to a period of sediment starvation. The following succession (from 16 to 17.15 m) consists of bioclastic wackestone rich in normal-marine fauna (corals, calcareous sponges, and brachiopods) and quartz. It is interpreted as semi-open to open lagoonal deposits.

Sequence-stratigraphic interpretation

The marly interval reveals protected lagoonal facies and is a candidate for medium-scale SB Ox6+. The rapid facies change (at 4.6 m) toward limestone-dominated facies suggests an increase of carbonate productivity due to the flooding of the platform during sea-level rise. This limit is considered to represent the transgressive surface TS Ox6+, previously identified by Pittet (1996) as the long-term TS 1.

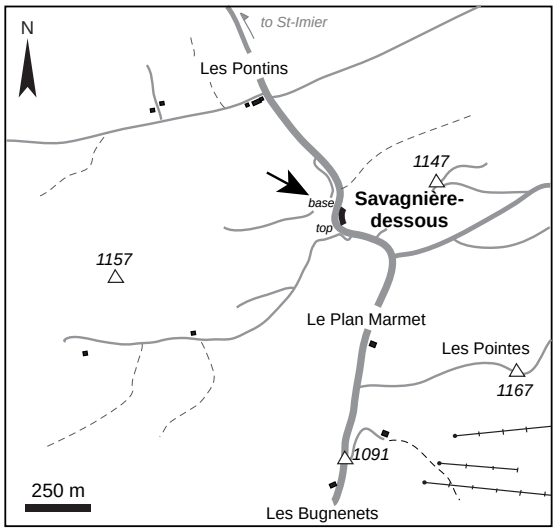

Fig. 4.12 - Location of the Savagnières section. Based on topographic map of Les Bois (1124), Carte nationale de la Suisse, 1:25 000.

Small-scale sequence 1 consists of five elementary sequences. The first elementary sequence displays massive packstone beds. The transgressive deposit is relatively rich in oncoids and the highstand deposit is placed in the more marly limestone with bioturbations. The second elementary sequence is entirely made of high-energy deposits, which makes the identification of sequence-stratigraphic elements difficult. The transgressive deposit of the third elementary sequence is also composed of high-energy deposits and the highstand deposit consists of coral bioconstructions. The fourth elementary sequence is entirely made of coral bioconstructions. The fifth elementary is the thinnest sequence but has large lateral thickness variations due to the platform morphology created in particular by coral patch-reefs.

The small-scale SB 2 is assumed to be located in the tidal-flat facies with birdeyes representing the shallowest facies. Small-scale sequence 2 also consists of five elementary sequences. The first elementary sequence consists of a relatively massive bed mainly dominated by corals. The overlying marly interval is considered to represent the sequence boundary of the second elementary sequence. The second and third elementary sequences are entirely composed of ooid-rich bars making their sequence-stratigraphic interpretation uncertain. However, the well-marked surface at 15.9 m, at the top of an ooid bar, is interpreted as the maximum-flooding surface of the third elementary sequence. By lateral correlation, this maximum-flooding surface is interpreted as belonging to the medium-scale MF Ox6+.

Savagnières (Figs 4.12 and 4.13a-b; Pl. 14/2)

Geography and stratigraphy

The Savagnières section, on the top of the Chasseral anticline, is approximately situated at half way between Les Bugnenets and Les Pontins, along the road relating Val-de-Ruz to St-Imier (Fig. 4.12). The Savagnières section is about 12.5 m thick and dominated by limestones. No important marl/clay deposits exist, contrary to all the other sections.

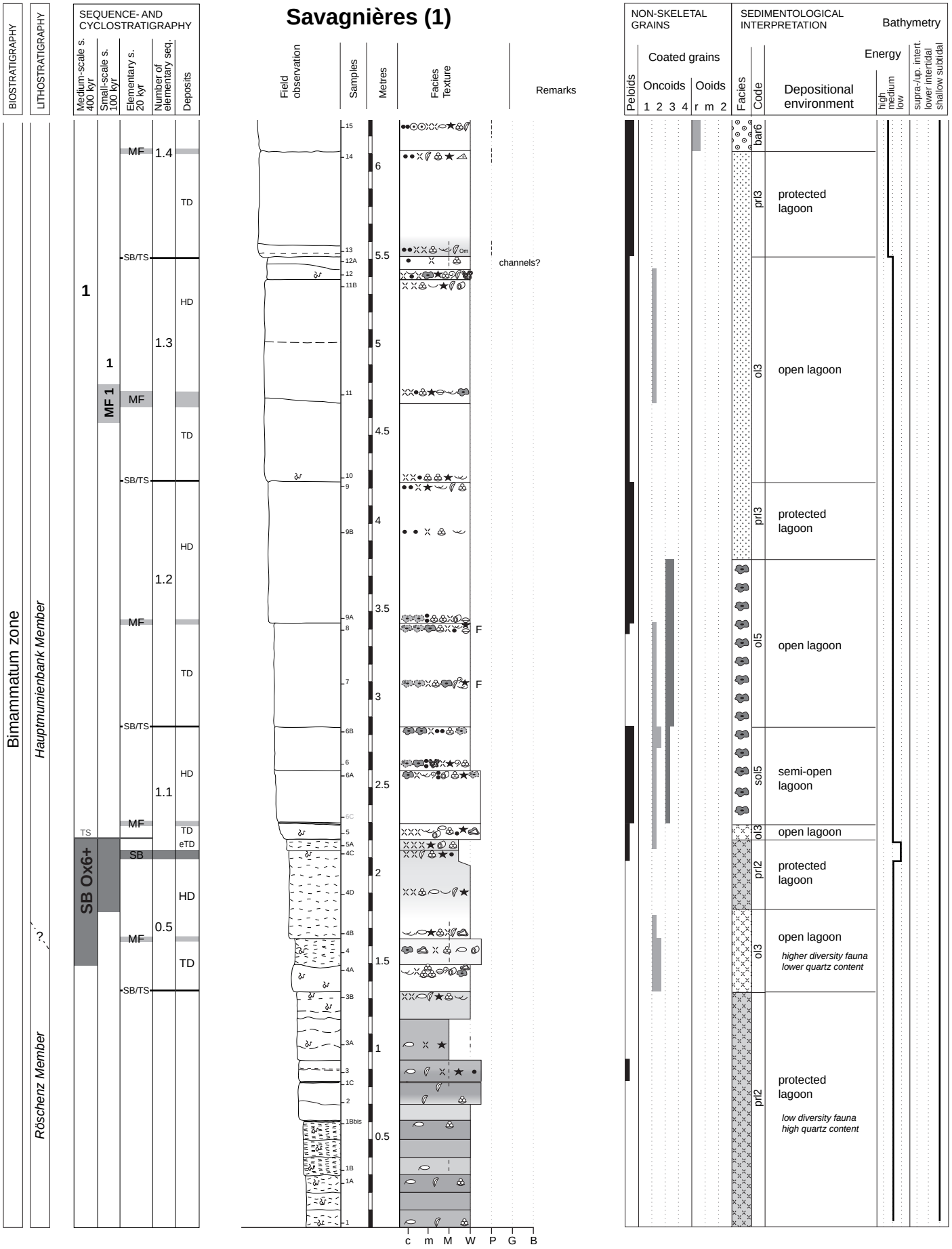

Fig. 4.13a - Savagnières section (1).

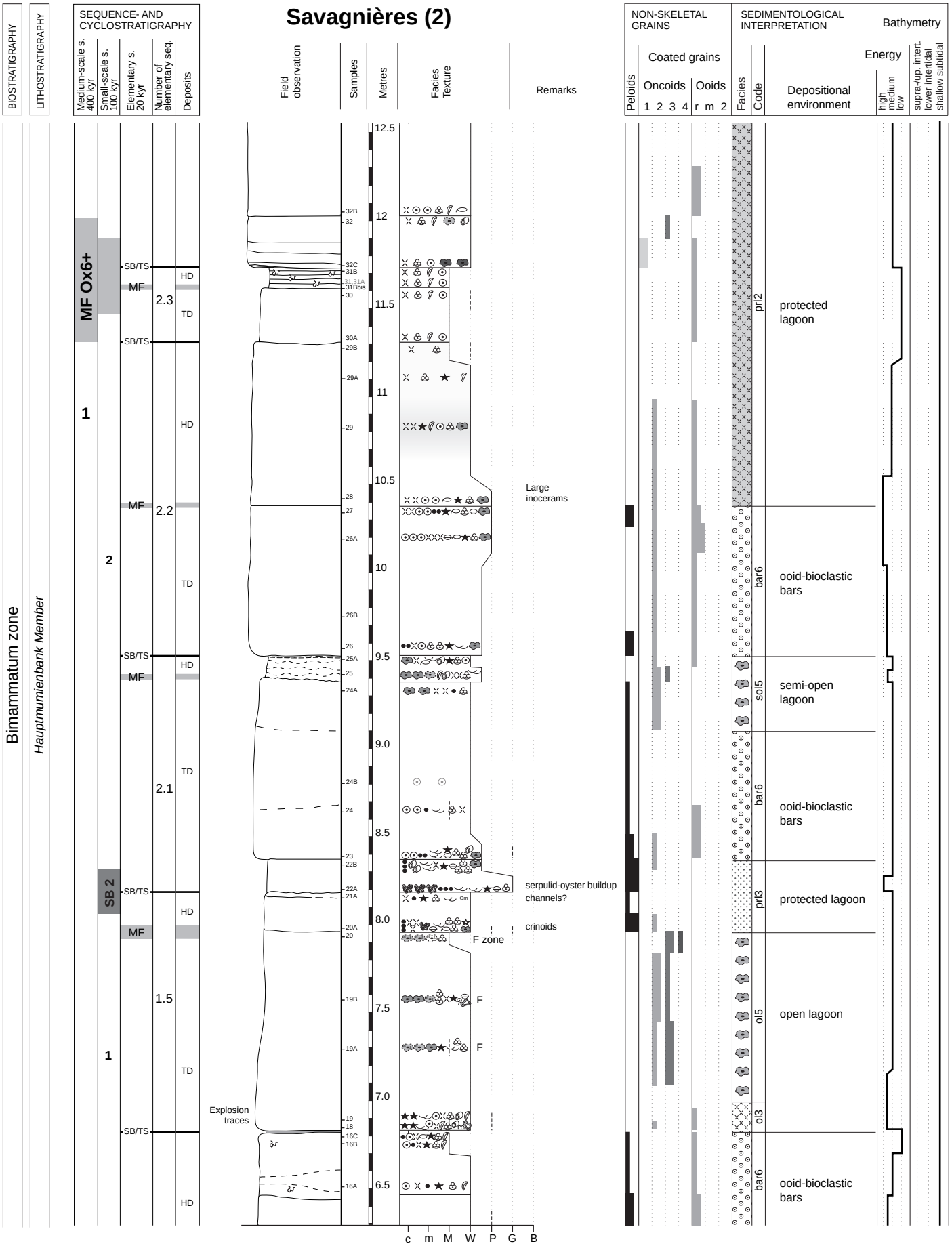

Fig. 4.13b - Savagnières section (2).

Sedimentological interpretation

The base of the section (from the base to 2.2 m) is characterized by thin nodular limestone beds mainly interpreted as protected lagoonal deposits. From the base to 1.35 m, the beds are bioturbated wackestones to mudstones rich in quartz and with a low-diversity fauna (i.e., ostracodes and inocerams). The following beds (from 1.35 to 1.8 m) show a higher-diversity fauna and a decrease of quartz content, indicating a slight opening of the depositional environment. Then, the inverse trend is observed (from 1.8 to 2.2 m) to less-diversified fauna and a smaller amount of quartz.

The deposition of relatively thick massive limestones and the disappearance of siliciclastics imply an important increase of accommodation space. Massive and thick beds from 2.3 to 2.85 m are packstones-wackestones composed of type 2 oncoids, interpreted as semi-open lagoonal deposits. The following beds from 2.85 to 3.8 m are wackestones composed of *Bacinella-Lithocodium* (type 3) oncoids and are interpreted as open lagoonal deposits. The peloid wackestones from 3.8 to 4.25 m are interpreted as relatively protected lagoonal deposits, whereas the bioclastic wackestones from 4.25 to 5.4 m are attributed to relatively open lagoonal deposits. Thinner beds (from 5.35 to 5.5 m) are considered as small channels. This succession (from 2.2 to 5.5 m) shows a thickening- and then thinning-up trend, suggesting accommodation space variations. At the base of the following bed (5.5 m), which is a peloid-bioclast wackestone, quartz reappears and rapidly disappears. From 6.1 to 6.85 m, some radial ooids are mixed with peloids and bioclasts pointing to the proximity of ooid bars. The following bed is characterized by echinoderm- and oyster-rich wackestone at its base, and by *Bacinella-Lithocodium* oncoid floatstone. This bed represents an open lagoonal environment. In the following thin bed (from 7.95 to 8.2 m), changes of texture and grain content point to relatively higher energy conditions in a shallower environment.

At 8.2 m the texture and facies change from (undifferentiated) bioclast wackestone to serpulid- and oyster-rich grainstone indicates a water energy change, probably related to a decrease of the accommodation space. This high-energy level contains a serpulid-oyster buildup. The following facies consist of peloid-bioclast wackestone-packstone (from 8.3 to 8.4 m), interpreted as relatively protected lagoon deposits, ooid-bioclast wackestones (from 8.4 to 9.1 m), interpreted as bar deposits, and type 2 oncoid wackestones-packstones (from 9.1 to 9.55 m), interpreted as semi-open lagoonal deposits. Then radial ooid- and peloid-rich packstone beds are deposited from 9.55 to 10.5 m and suggest the migration of oo-bioclastic bars abandoned in a shallow subtidal environment. A thinning-up trend from massive, thick beds to thin highly bioturbated beds is noticed from 9.55 to 11.75 m and is associated to a texture change from packstone-wackestone to mudstone and to a decrease of fauna diversity. This evolution points to decreasing energy probably due to protection behind a shoal field. In addition, the intense bioturbation in the thinnest beds probably resulted from a lower accumulation rate during a deepening phase. At the end of the section, thicker wackestone beds (at 11.75 m) dominate, suggesting a higher accommodation.

Sequence-stratigraphic interpretation

The medium-scale SB Ox6+ is placed in the nodular sandy limestones (2.1-2.2 m), interpreted as protected lagoon deposits. The base of the first massive limestones (at 2.2 m), showing the opening of the depositional environment, is interpreted as the medium-scale TS Ox6+, previously interpreted by Pittet (1996) as a long-term transgressive surface. This evolution points to a relative sea-level rise.

Small-scale sequence 1 consists of five elementary sequences. The first elementary sequence is composed of four wackestone-packstone beds. The first two beds, mainly composed of bioclasts, are interpreted as the early transgressive deposit and the transgressive deposit, respectively. The two following beds, dominated by oncoids, are interpreted as the highstand deposit. The maximum flooding is assumed to be located at 2.3 m between the second and third bed where laminations exist. The second elementary sequence consists of two thick and massive beds. The first bed is interpreted as the transgressive deposit and the second as the highstand deposit. The maximum-flooding surface is assumed to be located between these two beds (at 3.45 m) where *Bacinella-Lithocodium* oncoids, brachiopods, and benthic foraminifera are abundant. In the third elementary sequence, the maximum-flooding surface is placed at the top of the first bed where brachiopods are present. The top of the highstand deposit presents tidal channel structures, suggesting a decrease of accommodation space. The fourth elementary sequence consists of three beds. The maximum flooding is assumed to be located between the first and second bed. The fifth elementary sequence consists of two beds: one thick bed and one thinner

bed. The maximum flooding is placed at the *Bacinella-Lithocodium* oncoid-rich mudstone level (7.9 m).

The thin wackestone bed at the top of the fifth elementary sequence announces an important relative sea-level fall. The serpulid-oyster build-up is considered to represent the small-scale SB 2. In small-scale sequence 2 only the first three elementary sequences have been investigated. The transgressive deposit of the first elementary sequence consists of two beds. The second bed presents a slightly wavy surface, probably due to intense bioturbation. It is interpreted as the maximum-flooding surface. The following nodular bed is considered to represent the highstand deposit. The second elementary sequence consists of an ooid-rich transgressive deposit and a bioclastic highstand deposit. The third elementary sequence is composed of a massive bed, interpreted as the transgressive deposit and a level of thin bioturbated beds, interpreted as the highstand deposit. The top of this massive bed (at 11.6 m) is interpreted as the maximum-flooding surface. This MFS is attributed to the medium-scale MF Ox6+ by lateral correlation.

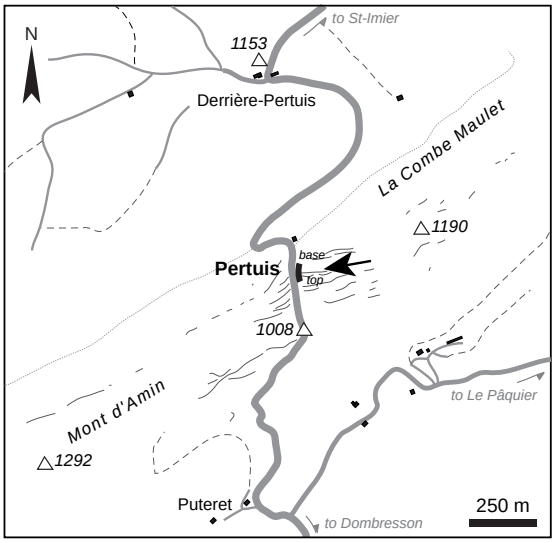

Fig. 4.14 - Location of the Pertuis section. Based on topographic map of Val de Ruz (1144), Carte nationale de la Suisse, 1:25 000.

Pertuis (Figs 4.14 and 4.15a-c; Pl. 14/3)

Geography and stratigraphy

The Pertuis section is located on the southern flank of the Mont d'Amin anticline halfway between Les Bugnenets and Vue des Alpes. The outcrop is along the road leading to Val de Ruz in direction of Dombresson (Fig. 4.14). The section begins after a forest clearing with a parking lot and old wood constructions. The section is about 15.5 m thick and exposes the top part of the clay-rich Röschenz Member, almost totally covered by vegetation, and the oncoid-rich Hauptmumienbank Member.

Sedimentological interpretation

This section presents three different intervals: (1) a marl-dominated interval with high quartz content in the limestones (from base to 3.85 m), (2) a limestone interval (from 3.85 to 12.7 m) and, (3) limestone-dominated interval with high quartz content (from 12.7 to 14.5 m). The base of the section (from base to 1.5 m) is characterized by marls with a low diversity fauna and plant debris, interpreted as protected lagoonal deposits. The following succession (from 1.2 to 3.85 m) consists of marls and peloid/bioclastic wackestones with a more diversified and normal-marine fauna (e.g., brachiopods) and high quartz content. These deposits are interpreted as semi-open lagoonal deposits.

The deposition of massive and thick oncoid-rich limestones (from 3.85 m) associated with the disappearance of detrital quartz marks an increase of accommodation space and deepening of the depositional environment. The first limestone beds are wackestones-packstones rich in radial ooids and/or type 3 and 2 oncoids (from 3.85 to 5.5 m), pointing to more open-marine environments. After these ooid-rich facies, *Bacinella-Lithocodium* (type 3) oncoid wackestones to floatstones predominate (from 5.5 to 9.3 m). This facies indicates lower-energy conditions in an open lagoon and thus reflects an important deepening of the depositional environment. It coincides with a thickening-up trend (from 5.5 to 10.7 m) that points to an increase of the accommodation space. The following beds are peloid-foraminifer wackestones (from 9.3 to 11.4 m), interpreted as open lagoonal deposits, and bioclastic mudstones with a small amount of quartz (from 11.4 to 12.05 m) interpreted as protected lagoonal deposits. This facies evolution and bedding pattern from 9.3 m upward point to a shallowing of the depositional environment and decrease of accommodation space. In addition, a change of oncoid types (from 11.8 to 12.0 m) in a mudstone bed from *Bacinella-Lithocodium* (type 3) oncoids to micrite-dominated (type 2) oncoids suggests an environmental change probably due to more eutrophic conditions (cf. Chap. 7).

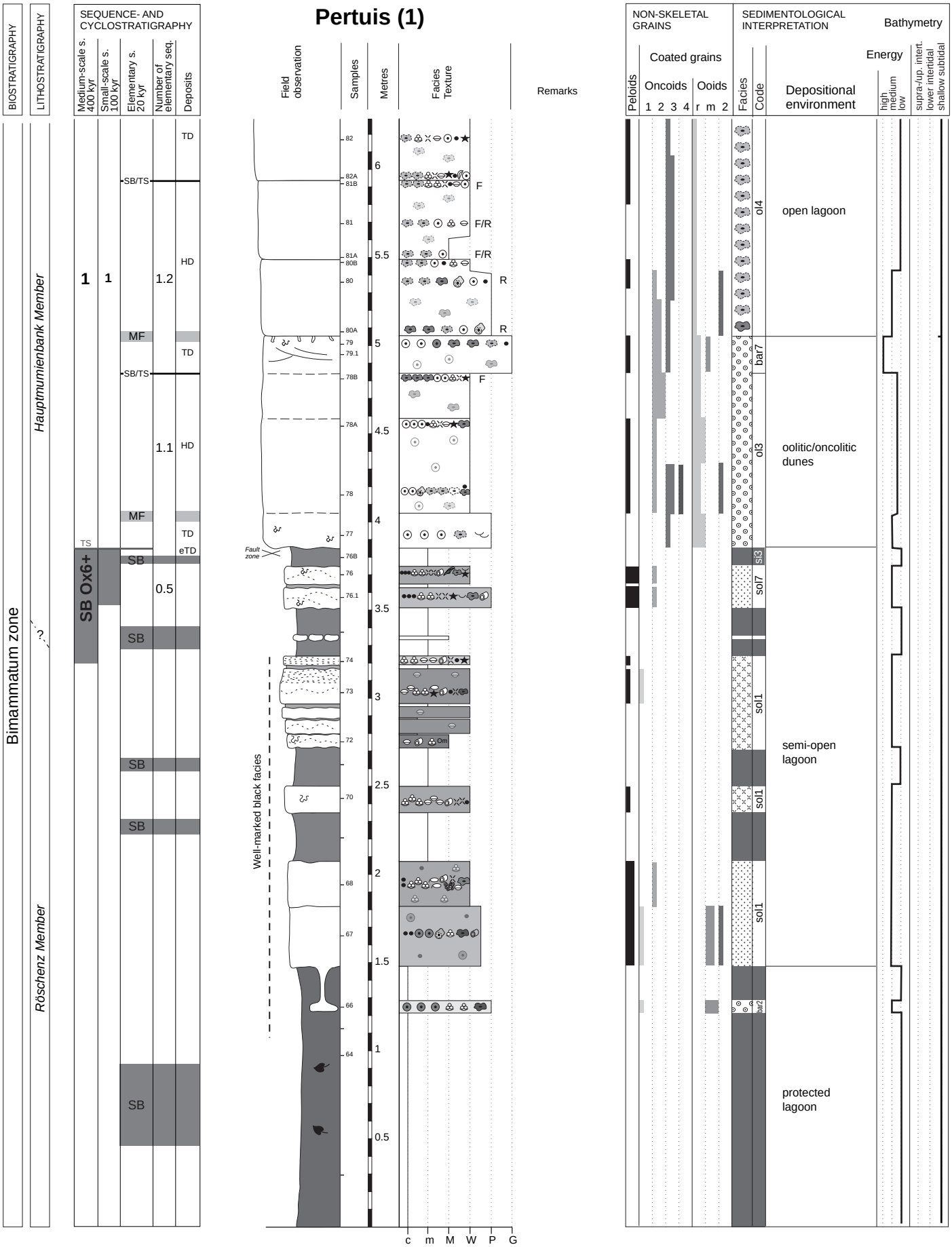

Fig. 4.15a - Pertuis section (1).

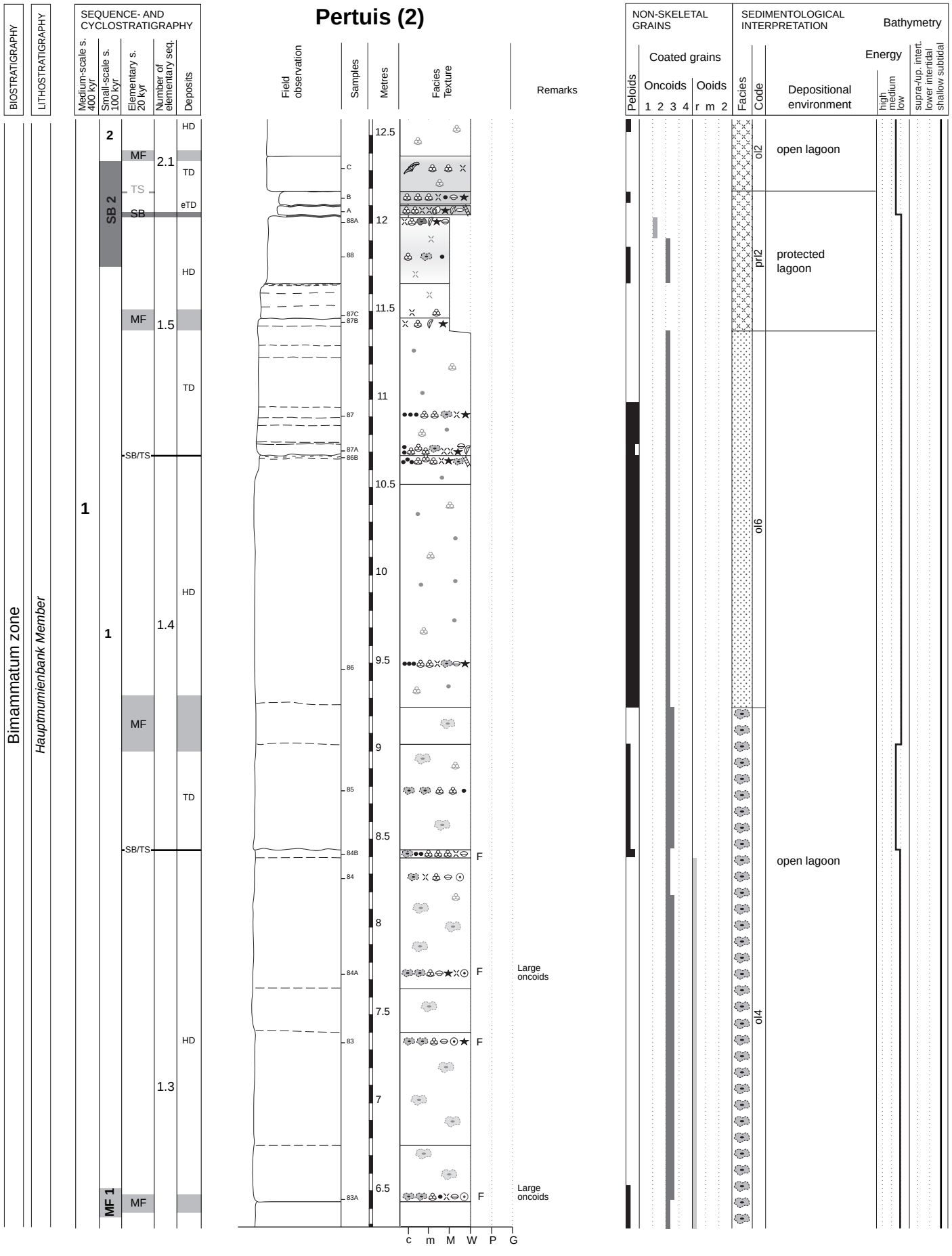

Fig. 4.15b - Pertuis section (2).

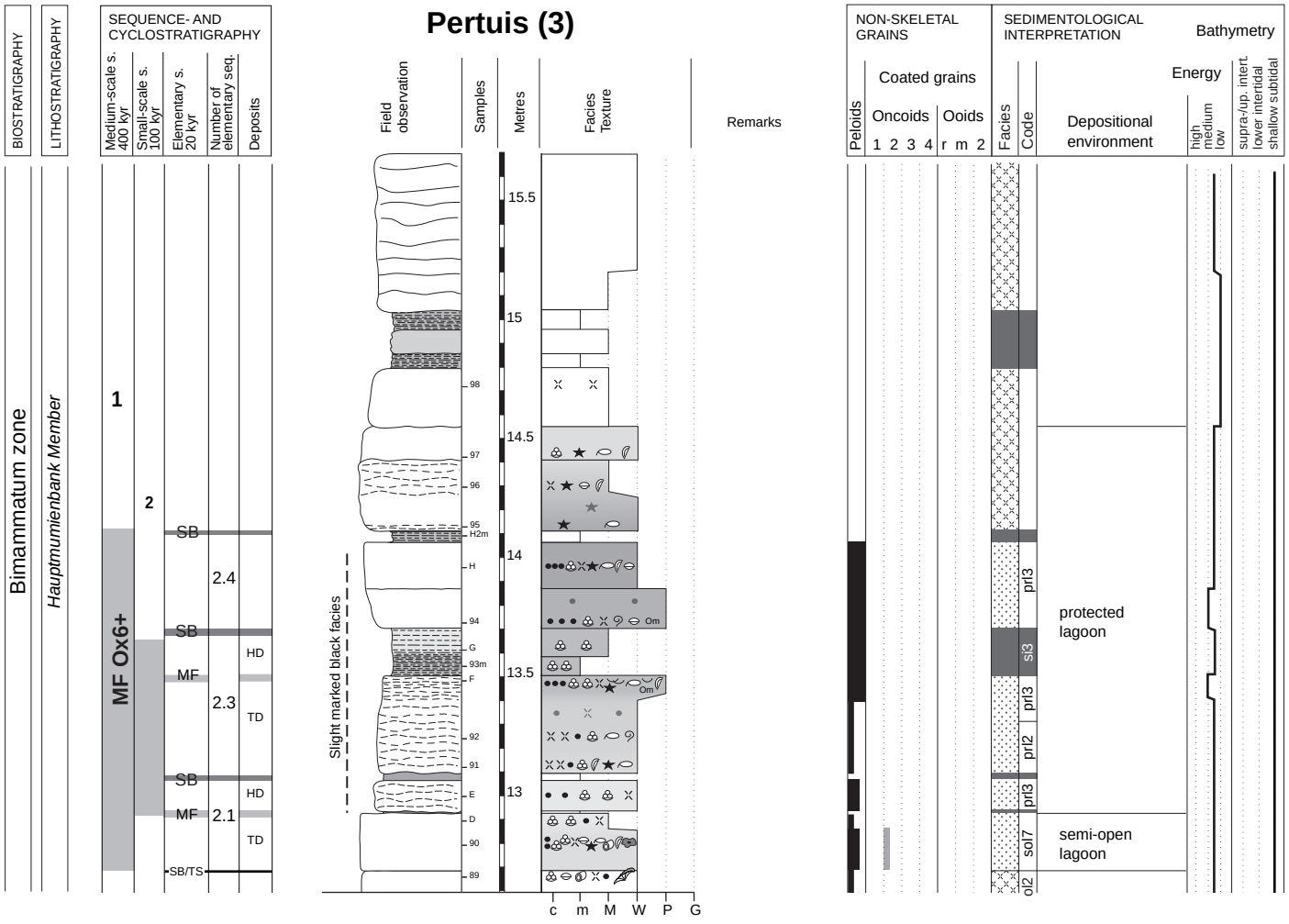

Fig. 4.15c - Pertuis section (3).

The following deposits consist of two slightly undulating beds interbedded with very thin marly layers. These beds consist of foraminifer wackestones with quartz and correspond to a protected lagoonal environment. Then, three relatively thick and massive bioclastic (e.g., benthic foraminifera, coral rubble) wackestones (from 12.3 to 12.95 m) are deposited and point to a new increase of accommodation space. The two following beds are nodular peloid-bioclast wackestones-packstones with quartz that are separated by a thin marly interval (at 12.95 m). The second bed is thicker than the first one and finely laminated in its top part. This bed is followed by a marly interval rich in quartz and benthic foraminifera (from 13.5 to 13.7 m). All deposits from 12.95 to 14.55 m are interpreted as relatively protected lagoonal deposits. The return to more massive limestone beds (at 13.7 m) points to an opening of the environment.

Sequence-stratigraphic interpretation

The facies change from marl-dominated to limestone-dominated facies suggests an opening of the environment with a significant decrease of siliciclastics. This facies change at 3.85 m is interpreted as a transgressive surface and as belonging to the medium-scale TS Ox6+. Pittet (1996) also interpreted this surface as a long-term transgressive surface. Consequently, the marly interval (3.75-3.85 m), below the base of the massive limestones, is interpreted as the sequence boundary and as belonging to the medium-scale SB Ox6+. This facies evolution indicates an important relative sea-level rise associated with an increase of accommodation space.

Small-scale sequence 1 consists of five elementary sequences. The first elementary sequence is dominated

by massive ooid-rich deposits. The interval with more *Bacinella-Lithocodium* oncoids (from 4.05 to 4.2 m) is interpreted as the maximum flooding. The transgressive deposit of the second elementary sequence consists of an ooid-dominated grainstone with cross-stratifications. Its top (at 5.05 m) reveals bioperforations and is assumed to represent the maximum-flooding surface. The two following beds consist of *Bacinella-Lithocodium* oncoid rudstones to floatstones and are interpreted as the highstand deposit. The third elementary sequence is the thickest sequence of the section and implies maximum accommodation gain. It consists of massive *Bacinella-Lithocodium* oncoid floatstones interpreted as open lagoon deposits. The fourth elementary sequence is also thick and composed of open lagoon facies: oncoid wackestones in the transgressive deposit and peloid-foraminifer wackestones in the highstand deposit. The transgressive deposit of the fifth elementary sequence consists of thin peloid wackestone beds, interpreted as open lagoonal deposits and the highstand deposit consists of more bioclastic mudstones, interpreted as more protected lagoonal facies. The general facies evolution from the third to the fifth elementary sequence points to general loss of accommodation.

The two slightly undulated beds rich in quartz and benthic foraminifera (from 12.05 to 12.2 m) and interbedded with very thin marly layers are interpreted as the small-scale SB 2. Small-scale sequence 2 presents thinner sequences than small-scale sequence 1. In the second small-scale sequence, only four elementary sequences have been examined. The first one consists of two undulated beds, interpreted as the early transgressive deposit and two more massive beds interpreted as the transgressive and highstand deposits, respectively. The second elementary sequence is relatively thin and consists of two peloid and foraminifer wackestone-mudstone beds with quartz, interpreted as the transgressive and highstand deposits, respectively. These beds are separated by a thin marly interval interpreted as the maximum flooding. The third elementary sequence consists of a nodular limestone bed and a marly interval, interpreted as the transgressive and highstand deposits, respectively. The maximum-flooding surface of this elementary is assumed to be located on the top of the nodular limestone bed. This MFS is correlated with the medium-scale MF Ox6+. The fourth elementary sequence is composed of two massive limestone beds, corresponding to the transgressive deposits and a thin marly interval that is thought to represent to the highstand.

Synthesis of the Swiss Jura sections

Detailed facies analyses of the sections allows to sketch the platform morphology at different time intervals (cf. Chap. 7). The facies distribution and thickness variations along the six studied sections point to a complex platform morphology with high areas and depressions, where silisiclastics preferentially accumulated.

The Voyeboeuf and Savagnières sections mainly reveal low-energy facies without important clay deposits and imply relatively protected environments. The geographical position of the Voyeboeuf section suggests a proximal position in comparison to the other sections. The Vorbourg section reveals more open-marine environments with bioclastic (coral rubble, brachiopods), oncolitic, and oolitic deposits. The low thickness of the Hautes-Roches section and the dominance of high-energy ooid deposits suggests a high position on the platform. The development of ooid bars but also of coral patch-reefs and carpets in the Court section points to normal-marine conditions in open lagoonal environments. The Pertuis section is dominated by open-marine facies, characterized by *Bacinella-Lithocodium* oncoids, peloids, and bioclasts. This indicates a relative distal position on the platform. As in the Savagnières section, the deposits of small-scale sequence 2 present more protected facies probably caused by the development of a barrier in distal position.

Through all the sections, siliciclastics (quartz and clays) preferentially occur in protected lagoonal environments.

4.1.2 Lorraine

Pagny-sur-Meuse (Figs 4.16 and 4.17a-b; Pl. 15/1-7, Pl. 16/1-3)

Geography and stratigraphy

The Pagny-sur-Meuse section is located 33 km west of Nancy in a large quarry exploited by the Novacarb society (Fig. 1.2c and 4.16). It provides fresh accessible outcrops due to continuous quarrying. These outcrops reveal Middle to Late Oxfordian deposits from the Lorraine shallow-water carbonate platform. Such outcrop conditions are favorable for detailed sedimentological and geochemical studies

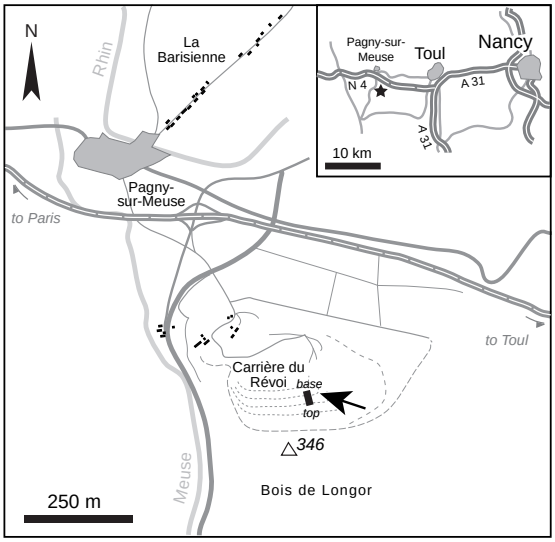

Fig. 4.16 - Location of the Pagny-sur-Meuse. Based on topographic map of Toul (3315O), IGN Topo 25 series.

(e.g., Vincent 2001; Carpentier 2004; Olivier et al. 2004a; Carpentier et al. 2006).

Logged in the upper part of the quarry, the section is about 10 m thick and exposes facies of the *Calcaires à polypiers de Pagny* (CPP), the *Oolithe de Saucourt inférieure* (OSI), and the *Marnes à huîtres de Pagny* (MHP) members (Fig. 4.17). A brief description of these members is given in Chap. 1. The biostratigraphic position of the Pagny-sur-Meuse section is based on the discovery of two ammonites, one at the base and the other at the top of the *Calcaires à polypiers de Pagny* (c.f. Fig. 4.17; Carpentier 2004). They indicate that the Bifurcatus-Bimammatum limit is positioned within the "Calcaires à polypiers de Pagny" and that the overlying deposits (the *Oolithe de Saucourt inférieure*, the *Marnes à huîtres de Pagny*, the *Oolithe de Saucourt supérieure*, and the *Marnes à serpules de Pagny*) are dated of the Bimammatum zone (Carpentier 2004; Carpentier et al. 2006).

The section has been logged through the *Oolithe de Saucourt inférieure* and the *Marnes à huîtres de Pagny*, which are situated in the lower part of the Bimammatum zone and thus are more or less time equivalent to the studied interval in the Swiss Jura.

Sedimentological interpretation

The base of the Pagny-sur-Meuse section is composed of relatively thick dark limestones (packstone-wackestone) with bioclasts, ooids, and locally detrital quartz. A packstone level of reworked and perforated mud pebbles occurs from 2.3 to 2.5 m. Laterally, these limestones pass into coral bioherms. These deposits represent an open lagoonal environment with local coral patch-reefs.

A decrease of accommodation space and a shallowing of the depositional environment are displayed by the marly interval (from 3.4 to 4.6 m) in the top part of the *Calcaires à polypiers de Pagny*. Marls are interbedded with argillaceous limestones, which are rich in bioclasts (e.g., oysters, echinoderms), quartz, and locally glauconite. The maximum of shallowing (4.55 m) is indicated by a reduction of faunal diversity (mainly ostracodes, gastropods, oysters) and coal debris. The following interval consists of marls (from 4.7 to 5.05 m) with lenticular bedding, commonly found in mud flats, and local coal debris (at 5 m). This interval reveals the shallowest facies corresponding to a low-energy environment (mud-dominated) with tidal currents (lenticular bedding).

The following deposits (from 5.05 to 7.65 m) consist of massive limestones rich in oysters and ooids. This abrupt lithological change points to an increase of the accommodation space during a deepening phase. The first carbonate bed has an erosive base (at 5.05 m), a wavy bed surface and consists of bioturbated (horizontal burrows) ooid- and oyster-rich grainstone-packstone. This bed presents important thickness variations and is interpreted as an ooid bar deposit. A tidal influence is demonstrated by herringbone cross-stratifications that indicate a bi-directionnal current. The following limestone beds (from 5.1 to 6.55 m) consist of oyster- and ooid-rich grainstone-packstone. Tidal influence is only observed at the base of these deposits from 5.05 to 5.45 m, suggesting a deepening of the depositional environment. At the top of a massive bed (at 6.55 m), an oyster accumulation (lumachella) probably reflects a reduction of the sedimentation rate. This level is followed by a relatively thin argillaceous oo-bioclastic (oysters, echinoderms) packstone with some quartz.

The deposition of three massive ooid- and oyster-rich packstone to grainstone beds (from 6.65 to 7.65 m), interpreted as ooid dunes (Pl. 15/6-7), points to a new increase of accommodation space and/or local migration of subtidal ooid bars. The top part of the third bed (at 7.55 m) is a wavy surface with oyster encrustations on top of the dunes and mud in depressions (Pl. 15/7). This remarkable surface is interpreted as a subtidal hardground, pointing to a period of sediment

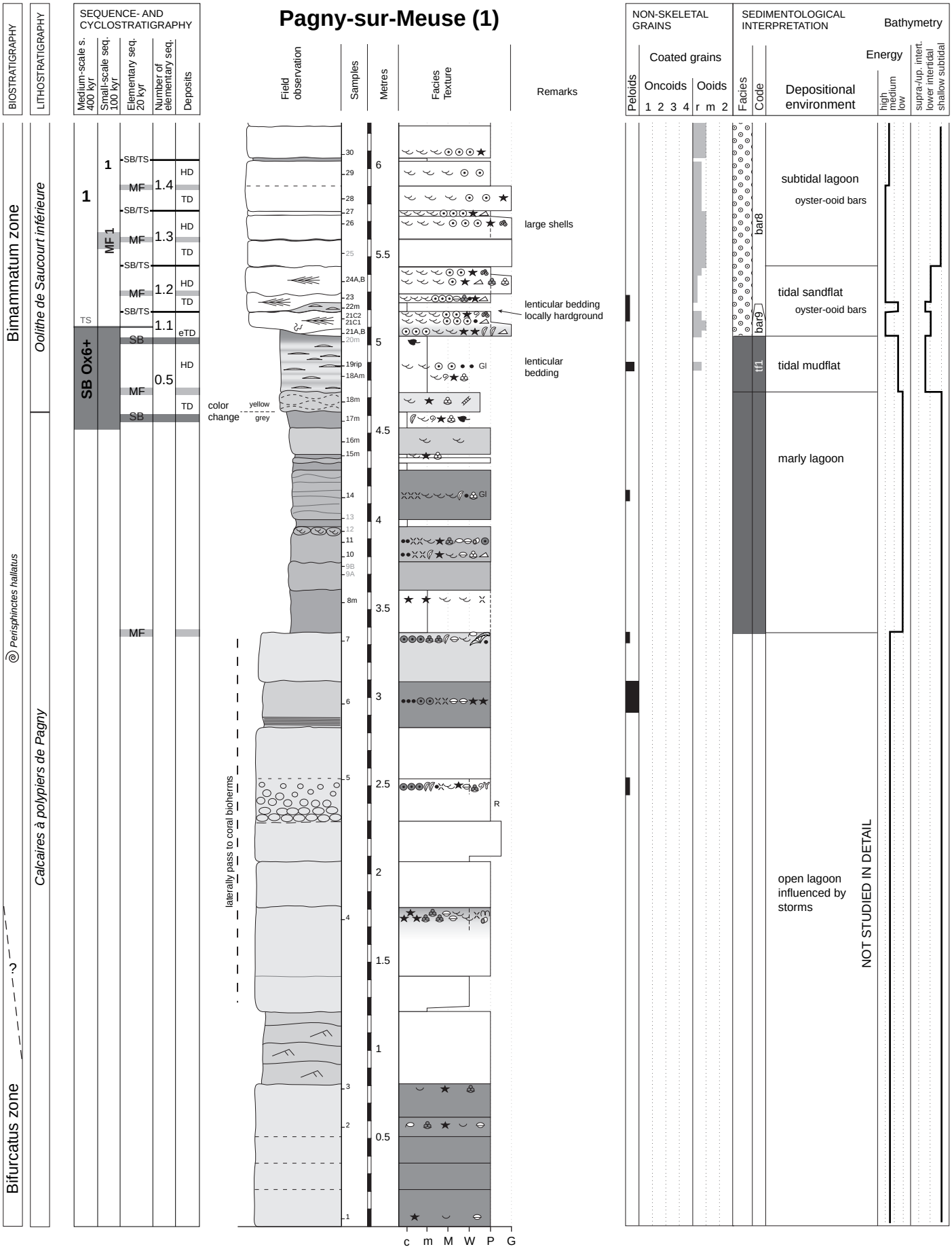

Fig. 4.17a - Pagny-sur-Meuse section (1).

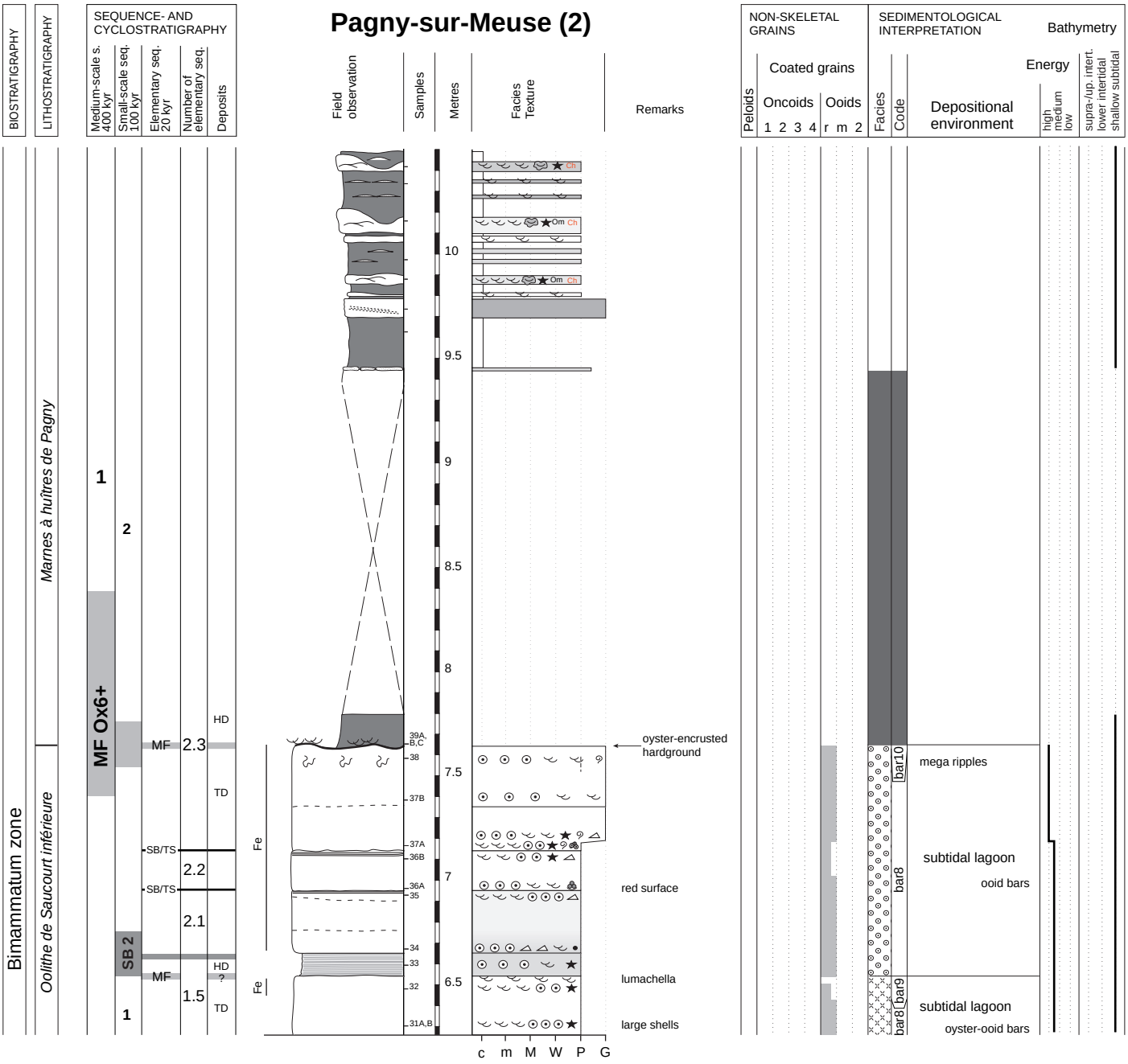

Fig. 4.17b - Pagny-sur-Meuse section (2).

starvation. Finally, marls, belonging to the *Marnes à huîtres de Pagny*, cap the ooid dunes. This facies change points to the turnover towards a siliciclastic-dominated sedimentary system, probably caused by a climatic change to more humid conditions.

Sequence-stratigraphic interpretation

Marls (from 4.75 to 5.05 m) with lenticular bedding, characteristic of upper intertidal environments, represent the shallowest facies and are interpreted as the medium-scale SB Ox6+. The base of the massive limestone is interpreted as the medium-scale TS Ox6+. This facies evolution reflects an important relative sea-level rise.

Small-scale sequence 1 consists of five elementary sequences. The first one is composed of one or two grainstone beds with herringbone cross-stratifications and a discontinuous marly level with lenticular bedding. These deposits present important lateral thickness variations. On the top of the limestone bed

(at 5.2 m), a hardground, representing an omission period, is interpreted as the maximum flooding surface. The second elementary sequence consists of two limestone beds with typical structures of tidal currents (i.e., herringbone cross-stratifications). The maximum flooding is assumed to be located between these two beds. The third elementary sequence consists of two limestone beds separated by a thin clay-rich interval, which is interpreted as the maximum flooding. A tidal influence is not recorded in the third elementary sequence, suggesting a general deepening of the depositional environment. The fourth elementary sequence comprises two limestone beds interpreted as the transgressive deposit for the first bed and the highstand deposit for the second bed. The fifth elementary sequence consists of two relatively thick limestone beds and an argillaceous packstone bed. The first two beds are interpreted as the transgressive deposit and the thick bed as the highstand deposit. The oyster lumachella (at 6.55 m) is a good candidate for the maximum-flooding surface.

In small-scale sequence 2, only three elementary sequences are investigated. Each consists of one ooid limestone bed. The sequence boundaries are assumed to be located at the base of these beds (at 6.65 m, 6.95 m, and 7.15 m), where ooids and/or quartz and lithoclasts are more abundant. The oyster-encrusted hardground at 7.65 m is considered to represent the maximum flooding of the third elementary sequence as well as of small-scale sequence 2. By lateral correlation with the Swiss Jura sections, this maximum flooding surface is interpreted as belonging to the medium-scale MF Ox6+.

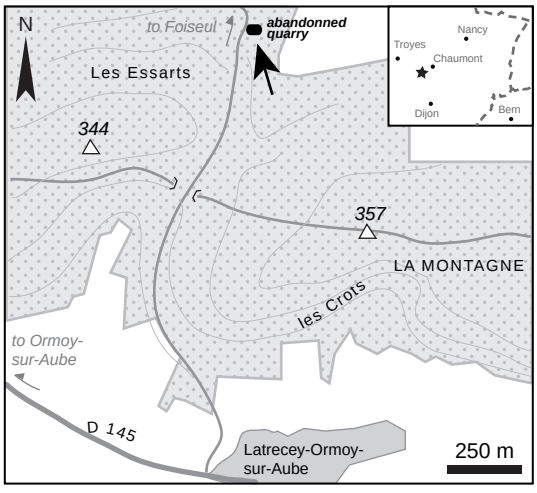

Fig. 4.18 - Location of the Latrecey-sur-Ormoy section. Based on topographic maps of Montigny-sur-Aube (3019O) and Châteauvillain (3019E), IGN Topo 25 series.

4.2 DEEP PLATFORM SECTIONS

Two sections of different geographical and palaeogeographical context as well as of different deep platform facies are investigated (cf. Chap. 1).

4.2.1 Haute-Marne

Latrecey-sur-Ormoy (Figs 4.18 and 4.19a; Pl. 16/4-5)

Geography and stratigraphy

The Latrecey-sur-Ormoy section is located in the Haute-Marne department in an abandoned quarry ("NW quarry" in COURVILLE & VILLIER 2003) close to Latrecey-sur-Ormoy (Figs 1.2c and 4.18). The logged section is only about 3.5 m thick and exposes the "Calcaires de Latrecey" This member is characterized by homogeneous carbonate facies with quite poor and poorly diversified benthic macrofauna (COURVILLE & VILLIER 2003) and represents an outer, (relatively deep) distal platform environment (cf. Chap. 1).

Lithostratigraphy and biostratigraphy of this section were first described by COURVILLE & VILLIER (2003). *Zoophycos* trace fossils commonly occur and point to offshore environments (e.g., LORIN et al 2004). Biostratigraphy is based on the discovery, at the base of the Calcaires de Latrecey, of two ammonites (*Epipeltoceras semimammatum*) indicating the beginning of the Bimammatum zone (i.e., Semimammatum subzone; COURVILLE & VILLIER 2003).

Sedimentological interpretation

This section presents homogeneous facies (always mudstones) with very poor fauna (i.e., benthic foraminifera, bivalves, echinoderms and serpulids ; Tab. 2.2). Bioturbation is commonly present, indicated by a difference of colors. At the base of the section (at 0.1m), a clay-rich level, surrounded by mudstone beds, contains coal debris. This level represents the shallowest facies of this section. From this level to 2.55 m, relatively thick limestone beds predominate. The deposition of a thin marly level at 2.55 m points to a change in the system. The following succession is formed by thinner limestone beds with more frequent clay levels. This facies change towards more clay-rich deposits indicates a generally higher terrigenous input.

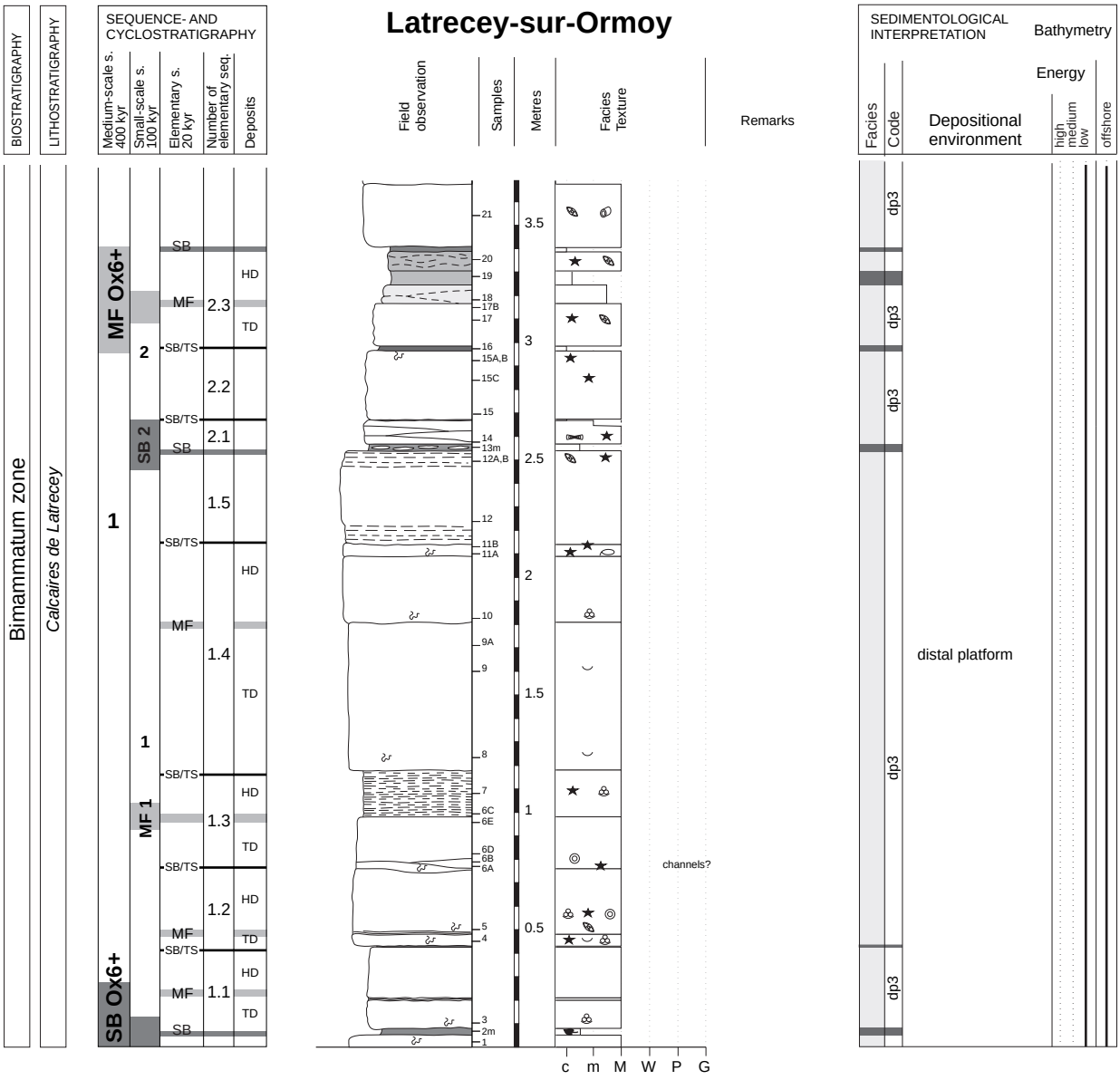

Fig. 4.19 - Latrecey-sur-Ormoy section (1).

Sequence-stratigraphic interpretation

Because of low facies variations, the sequence-stratigraphic interpretation of the Latrecey section is mainly based on the bedding pattern, the bioturbation, and some sedimentary structures. The clay-rich interval at the base of the section is interpreted as the medium-scale SB Ox6+. Small-scale sequence 1 includes five elementary sequences. Each one is composed of two beds. The maximum-flooding surface of elementary sequence 1.3 is placed at the base of the marly interval (at 0.98 m). This surface is interpreted as the maximum flooding of the small-scale sequence 1 (MF1).

The marly interval at 2.55 m is considered to represent the small-scale SB 2. In small-scale sequence 2 only three elementary were investigated. The first two elementary sequences consist of one bed. The third elementary sequence is composed of a limestone bed and a more marly interval. The maximum-flooding surface of this elementary sequence is assumed to be located at the top of the limestone bed (at 3.15 m) and is interpreted to correspond to medium-scale MFOx6+.

4.2.2 Swabian Jura

Balingen-Tieringen (Figs 4.20 and 4.21a-c; Pl. 17/1-2)

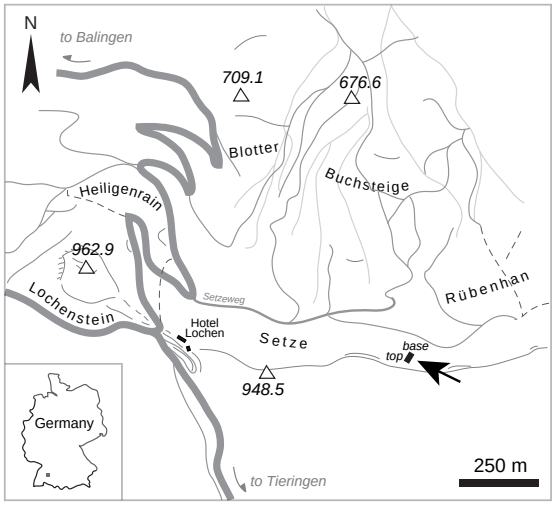

Fig. 4.20 - Location of the Balingen-Tieringen section. Based on topographic maps of Balingen (7719), TK 25.

Geography and stratigraphy

The Balingen-Tieringen section is located in the western Swabian Jura (southern Germany; Fig. 1.2c and 4.20). The section exposes deep-water carbonate facies, characterized by marl-limestone alternations and siliceous sponge facies, probably deposited in 100-200 m water depth (Olivier et al. 2004b). The studied interval concerns 14.5 m of deposits dated of the Bifurcatus and Bimammatum zones (Fig. 4.21).

Sedimentology, nannofossil assemblages, and stable isotopes of this section have already been studied by Pittet & Strasser (1998a), Pittet et al. (2000), Pittet & Mattioli 2002, and Bartolini et al. (2003). Similar sections in the Swabian Jura have also been investigated by, e.g., Olivier et al. (2004b).

Sedimentological interpretation

The Balingen-Tieringen section is marl-dominated at the base (from base to 6.4 m) and limestone-dominated in the top (from 6.4 m to top). The base of the section is characterized by unfossiliferous grey to brown marls and relatively thin limestone beds. These beds are bioclastic mudstones from the base to 4.25 m and dominated by tuberoid wackestones-packstones, commonly interpreted as deposits close to sponge reefs, and thin sponge boundstones from 4.25 to 6.4 m. This marl-dominated interval points to a low carbonate input from the adjacent platform and/or to high clay input (Pittet & Strasser 1998a; Pittet et al. 2000).

A major facies change (at 6.4 m) from marl-dominated facies to more massive limestone beds points to an increase of carbonate production and export and/or to a reduced clay input. The first two thin limestone beds (from 6.4 to 6.85 m) are tuberoid and bioclast packstone to wackestones. The two following thick and massive beds (from 6.85 to 8.6 m) are sponge boundstones with mudstone matrix. Another level of tuberoid packstone is observed between these two beds. The following bed (from 8.6 to 9.8 m) has a nodular aspect and a finely laminated bed surface. It consists of wackestones with tuberoids and sponge fragments. This bed is followed by a relatively thin tuberoid-rich wackestone to packstone, nodular in the top and a thin clay-rich level (10.1-10.15 m). Pittet & Strasser (1998a) suggest that intervals rich in tuberoids may correspond to low sedimentation rates.

The following succession consists of tuberoid and bioclastic packstones to wackestones interbedded with thin marly limestones (from 10.15 to 11.7 m). The fifth limestone bed (from 11.45 to 11.7 m) is bioturbated, richer in bioclasts (e.g., ostracodes, Protoglobigerinids, and brachiopods) and has a wavy bed surface. A thin clay level (at 11.7 m), containing benthic foraminifera and sponge fragments, covers this bed. The following succession mainly consists of tuberoid and peloid facies that pass laterally into sponge bioherms. From 13.95 to 14.15 m, thin limestone beds rich in tuberoids and marls imply a condensed interval with a low accumulation rate. Finally, massive limestones re-appear at the top of the section and suggests an increase of carbonate input.

Sequence-stratigraphic interpretation

Based on facies, stacking pattern and bed surfaces, a sequence-stratigraphic interpretation is proposed between SB Ox6+ and SB Ox7. It is assumed that sea-level variations play an important role in the exportation of carbonate mud from platform to deeper environments (e.g., Schlager et al. 1994; cf. Chap. 5). It has been demonstrated that carbonate mud is preferentially exported from the platform during transgression when carbonate productivity is high on the platform, and during sea-level fall when progradation of the platform is forced (e.g., Schlager et al. 1994; Pittet & Strasser 1998a). Marly layers correspond to flooding of the platform or to emersion when only a small amount of carbonate mud is exported to the basin. Furthermore, pelagic carbonate

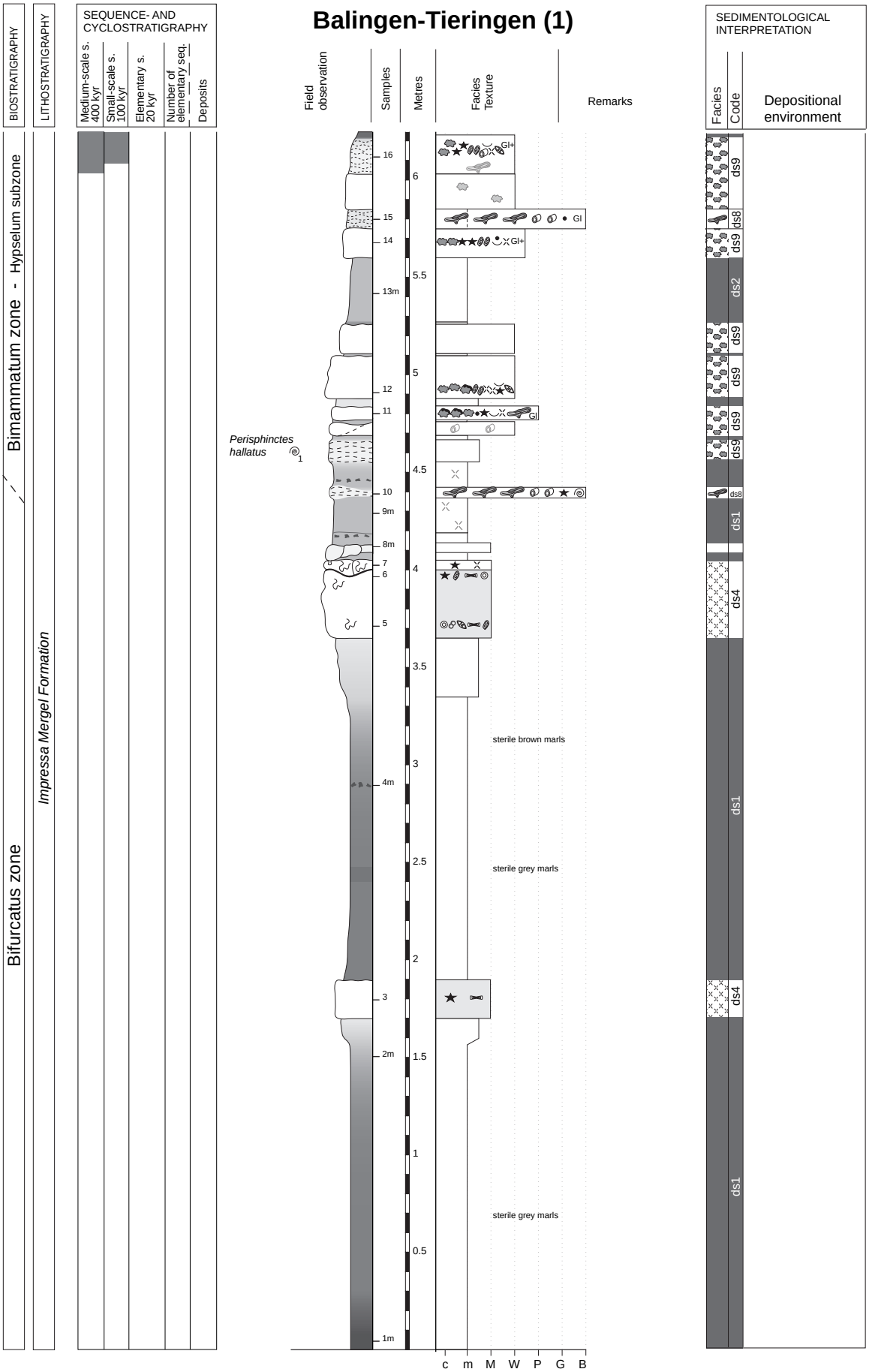

Fig. 4.21a - Balingen-Tieringen section (1).

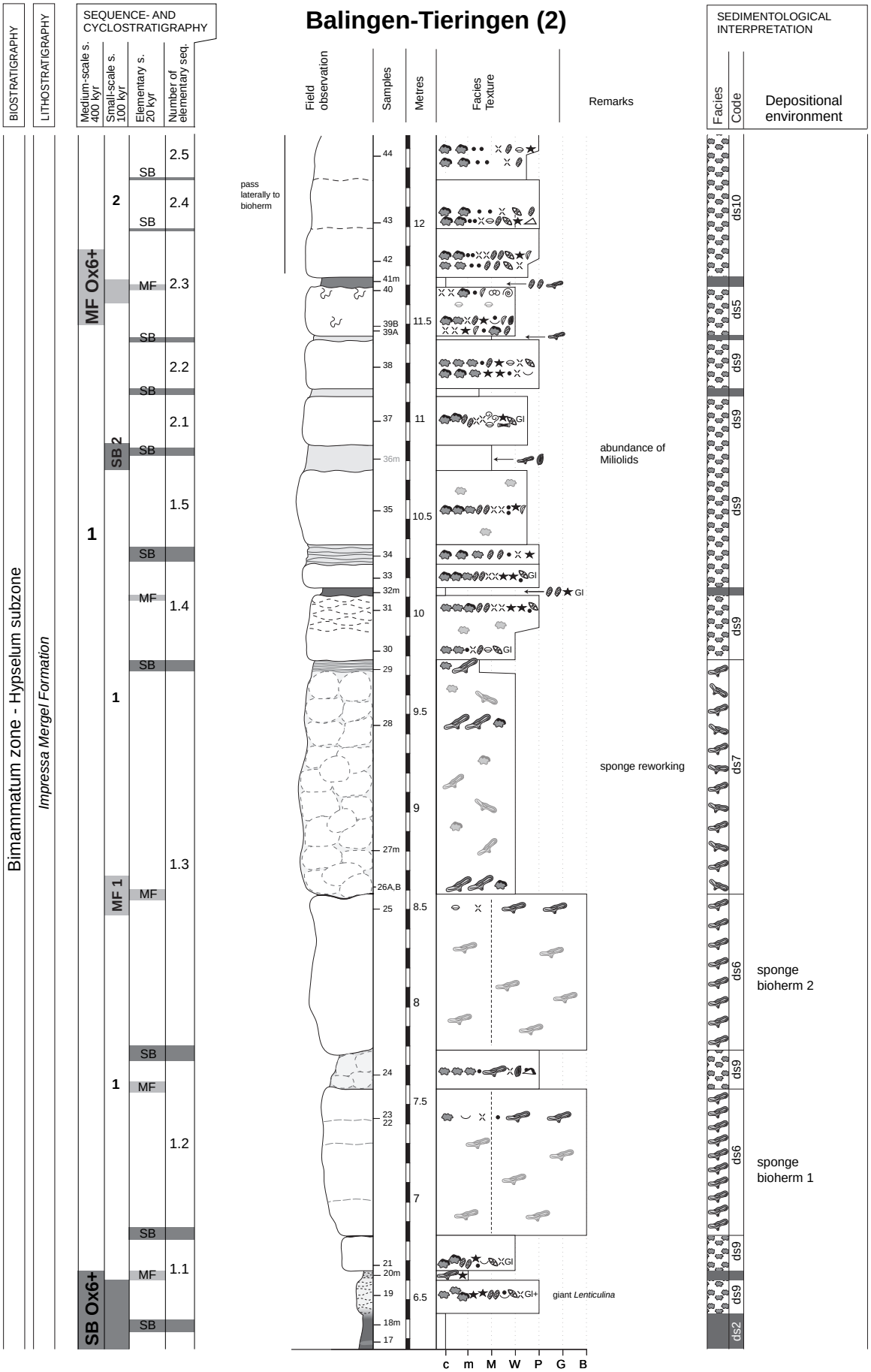

Fig. 4.21b - Balingen-Tieringen section (2).

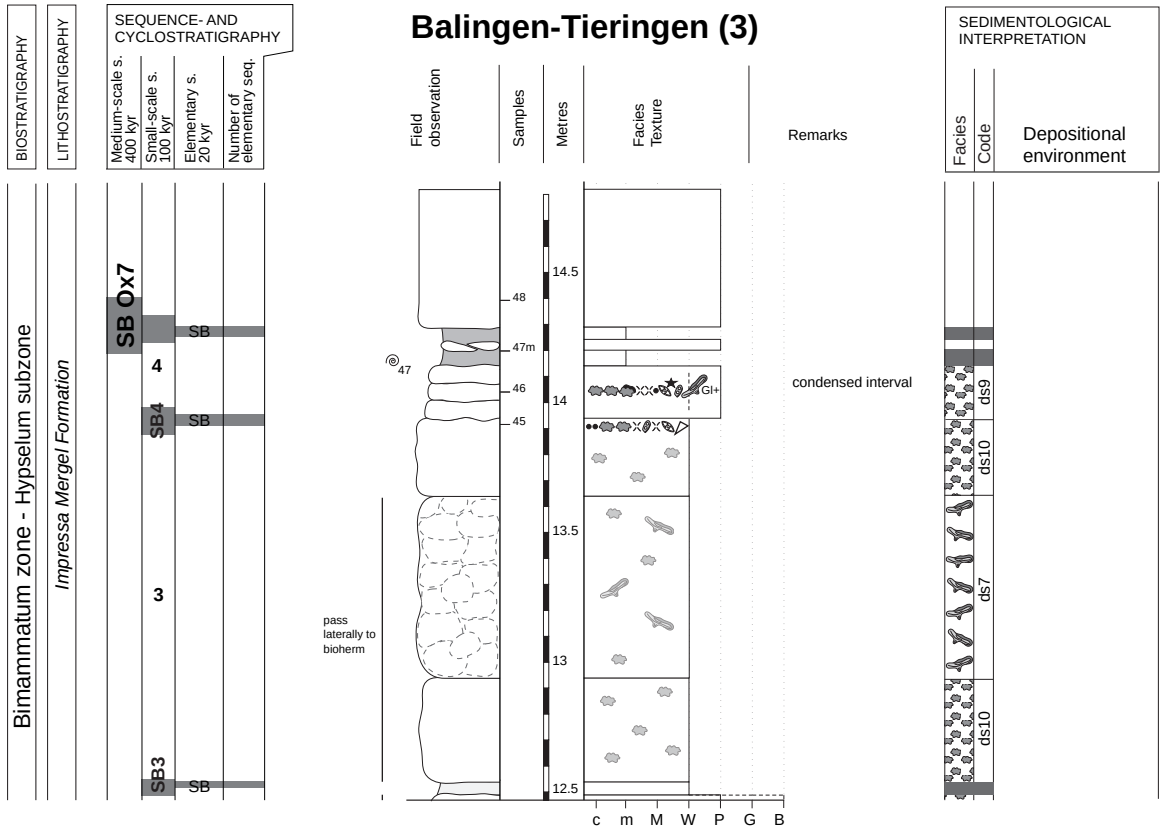

Fig. 4.21c - Balingen-Tieringen section (3).

productivity and input of clay were certainly also modulated by climate changes.

The marl-dominated interval at the base of the section (from 0 to 6.4 m) suggests a relatively low sea level during which carbonate productivity was low on the platform. The clay-rich level at the base of the section (from 6.2 to 6.4 m) is assumed to represent the medium-scale SB Ox6+. The marly interval at the base of the massive limestones (at 14.25 m) is interpreted as the medium-scale SB Ox7. Four small-scale sequences are identified within this medium-scale sequence (between Ox6+ and Ox7).

Small-scale sequence 1 consists of five elementary sequences. The first elementary sequence is composed of two tuberoid-rich beds (packstone and wackestone). The maximum flooding is placed in the marly interval between these two beds (at 6.55 m). The second and third elementary sequence each consists of one thick and massive sponge boundstone and one reworked sponge and tuberoid packstone-wackestone. The maximum flooding of these sequences is placed on top of the boundstones. The third elementary sequence (from 7.8 to 9.75 m) is the thickest sequence of this small-scale sequence and includes the maximum flooding of small-scale sequence 1. This probably indicates good conditions for sponge growth: low to moderate trophic level, low background sedimentation rate (e.g., Olivier et al. 2004b). The fourth elementary sequence is thinner and composed of two tuberoid wackestone-packstone beds separated by a clay level rich in benthic foraminifera, echinoderms, and glauconite. The top of the first bed is nodular and has a slight wavy bed surface interpreted as the maximum-flooding surface. The fifth elementary sequence is composed of a massive tuberoid wackestone-packstone bed and a marly limestone bed rich in benthic foraminifera (Miliolids) and reworked sponges. This level (from 10.75 to 10.9 m) suggests the exportation of coarse elements from the platform and thus represents a good candidate for the small-scale SB 2.

Small-scale sequence 2 consists of five elementary sequences. The first and second elementary sequence are relatively similar and composed of one massive tuberoid wackestone-packstone and one thin marly limestone. The third elementary sequence is composed

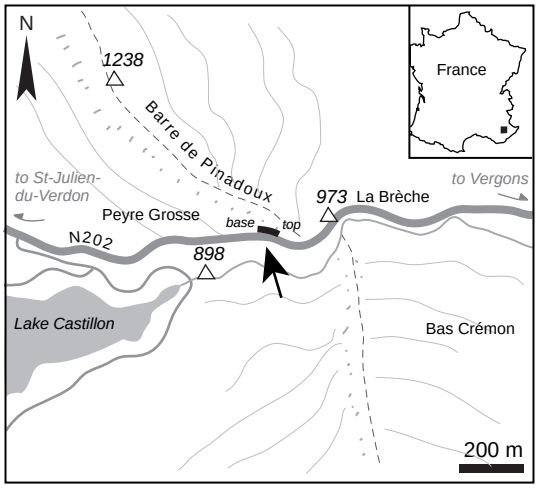

Fig. 4.22 - Location of the Vergons section. Based on topographic map of Castellane (3442OT), IGN Topo 25 series.

of two limestone beds separated by a clay-rich level. The first limestone bed presents bioturbation and more bioclastic facies (e.g., brachiopods, protoglobigerinids). These observations point to a maximum-flooding surface. The fourth and fifth elementary sequence are each composed of one tuberoid and peloid packstone.

Small-scale sequence 3 is thinner than sequences 1 and 2. This sequence is composed of three limestone beds relatively rich in tuberoids that pass laterally into sponge reefs.

Small-scale sequence 4 is the thinnest (around 40 cm) compared to the three other small-scale sequences and only consists of four limestone beds. This sequence corresponds to a condensed interval. By lateral correlation, the top of this small-scale sequence is interpreted as the medium-scale SB Ox7.

The small-scale sequences above the medium-scale MF Ox 6+ are thinner than those before. This difference is probably due to the highstand conditions of the large-scale trend.

4.3 Basin sections

4.3.1 South-East France

Vergons (Figs 4.22 and 4.23a-c; Pl. 17/3-6)

Geography and stratigraphy

The Vergons section is located in the Alpes de Haute-Provence (France) along the road N202 between St. Julien du Verdon and Vergons (Fig. 4.22). The whole section comprises about 115 metres of basin deposits and covers the Middle Oxfordian to Early Tithonian time interval. Sedimentology and stratonomy have already been studied by Killian (1889), Beaudoin (1977), Pellaton & Ullrich (1997), the geochemistry by de Rafélis Saint-Sauveur (1996), Pellaton & Ullrich (1997), the sedimentary organic matter by Bombardière (1998), and the clay-mineralogy by Deconinck & Debrabant (1985).

The studied section only concerns 16.5 m of deposits, analyzed with great detail (Fig. 4.23). The bed numbers are taken from Pellaton & Ullrich (1997). The biostratigraphy of this section is based on ammonites and partly on dinocysts (Atrops 1982, 1984). Ammonite specimens attributed to the Bifurcatus zone are present between beds 33 and 46 and those of the Bimammatum zone are found in beds 69 and 74 (determination by F. Atrops; Pellaton & Ullrich 1997). The section corresponds to the topmost part of the Middle to Late Jurassic "Terres Noires" facies, well known in SE France. The progressive transition from the Oxfordian Terres Noires facies to marl-limestone alternations is well exposed in the abrupt cliff on the other side of the Riou River.

Sedimentological interpretation

This section is characterized by pelagic to hemipelagic facies with marl-limestone alternations and, locally, gravity deposits (calcarenites, breccias, and slumps). Such deposits are mainly controlled by changes of planktonic productivity, carbonate mud export from the platform, and clay input, as well as by gravity flows and slope instabilities (cf. Chaps 3 and 5).

The base of the section is marl-dominated (from base to bed 52) while the top part is limestone-dominated (from bed 53 to top). In the marl-dominated part, relatively thick limestone beds occur (i.e., beds 43, 45, 47, 49; Tab. 2.3) and mark changes in sediment supply and carbonate productivity. Then, in the mid-part of the section, gravity flow deposits appear (i.e., beds 48, 50, 53) that are interbedded with marl-limestone alternations. These beds are peloidal and bioclastic packstones with some radial ooids and are interpreted as turbidites reworked by contour currents. Beds 47 and 48 show synsedimentary deformations (Plate 17/4) interpreted as slumps. Consequently, the interval from 5.5 to 7 m indicates a phase of instability of deposits.

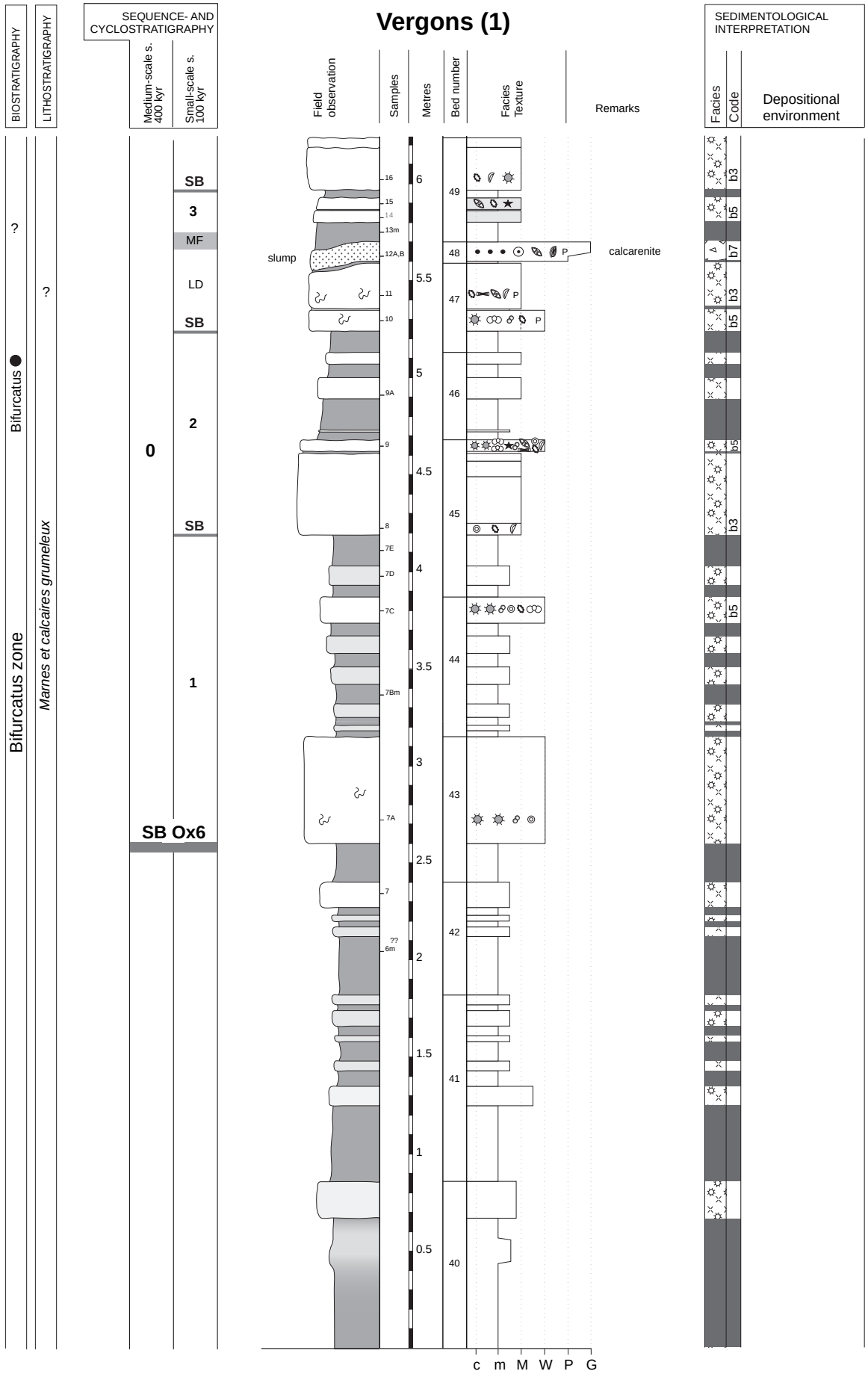

Fig. 4.23a - Vergons section (1).

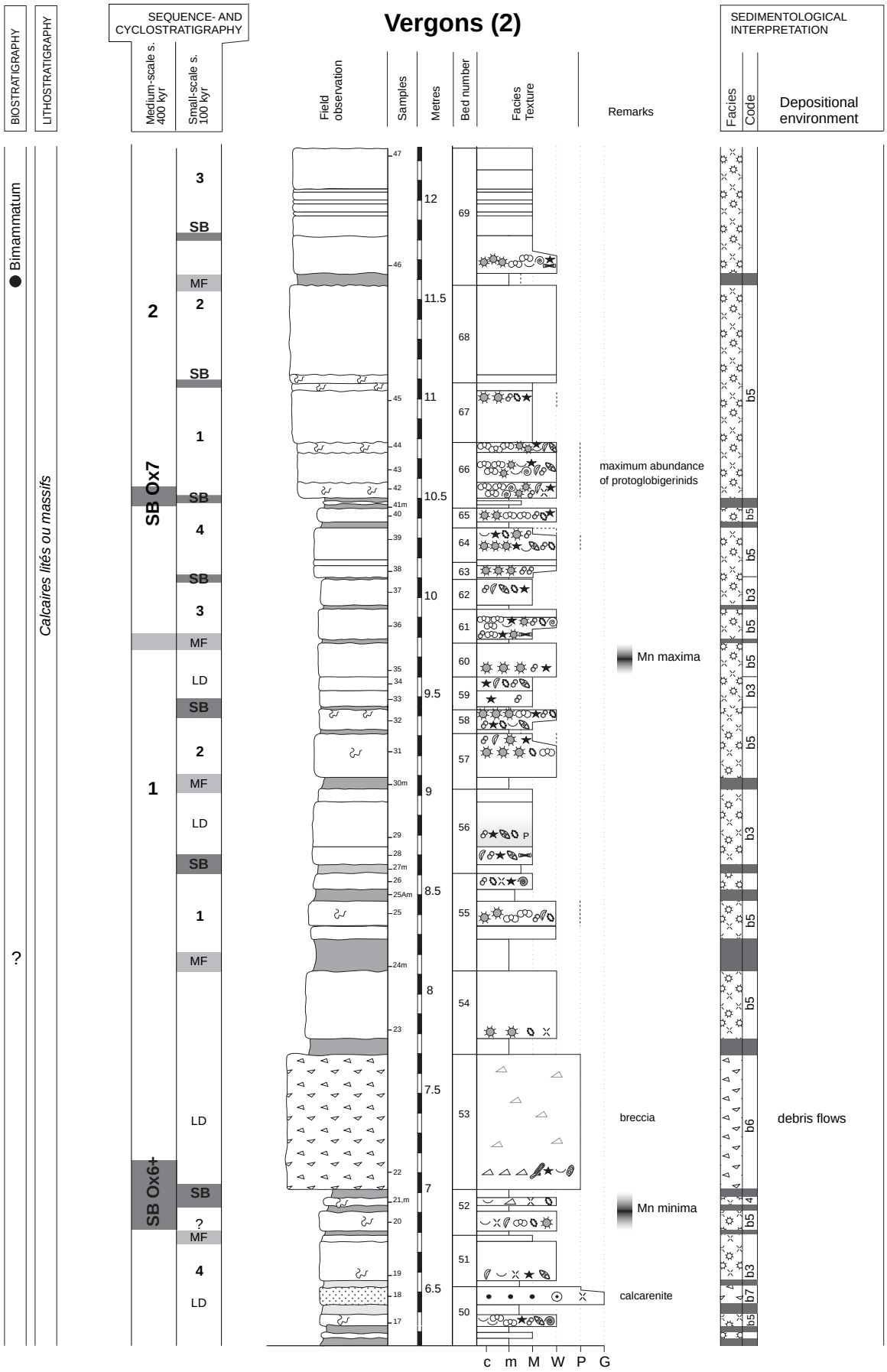

Fig. 4.23b - Vergons section (2).

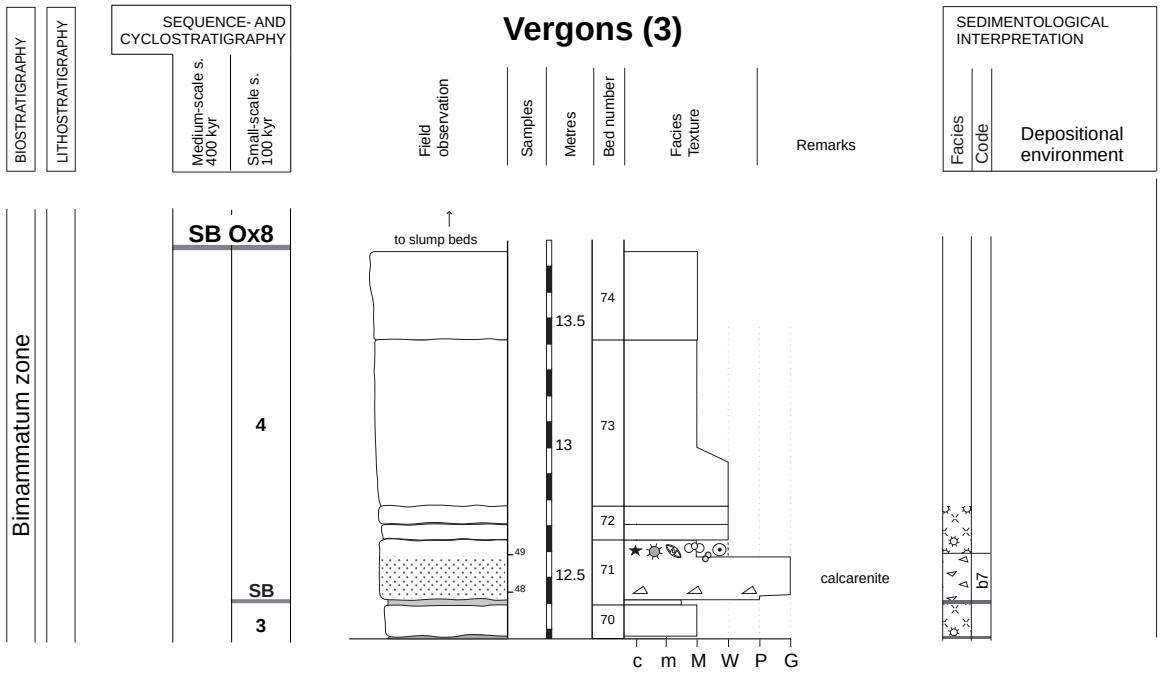

Fig. 4.23c - Vergons section (3).

Bed 53 is a lithoclastic–bioclastic packstone with breccia facies, interpreted as a debris flow (microfacies b6, Tab. 2.3). Bed 54 to 65 are relatively thin (10-30 cm) with more and more radiolarians, protoglobigerinids, and ammonites. The top part of the section (from bed 66) is dominated by thick limestone beds, rich in radiolarians, Protoglobigerinids, and locally allochthonous particles (bed 71). Higher up, slumps appear.

Sequence-stratigraphic interpretation

Based on the hierachical stacking pattern, bed surfaces, and facies, four medium-scale sequence boundaries have been identified. The first one is placed below the first thick radiolarian limestone (bed 43) in the Bifurcatus zone. According to this biostratigraphic position, it is assumed to correspond to SB Ox6 of HARDENBOL et al. (1998). The medium-scale SB Ox6+ is placed below the thick lithoclastic limestone (bed 53) between the Bifurcatus and Bimammatum zones. This interval approximately coincides with the relatively lowest manganese concentrations, which is generally associated to a low sea level (EMMANUEL & RENARD 1993). The medium-scale SB Ox7 is placed below the interval of amalgamated limestone beds at the base of bed 66, below the first ammonite indicating the Bimammatum zone. SB Ox8 is placed below slumped beds (bed 75) in the Bimammatum zone.

Medium-scale sequence 0, between Ox6 and Ox6+, consists of four small-scale sequences. The first two small-scale sequences display marl-limestone alternations. The two following sequences contain gravity flow deposits in the first part of each sequence. These deposits are interpreted as lowstand deposits because they correspond to periods of slope instability commonly occuring during low sea level (STROHMENGER & STRASSER 1993).

Medium-scale sequence 1, between Ox6+ and Ox7, consists of four small-scale sequences. The first small-scale sequence consists of five marl-limestone couplets. The first bed is a breccia and thus indicates a period of instability during a low sea level. The maximum flooding of this small-scale is placed in the thinnest marly level of this sequence (at 8.35 m), probably suggesting a condensed interval. The three following small-scale sequences each consist of five beds or marl-limestone couplets. For each small-scale sequence, the maximum flooding is placed in a marly level. The maximum flooding of medium-scale sequence 1 is placed around 9.7-9.8 m in the third elementary sequence of the third small-scale sequence (bed 60), where radiolarians and then Protoglobigerinids are abundant. This interval also coincides with the highest manganese concentrations generally associated with a high sea level (EMMANUEL & RENARD 1993).

Medium-scale sequence 2, between Ox7 and Ox8, also consists of four small-scale sequences. Sequence boundaries are placed at the base of thick massive limestones. The identification of deposits is more difficult than in the previous medium-scale sequences mainly because of a different stacking pattern with thick massive limestones but rare marly intervals.

* * *

5 - STRATIGRAPHIC CORRELATIONS

For the high-resolution stratigraphic correlation of all studied sections different tools are used: ammonite biostratigraphy, lithostratigraphy, and sequence stratigraphy. While biostratigraphy and major lithological changes furnish a general framework, the highest resolution is obtained by sequence-stratigraphical correlations on the scale of elementary sequences. In one section alone, it is often difficult to place these boundaries (i.e., sequence boundaries, transgressive surfaces, maximum-flooding surfaces) unequivocally and to estimate their magnitude (i.e., if they belong to elementary, small-scale, or medium-scale sequences). Through correlation with other sections over short and long distances, however, a "*best-fit solution*" can be found.

This study provides a high-resolution sequence-stratigraphical correlation from shallow-water platform (Jura, Lorraine) to deeper platform (Haute-Marne, Swabian Jura) and to basin sections (SE France) during the early Bimammatum zone (Late Oxfordian). One of the targets of this study is to have a closer look at the transgression that led to the accumulation of the Hauptmumienbank and Steinebach members (Swiss Jura) with regard to its evolution in time and space (cf. Chap. 7).

No palinspastic reconstructions have been undertaken in this study. The indicated distances between the sections are measured on today's geographical maps. The distances would have to be stretched by a few kilometers between the sections along a general N-S axis. Moreover, some lateral offsets by a few kilometers between sections cannot be excluded. However, the relative proximal-distal position of the sections is not affected.

5.1 METHODS OF CORRELATION

5.1.1 Biostratigraphy

The biostratigraphic framework of the platform and basin sections was established using ammonites (ENAY et al. 1988 and GYGI 1995 for the Swiss Jura; CARPENTIER 2004 for the Lorraine; COURVILLE & VILLIER 2003 for the Haute-Marne; SCHWEIGERT 1995a, b for the Swabian Jura, and ATROPS 1982, 1984 for SE France). However, due to infrequent data on most shallow-water carbonate platforms, alternative correlation methods are demanded for the correlation of platform sections.

5.1.2 Lithofacies

Major lithostratigraphic changes occur regularly on the Jura platform (e.g., GYGI 1995). The base of the massive Hauptmumienbank and Steinebach beds has thus been used for regional correlations (GYGI 1995; PITTET 1996; HUG 2003). Furthermore, GYGI & PERSOZ (1986) have performed mineralostratigraphic correlations (based on quartz and clay minerals) between the biostratigraphically better dated epicontinental basins and the less well dated Jura platform.

However, lithological boundaries are not necessarily isochronous. Small-scale diachronisms and lithological heterogeneities deriving from spatial and temporal variations of facies distribution and/or lateral migration of facies belts certainly occur but are difficult to evaluate without applying facies-independent methods of correlation.

5.1.3 Discontinuity surfaces and depositional sequences

In the wake of sequence stratigraphy, great attention has been paid to the chronostratigraphic value of discontinuities. High-resolution correlations over long distances are usually based on diagnostic surfaces and/or intervals, which are assumed to be more or less isochronous. However, especially in marginal-marine and slope environments sequence boundaries include hiatuses caused by erosion and/or non-deposition (Fig. 5.1a). Transgressive surfaces are generally not isochronous if there is a pre-existing morphological relief (Fig. 5.1b). Maximum-flooding surfaces or intervals have the best chance to homogenize a morphological relief in shallow-marine settings and, consequently, to be isochronous (Fig. 5.1c). Accordingly, they are considered to be the most appropriate for high-resolution correlation over long distances (e.g., SANDULLI & RASPINI 2004; TRESCH 2007).

In platform sections, the stacking pattern of depositional sequences can be used to identify trends in accommodation change. However, the comparison of thickness variations of laterally corresponding depositional sequences can only be made as a first approximation. In order to translate the thickness of a sequence into accommodation and eventually sea-level change, the sequence would first have to be decompacted according to facies and water depth for the deposition of each facies would have to be estimated (STRASSER et al. 2004; HILLGÄRTNER & STRASSER 2003). This very time-consuming procedure has not been performed in the present study.

The investigated sedimentary record lies between two well-marked discontinuities, which are attributed to the 3rd-order (large-scale) sequence boundaries Ox6 and Ox7 according to HARDENBOL et al. (1998). These sequence boundaries have been dated and define the general chronostratigraphic time framework. The cyclostratigraphical analysis can further improve the time resolution (cf. Chap. 6). Two medium-scale sequences, identified between these major sequence boundaries, create a correlation framework, which has already been established in previous studies for the Swiss Jura platform (PITTET 1996; HUG 2003). The first half of the second medium-scale sequence at the base of the long-term transgressive trend has been chosen to investigate small-scale and elementary depositional sequences in more detail.

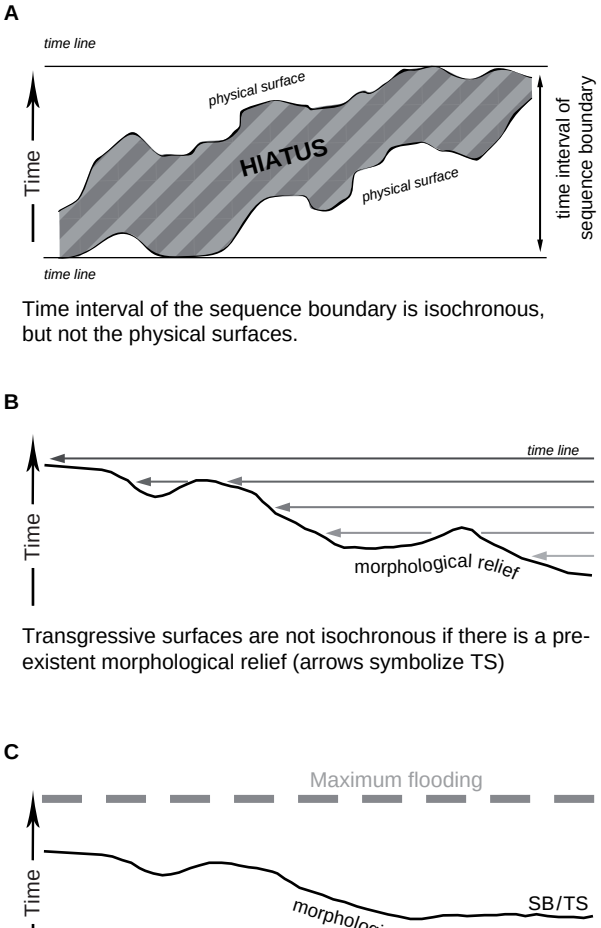

Fig. 5.1 - Models illustrating diagnostic intervals or surfaces in time and space. a) Sequence boundaries; b) Transgressive surfaces; c) Maximum floodings. Modified from TRESCH (2007).

High-resolution sequence-stratigraphic correlations are presented for each sedimentary domain (i.e., shallow platform, deep platform, basin) and then are discussed together.

5.2 CORRELATION ON THE SHALLOW PLATFORM

The base of the Hauptmumienbank and Steinebach members for the Swiss Jura sections and the base of the Oolithe de Saucourt inférieure Member for the Lorraine section are used as regional markers. The biostratigraphic framework of the platform sections is based on ammonites (GYGI 1995; CARPENTIER 2004).

Based on these sequence-stratigraphic elements presented in Chapter 4, a bed-by-bed correlation of the six Swiss Jura sections and the Lorraine section has been attempted providing the most consistent *best-fit correlation* (Figs 5.2 and 5.3).

The Swiss Jura sections are correlated between the medium-scale SB Ox6+ and the medium-scale MF Ox6+. The sections are distant of a few kilometres to tens of kilometres. They are positioned from "proximal" (Voyeboeuf section) to "distal" (Savagnières and Pertuis sections) based on the dominant facies and on their palaeogeographical positions. However, because platform morphology has changed through time, these attributions can only indicate the general trend.

The best-fit high-resolution correlation of the Swiss Jura sections shows that sequence boundaries and maximum floodings of the small-scale and elementary sequences have a good lateral continuity (Fig. 5.2). This suggest that the formation of the small-scale sequences was controlled by an allocyclic mechanism.

Elementary sequences can be produced by allo- and autocyclic processes. Most small-scale sequences include five elementary sequences suggesting a control on the sedimentation by a common external factor such as orbitally controlled sea-level changes. However, Fig. 5.4 shows the intervals consisting of migrating high-energy ooid bars, controlled by autocyclic processes (cf. Chap. 3). Nevertheless, the good correlation of many elementary sequences suggests an allocyclic control also for these sequences, even if it is occasionally overprinted by autocyclicity.

When comparing the facies of time-equivalent small-scale and elementary sequences between the Swiss Jura sections, significant lateral facies changes appear. For example, ooid shoals are laterally replaced by oncoid lagoons, or tidal flats are juxtaposed to marly depressions (Fig. 5.2). Ooid shoals do not always occur at the same time in the studied sections, which suggests that they migrated across the platform through time or were stranded in one position and later re-initiated in another one. This points to a facies mosaic on the Swiss Jura platform. It reflects the dynamics and complexity of sedimentary systems where juxtaposed sub-environments evolved and shifted through space and time (Samankassou et al. 2003; Wright & Burgess 2005; Strasser & Védrine in press; cf. Chap. 7).

The presence of thickness variations at the scale of small-scale and elementary sequences reveals variable sediment accumulation rates. This is interpreted as resulting mainly from differential subsidence due to the activity of tectonic blocks (Allenbach 2002). The relief created by tectonics therefore contributed significantly to the general facies distribution. Furthermore, the irregular distribution of siliciclastics can be explained by localized depressions, which were created by differential subsidence and served as conduits (Pittet 1996; Hug 2003). In addition, carbonate production and accumulation, i.e. the preferential growth of reefs and the initiation of ooid shoals on tectonic highs, further enhanced the relief.

The Swiss Jura sections are then correlated with an additional shallow platform section from Lorraine. Two Swiss Jura sections, representative of proximal and distal facies (Voyeboeuf and Pertuis, respectively), have been selected for the correlation with the Pagny-sur-Meuse section (Lorraine). This section is less thick than the Swiss Jura sections, probably due to a lower subsidence rate. The correlation of sequence boundaries and maximum floodings of small-scale and elementary sequences between the seven shallow platform sections is relatively straightforward (Fig. 5.3). A similar number of elementary sequences is counted in all sections and thus implies an external controlling factor. In all studied shallow platform sections, the distribution of siliciclastics shows a similar pattern with more or less developed levels at the medium-scale SB Ox6+, and MF Ox6+, and at the small-scale SB 2.

5.3 Correlation from deep platform to basin

Based on a well-established biostratigraphic framework, the interpreted sequence stratigraphic boundaries are correlated at the scale of elementary and small-scale sequences from the deep platform sections to the basin section (Figs 5.5 and 5.6). The larger time framework of the Balingen-Tieringen and Vergons sections (between Ox6 and Ox8) allows to better constrain the studied time interval.

Fig. 5.2 - (following pages) High-resolution best-fit correlation of the one and a half small-scale sequence and elementary sequences of the six sections of the Swiss Jura platform.

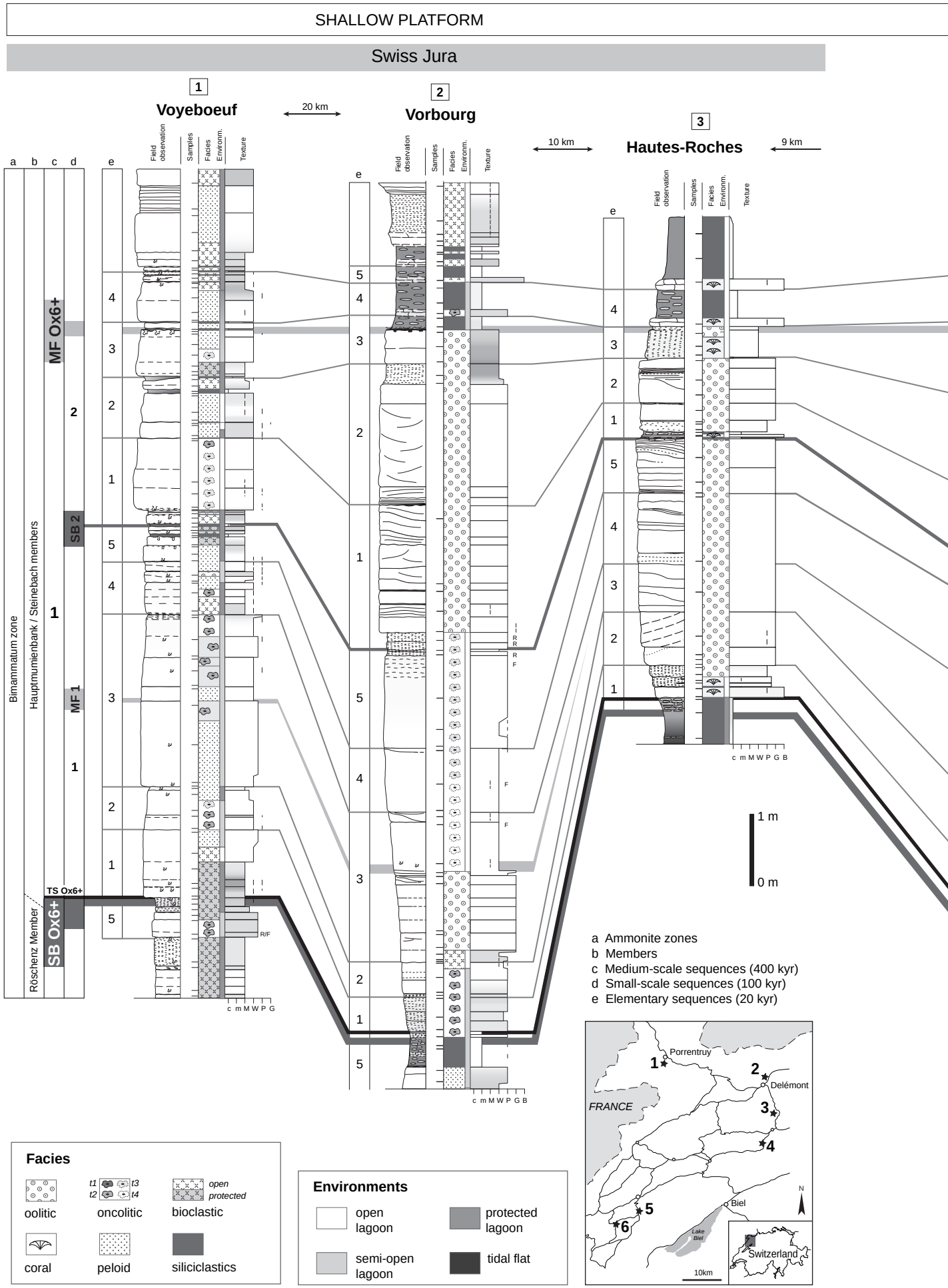
SHALLOW PLATFORM
Swiss Jura
1
Voyeboeuf
20 km
2
Vorbourg
10 km
3
Hautes-Roches
9 km
a b c d e
Field observation
Samples
Facies
Environm.
Texture
Bimammatum zone
Hauptmumienbank / Steinebach members
Röschenz Member
MF Ox6+
SB 2
MF 1
SB Ox6+
TS Ox6+
c m M W P G B
R/F
1 m
0 m
a Ammonite zones
b Members
c Medium-scale sequences (400 kyr)
d Small-scale sequences (100 kyr)
e Elementary sequences (20 kyr)
Facies
oolitic
oncolitic
bioclastic
coral
peloid
siliciclastics
open
protected
Environments
open lagoon
protected lagoon
semi-open lagoon
tidal flat
Porrentruy
Delémont
FRANCE
Biel
Lake Biel
Switzerland
10km
N

SHALLOW PLATFORM

Swiss Jura

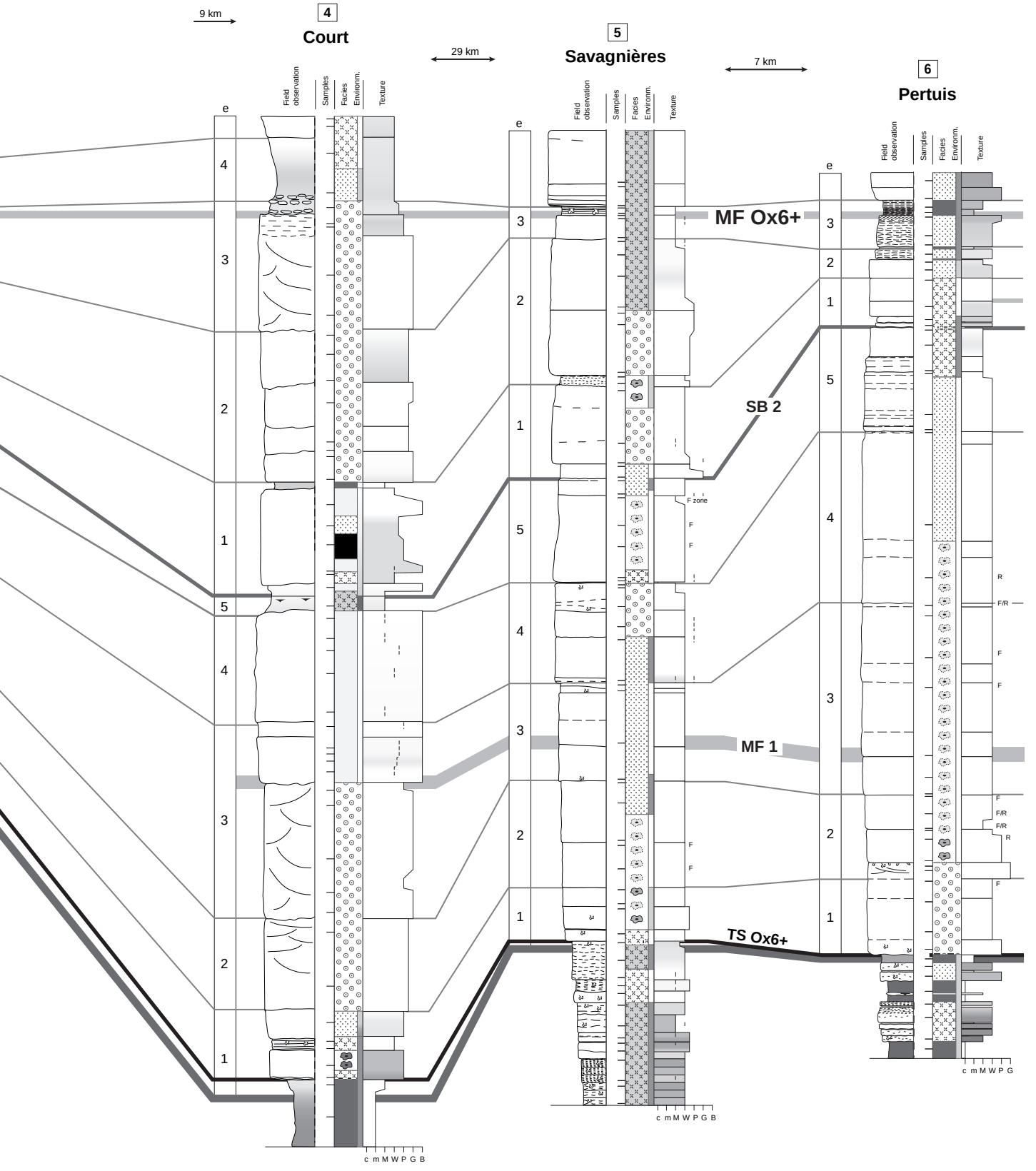

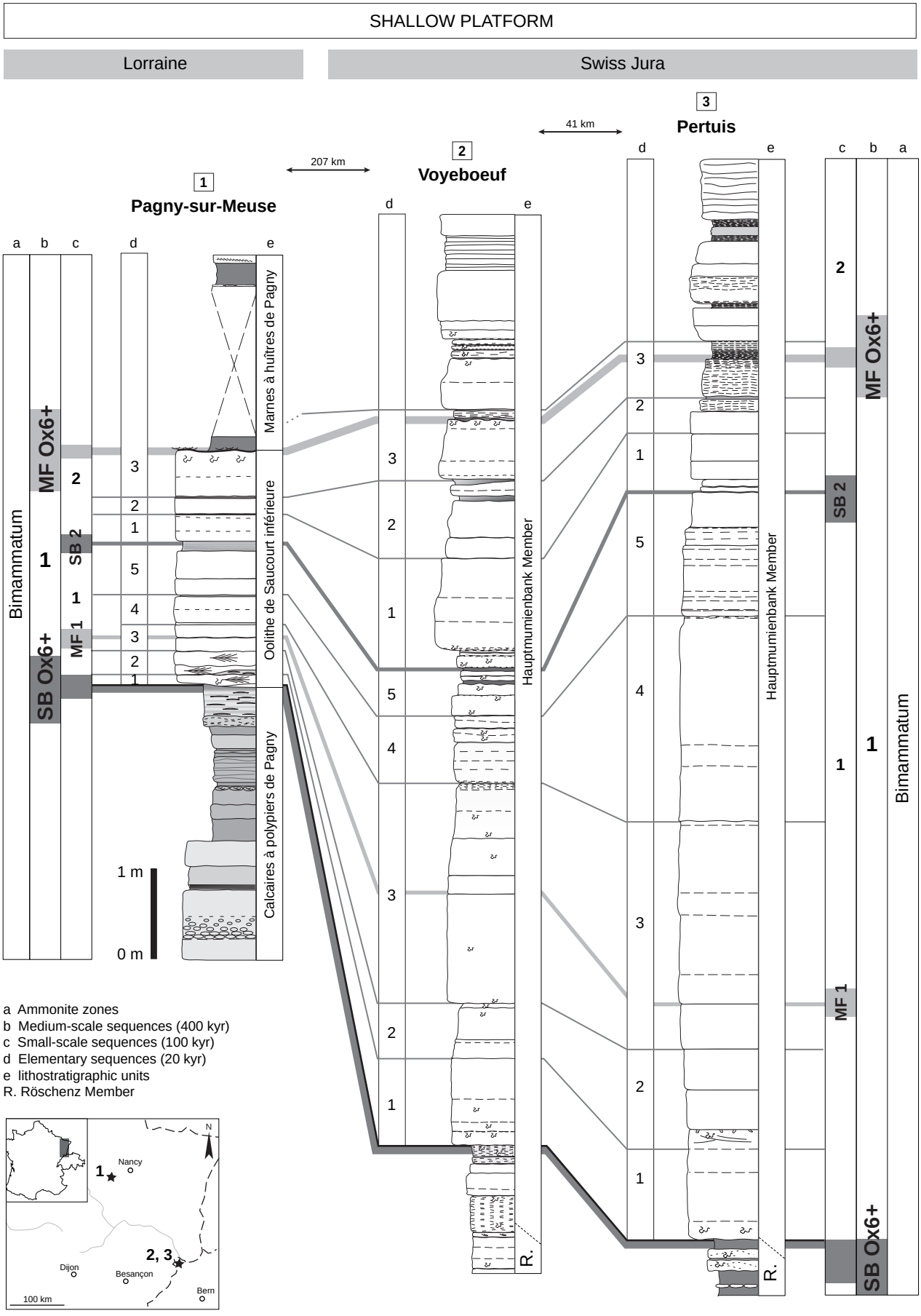

Fig. 5.3 - High-resolution best-fit correlation of the platform sections: two selected sections of the shallow-water Swiss Jura platform and the section of the Lorraine platform.

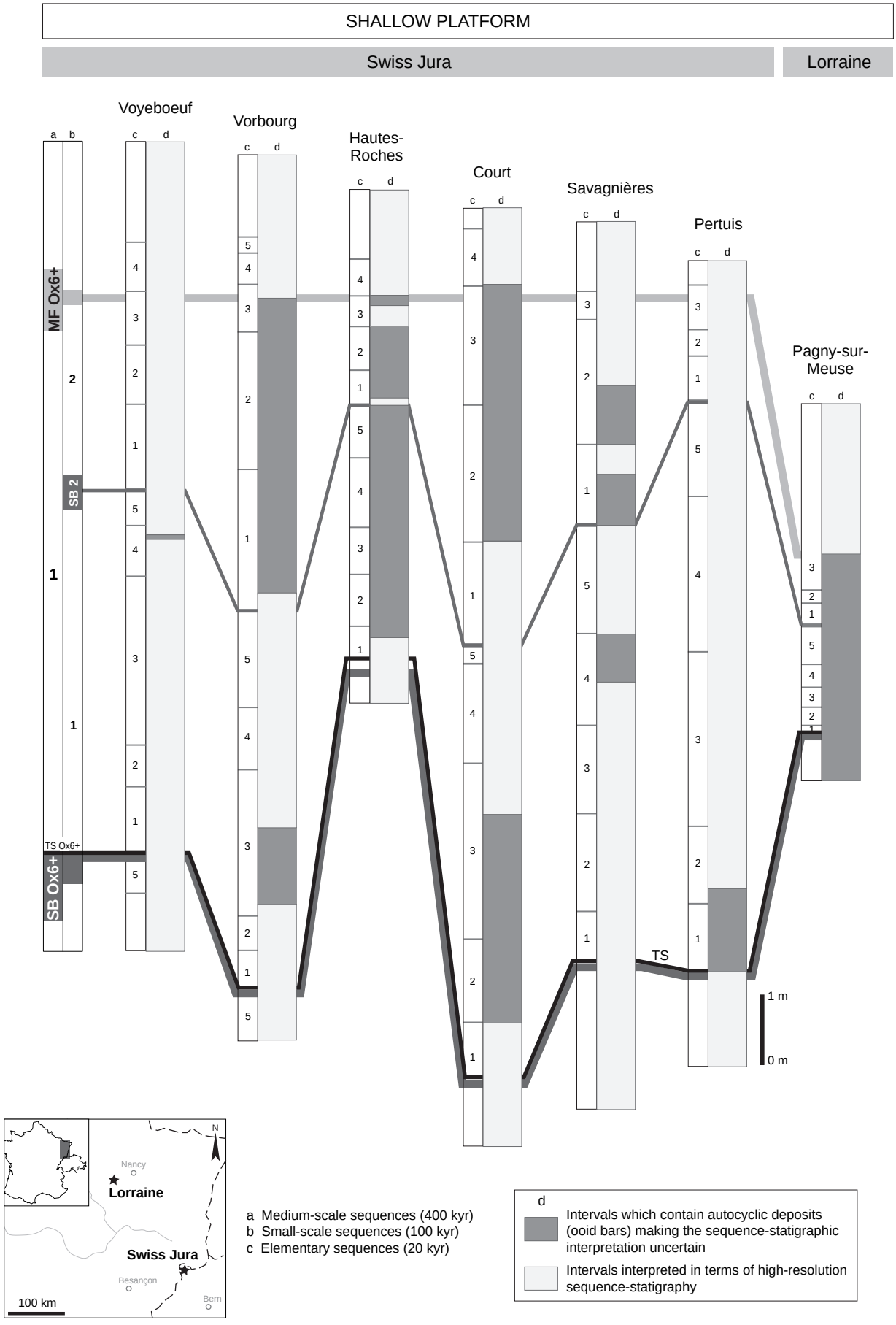

Fig. 5.4 - Intervals with autocyclic deposits where the sequence-stratigraphic interpretation is uncertain in the platform sections.

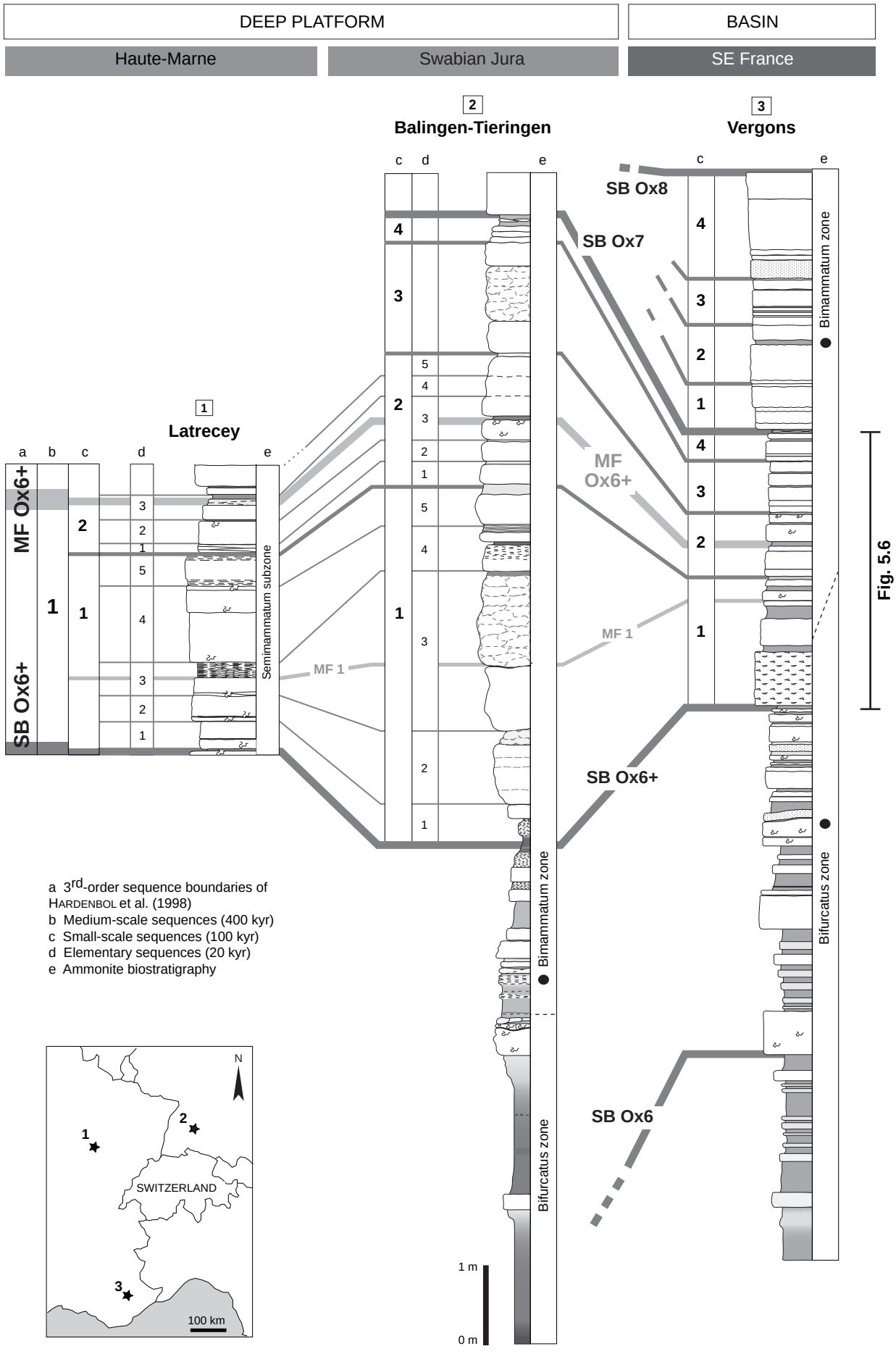
DEEP PLATFORM
BASIN
Haute-Marne
Swabian Jura
SE France
1
Latrecey
2
Balingen-Tieringen
3
Vergons
a b c d e
MF Ox6+
SB Ox6+
SB Ox8
SB Ox7
SB Ox6
MF Ox6+
MF 1
Semimammatum subzone
Bimammatum zone
Bifurcatus zone
a 3rd-order sequence boundaries of Hardenbol et al. (1998)
b Medium-scale sequences (400 kyr)
c Small-scale sequences (100 kyr)
d Elementary sequences (20 kyr)
e Ammonite biostratigraphy
N
SWITZERLAND
100 km
1 m
0 m

Fig. 5.6

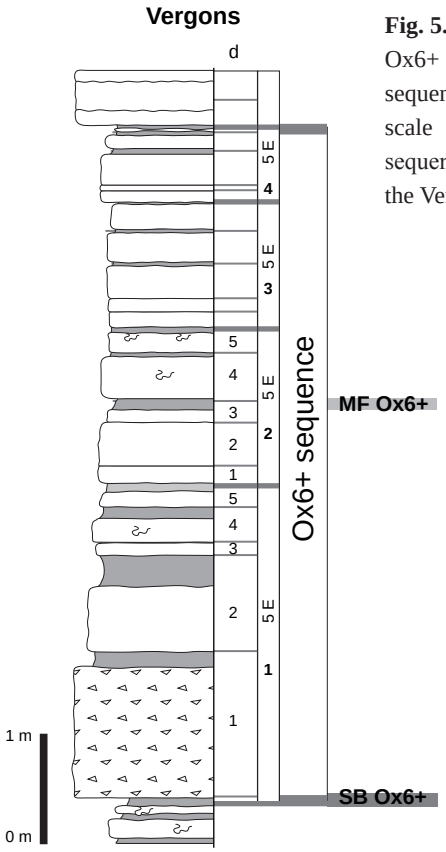

Fig. 5.6 - Detail of the Ox6+ medium-scale sequence with small-scale and elementary sequences identified in the Vergons section.

The first small-scale sequence shows important sediment thickness variations. The highest sediment thickness is observed in the Balingen-Tieringen section where sponge reefs develop (cf. Figs 5.5 and 4.21). The lowest sediment thickness appears in the basin section. However, the sections are not decompacted and as the Latrecey section is entirely composed of mudstones, its original thicknesses was considerably larger. If a decompaction factor of 2.5 is applied for deposits of the first small-scale sequence at Latrecey (Strasser & Samankassou 2003), the original thickness is higher than the one of the decompacted Balingen-Tieringen section, containing wackstones, packstones, and boundstones. At Vergons, the relatively thick first small-scale sequences owes this to the debris flow at its base. Elsewhere in this section, the limestone-marl alternation had low accumulation rates. This comparison shows the different sediment accumulation rates from deep platform to basin. Due to the disappearance of sponge boundstones and the deposition of marl-limestone couplets in the first half of the second small-scale sequence at Balingen-Tieringen, sediment thicknesses are generally lower there.

As for the shallow platform sections, five elementary sequences have been identified in the first small-scale sequence of all three sections (cf. Chap. 4; Fig. 5.6). Elementary sequence 1.3, where the maximum flooding of the small-scale sequence 1 (MF1) is inferred, is thickest in the Balingen-Tieringen section and thinnest in the Vergons section. A similar pattern is observed for the next small-scale maximum flooding, which is equivalent to the medium-scale maximum flooding (MF Ox6+) recognized on the shallow platform. However, facies analysis of the Vergons section suggests that the best expressed MF is the one of the third small-scale sequence (Fig. 4.23). This observation is supported by the highest manganese value usually interpreted as a maximum flooding. Depending on basin morphology, the best-expressed MF apparently may shift by one or two cycles from one location to another (Strasser et al. 2000).

5.4 Platform-to-basin correlation

The high-resolution sequence-stratigraphical interpretation enables for the first time a best-fit correlation on the scale of elementary sequences between sections from shallow platform to basin in the Tethyan realm during the Late Oxfordian (cf. Fig. 5.7).

The number of elementary and small-scale sequences, identified in the shallow platform sections, is equivalent to the one of the deep platform and basin sections. This suggests a common controlling factor.

5.5 Discussion

In the studied interval, siliciclastics (quartz and/or clays) preferentially occur at three time levels in all sections: SB Ox6+, SB 2, and MF Ox6+. On the shallow platform, humidity and/or base-level changes in the hinterland act on the terrigenous run-off and thus on the distribution of siliciclastics. On the Swiss Jura platform, the occurrence of siliciclastics around sequence boundaries are mainly explained by more humid conditions in the hinterland during the relatively low sea level (Pittet & Strasser 1998a, b). This model explains the presence of siliciclastics around SB Ox6+

Fig. 5.5 - (facing page) High-resolution best-fit correlation of the sections from the deep platform to the basin.

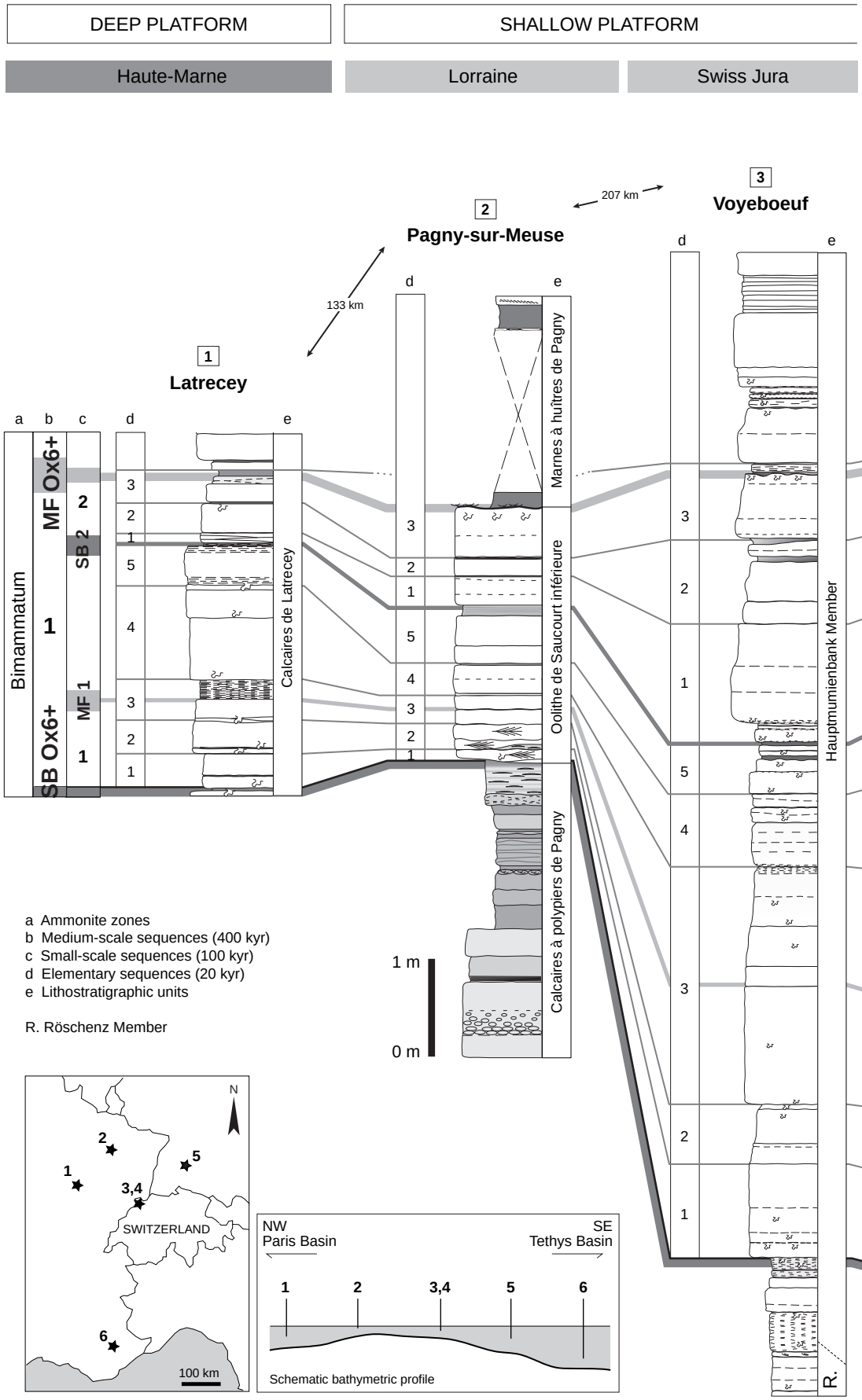

Fig. 5.7 - High-resolution best-fit correlation of the platform, deep platform and basin sections for the studied interval.

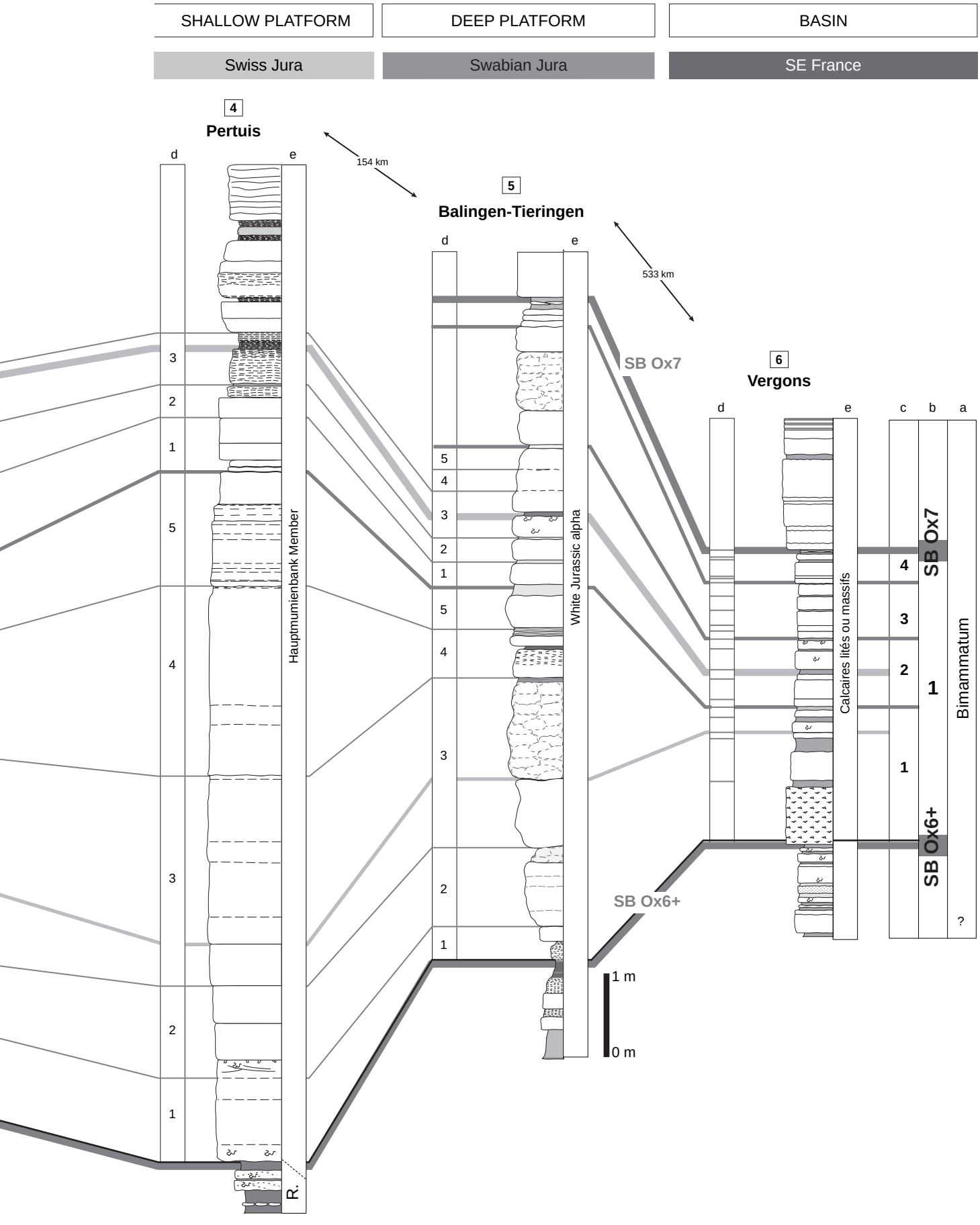
SHALLOW PLATFORM
DEEP PLATFORM
BASIN
Swiss Jura
Swabian Jura
SE France
4
Pertuis
d
e
154 km
5
Balingen-Tieringen
d
e
533 km
6
Vergons
d
e
c
b
a
SB Ox7
SB Ox6+
Hauptmumienbank Member
White Jurassic alpha
Calcaires lités ou massifs
Bimammatum
SB Ox7
SB Ox6+
1 m
0 m
R.

and SB 2. During the maximum floodings, relative sea-level rise is fastest and the erosion potential is reduced. Therefore, siliciclastics probably come from the remobilization of siliciclastics formerly stored on the proximal platform and are preferentially deposited in depressions on the shallow platform (Fig. 3.2; STRASSER & HILLGÄRTNER 1998).

5.5.1 On the shallow platform

The hierarchical stacking pattern observed in the studied sections implies that sedimentation was influenced by cyclical or periodic changes of controlling factors. The good correlation of depositional sequences over long distances between different sedimentary basins is a valuable argument that processes other than local tectonic activity or migration of sediment bodies must have been involved in the formation of these depositional sequences. It is assumed that high-frequency **sea-level fluctuations** were at least partly responsible for the repetitive stacking of depositional sequences on several scales, as observed in the studied sections.

On shallow-carbonate platforms, the thickness of a sedimentary sequence reflects as a first approximation the changing accommodation space over time. However, it has to be kept in mind that bed thickness and accommodation generally do not have a linear relationship. This is due to facies-dependent differential compaction and because sediment not always fills up the available space (STRASSER et al. 1999). The studied sections displayed here are not decompacted. Therefore, the comparison of thickness changes of laterally corresponding depositional sequences have to be interpreted with caution. Assuming that the sequence boundaries of the depositional sequences are more or less time-equivalent, the lateral changes of accommodation across the regions of investigation can be compared. The causes of these changes result from the combination of eustatic sea-level changes, tectonic movements (i.e., differential subsidence, block faulting), and the production and accumulation rates of sediment.

Additional factors have to be considered in the formation of depositional sequences on a shallow platform. The **position on the platform** is the first important parameter. Generally, restricted and/or protected facies are common in proximal positions while open-marine facies predominate in distal position (cf. Chap. 2). A **pre-existing morphology** determines the geometry of the coast line and the distribution of depocentres on the platform. The pre-existing relief also modifies the hydrodynamic setting (current and/or wave directions and intensity), the pattern of sediment production and deposition, and ecological conditions (e.g., water depth, salinity, turbidity, nutrient distribution).

Climate changes also play a role on the distribution of carbonate facies on the shallow platform. Terrigenous input, controlled by humidity changes in the hinterland, mainly influences the carbonate production and accumulation (see below).

5.5.2 On the deep platform and in the basin

In basinal, hemipelagic to pelagic sections, the expression of environmental changes is completely different from that in shallow platform sections. Environmental changes there are indicated by variations in palaeoecology (i.e., macro-, micro-, and nannofossils), different composition of organic matter, and/or changes of mineralogy and geochemistry. These variations can be used for sequence-stratigraphic interpretations (e.g., JAN DU CHÊNE et al. 1993; PITTET & MATTIOLI 2002). Additionally, facies analyses and variations of the stacking pattern in different basinal successions have been related to environmental changes associated with relative sea-level changes (e.g., STROHMENGER & STRASSER 1993; PASQUIER & STRASSER 1997; HILLGÄRTNER 1999; COLOMBIÉ & STRASSER 2003; cf. Chap. 3.4). Different factors control the changes in stacking pattern in deep-marine depositional systems. The main factors are winnowing of fine-grained sediments by bottom currents, intensified export of platform material to more distal, basinal depositional settings (e.g., slumps and turbidites in basin floor fans, slope fans and lowstand prograding wedges, highstand shedding), fluctuations in the calcite compensation depth (CCD) and oxygen-minimum zones, and changes of climate and/or oceanic circulation patterns, which influence the planktonic productivity and the clay input and distribution (e.g., EINSELE & RICKEN 1991; HILLGÄRTNER 1999).

5.5.3 Platform-basin relationships: a conceptual model

For the Oxfordian, PITTET & STRASSER (1998a) and PITTET et al. (2000) propose a model for the relationships between the Swiss Jura shallow

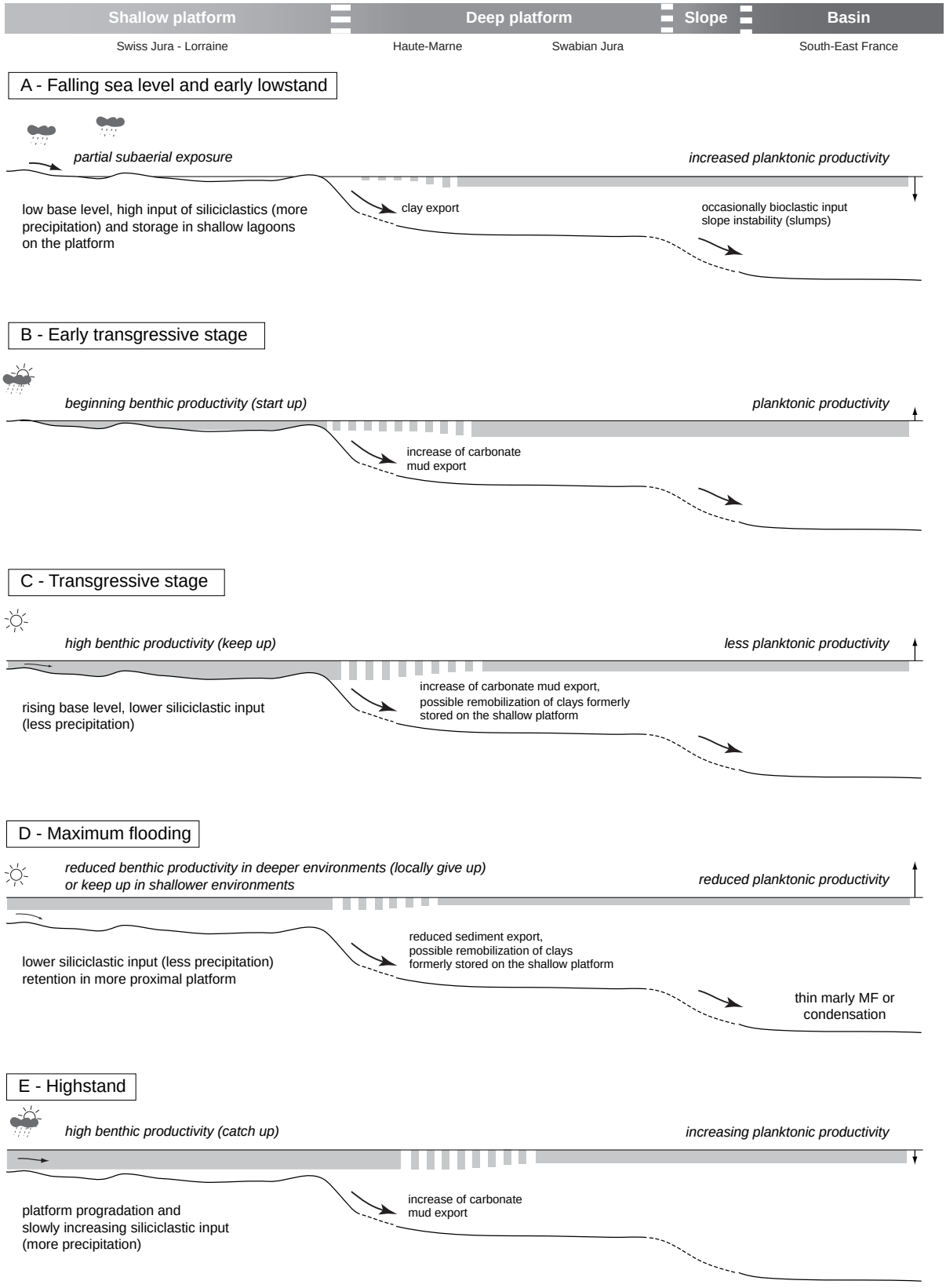

Fig. 5.8 - Conceptual model linking trends in relative abundance of carbonate mud and siliciclastics between the platform and the basin. Modified from Pasquier & Strasser (1997) and Hillgärtner (1999).

platform and the Swabian deep platform. In this model, carbonate production in shallow platform areas and export of carbonates from the platform to more distal environments are considered as the factors controlling deep platform sedimentation (i.e., marl-limestone couplets/sponge reefs). From nannofossil assemblage composition, PITTET & MATTIOLI (2002) suggest that deep platform deposition (Balingen-Tieringen section) results from cyclical export of carbonate mud from shallow platforms basinwards and, only secondarily, by changes in nannoplankton productivity. To explain the hemipelagic to pelagic Kimmeridgian deposits from the Vocontian basin, COLOMBIÉ & STRASSER (2003) propose the same controlling factors.

Based on the studied sections and their correlation, a conceptual model applicable for small-scale (100-kyr) sequences is proposed (Fig. 5.8). During **low relative sea level**, accommodation potential on the platform is reduced, leading to frequent periods of non-deposition and/or erosion. Base level is low, forcing terrigenous input, which generally coincides with more humid conditions (PITTET & STRASSER 1998a, b). Siliciclastics are mainly concentrated in shallow lagoons on the platform but sediment export, particularly clays, also occurs (cf. Fig. 5.8a). In the basin, slumps or debris flows are common due to slope instability during low sea level.

During the **(early) transgressive** period, benthic productivity on the platform increases significantly (start-up and keep-up phases, KENDALL & SCHLAGER 1981) leading to an increase of carbonate mud export (cf. Fig. 5.8b-c). In addition, clays formerly stored on the shallow platform can be remobilized and preferentially accumulated in deeper environments.

During accelerated sea-level rise and **maximum flooding**, benthic carbonate productivity on the platform decreases locally (give-up phase, KENDALL & SCHLAGER 1981) because water depth increases too rapidly for the system to keep up, and carbonate producers find themselves below the photic zone. Less humid conditions lead to reduced siliciclastic influx to platform areas and to the basin (cf. Fig. 5.8d). However, clays may also be reworked from proximal areas and spread across the platform and into the basin. At the same time, carbonate accumulation in the basin diminishes to a degree that marly sediments predominate because of decreasing planktonic carbonate production (e.g., PASQUIER & STRASSER 1997) and reduced carbonate export from the platform (PITTET et al. 1998a). The maximum flooding is thus marked by a marly and/or condensed level.

During the **highstand** period, decreasing bathymetry on the platform successively hinders the export of clays to basinal depositional settings but increases highstand shedding of carbonate mud, resulting in thin marl intervals and thick limestone beds (e.g., SCHLAGER et al. 1994; cf. Fig. 5.8e).

5.5.4 Elementary sequences : a challenge

In the shallow platform sections, an elementary sequence generally consists of one to four beds including more or less developed marl intervals. In the deep platform sections, an elementary sequence generally consists of one or two limestone beds with a more or less developed marl interval. In the basin section, an elementary sequence is commonly defined by one marl-limestone couplet.

The identification of elementary sequences is based on a very detailed facies and microfacies analysis (cf. Chap. 4). In the shallow and deep platform sections, these sequences are defined based on sometimes very subtle changes of texture and fauna. Sequence boundaries are defined by more restricted or protected facies, while the maximum floodings are characterized by the most open-marine facies. The high-resolution correlation of sections, at the scale of the 20-kyr sequences, shows the great variability of facies within an elementary sequence (cf. Chap. 7), suggesting the influence of intrinsic factors (cf. Chaps 7 and 9). In the basin section, the relatively homogenous facies make the identification of sequence boundaries difficult, transgressive surfaces, or maximum floodings. Consequently, the correlation of elementary sequences from shallow platform to basin is a best-fit solution and may be improved by complementary analyses (e.g., nannofossil assemblages, stable isotopes, trace elements).

* * *

6 - CYCLOSTRATIGRAPHY

Cyclostratrigraphy is the subdiscipline of stratigraphy that deals with the identification, correlation, and interpretation of cyclic variations in the stratigraphic record. Cycles take their origin in the orbital dynamics of the Earth-Moon-Sun system. The two main families of orbital cycles that are known to be recorded in the sedimentary deposits are the tidal and the Milankovitch cycles (HILGEN et al. 2004). This chapter focuses on the Milankovitch cyclicity records in the studied shallow platform deposits. The goal is to obtain a much more precise chronostratigraphic framework than through biostratigraphy or geochronology and thus to allow for the estimation of rates of ecological and sedimentary processes and to give a high-resolution time scale for the reconstruction of the evolution of the depositional environments.

6.1 CONCEPTS AND METHODOLOGY

Orbital forcing is an astronomical theory on the link between variations of the Earth's orbit and climate changes. Quasi-periodic variations of the Earth's orbital parameters modify the distribution and the intensity of insolation and engender climatic changes (MILANKOVITCH 1941; BERGER 1978; SMITH 1989; DE BOER & SMITH 1994). Insolation changes influence air temperature, growth and decay of ice sheets, atmospheric and oceanic circulation, rainfall pattern, and evaporation as well as terrestrial and oceanic ecosystems.

The main astronomical parameters are the changing eccentricity of Earth's orbit around the sun, the Earth's cycle in axial obliquity, and the cycle of precession of the equinoxes (e.g., FISCHER et al. 1990). The controlling orbital parameters (precession, obliquity, eccentricity; Fig. 6.1) are well defined in terms of cycle duration back to Mesozoic times (BERGER et al. 1989; BERGER & LOUTRE 1994). In the geological past, the periods of precession and obliquity were shorter because of the slowing of the Earth's rotation and the increasing Earth-Moon distance (BERGER et al. 1989). In the Oxfordian, the peaks of the precession signal were approximately at 18 kyr and 22 kyr and at about 37 kyr and 48 kyr for the obliquity (BERGER et al. 1989). Eccentricity stays constant at 100 and 400 kyr.

The formation of high-frequency sedimentary cycles on shallow platforms is mainly explained by eustatic variations. During glacial periods, there were dependent on glaciation/deglaciation cycles of polar ice-caps and mountain glaciers linked to the Earth's orbital parameters. The Oxfordian is interpreted as a "greenhouse" period (HALLAM 1984). No evidence of polar ice-caps is found, but they can not be excluded, and mountain glaciers were probably present (e.g., FRAKES et al. 1992; PRICE 1999, cf. Chap. 8). Sea-level changes of a few metres amplitude can also be created by thermal expansion and retraction of the uppermost layer of the ocean water (GORNITZ et al. 1982), by thermally induced volume changes in deep-water circulation (SCHULZ & SCHÄFER-NETH 1998), and/or by water retention and release in lakes and aquifers (JACOBS & SAHAGIAN 1993).

In the sedimentary record, the 5:1 relationship between elementary and small-scale sequences and the 4:1 relationship between small-scale and medium-scale sequences reflect the hierarchy of Milankovitch cycles. The relatively good biostratigraphic control associated with the absolute dating of GRADSTEIN et al. (1995), it makes thus possible to estimate time comprised in the studied sections (including of course the error bars of radiometric dating). By counting the identified depositional sequences between dated levels (boundaries of ammonite zones or subzones,

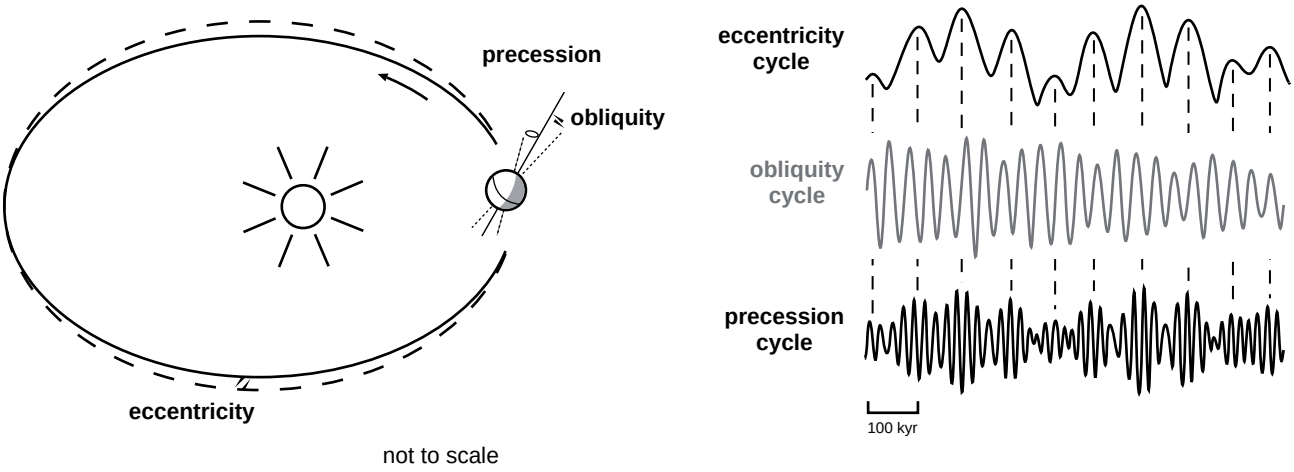

Fig. 6.1 - Astronomical parameters that control insolation on Earth (precession, obliquity, and eccentricity). Modified from STRASSER et al. (2007). Schematic insolation curves of the different orbital parameters. Note that the eccentricity cycles act as an amplitude modulator of the precession cycles. The obliquity cycle is not visible in the studied deposits. Based on EINSELE & RICKEN (1991).

sequence boundaries, or maximum floodings), their order of duration can be inferred (STRASSER et al. 1999) and compared with the known durations of the Milankovitch cycles.

6.2 ADVANTAGES AND LIMITS

Cyclostratigraphy allows obtaining a high-resolution stratigraphic framework, superior to that of biostratigraphy (PITTET 1994, 1996; HILLGÄRTNER 1999; HUG 2003; STRASSER et al. 2004; TRESCH 2007). As each sedimentary cycle represents a given duration (approximately 20, 40, 100, or 400 ka), the resulting time scale is very accurate but still floating because the age of the stage boundaries has large error margins ("floating astronomical timescale"; HILGEN et al. 2004; STRASSER et al. 2006).

The following effects or mechanisms may prevent and/or distort the record of orbital forcing in shallow platform environments and, consequently, they have to be taken into account when establishing a cyclostratigraphic time frame (STRASSER et al. 1999):

- Uncertainty about the completeness of the stratigraphic record (non-deposition or non-preservation of depositional sequences).
- In shallow carbonate platform deposits, autocyclic processes may mask or imitate orbitally forced depositional sequences.
- One cycle of environmental change can lead to the formation of multiple beds and, therefore, no constant time span can be attributed per bed (PITTET & STRASSER 1998b).
- Bed thickness and accommodation do not have a linear relationship because of facies-dependent differential compaction. Observed bed thickness consequently does not correspond to the original accommodation.
- The estimation of accommodation potential is difficult within subtidal facies.
- Loss of record of high-frequency sea-level and/or climatic fluctuations when sedimentological and/or biological thresholds were not passed and thus no facies contrast was created.
- Interference of long-term and short-term sea-level fluctuations leading to enhancement and attenuation of high-frequency signals.
- Imprecise chronostratigraphic data that introduce large error ranges in mean cycle durations.

Despite of all these difficulties, cyclostratigraphy is the tool of choice for establishing a high-resolution time frame.

6.3 CYCLOSTRATIGRAPHIC TIME FRAME

A cyclostratigraphic time frame is proposed for the studied interval (Fig. 6.2). Based on the radiometric ages given by GRADSTEIN et al. (1995) for the Oxfordian and Kimmeridgian stage boundaries, HARDENBOL et al. (1998) date the 3rd-order SB Ox6 at 155.81 Ma and the 3rd-order SB Ox7 at 155.15 Ma by interpolation between the stage boundaries (Figs 1.5 and 6.2).

This implies a time span of 600 to 700 kyr between these two sequence boundaries. Between the 3rd-order sequence boundaries Ox6 and Ox7, two medium-scale sequences, each containing four small-scale sequences, were identified in the shallow platform and in the basin sections (Fig. 6.2). Consequently, it is suggested that a medium-scale sequence formed within 300 to 350 kyr and a small-scale sequence within 75 to 87.5 kyr. These values coincide well with those of the short and long eccentricity cycles (100 and 400 kyr, respectively; Berger et al. 1989; Berger & Loutre 1994). In the studied sections it is commonly observed that five elementary sequences group into a small-scale sequence. Consequently, the observed depositional sequences are the sedimentological expression of orbital cycles and are attributed to the precession of the equinoxes (20 kyr) for the elementary sequences, and to the short- and long-eccentricity cycles (100 and 400 kyr) for the small- and medium-scale sequences, respectively. Despite the attenuated effects of the obliquity cycle (40 kyr) on the insolation in low latitudes (Berger 1978), an influence of this cycle is possible, particularly during greenhouse periods (Read 1995). This cyclostratigraphic time frame is comparable to the one of Strasser in press (Fig. 6.2) and now helps to improve the timing between the 3rd-order sequence boundaries Ox6 and Ox7.

In the Late Oxfordian deposits of the Jura platform, 100-kyr sequences are quite easily recognized whereas 20-kyr sequences may be locally more difficult to identify (Pittet 1996; Hug 2003). However, this study has confidently identified elementary sequences with the help of detailed facies and microfacies analyses. The obliquity cycle seems not to be expressed in the sedimentary record of the studied sections. However, from the study of more marly intervals, for example in the top part of the Röschenz Member, Pittet

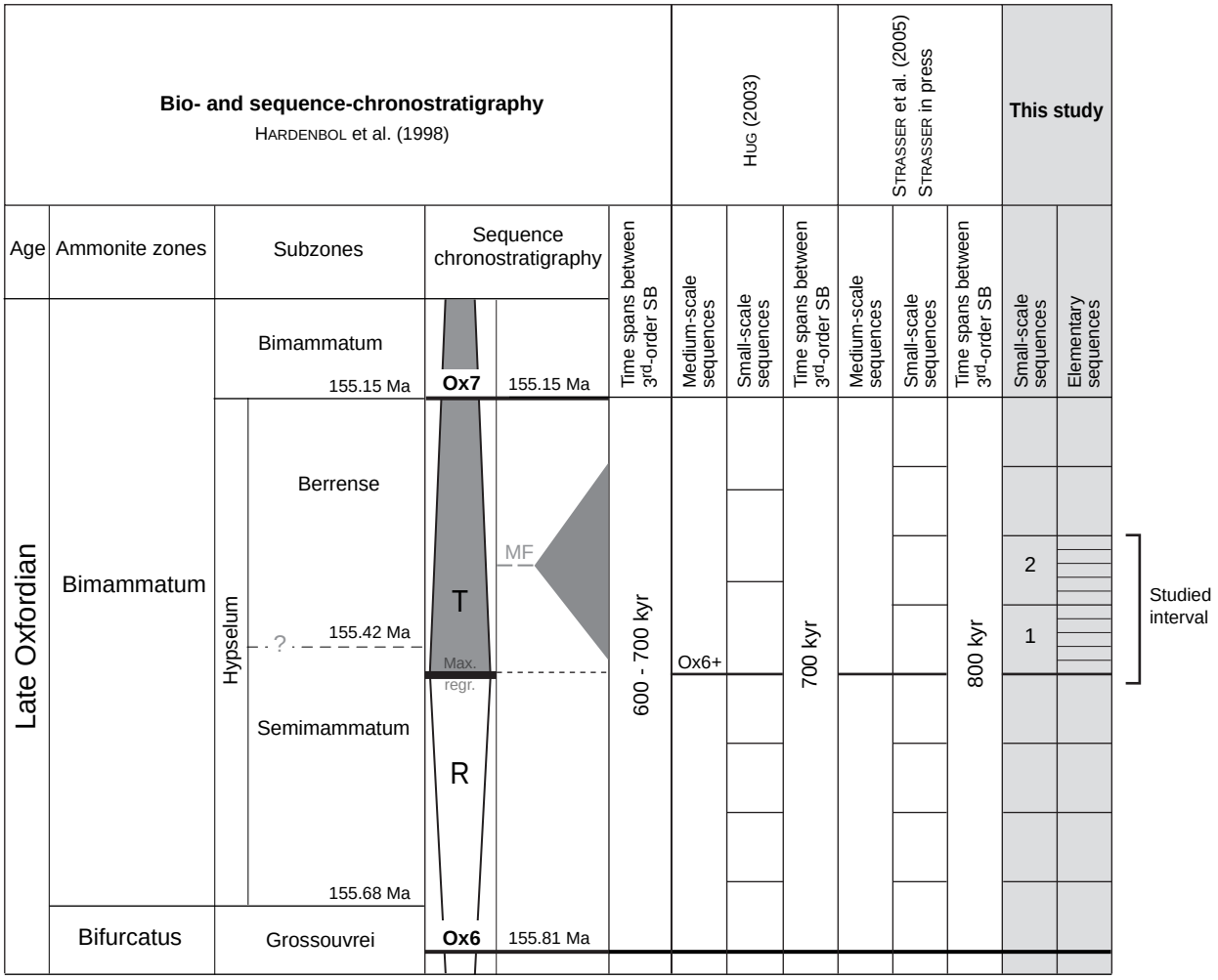

Fig. 6.2 - Cyclostratigraphic time framework proposed for the studied interval. Bio- and sequence-chronostratigraphy are from Hardenbol et al. (1998).

(1996) related obliquity to humidity cycles acting on carbonate production and terrigenous input and not to cycles of sea-level changes.

6.4 Comparison with other studies

Only a few studies exist on the record of Milankovitch cycles in Late Oxfordian sedimentary successions. Pittet (1996) investigated, for the first time, the orbital cycles in the deposits of the Röschenz Member and Hauptmumienbank/Steinebach members (Vellerat Formation, Swiss Jura). This author observed a hierarchy of four orders of sequences related to orbital cycles (precession, obliquity, and short and long eccentricity). Hug (2003) studied the top part of the Vellerat Formation and the Courgenay Formation and established a precise sequence- and cyclostratigraphic framework with a 100-kyr resolution used as a starting point of this study (Fig. 6.2).

Strasser et al. (2005) performed a sequence- and cyclostratigraphic analysis from platform to basin on sections in Spain. They identified eight small-scale sequences within the 3rd-order sequence between SB Ox6 and Ox7, leading to the same duration (800 kyr) as proposed by Strasser (2007) for the Swiss Jura. However, a comparison at the scale of elementary sequences is not proposed in any of these studies.

* * *

7 - HIGH-FREQUENCY PALAEOENVIRONMENTAL CHANGES ON THE SWISS JURA PLATFORM

This chapter examines the high-frequency palaeoenvironmental changes that occurred on the Swiss Jura platform in the narrow time framework established from facies analysis coupled with sequence- and cyclostratigraphic analysis (cf. Chaps 5 and 6). The stratigraphic and lateral distribution of facies, oncoids, and benthic foraminifera is investigated within an interval of 180 kyr at the scale of elementary sequences (20 kyr), which allows to reconstruct the platform evolution through time and to interpret the palaeoecological conditions.

7.1 PLATFORM EVOLUTION THROUGH TIME

The shallowest facies appears at the base of all sections (Fig. 7.1a). At Vorbourg, Hautes-Roches, Court, and Pertuis, they consist of marly deposits, characterizing protected lagoonal sedimentation. In Voyeboeuf and Savagnières, the shallowest facies are made of bioclastic (mainly ostracodes and inocerams) mudstones-wackestones. These two facies types mark a major sequence boundary: **the medium-scale SB Ox6+** (see chapter 5 for the definition of this sequence boundary). Then, a rapid facies change, easily recognizable in most of the Swiss Jura deposits, occurs from marly deposits to massive limestone beds (cf. Chap. 5; Fig. 7.1a). These limestones correspond to higher energy facies and/or contain more open-marine faunal assemblages, which overlie the transgressive surface TS Ox6+. Elementary sequence 1.3 is the thickest one of the first small-scale sequence (Fig. 7.1b) suggesting maximum accommodation gain. The maximum flooding of this elementary sequence coincides with the maximum flooding of small-scale sequence 1. At the end of the first small-scale sequence, a shallowing and possibly also a climate change to more humid conditions are indicated by a minor siliciclastic input (Fig. 7.1c) marked by relatively thin clay layers (Voyeboeuf, Hautes-Roches, and Pertuis sections), by oncoid rudstones (Vorbourg section), by bioclast mudstones with birdseyes (Court section), and by a serpulid-rich layer (Savagnières section). This interval with thin beds and more or less rich in clays is interpreted as the **small-scale SB 2**. At the top of the carbonate-dominated part of the sections, a wavy to planar surface is observed (Fig. 7.1d), which is overlain by more or less siliciclastics. In the "proximal" sections (Voyeboeuf, Vorbourg, Hautes-Roches, and Court) this wavy surface consists of a hardground, indicating sediment starvation. In the most "distal" sections (Savagnières and Pertuis), it consists of a relatively flat surface. This level belongs to the **medium-scale MF Ox6+** (for definition see chapter 5). The overlying siliciclastics, more abundant in the 'proximal' part of the platform, possibly indicate more humid conditions in the hinterland. However, during transgression clays may also have been remobilized and transported by currents over kilometres and preferentially deposited in depressions (PITTET 1996; STRASSER et al. 1999).

Assuming that the observed depositional sequences formed through superimposed frequencies of sea-level fluctuations controlled by orbital cycles, a precise time frame can be constructed (Fig. 7.2). Dominant facies and environments within each elementary sequence are represented in a time-space diagram (Fig. 7.3). **Siliciclastics** (clays and quartz) occur abundantly at the base (sequence 0.5 and around SB Ox6+) of the Vorbourg, Hautes-Roches, and Court sections. Then siliciclastics disappear but reappear around SB 2, especially in the Voyeboeuf and Hautes-Roches sections. Siliciclastics are flushed onto the platform by terrigenous input controlled by increased rainfall in the hinterland and/or by sea-level drop. The source

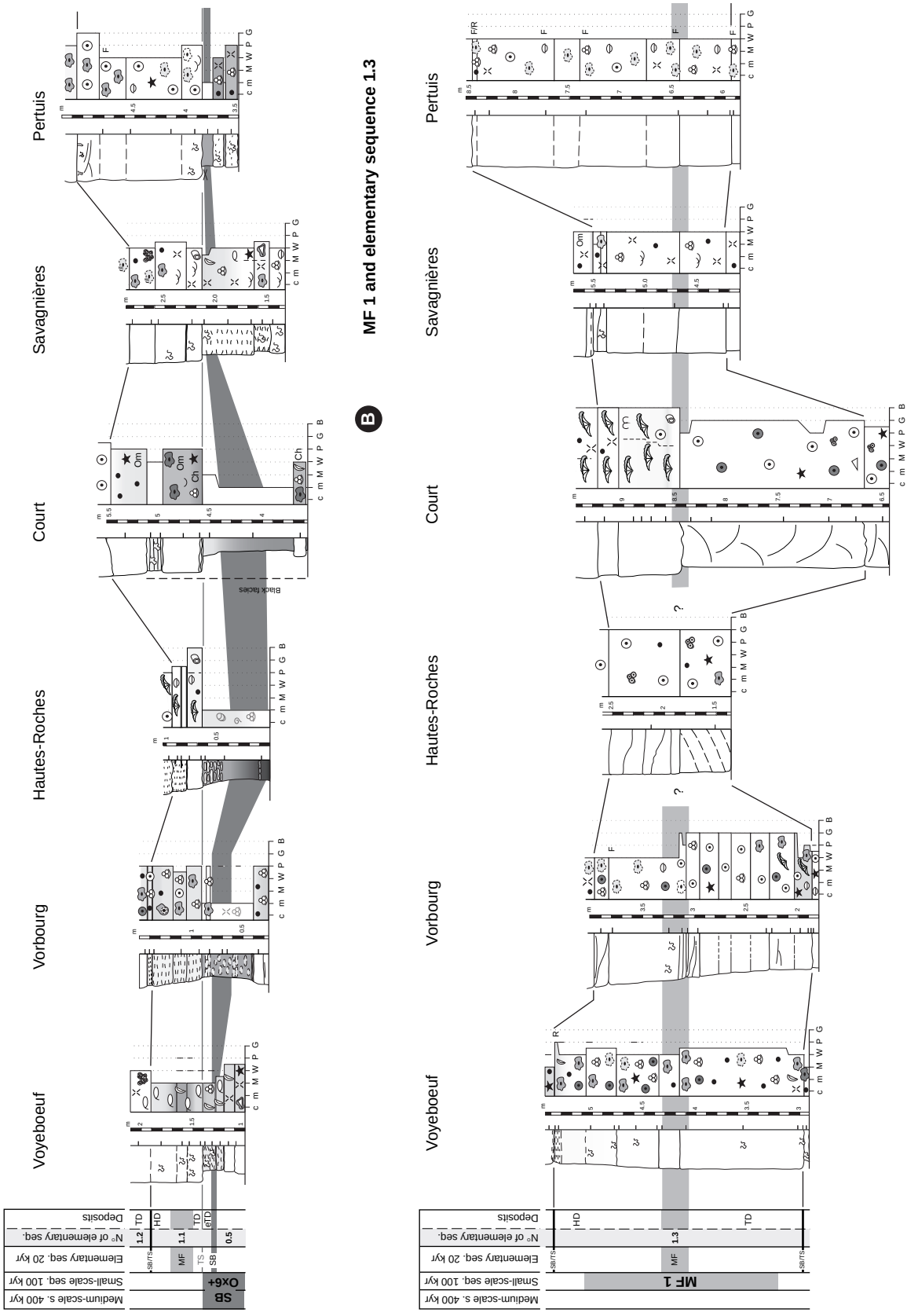

Fig. 7.1 - Focus on major sequential limits and their concomitant elementary sequences. (a) SB Ox6+ and elementary sequence 1.1, (b) MF 1 and elementary sequence 1.3.

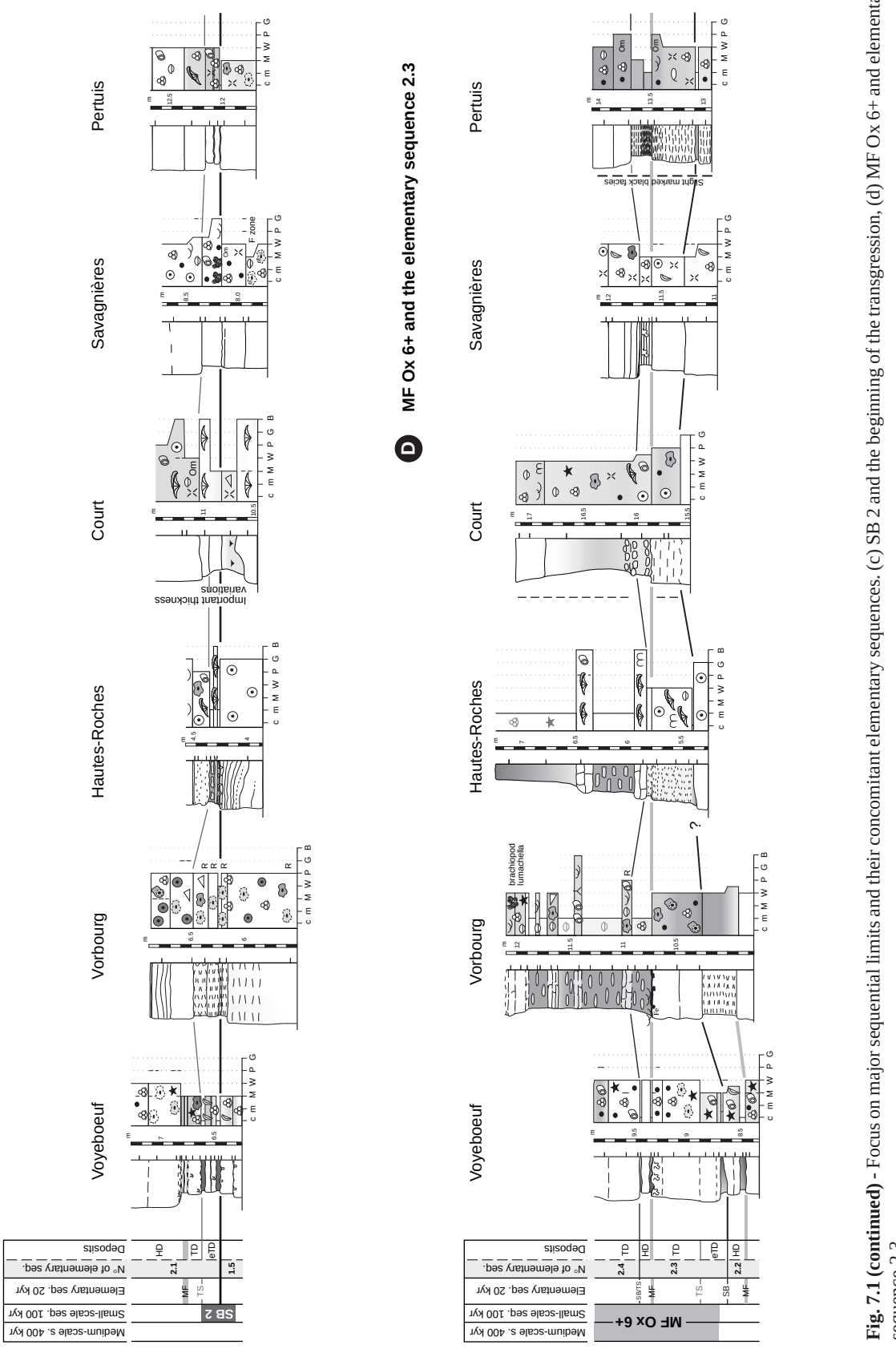

Fig. 7.1 (continued) - Focus on major sequential limits and their concomitant elementary sequences. (c) SB 2 and the beginning of the transgression, (d) MF Ox 6+ and elementary sequence 2.3.

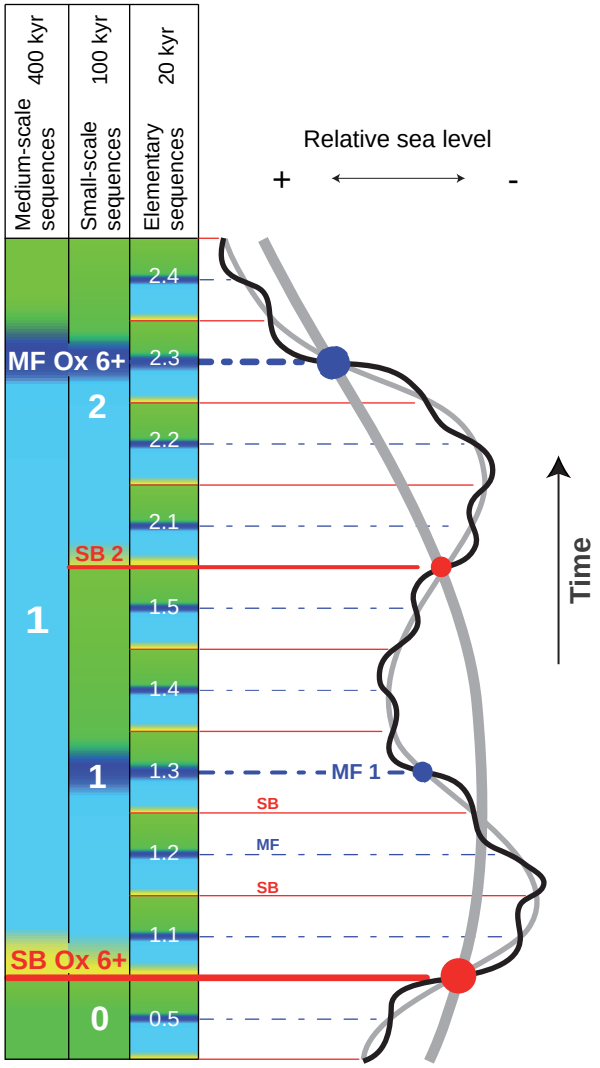

Fig. 7.2 - High-resolution time framework used in this study related to superimposed sea-level fluctuations.

area was located in the London-Brabant and/or Bohemian massifs, 400 km to the North (Fig. 1.3). Between the emerged lands and the shallow-carbonate platform, a fluvial plain with an important potential of siliciclastic capture and storage has probably existed. However, the climatic conditions on the platform were not necessarily the same as in the hinterland (Pittet 1996; Dupraz 1999; Hug 2003). For example, siliciclastics could have been mobilized when it rained in the hinterland and flushed onto the platform that experienced a semi-arid climate.

Oncoid growth is mainly controlled by the water energy, trophic level, and sediment accumulation rate (see below). **Oncoid-rich facies** appear more abundantly in the first small-scale sequence than in the second one. The Vorbourg and Pertuis sections are essentially composed of oncolitic facies in the first small-scale sequence whereas in the Voyeboeuf, Court and Savagnières sections oncolitic facies are patchily distributed and even inexistent in the Hautes-Roches section.

The various origins of peloids (e.g., bacterial, fecal, reworked cohesive mud, internal molds of fossils, complete micritization of grains) may explain the relatively widespread distribution of the **peloid-rich facies** in almost all sections.

Bioclastic facies result from the accumulation of debris of organisms. The fauna and flora association reflects the environmental conditions during their life under the condition that they have been deposited in situ. However, taphonomic processes such as time averaging through bioturbation and transport through currents cannot be excluded. Bioclastic facies with semi-restricted fauna, characteristic of protected lagoonal environments, are mainly present at the base (sequences 0.5 and 1.1) of the Voyeboeuf and Savagnières sections, and around SB 2 of the Voyeboeuf, Court, and Savagnières sections. They also exist at the top of the Savagnières section around MFS Ox6+. Bioclastic facies with normal-marine fauna, representing open-lagoonal environments, are less abundant and occur only patchily (Fig. 7.3).

Coral facies, mainly composed of coral boundstones, reflect open-marine environments (i.e., semi-open and open lagoon in this study). Coral facies occur in the Court and Hautes-Roches sections. The first coral reefs appear in the Hautes-Roches section in sequence 1.1 and in the Court section in sequences 1.3 and 1.4. In the second small-scale sequence, coral facies are less abundant and correspond to small patch-reefs.

Ooids are formed and transported by tidal currents in shallow waters. **Oolitic facies** predominate in the Hautes-Roches, Court, and Vorbourg sections. The spatial and temporal distribution is patchy. In the first small-scale sequence, the Pertuis section reveals the first and single oolitic deposit while in the Hautes-Roches and Court sections ooid accumulation starts somewhat later but then dominates especially at Hautes-Roches. The second small-scale sequence exhibits ooid deposits mainly in the Vorbourg, Hautes-Roches, and Court sections, and a few in the Savagnières section. Oolitic deposits are mainly driven by autocyclic processes (e.g., progradation or lateral migration of sedimentary bodies), which can simulate depositional sequences

or mask sequence boundaries and maximum flooding surfaces (STRASSER 1991). However, hydrodynamic changes denoted by sedimentary structures can point to relative sea-level fluctuations. Consequently, also oolitic deposits were precisely logged in order to identify potential sequential limits.

Figure 7.3 demonstrates the complexity of facies and depositional environment distribution across the platform and through time and illustrates the **facies mosaic** on the Swiss Jura platform (STRASSER & VÉDRINE in press). The observed facies distribution reveals a difference between 'proximal' and 'distal'

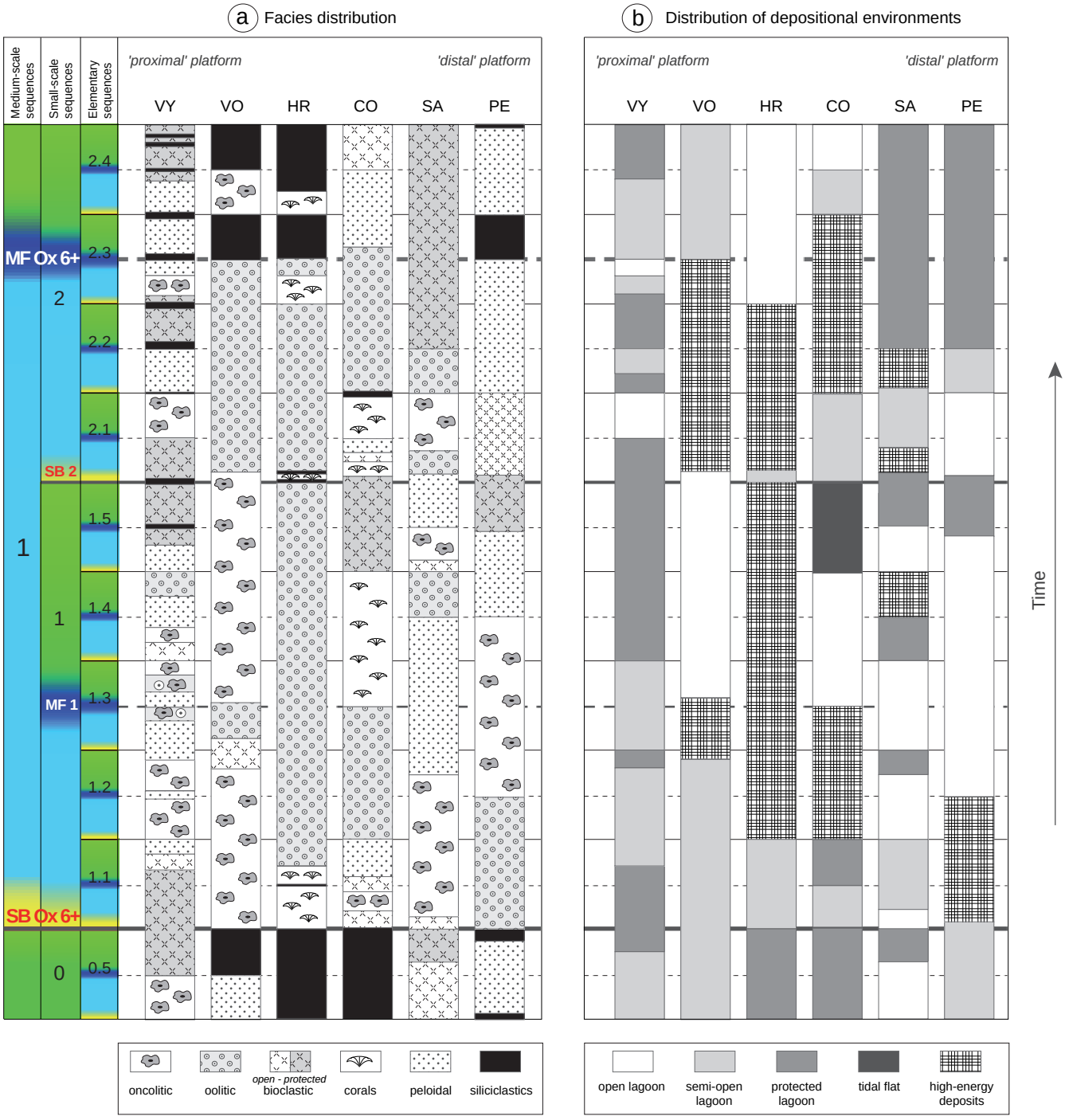

Fig. 7.3 - Time-space diagram illustrating the distribution of (a) major facies and (b) depositional environments of the six sections studied in the Swiss Jura Mountains (cf. Chap. 2 for details on facies and depositional environments). The sequence boundaries of the small-scale and the elementary sequences are considered as time lines delimiting the 100- and 20-kyr orbital cycles.

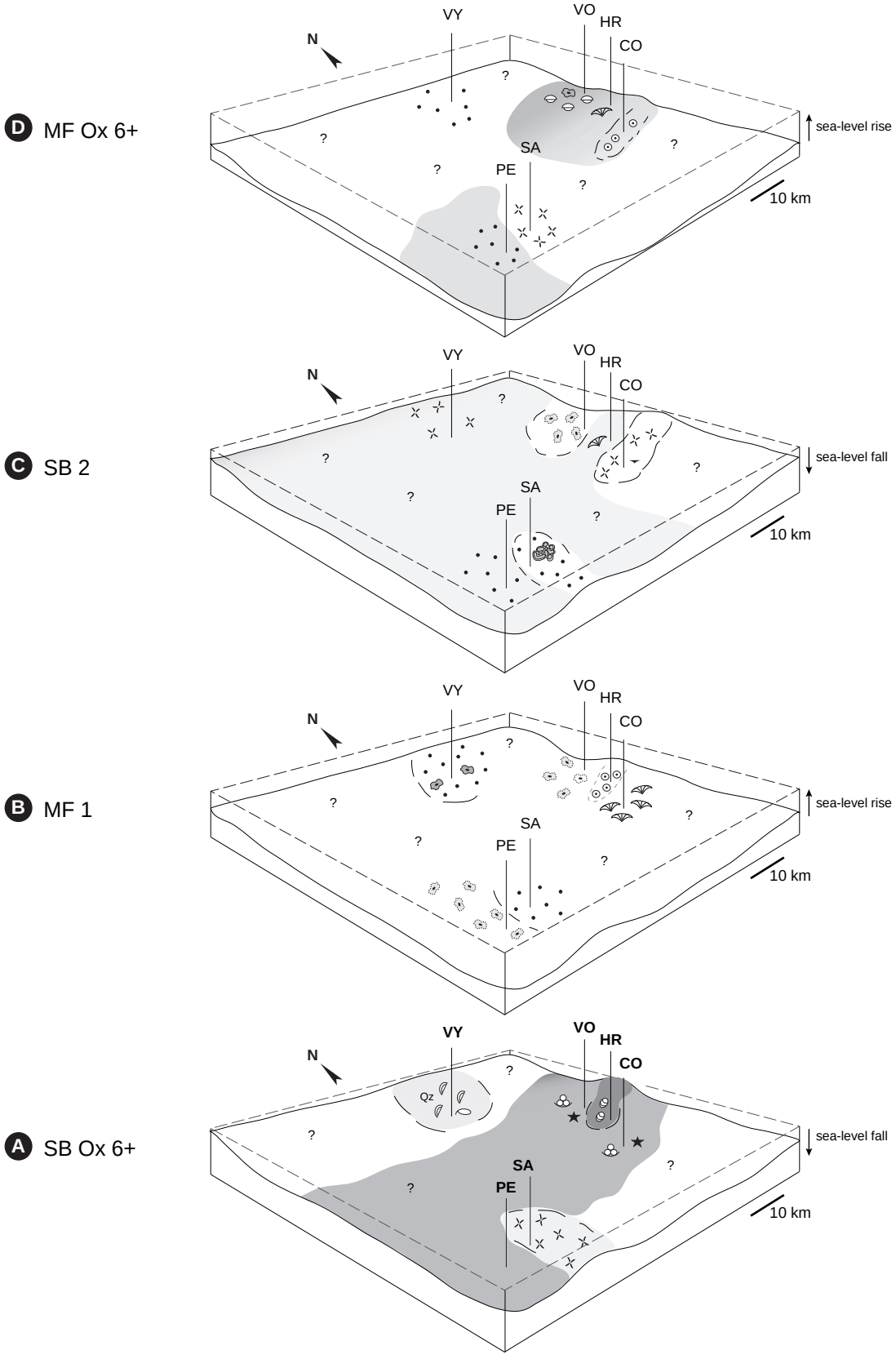

Fig. 7.4 - Platform evolution through time of the Swiss Jura platform at selected time intervals (a) medium-scale SB Ox6+; (b) small-scale MF 1; (c) small-scale SB 2; (d) medium-scale MF Ox6+. Symbols as in Fig. 4.1.

platform environments (Fig. 7.3b). Open lagoonal environments are more common in the "distal" platform positions and particularly in the Pertuis section. Inversely, protected lagoonal environments abound in Voyeboeuf, in the most "proximal" platform positions. The facies distribution of the Swiss Jura platform is thus partly linked to platform morphology. The latter is variable and was created by differential subsidence (Wetzel et al. 2003; Allenbach 2001). The sediment accumulation rates (carbonates and siliciclastics) accentuate or attenuate the relief of the platform. For example, during periods of coral reef growth and ooid production, equivalent to high carbonate productivity, the irregular morphology was enhanced. Reefs formed on structural highs along the platform margin but could later find themselves in rapidly subsiding areas due to tectonic inversion. Ooid bars not only occurred on the platform margin but also in the platform interior where morphological highs created favourable conditions. Locally, wide channels brought relatively open-marine conditions into more central platform positions, generating high-energy depositional environments. Behind reefs and bars, lagoons were isolated or protected from open-marine influence and from wave or current energy (Fig. 2.3; Hug 2003; Strasser & Védrine in press). Lagoonal facies with oncoids shows a patchy distribution. No systematic relationship with the other facies is recognizable, although the most persistent oncoid lagoons appear to be situated preferentially on the inner platform when compared to ooid bars and coral reefs.

The spatial facies distribution is monitored for different selected time intervals corresponding to major sequential limits of medium-scale and small-scale sequences (Fig. 7.4). At the SB Ox6+, a major sea-level fall caused the flushing of the platform by siliciclastics (Fig. 7.4a). The Voyeboeuf and Savagnières sections are dominated by bioclasts and do not present marls, suggesting that these sections were topographic highs. Then the transgression begins and leads to the disappearance of siliciclastics. The increase of accommodation favors homogenization and diversification of lagoonal facies and marks the small-scale MF 1 (Fig. 7.4b). The Voyeboeuf and Savagnières sections still present similar facies (micrite-dominated oncoid and peloidal facies). The Vorbourg and Pertuis sections show *Bacinella-Lithocodium* oncoid facies. High-energy deposits dominate in the Hautes-Roches section and a large coral patch-reef develops in the Court section. Then, sea level falls again. At this time, minor inputs of siliciclastics are noticed especially in the Hautes-Roches and Voyeboeuf sections (Fig. 7.4c), birdseyes representing tidal flat facies are observed in the Court section, a serpulid-rich level occurs in the Savagnières section, and peloidal facies dominates in the Pertuis section. Finally, sea level rises again, creating an increase of the accommodation space (around the MF Ox6+; Fig. 7.4d). Peloid- and bioclast-rich facies exist in the Voyeboeuf, Pertuis, and Savagnières sections. As for MF 1, the Court and Hautes-Roches sections present ooid bars and coral patch-reefs while the Vorbourg section is rich in brachiopods and micrite-dominated oncoids.

7.2 Oncoids

Based on thin sections and macroscopic samples from the Hauptmumienbank Member, four types of oncoids are distinguished (cf. Chap. 2, Fig. 2.1). Based on the well-defined high-resolution time framework, stratigraphic and spatial oncoid distribution is examined and the main environmental controlling factors of oncoid growth and distribution are discussed (see also Védrine et al. 2007).

7.2.1 Stratigraphic and spatial distribution

From the high-resolution sequence-stratigraphic framework, a time-space diagram illustrating the distribution of oncoid types is synthesized (Fig. 7.5). A proximal-distal trend is revealed by the greater abundance of type 3 oncoids in the "distal" platform sections (Pertuis and Savagnières); while in the "proximal" section (Voyeboeuf) type 2 and 1 oncoids predominate. Hautes-Roches and Court, which are mainly composed of ooid-rich deposits and patch-reefs, almost exclusively present type 2 oncoids. The different oncoid types coexist, except types 1 and 4 that occur in very different environmental settings concerning mainly water energy. Regardless of these general trends, it appears that local conditions (e.g., clay input) played an important role in oncoid development. Migrating ooid bars locally interrupted the oncoid sedimentation (Fig. 7.3).

A specific evolution of oncoid types is occasionally observed within small-scale and elementary depositional sequences. Oncoids are generally more abundant in the first small-scale sequence than in the second one (Fig. 7.5). Based on the high-resolution sequence-stratigraphic framework, a detailed description of the oncoid type distribution is given for the Vorbourg sec-

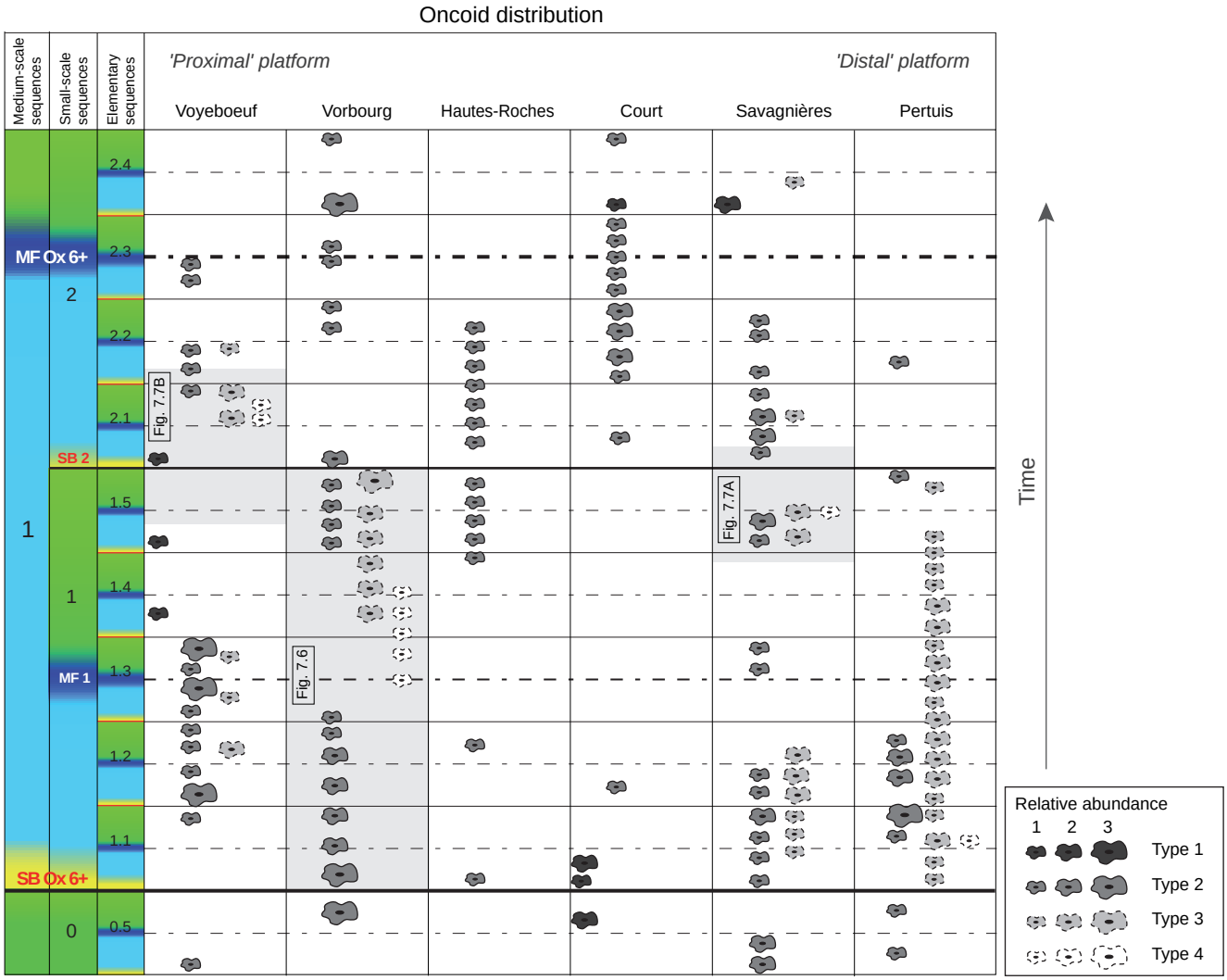

Fig. 7.5 - Distribution of oncoid types in the elementary sequences within the transgressive deposits of the Ox 6+ medium-scale sequence for the six studied sections in the Swiss Jura. Sections are arranged from "proximal" to "distal" platform. Relative abundance (1-present, 2-common, 3-abundant) for each oncoid type is estimated from thin section analysis. Intervals detailed in Figs 7.6 and 7.7 are shaded.

tion (Fig. 7.6). The (early) transgressive deposits of the first small-scale sequence contain abundant type 2 oncoids. Migration of ooid bars locally interrupts oncoid formation in the upper part of the transgressive deposits of elementary sequence 1.3. Around and after the maximum flooding of this elementary sequence, type 3 and 4 oncoids appear. In the two last elementary sequences, type 3 oncoids dominate and type 2 oncoids reappear. Small-scale SB 2 is marked by Miliolid foraminifera and type 3 oncoid rudstones. Within the elementary sequences of Vorbourg, no particular trend is observed.

However, in the Voyeboeuf and Savagnières sections (Fig. 7.7), some elementary sequences display the same evolution as the small-scale sequence of Vorbourg. Elementary sequence 1.5 in Savagnières presents two beds, interpreted respectively as transgressive and highstand deposits. The transgressive bed can be subdivided into bioclastic wackestone with normal-marine fauna and oncoid-rich wackestone-floatstone. The maximum flooding is marked by type 3 and 4 oncoid mudstone to floatstone. The highstand deposit is dominated by peloidal and bioclastic wackestone. The small-scale sequence boundary is placed at the base of a serpulid bioherm with peloids and oysters. The next elementary sequence 2.1 has an early transgressive deposit rich in peloids, serpulids, oysters, Textulariid foraminifera, and a few type 2 oncoids. In Voyeboeuf, elementary sequence 1.5 is

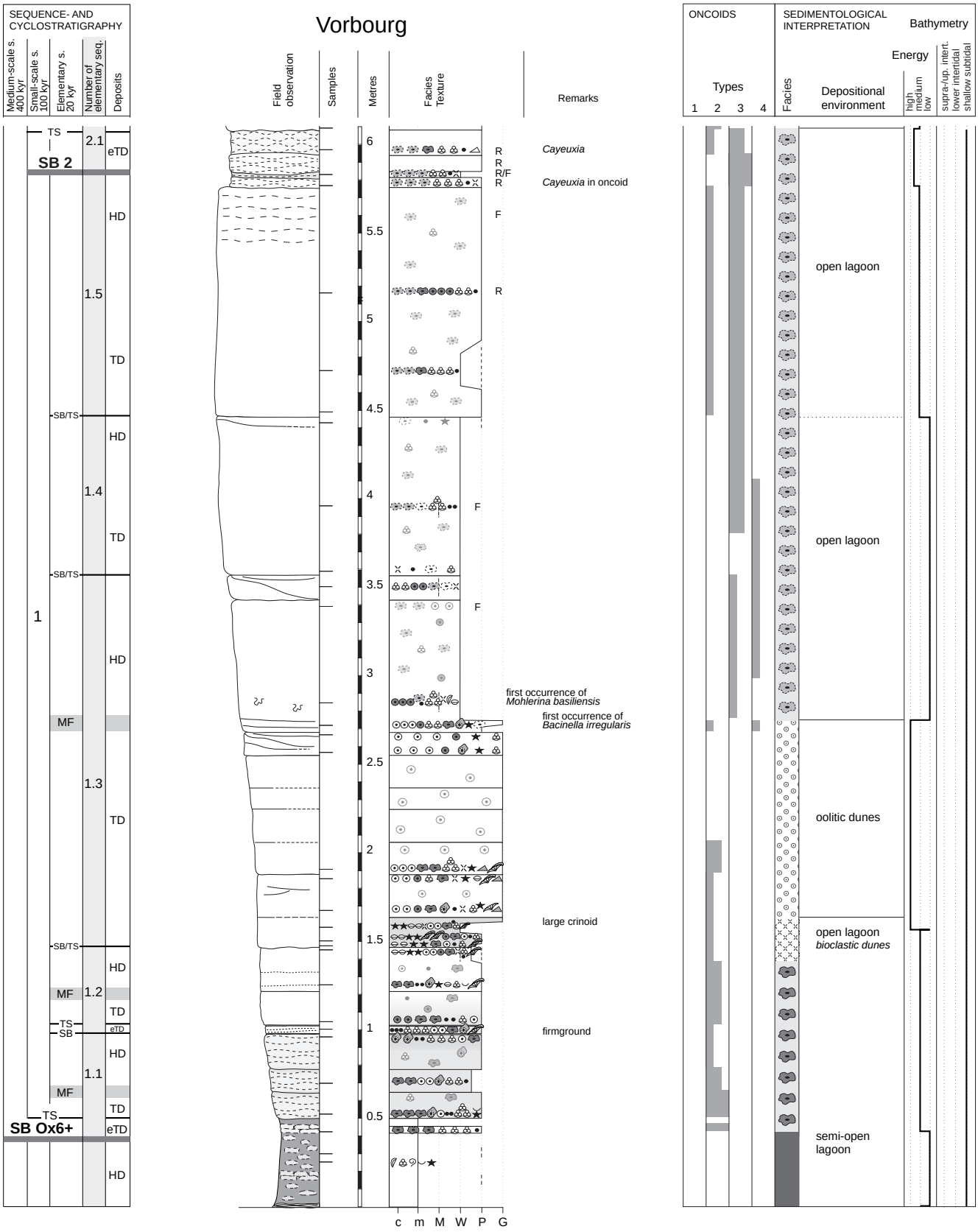

Fig. 7.6 - Detail of the first small-scale sequence of the Vorbourg section, showing the distribution of the four oncoid types, facies types, palaeoenvironmental interpretation, and the sequence-stratigraphic framework. For discussion refer to text. For symbols refer to Fig. 4.1.

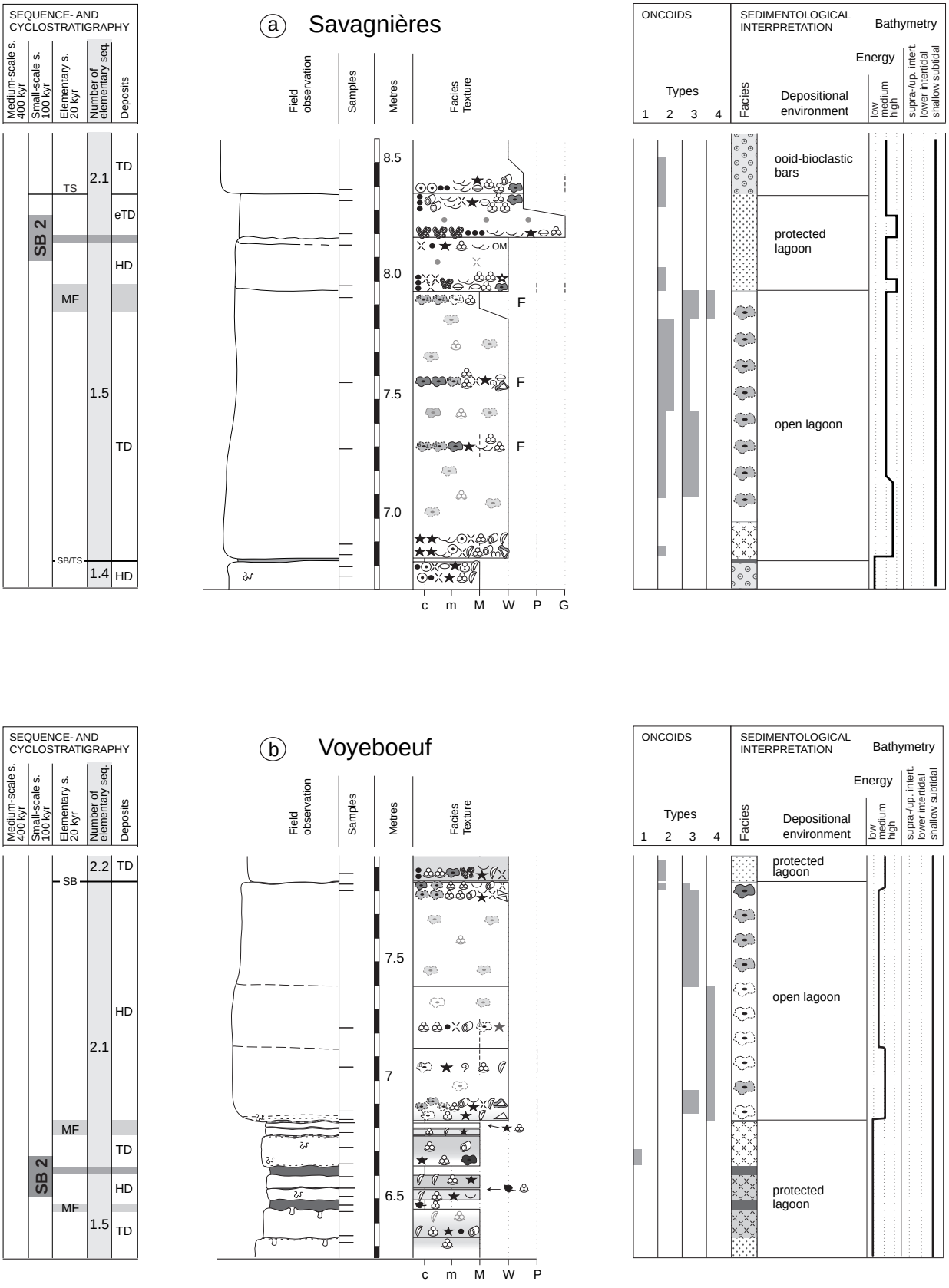

Fig. 7.7 - Selected elementary sequences of the Savagnières and Voyeboeuf sections around small-scale sequence boundary SB 2, showing the distribution of the four oncoid types, facies types, the palaeoenvironmental interpretation, and the sequence-stratigraphic framework. For discussion refer to text. For symbols refer to Fig. 4.1.

composed of ostracode and Textulariid foraminifer mudstones (Fig. 7.7b). The highstand deposit of this elementary sequence consists of clays with coal debris, detrital quartz, and serpulids, indicating relatively proximal and semi-restricted conditions, and two thin wavy limestone beds composed of ostracode and foraminifer mudstone. The small-scale sequence boundary is placed at 6.6 m in a clay-rich level. The transgressive deposit consists of foraminifer mudstone with some type 1 oncoids. The maximum flooding is placed around thin wavy beds surrounded by marls. The highstand deposit is made of a massive bed, which is rich in type 3 and 4 oncoids and benthic foraminifera at the base. In its upper part, type 3 oncoids and foraminifera (Textulariid and Miliolid) dominate. The next sequence boundary SB 2.2 is marked by peloid and foraminifer (Miliolid and less Textulariid) wackestone rich in detrital quartz. In this transgressive deposit, some type 2 oncoids are observed.

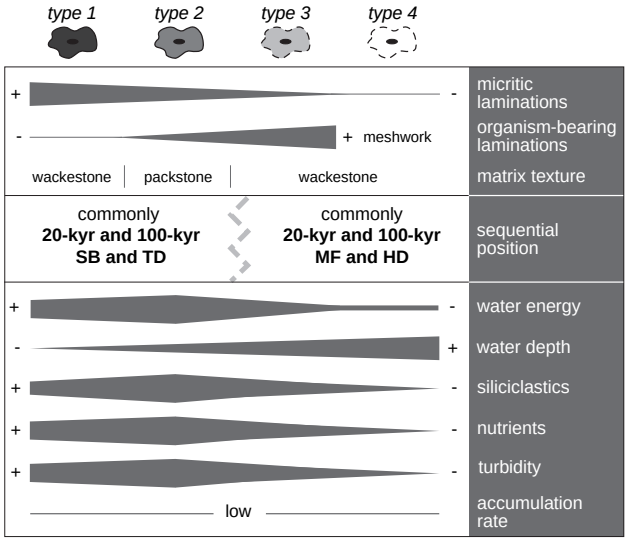

Fig. 7.8 - Oncoid types, their preferred position in a depositional sequence, and main controlling factors. For discussion refer to text.

This study on the spatial and stratigraphic distribution of oncoids in lagoonal deposits shows that type 1 and 2 oncoids have both a similar distribution and preferentially form around the sequence boundaries and during transgressive conditions of elementary and small-scale sequences, indicating that enough energy was furnished to roll the particles (Fig. 7.8). Type 3 and 4 oncoids have an inverse occurrence because they mainly occur around small-scale and elementary maximum-flooding intervals and in highstand deposits, characterizing periods of low-energy and increase of *Bacinella-Lithocodium* growth (Fig. 7.8).

7.2.2 Controlling factors

Oncoid growth and distribution are mainly controlled by sea level and climate (Figs 7.8 and 7.9). The main direct environmental parameters are water energy, water depth, trophic level, and sediment accumulation rate. Their influence is recognized in the stratigraphic and spatial distribution of oncoids in large-scale to elementary sequences as well as in the oncoid surface morphology, the biotic composition of the oncoid cortex, and the encasing sediment.

Water energy and water depth

The oncoid-rich facies of the Hauptmumienbank Member appears at the beginning of a 2nd-order sea-level rise, covers the entire medium-scale Ox6+ sequence and then disappears above the 3rd-order SB Ox7 (Fig. 1.4). This stratigraphic distribution points to a link with changes of relative sea level. Sea-level fluctuations play an important role in opening and closing shallow lagoons behind barrier systems and thus strongly modify environmental factors (e.g., water energy, oxygenation, salinity, temperature, sediment transport). The specific evolution of oncoid types within small-scale and elementary sequences confirms the link also to high-frequency sea-level fluctuations. The sub-spherical type 1 and 2 oncoids, mainly resulting from sediment trapping by micro-organisms, preferentially occur around sequence boundaries and in transgressive deposits where higher energy conditions predominated in relatively shallow water (Fig. 7.8). This implies that these particles needed energy to be overturned and rolled. On the other hand, the lobate type 3 and 4 oncoids are characteristic of low-energy environments where microbial meshwork had time to grow. Type 3 and 4 oncoids are concentrated around maximum floodings and in highstand deposits where low-energy conditions existed in relatively deep water but still in the photic zone (Fig. 7.8). Consequently, the oncoid surface morphologies indicate the intensity of rolling on the sea floor and thus the degree of wave or current energy and, indirectly, water depth. The biotic composition and diversity in the oncoid cortex and the encasing sediment (e.g., texture, faunal association) provides additional information on water energy and water depth.

Platform morphology was created by differential subsidence of tectonic blocks and by differential sediment accumulation (e.g., Pittet 1996; Allenbach 2001; Hug 2003; Wetzel et al. 2003). The already

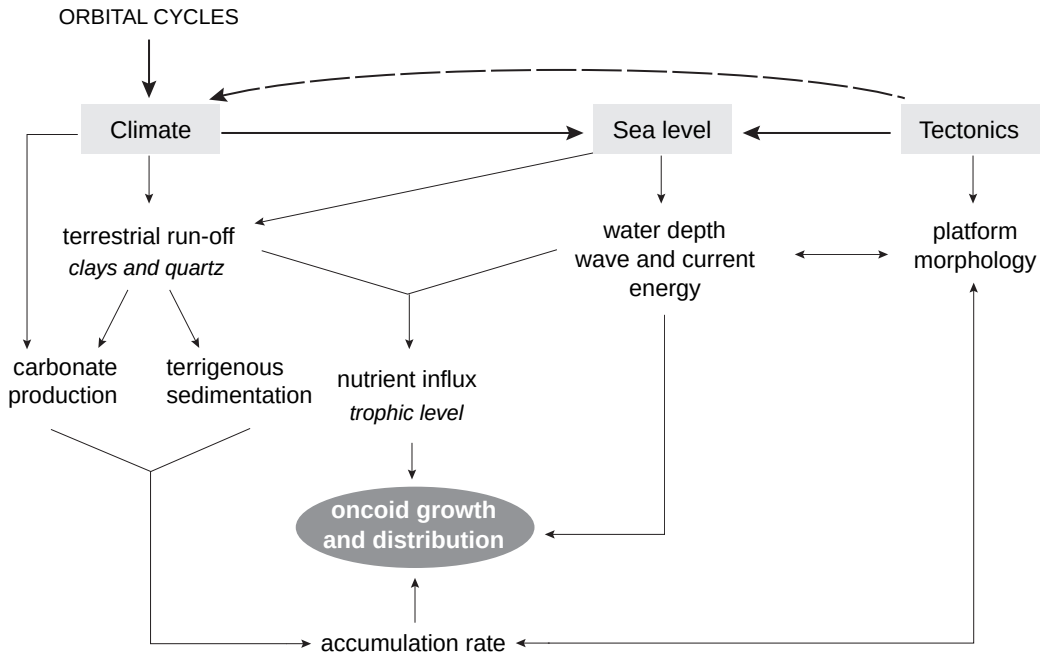

Fig. 7.9 - Interrelated factors controlling oncoid growth and distribution. For discussion refer to text.

existing highs and depressions were further accentuated by the increase of carbonate production in reefs and on ooid shoals. Oncoids were preferentially accumulated in depressions. HALLOCK (1988) also suggests that the point sources of terrigenous input and the platform morphology increase the spatial heterogeneity of nutrient distribution and thus trophic level. Consequently, variable platform morphology was partly responsible for the patchy distribution of oncoid-rich facies and oncoid types.

In the studied sections, some oncoid-rich beds are capped by ooid bars, which may have been controlled by autocyclic processes. On shallow carbonate platforms, such processes are inherent and involve lateral migration of sediment bodies (GINSBURG 1971; PRATT & JAMES 1986; STRASSER 1991). Consequently, autocyclic processes were superimposed on the orbitally controlled sea-level fluctuations and represented an additional factor in oncoid growth and distribution.

Accumulation rate

Carbonate accumulation rates mainly depend on the local carbonate production but can also be modified by carbonate transport (supply or exportation). On the Swiss Jura platform, the accumulation rate of oncoid-rich lagoons has been estimated at around 0.11 mm/year (after sediment decompaction), which is low in comparison to modern lagoonal environments (STRASSER & SAMANKASSOU 2003; STRASSER & VÉDRINE in press).

Microbial crusts commonly grow slowly. Their occurrence is considered to be diagnostic for low background sedimentation rates (LEINFELDER et al 1993). Similar requirements are probable for oncoids, which are partly or totally composed of the same microencrusters such as the *Bacinella-Lithocodium* association (e.g., PERYT 1983; DUPRAZ 1999).

Trophic level

The deposition of the massive Hauptmumienbank limestones on top of the Röschenz marls points to a general trend toward a lower input of siliciclastics and a higher carbonate productivity. Decreasing terrigenous input may have been related to a change to less humid climate conditions in the hinterland.

In the studied sections, oncoids occur abundantly in limestones and occasionally in marls. In the limestone beds, type 1, 2, 3 and 4 oncoids are present whereas in the marly intervals only type 2 oncoids are found. The biotic composition of the oncoid cortex

and the encasing sediment imply specific trophic conditions. Type 2 oncoids enclose serpulids and Textulariid foraminifera, which tolerate meso- to eutrophic conditions (e.g., Brasier 1995; Fugagnoli 2004). The concomitant growth of type 2 oncoids with such organisms and their occurrence in clay-rich environments suggest that they were adapted to low water transparency and potentially high trophic levels. Type 1 oncoids are rare in the studied sections and found in limestone beds. They show affinity with type 2 oncoids: the scarcity of associated fauna probably indicates mesotrophic or eutrophic conditions, making life difficult for carbonate producing organisms. Type 3 and 4 oncoids are constituted of light-dependent microencrusters (i.e., *Bacinella* and *Lithocodium*) implying clear water and oligotrophic conditions (Dupraz & Strasser 1999). They occur in the massive limestone beds, which formed when siliciclastic and nutrient input was reduced. Growing under water on the sediment surface, oncoids thus monitor water transparency and trophic level, which are both driven by the episodic influx of terrigenous sediment (quartz, clays, organic matter, and nutrients) onto the shallow carbonate platform (Fig. 7.9). This study demonstrates that oncoids are valuable proxies for high-resolution palaeoenvironmental and palaeoecological studies.

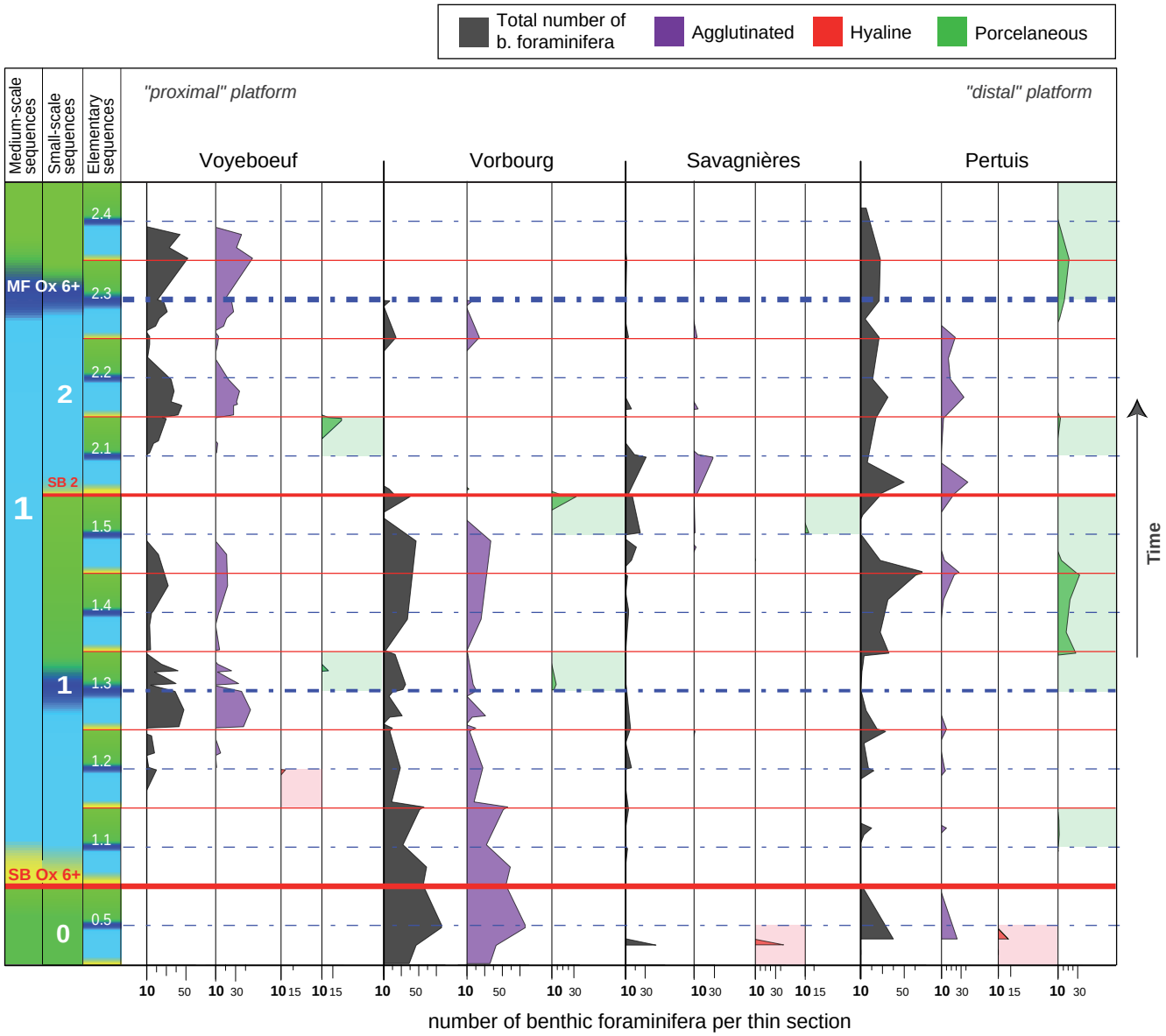

Fig. 7.10 - Benthic foraminifer distribution (all foraminifera, agglutinated, hyaline, porcelaneous) in the Voyeboeuf, Vorbourg, Savagnières, and Pertuis sections placed in the high-resolution time-space diagram. Specific occurrences of foraminifera in the transgressive and highstand deposits of some elementary and small-scale sequences are highlighted.

7.3 BENTHIC FORAMINIFERA

Benthic foraminifera have a great potential as indicators of depositional environments in the geologic past (e.g., SMITH 1955; MARTIN 1988; CANNARIATO et al. 1999). These bottom dwelling organisms occur in a wide range of marine environments from normal-marine to hypersaline, and from deep to shallow (GEEL 2000). Temperature and salinity have been considered as the main factors controlling the spatio-temporal distribution (e.g., MITCHELL 1996). However, trophic level and oxygenation appear as more determinant factors (concept of the organic flux, e.g., VAN DER ZWAAN et al. 1999). Hence, indirectly, also climate and sea level play an important role in the distribution of benthic foraminifera.

This study proposes to investigate the role of sea level on foraminifera in the Hauptmumienbank Member. Based on the high-resolution time framework (20-kyr time resolution) established by sequence- and cyclostratigraphy, the stratigraphic and spatial distribution of foraminifera is examined in four of the six studied Swiss Jura sections. The lagoonal deposits reveal three main suborders of benthic foraminifera: Textulariina, Miliolina, and Lagenina, characterized by three different types of wall (agglutinated, hyaline, porcelaneous respectively; cf. Chap. 2). For each category, the number (absolute abundance) of foraminifera has been counted per thin section (each thin section has the same surface area). In the graphical representation of the foraminifer distribution, samples with less than ten specimens have been masked in order to remove the potential noise caused by reworking. In addition, foraminifer and oncoid distribution are compared and discussed.

7.3.1 Stratigraphic and spatial distribution

Agglutinated, porcelaneous, and hyaline foraminifera

The foraminifer assemblages of the studied sections are mainly composed of forms with agglutinated tests (Textularids) and in a lower amount of those with porcelaneous tests (Miliolids). Hyaline foraminifera (only *Lenticulina*) are much rarer (Fig. 7.10).

The distribution of the total abundance of benthic foraminifera shows a relatively patchy distribution without any "proximal-distal" trend. Due to the predominance of agglutinated foraminifera in the studied deposits, the agglutinated foraminifer distribution is relatively similar to the one of the total number. Agglutinated foraminifera apparently occur without a clear facies dependence. The determination of genera and species would possibly give more detailed information (MURRAY 1991). This, however, is outside of the scope of this thesis. The porcelaneous and hyaline foraminifera show a correlation with the sequence-stratigraphic evolution. Miliolids are preferentially found in the highstand deposits of the elementary and/or small-scale sequences (Figs 7.10 and 7.11). The hyaline foraminifera, rare in the studied sections, are preferentially found in the transgressive deposits of elementary sequences (Figs 7.10 and 7.11). A similar distribution of benthic foraminifera has been suggested by ARNAUD-VANNEAU (1994) and was interpreted as being related to changes of accommodation and sediment and nutrient input. Consequently, the benthic foraminifera are indirectly linked to relative sea-level and indirectly also to climate changes. As for the oncoids, the variations in the foraminifer distribution are due to the combination

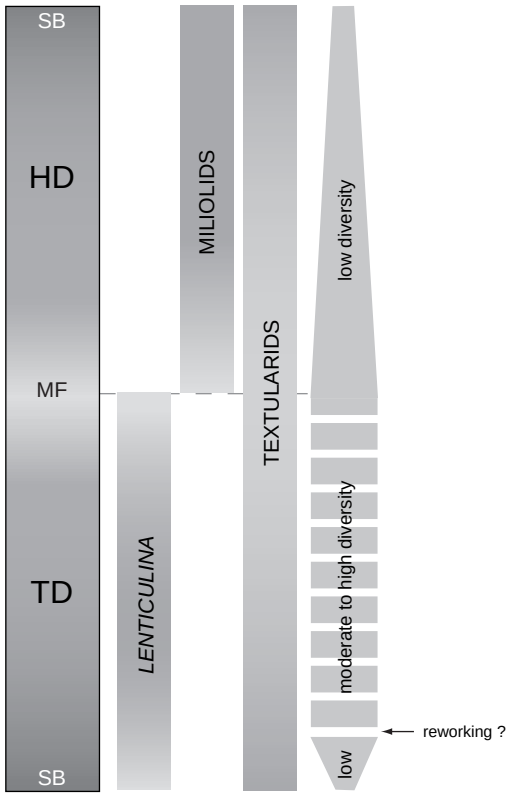

Fig. 7.11 - Schematic distribution of Textularids, Miliolids, and *Lenticulina* in relation with the sequence-stratigraphic evolution.

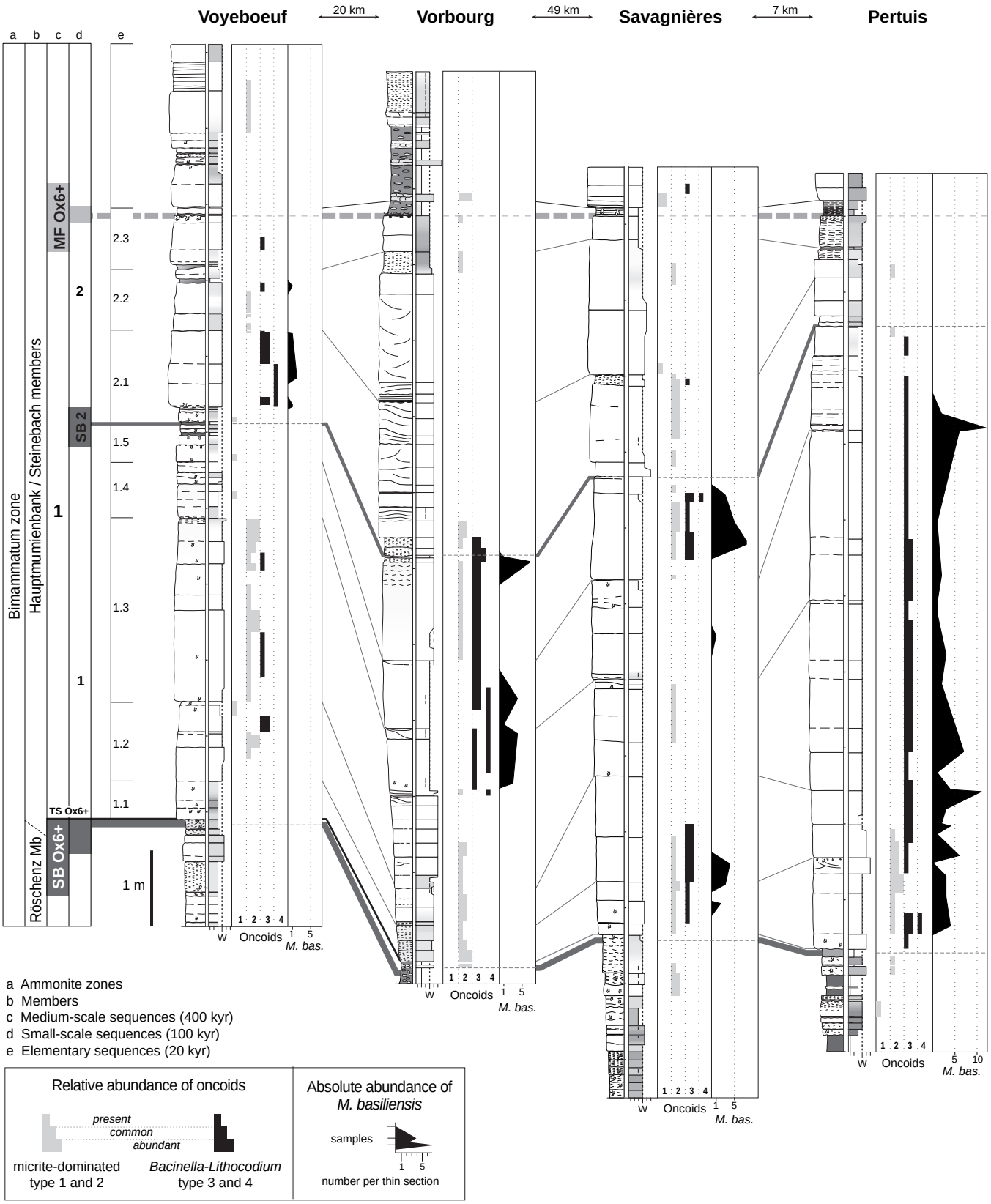

Fig. 7.12 - Distribution of *Mohlerina basiliensis* and oncoids along the studied sections.

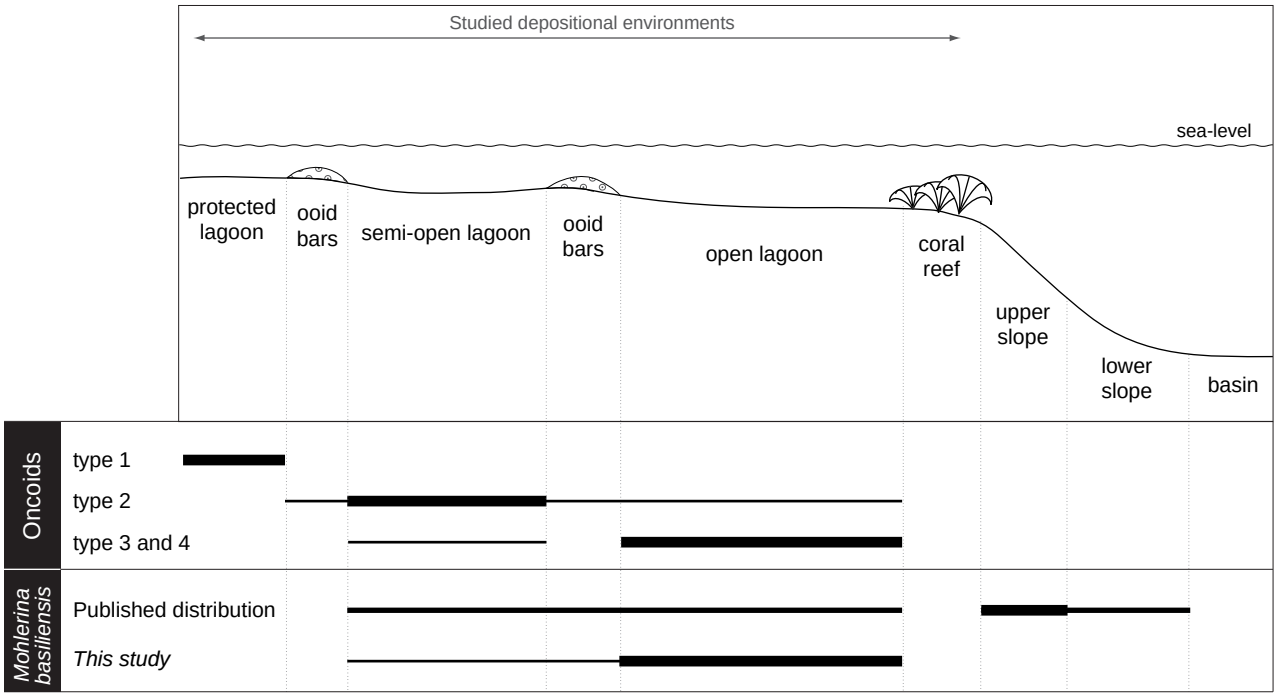

Fig. 7.13 - Distribution of *Mohlerina basiliensis* and oncoids from protected lagoon to basin. Published distribution according to DARGA & SCHLAGINTWEIT (1991), SCHLAGINTWEIT & EBLI (1999), SASARAN et al. (1999), VELIĆ et al. (2002), GAWLICK et al. (2003), and FLÜGEL (2004).

of physical, chemical, and biological factors (see below).

Co-occurrence of the benthic foraminifer Mohlerina basiliensis and Bacinella-Lithocodium oncoids

Together with Textularids, Miliolids and *Lenticulina*, the foraminifer *Mohlerina basiliensis* occurs in small amounts and is sparsely distributed in the studied sections (VÉDRINE & SPEZZAFERRI 2007; VÉDRINE 2008; Fig. 7.12). *Mohlerina basiliensis* was found in only 40 of the 265 analyzed thin sections. In the oncoid-rich Hauptmumienbank Member, *M. basiliensis* is mostly found in oncoid-rich and bioclastic (brachiopods, echinoderms) wackestones, characterizing low-energy and normal-marine conditions (Pl. 9/10-11, cf. Chap. 2). Sporadically, *M. basiliensis* appears in higher energy deposits such as ooid- and peloid-rich packstones (Pl. 9/10). Several authors found this foraminifer preferentially in high-energy facies from the internal platform to the slope, commonly associated with *Protopeneroplis* sp., *Trocholina* sp., *Pseudocyclammina* sp., *Andersolina* sp., *Nautiloculina* sp., *Lenticulina* sp. *Valvulina* sp., and Miliolids (DARGA & SCHLAGINTWEIT 1991; SCHLAGINTWEIT & EBLI 1999; SASARAN et al. 1999; VELIĆ et al. 2002; GAWLICK et al. 2003). Recently, FLÜGEL (2004) and VELIĆ et al. (2002) described *M. basiliensis* as characteristic of upper slope facies (Fig. 7.13).

The *M. basiliensis* distribution is relatively patchy. The 'distal' platform facies present a higher abundance of this foraminifer (Figs 7.12 and 7.14). Its minimum abundance (only 2 specimens per thin section) is found in the relatively "proximal" Voyeboeuf section, and the maximum abundance (up to 12 specimens per thin section) in the relatively "distal" Pertuis section. In the latter, *M. basiliensis* has a more extensive stratigraphic occurrence than in the other sections (Figs 7.12 and 7.14).

The distribution of *Bacinella-Lithocodium* oncoids is also relatively patchy. However, *Bacinella-Lithocodium* oncoids are more abundant in "distal" platform facies, especially in the Pertuis section (Fig. 7.12). Micrite-dominated oncoids are present in all sections but less abundant in Pertuis. Occasionally, *Bacinella-Lithocodium* and micrite-dominated oncoids coexist.

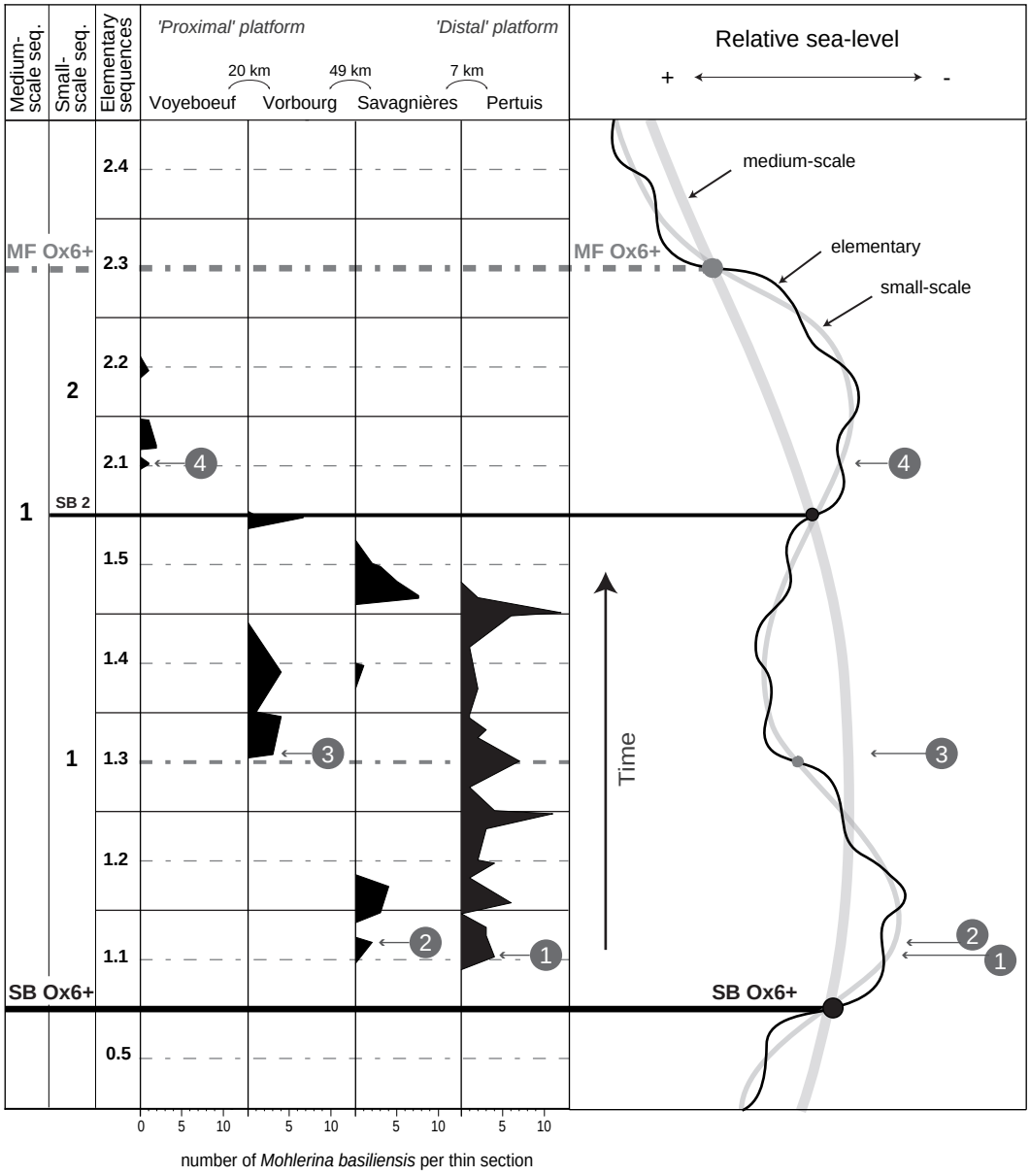

Fig. 7.14 - *Mohlerina basiliensis* distribution within elementary and small-scale depositional sequences. The encircled numbers indicate the first occurrence of *M. basiliensis* in each section.

In a time-space diagram, the *M. basiliensis* distribution shows a particular evolution (Fig. 7.12). The first occurrence of the foraminifer differs between sections through time and space but follows the "proximal-distal" trend. In the most "distal" section (Pertuis), the first occurrence is coeval with the beginning of the 2nd order marine transgression (arrow 1, Fig. 7.14). In the three other sections, the first occurrence appears successively later. This illustrates the stepwise flooding and opening of the shallow platform during the transgression (Fig. 7.15).

Contrary to oncoids, the *Mohlerina basiliensis* distribution does not reveal a clear preferential occurrence within small-scale and elementary sequences or around sequence boundaries or maximum floodings (Fig. 7.14).

However, the distribution of *Mohlerina basiliensis* and *Bacinella-Lithocodium* oncoids shows a strong correlation (Fig. 7.12). *M. basiliensis* preferentially occurs when *Bacinella-Lithocodium* oncoids are

present. On the other hand, the presence of *Bacinella-Lithocodium* oncoids does not necessarily imply an occurrence of *M. basiliensis*. For example, the base of the Voyeboeuf section contains *Bacinella-Lithocodium* oncoids in three intervals but no *M. basiliensis* (elementary sequences 1.2 and 1.3; Fig. 7.12). The co-occurrence of these two components thus suggests common environmental factors.

7.3.2 Controlling factors

The distribution of benthic foraminifera is controlled by biological, physical, and chemical factors. Water depth and water turbidity are important parameters because they control the amount of light received by the benthos. The substrate on or in which they live influences the test morphology (Murray 1991). Other important factors are oxygen content and food availability, which act on the foraminifer

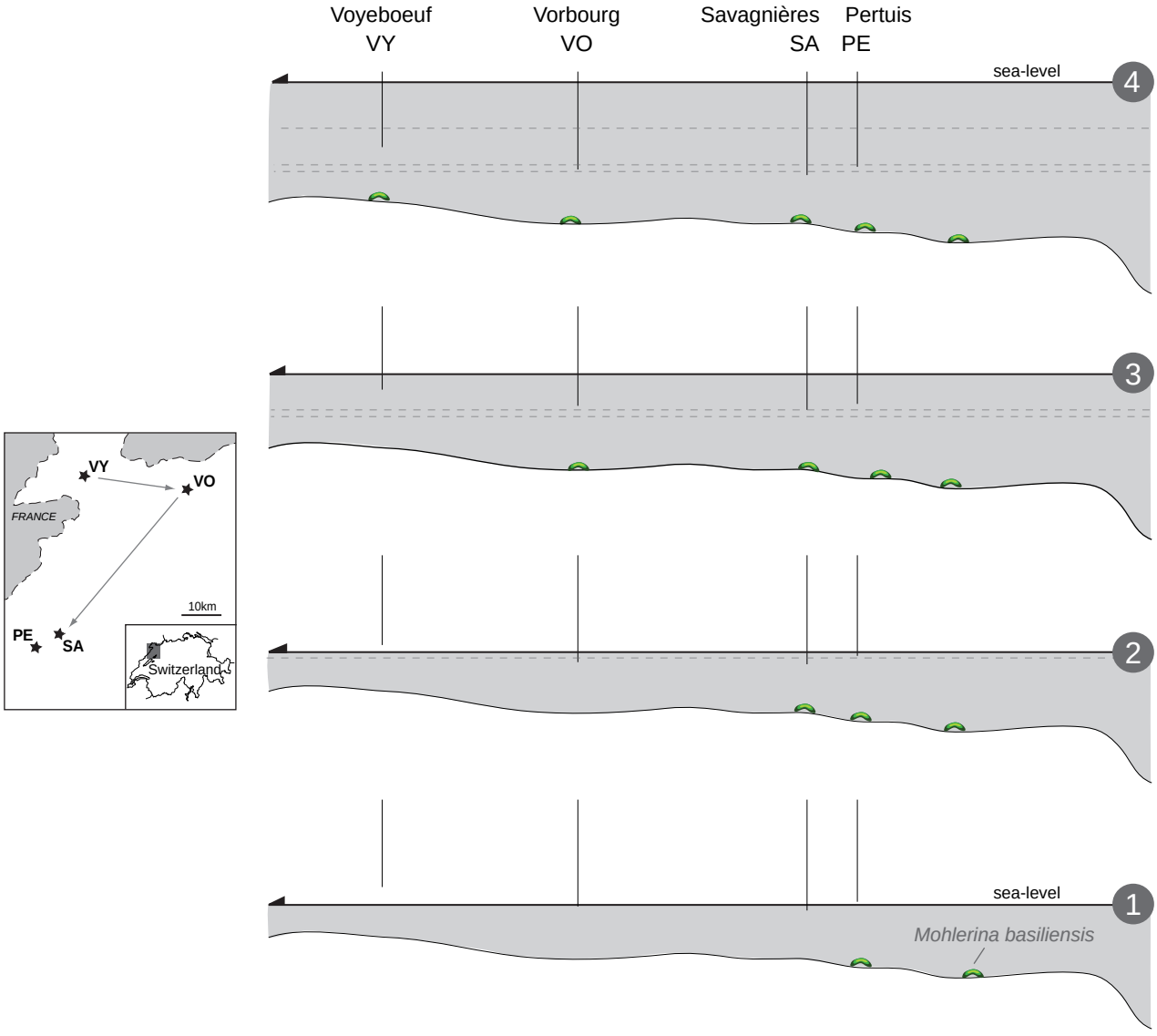

Fig. 7.15 – Platform flooding illustrated by the distribution of *Mohlerina basiliensis*. The platform morphology suggested by facies analysis allows to explain the successive first occurrences of *M. basiliensis*. Concerning the Savagnières and Pertuis sections, which are relatively close, the first occurrence and the abundance of *M. basiliensis* suggest a deeper bathymetry for the Pertuis section. Refer to text for more discussion.

diversity (e.g., JORISSEN et al. 1995; FUGAGNOLI 2004). Temperature and water chemistry also play a role in foraminifer distribution by modifying the $CaCO_3$ solubility in seawater, which acts on the nature of the test (GREINER 1969).

The palaeoenvironmental and palaeoecological requirements of *Mohlerina basiliensis* are not well known. The successively later occurrence of *M. basiliensis* from "distal" to "proximal" sections illustrates the stepwise flooding of the platform and thus implies a dependence on normal-marine conditions. Its occurrence in high-energy as well as in low-energy facies probably suggests a reworking by waves and currents. Good living conditions were rather in low-energy environments, which is supported by the co-occurrence of this foraminifer with *Bacinella-Lithocodium* oncoids. Oncoids and their associated microencrusters grow on the sediment surface and thus monitor water transparency and trophic level, which are both controlled by terrigenous influx (clays and nutrients) onto the shallow carbonate platform. The *Bacinella-Lithocodium* association, included in the oncoid cortex, indicates oligotrophic, clear, oxygenated, and normal-marine waters (e.g. DUPRAZ & STRASSER 1999). Hence, the co-occurrence of *Bacinella-Lithocodium* oncoids and *M. basiliensis* suggests that this foraminifer required similar ecological conditions (VÉDRINE & SPEZZAFERRI 2007; VÉDRINE 2008).

* * *

8 - PALAEOCLIMATE

Jurassic climate has classically been considered as warm and equable with minimal equator-to-pole thermal gradient, extensive evaporite deposition, and temperate conditions at high latitudes without permanent ice caps (e.g., FRAKES et al. 1992; HALLAM 1993; PRICE 1999). This global greenhouse period is consistent with the recent estimations of atmospheric concentrations of the greenhouse gas carbon dioxide, which is estimated to have been 4-10 times higher than modern (pre-industrial) values (e.g., VAN AARSSEN et al. 2000; RETALLACK 2001). However, there is increasing evidence for cooler climate periods that were superimposed on this generally warm trend. For example, FRAKES et al. (1992) consider the Middle Jurassic to Early Cretaceous (Bajocian to mid-Albian; 171.6–106 Ma) as a time of cool non-glacial conditions with high-latitude seasonal ice ("cool mode"). Recent General Circulation Model results indicate that Antarctica and Australia may have sustained an ice/snow-sheet during the Oxfordian to Middle Tithonian (SELLWOOD et al. 2000). Therefore, the Late Jurassic climate may have been interspersed with cool phases, and/or with a major cold phase associated with the development of an ice/snow-sheet in the southern hemisphere (GRÖCKE et al. 2003).

Most climate information comes from land plant fossils that are the most valuable palaeoclimate indicators. During the Late Jurassic, warm and arid conditions prevailed all over the Eurasian hinterland (VAKHRAMEEV 1991) whereas chilly and humid conditions predominated in the North Pacific region (PARRISH 1992), leading to strong contrasts in the longitudinal thermal gradients in the northern hemisphere.

8.1 PALAEOCLIMATE DURING THE OXFORDIAN

For the northern Tethys margin, several studies have suggested a relatively cool and humid climate during the Late Callovian-Early Oxfordian, whereas the Middle and Late Oxfordian were characterized by warmer and more arid conditions (e.g., VAKHRAMEEV 1991; BAUSCH et al. 1998; ABBINK et al. 2001; DROMART et al. 2003a, b). The onset of this warming was in the earliest Middle Oxfordian (Fig. 8.1). This pattern of climate change is in agreement with the pattern of sedimentation. In the European Tethys realm, the Late Callovian and Early Oxfordian are marked by a decrease of marine carbonate sedimentation: absence of sediments, condensed and iron-rich (COLLIN et al. 2005), organic carbon-rich shales (e.g., Terres Noires, DE GRACIANSKY et al. 1999), or siliceous deposits (e.g., radiolarites, BARTOLINI et al. 1996). Then, carbonate sedimentation recovered significantly during the Middle and Late Oxfordian (DROMART et al. 1996, 2003a, b). This evolution is probably linked to oceanographic changes related to the opening of the North Atlantic (ABBINK et al. 2001; RAIS et al. 2005). However, the greater spread of limestone facies in the Late Jurassic is probably more a consequence of the greater extent of epicontinental seas at that time than of higher temperatures (HALLAM 1975).

Sedimentological, floral, faunal, and geochemical indicators for palaeoclimate in the Oxfordian will be discussed only briefly. Clay minerals and stable isotopes (C, O) have been analysed in detail and are discussed in separate chapters.

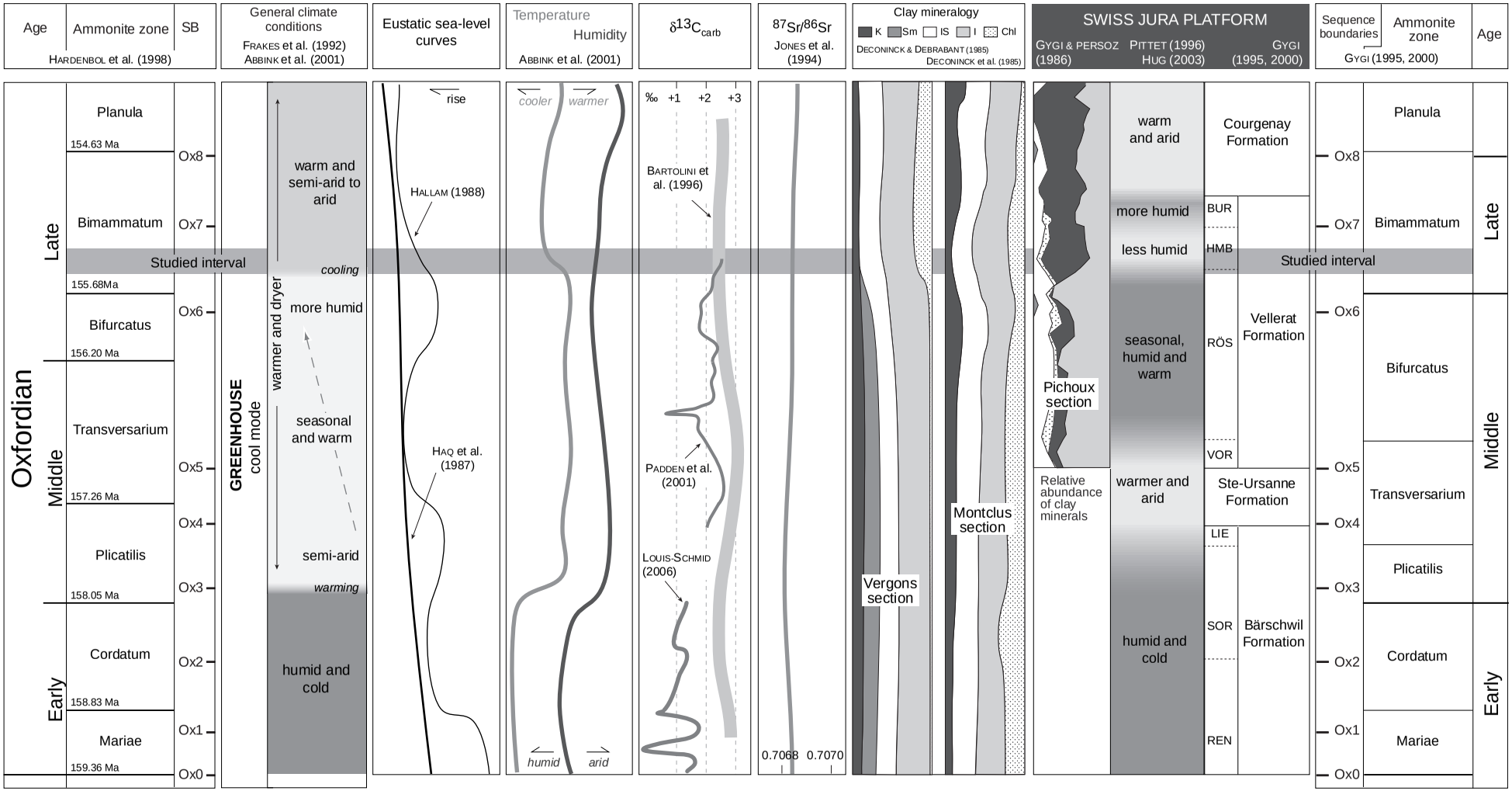

Fig. 8.1 - General palaeoclimatic evolution (FRAKES et al. 1992; ABBINK et al. 2001), eustatic sea-level curves (HAQ et al. 1987; HALLAM 1988), composite temperature and humidity curves from palynological data (ABBINK et al. 2001), $\delta^{13}C$ record (BARTOLINI et al. 1996; PADDEN et al. 2001; LOUIS-SCHMID 2006), strontium isotope record (JONES et al. 1994), and clay mineralogy of basin sections for the Oxfordian of NW and Central Europe (DECONINCK & DEBRABANT 1985; DECONINCK et al. 1985) compared to the Swiss Jura platform climatic evolution (GYGI & PERSOZ 1986; PITTET 1996; HUG 2003). Note that the limit between Middle Oxfordian and Late Oxfordian is placed between the Transversarium and Bifurcatus ammonite zone in HARDENBOL et al. (1998) and between the Bifurcatus and Bimammatum ammonite zone in GYGI (1955, 2000). The studied time interval is shaded.

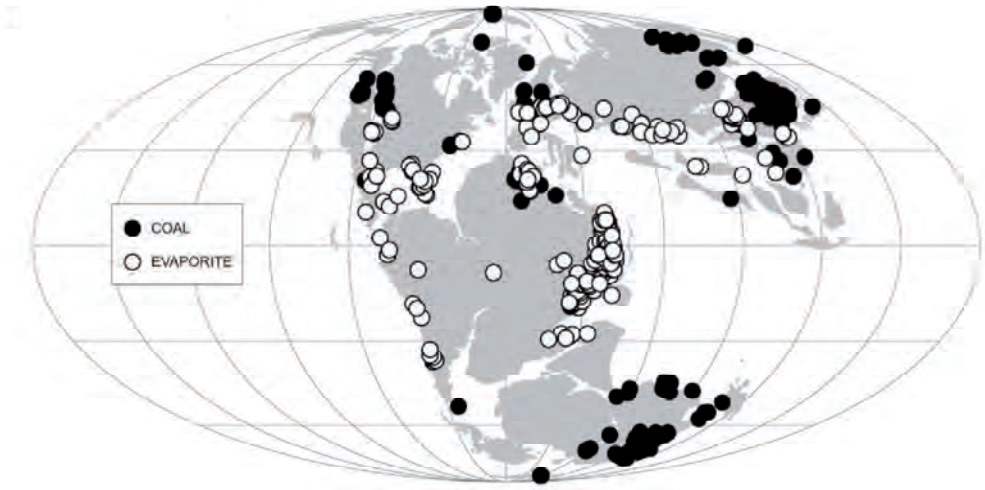

Fig. 8.2 - Coal and evaporite distribution during the Late Jurassic (from Rees et al. 2004).

8.1.1 Sedimentological indicators

The distribution of evaporites and coals is the best means of distinguishing more humid and more arid conditions (Frakes 1979). Substantial deposits of evaporites (notably gypsum, anhydrite, and halite) indicate conditions of both warmth and aridity, whereas coals indicate swampy conditions in generally humid regimes, though there is no particular temperature connotation. In the Late Jurassic, evaporites preferentially occur in the low to mid latitudes while coals are more present in mid to high latitudes (Rees et al. 2004, cf. Fig. 8.2). On the Swiss Jura platform, Hug (2003) found evaporites in the Late Oxfordian from SB Ox7 to SB Ox8 (cf. Fig. 8.1).

On the Swiss Jura platform, siliciclastics occur during the Early Oxfordian and at the Middle-Late Oxfordian transition (Fig. 8.1). Generally, the relative abundance and distribution of siliciclastics mainly reflects the intensity of continental run-off, which is related to the abundance of rainfall in the source areas and thus to local palaeoclimatic conditions (Hallam 1984). Figure 8.3 shows Late Oxfordian palaeogeography with the different source areas and the directions of sediment export. In the Swiss Jura, siliciclastics are observed mainly at the 100-kyr sequence boundaries and are explained by rainfall controlled by palaeolatitudinal variations of atmospheric cells in tune with orbitally induced

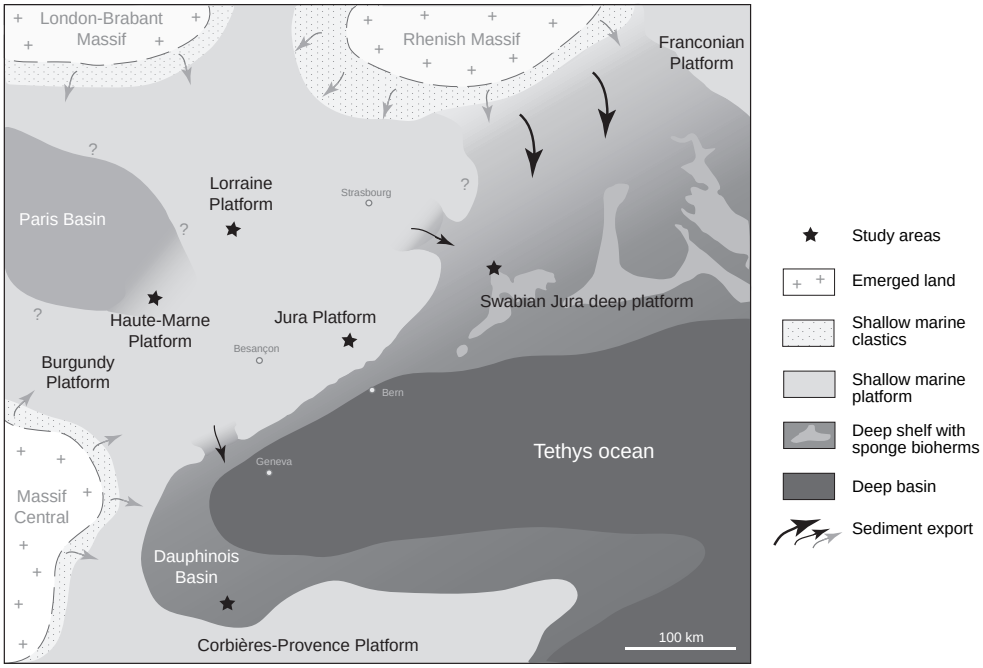

Fig. 8.3 - Palaeogeographic map of the study areas for the Late Oxfordian showing the different sedimentation areas, the emerged lands and the direction of sediment export (arrows). Modified from Meyer & Schmid-Kaler (1989, 1990), Thierry et al. (2000), and Hug (2003).

insolation cycles (Pittet 1996; Pittet & Strasser 1998b). However, tectonic uplift in the hinterland or sea-level fall may also contribute to increasing siliciclastic input into the sedimentary basins. Hence, the siliciclastic-carbonate relationship alone is not sufficient for palaeoclimatic interpretations (Ruffell & Rawson 1994).

Terrigenous particles such as quartz are common in mixed carbonate-siliciclastic platform systems. Their fluvial origin (Gygi & Persoz 1986) allows to relate the quartz proportions to the intensity of hinterland erosion. Authigenic quartz (neoformation and/or overgrowth on detrital grains) is present only in minor proportions Pittet (1996).

8.1.2 Floral and faunal indicators

The distribution and thermal tolerances of land plants provides one of the main sources of climatic evidence for the Late Jurassic (Frakes et al. 1992). In mid to low latitudes, particularly in the northern hemisphere, the vegetation was dominated by Cheirolepidicean conifers, which shed *Classopollis* pollen. These conifers grew on drained slopes, often near areas of evaporite deposition. Pollen of this type is most commonly found in association with evaporitic sediments and thus the presence of this conifer family has been used as an indicator of arid climates (Vakhrameev 1981). A high abundance of *Classopollis* pollen occurs at the Oxfordian in the former URSS region. Evaporites also increased in quantity at this time, there were fewer clastics, and corals spread further north in the northern hemisphere (Frakes 1979). This coincides with a long-term transgressive trend, and it may be that the increase in area of shallow seas provided greater areas for the formation and preservation of evaporites and the entrapment of pollen, rather than reflecting a great increase of aridity (Frakes et al. 1992).

Fluctuations in the biogeographical distribution of coral reefs during the Oxfordian suggest a latitudinal shift of climatic belts. After the cooling event of the Late Callovian-Early Oxfordian, the recovery of coral reefs in the Middle Oxfordian is limited to the European epicontinental platform between about 25° and 35°N. These reefal formations seem to indicate oligotrophic conditions at their climax stage, and hence scarce nutrient supply, suggesting an arid climate on the bordering landmass (Cecca et al. 2005). However, the maximum extent of radiolarites in the Middle Oxfordian in the deep basin of the Mediterranean Tethys implies humid conditions marked by increased run-off and nutrient input (Bartolini et al. 1999). In the Late Oxfordian, coral reefs recovered completely and were distributed between 10°S to 32°N, implying generally more arid conditions and/or platform isolation (Cecca et al. 2005). These coral reefs differ from those of the Middle Oxfordian by the occurrence of microbialites suggesting mesotrophic to eutrophic conditions and implying more nutrient input from the hinterland and more humid climatic conditions (Pittet 1996; Dupraz & Strasser 1999, 2002).

During the Oxfordian, two major faunal provinces existed in the northern hemisphere: the northern Boreal realm and the low-latitude Tethyan realm (Hallam 1994; Cecca 2002 and references therein). The limits of these realms varied in response to eustatic, climatic, and tectonic changes. In the latest Callovian to Kimmeridgian, Tethyan ammonite fauna migrated from the south into the Boreal realm, following a long-term palaeotemperature increase (Malchus & Steuber 2002).

8.1.3 Geochemical indicators

The Oxfordian is characterized by the lowest $^{87}Sr/^{86}Sr$ values in the Phanerozoic (Jenkyns et al. 2002). This may be related to decreased input of Sr from continental erosion and/or to increased input of mantle strontium with a low $^{87}Sr/^{86}Sr$ ratio (Cogné & Humler 2004). Generally, increased humidity (Van Aarssen et al. 2000; Abbink et al. 2001) and increased siliciclastic input (Gygi & Persoz 1986) in the Early Oxfordian imply a high weathering rate if compared to the Middle and Late Oxfordian. Hence, low input of continental Sr is unlikely to be the cause of low $^{87}Sr/^{86}Sr$. Jones et al. (1994) interpreted these low values, also found in the Early-Middle Oxfordian (Cordatum-Densiplicatum zones) from the British Isles, as the result of a major pulse of hydrothermalism related to the onset of the rifting in the North and South Atlantic regions.

8.2 Clay minerals

8.2.1 Introduction

The analysis of clay-mineral assemblages from marine deposits can provide significant palaeoclimatic information on the provenance, sediment sorting, and

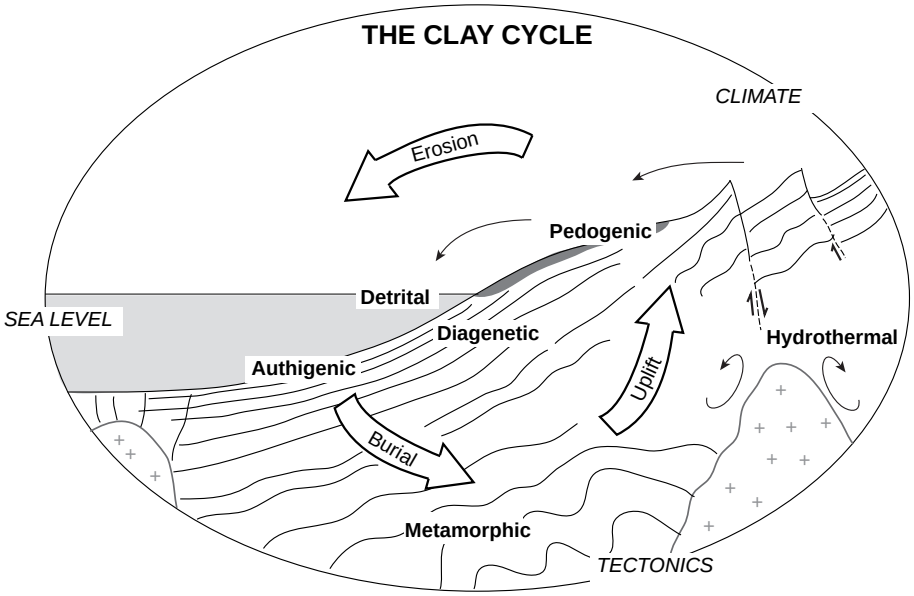

Fig. 8.4 - Origin of clays (detrital, pedogenic, authigenic, diagenetic, metamorphic, and hydrothermal) and their link with the sedimentary cycle (uplift, erosion, and burial). Modified from Eslinger & Pevear (1988).

weathering processes on the adjacent continental areas (e.g., Chamley 1989; Sellwood & Price 1993; Ruffell et al. 2002). However, clay-mineral assemblages are not only controlled by climate changes (erosion and weathering) but also by tectonics (platform morphology, uplift, burial) and eustatic sea-level changes (Chamley 1989). The different types of clay minerals (detrital, pedogenic, authigenic, diagenetic, metamorphic, and hydrothermal) thus result from the interaction of climate, tectonics, and sea level (Fig. 8.4).

The formation of clay minerals in soils strongly depends on the weathering environment (Sladen 1983). It results, either directly or indirectly, from the hydrolytic decomposition of primary aluminosilicates. Leaching potential (wash out of cations and silica oxides by percolating waters) depends on vertical water movement, weathering profiles, and parent rock and is controlled by the relationship between precipitation and evaporation (Singer 1980). Clay minerals are formed in soils or eroded from parent rocks. Tectonic uplift favours the direct removal of materials from rocky substrates and is less favourable for pedogenesis (Blanc-Vernet et al. 1979; Chamley 1989). Erosion, reworking and transport from the continental source area to marine settings by water or wind may modify the composition of clay-mineral assemblages, e.g., by mixing different horizons with different degrees of alteration (e.g., Curtis 1990). The transformation of kaolinite in sea water may also change the clay-mineral assemblages (Rex & Martin 1966).

The relationship between climatic parameters (particularly seasonality, average annual temperature and precipitation) and clay-mineral formation is complicated by the intervention of other factors such as topography, type of vegetation and organisms, parent rock composition, and length of time available for soil formation (e.g., Singer 1980; Sladen 1983; Chamley 1989; Velde 1995). The longer the transport distance, the higher is the possibility that complex alteration processes happen during intermediate sediment storage, and less the palaeoclimatic message of the deposited clay-mineral assemblage is clear (Thiry 2000).

Once deposited in the sedimentary environment, clay-mineral assemblages may be further modified by diagenetic processes (Chamley 1989; Kübler & Jaboyedoff 2000; Deconinck et al. 2001) and thus the original climatic signal will be distorted. Post-depositional diagenetic changes include alteration and neoformation of clay minerals (e.g., Chamley 1989; Ruffell et al. 2002). The most common process is the transformation of smectite to illite during burial diagenesis (Chamley 1989). However, this transformation may also happen under surface conditions (e.g., in hypersaline lagoons; Deconinck et al. 1988, 2001).

In marginal-marine settings, the clay-mineral assemblages are mainly characterized by kaolinite, illite, smectite, mixed-layer minerals, and palygorskite. **Kaolinite** formation is supported by deep weathering

associated with perennial precipitation and a soil temperature not dropping below 15°C (e.g., HALLAM et al. 1991). Fairly high evaporation in combination with high annual precipitation in humid warm to temperate climates leads to extensive leaching and to deep weathering profiles, creating kaolinite- and gibbsite-rich acid soils (e.g., SINGER 1980; SLADEN 1983; WRIGHT 1994). Consequently, kaolinite in marine sediments is mainly considered as a detrital mineral resulting of soil reworking. **Illite** and **chlorite** may derive from the erosion of unaltered bedrock. An increase in these minerals is often observed in areas with steep relief, where rapid erosion does not allow for soil formation and maturation (DECONINCK et al. 1985; GAWENDA 1999). **Illite** is often thought to be the product of physical erosion dominating in the hinterland (CHAMLEY 1989; RUFFEL & BATTEN 1990). According to DECONINCK (1993), low relative sea level causes a high erosion rate and thus favours the development of illite-rich sediments. SINGER (1984) claims that well-crystallized illite indicates formation in either cold or dry conditions with minimum hydrolysis. Chlorite mainly derives from the alteration of crystalline (basic igneous or low-grade metamorphic) rocks. Hence, regional variations in the source-rock composition may influence the chlorite content (LAMY et al. 1998).

Palygorskite and **smectite** are characteristic for soils with a shallow weathering profile in seasonal, semi-arid climates (Mediterranean-type climate). Palygorskite is an excellent marker for arid to semi-arid conditions (SINGER 1980). Smectite forms preferentially under tropical and subtropical conditions that are characterized by an elevated seasonality of alternating wet and dry periods (ROBERT & KENNET 1994; GAWENDA 1999). Moreover, smectite may be entirely volcanic in origin, deriving directly from the weathering of lava and ash (bentonites; e.g., PELLENARD et al. 2003).

The **kaolinite-illite ratio (K/I)** is commonly used for palaeoclimatic reconstruction and reflects the influence of climate and relief changes on chemical weathering and soil formation. The main influences on the K/I ratio are interpreted to be changes in climate and relative sea level (THIRY 2000; CURTIS 1990). A high K/I ratio generally indicates a more humid, warm climate.

The **illite crystallinity index (IC)** gives information on the chemical weathering intensity in the source area of the mineral (SINGER 1984; CHAMLEY 1989). Well-crystallized illites indicate a low chemical weathering activity while poor illite crystallinities reflect stronger chemical weathering intensity (e.g., SINGER 1984). However, another source of illite is the replacement of smectite during burial diagenesis (diagenetic illites IC >0.42° $\Delta 2\theta$ CuKα, CHAMLEY 1989) but also at surface temperature and pressure in seawater of elevated salinity under a hot and arid climate (DECONINCK et al. 1988). RAMEIL (2005) noted a correlation between illite crystallinity index and regressive-transgressive phases of superimposed large- and medium-scale sequences. During large-scale maximum flooding periods, only detrital, well-crystallized illites (IC <0.42° $\Delta 2\theta$ CuKα) are deposited while around large-scale sequence boundaries illite neoformation is dominant. Additionally, illite crystallinity can also serve as a proxy of proximal-distal facies trends (RAMEIL 2005).

8.2.2 Material and analytical methods

Clay mineral analyses were performed on 70 samples from the Savagnières, Balingen-Tieringen, and Vergons sections. Sample preparation and X-ray diffraction (XRD) analyses were carried out at the Institute of Geology of the University of Neuchâtel (Switzerland) on a SCINTAG XRD 2000 diffractometer. Sample preparation is based on the methods described by KÜBLER (1987): The crushed sediment is mixed with an ionized aqueous solution (pH 7-8) and agitated. The carbonate fraction is then eliminated by the addition of HCl 10% (1.25 N) at room temperature. During a reaction time of 20 minutes or more, physical disintegration is stimulated in an ultrasound bath every 3 minutes, until all carbonate is dissolved. The insoluble residue is then repeatedly concentrated in a centrifuge and washed (5-6 times) until obtaining a neutral suspension (pH 7-8). The separation of various particle sizes (<2 µm and 2-16 µm) is obtained using the relation between sedimentation time and the depth of pipettage based on STOKES' Law. The <2µm fraction is transferred by pipette to a glass object tray and air-dried at room temperature. Then the <2 µm fraction is analysed after saturation with ethylene glycol and subsequent air-drying.

The intensities of the peaks that characterize each clay mineral (smectite, chlorite, illite, kaolinite, interstratified) are measured in *counts per second* (cps) for the semi-quantitative estimation of the proportion of clay minerals, which is therefore given in relative percent without correction factors (Annex 6). Variations of more than 10% are considered as significant. Quartz content has been estimated from thin sections and from

X-ray diffraction analyses of bulk-rock in percent, or from the 2-16 µm fraction in counts per second when the total amount of quartz in bulk was not sufficient. The illite crystallinity index (IC) is expressed as the ratio of the width of the (001) basal peak at mid-height to the peak height above background measured on <2 µm fraction diffractograms (KÜBLER 1987).

8.2.3 Results and interpretations

Swiss Jura (shallow platform)

Only the Savagnières section has been analysed for the clay minerals and is considered as representative for the Swiss Jura sections. Clay mineral assemblages of the Hauptmumienbank Member are mainly composed of kaolinite (40-60%), illite (30-50%), mixed-layer illite-smectite (2-15%), and chlorite (2-8%).

The illite and chlorite trends are relatively similar and are both inverse to the kaolinite trend (Fig. 8.5). The mixed-layer illite-smectite trend preferentially correlates with the kaolinite trend. The scarcity of smectites and the relative abundance of mixed-layer clays are a fundamental feature of the clay mineral associations of the Oxfordian of the Swiss Jura (GYGI & PERSOZ 1986). This scarcity can be explained in two ways: (1) the absence of smectite is an original feature; (2) it is due to the transformation of smectites into mixed layer illite-smectite and illite by burial diagenesis or by transformation in soils (GYGI & PERSOZ 1986; CHAMLEY 1989).

The comparison between clay-mineral assemblages and sequence stratigraphy (Figs 8.5 and 8.6) shows that illite content commonly is higher around sequence boundaries and lower around maximum floodings essentially at the scale of small-scale (100-kyr) sequences. Chlorite content is generally higher around the small-scale and elementary (100- and 20-kyr) SBs and lower around the small-scale and elementary MFs. Mixed-layer illite-smectite content is higher around the small-scale SBs and occasionally around the elementary SBs. In addition, high content of mixed-layer illite-smectite also occurs around the small-scale MF while the lowest values exist around the elementary MF. The kaolinite trend presents low values (45%) at the base of the section (i.e., in the first two elementary sequences 0.5 and 1.1) and then increases significantly (55-60%). High kaolinite contents appear in the elementary sequences 1.2 and 1.3, in the elementary sequence 1.5, and (3) in the elementary sequences 2.2 and 2.3 but a link with the sequence stratigraphy is not evident.

The kaolinite-illite ratio is mainly controlled by the kaolinite content. High values occur around the small-scale (100-kyr) MF 1, at the small-scale (100-kyr) SB 2, and the highest values at the medium-scale (400-kyr) MF Ox6+. High quartz content preferentially occurs around the small-scale and elementary SBs (Fig. 8.5).

Most of the samples present low IC values (<0.42° $\Delta 2\theta$ CuKα, well-crystallized illites) rather indicating detritic illites. This is in agreement with the low burial depth (<2 km) of the Swiss Jura suggested by TRÜMPY (1980). Five samples present higher IC values pointing to poorly crystallized illites. These samples are preferentially positioned around small-scale and elementary sequence boundaries as found by RAMEIL (2005) for large- and medium-scale sequence boundaries. However, in this study, the IC is interpreted in terms of chemical weathering in the source area rather than as an indicator for aridity and elevated evaporation (see above, SINGER 1984; RAMEIL 2005).

In the Pichoux section, an increase of the K/I ratio from the Röschenz Member to the Hauptmumienbank Member (GYGI & PERSOZ 1986) can be interpreted as a change to more humid conditions. However, this evolution is in disagreement with the general facies evolution on the Swiss Jura platform that suggests a trend towards less humid conditions (cf. Fig. 8.1; GYGI 1995, 2000).

The clay-mineral distribution is mainly explained by sea-level and humidity changes (Fig. 8.6). **Humidity changes** act on the hydrological cycle that influences the continental run-off. In the Oxfordian, the sediment supply probably came from the Rhenish, London-Brabant and/or Bohemian Massifs (Fig. 8.3). **Sea-level changes** modify the base level that acts on the erosion potential (Fig. 8.6). During low sea-level periods, the terrigenous sediments (quartz) increase pointing to an intensification of land erosion in the source area, probably also intensified by more humid conditions. In contrast, during high sea-level periods, less erosion potential and probably humid conditions are evidenced by a decrease of siliciclastics (PITTET 1996; PITTET & STRASSER 1998b).

The kaolinite distribution in the studied shallow-carbonate platform section indicates that it occurred

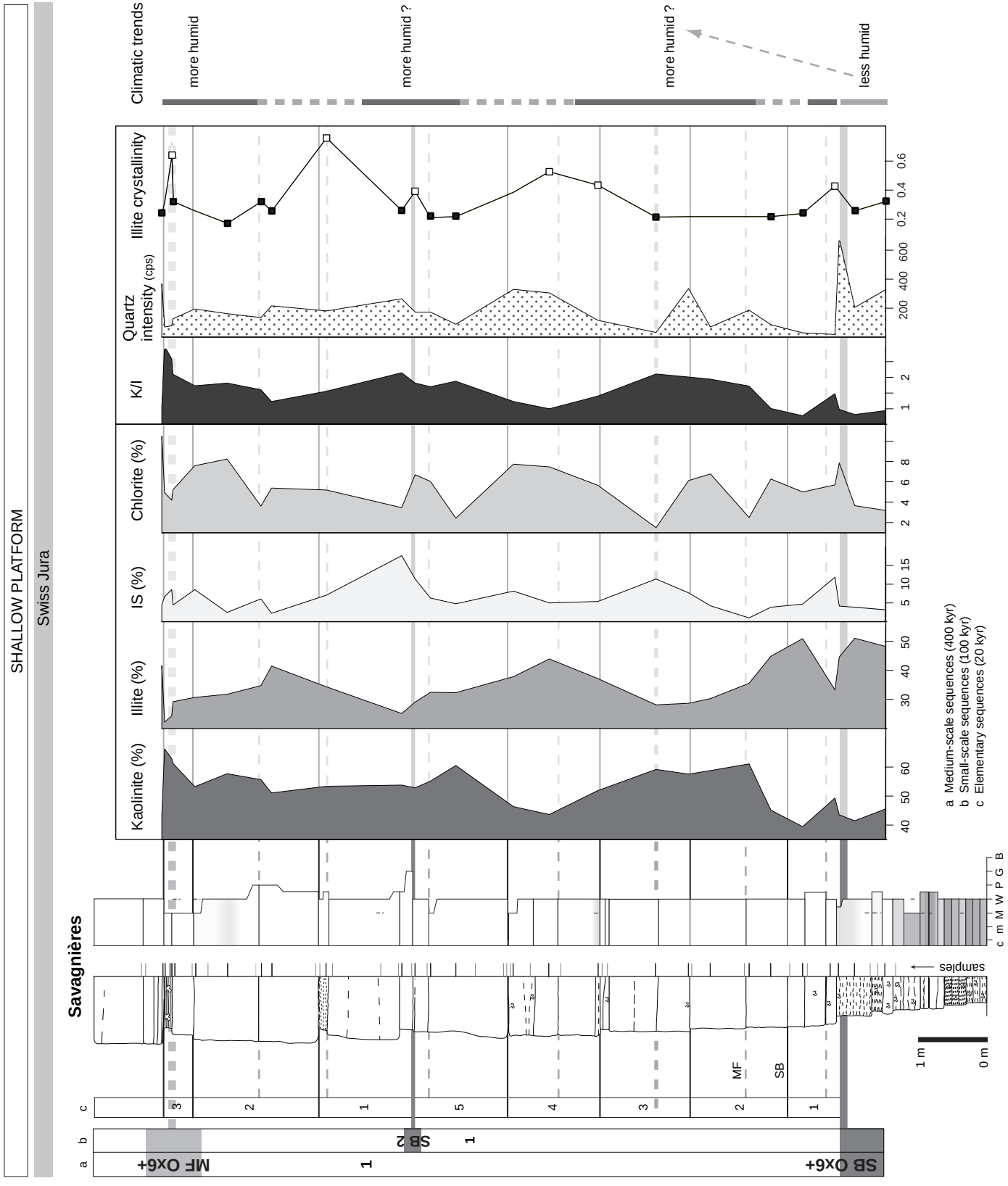
SHALLOW PLATFORM
Swiss Jura
Savagnières
Climatic trends
more humid
more humid ?
more humid ?
less humid
Quartz intensity (cps)
Illite crystallinity
K/I
Chlorite (%)
IS (%)
Illite (%)
Kaolinite (%)
a Medium-scale sequences (400 kyr)
b Small-scale sequences (100 kyr)
c Elementary sequences (20 kyr)
samples
MF
SB
SB Ox6+
MF Ox6+
1 m
0 m

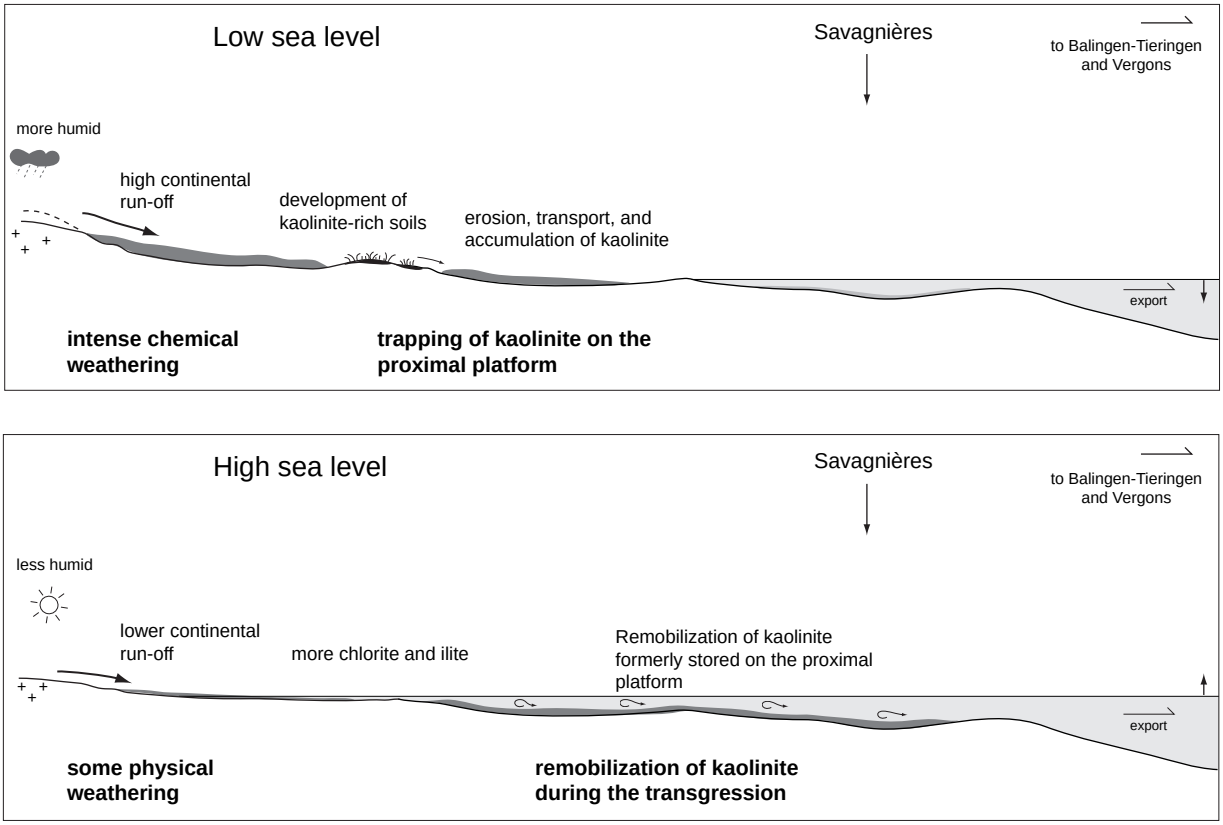

Fig. 8.6 - Models explaining the clay-mineral distribution, particularly the kaolinite formation and accumulation during a low sea level (more humid conditions) and a high sea level (less humid conditions). Refer to text for discussion.

during low as well as during high sea-level periods (Fig. 8.7). Kaolinite occurrence during low sea level is explained by favourable conditions (i.e., more humid) for kaolinite-rich palaeosoil formation and an increase of kaolinite erosion, transport, and accumulation. DECONINCK (1993) suggests that kaolinite preferentially accumulates in proximal platform areas. During high sea-level periods, kaolinite formation is reduced due to a less humid climate. Therefore, the observed high kaolinite contents around small-scale (100-kyr) maximum floodings probably suggest the remobilization of kaolinite formerly stored in the proximal part of the shallow platform.

Fig. 8.5 - (facing page) Distribution of clay minerals, K/I ratio, quartz intensity and illite crystallinity within the transgressive part of medium-scale sequence 1 of the Savagnières section. Interpretations on climate evolution are proposed (on the right side).

Swabian Jura (deep platform)

Clay mineral assemblages of the Impressa Mergel Formation of the Balingen-Tieringen section are mainly composed of kaolinite (30-55%), illite (20-50%), chlorite (5-20%), and mixed-layer illite-smectite (5-20%). The kaolinite trend correlates negatively with the illite, chlorite, and mixed-layer illite-smectite abundances (Fig. 8.7).

The comparison between clay-mineral assemblages and sequence stratigraphy shows a certain correlation (Figs 8.7 and 8.8): the illite content is generally higher around MFs and lower around SBs at the scale of small-scale (100-kyr) and elementary (20-kyr) sequences. Inversely, the chlorite and kaolinite contents are higher around SBs and lower around MFs of the small-scale and elementary sequences. In addition, high contents of mixed-layer illite-smectite occur around small-scale SBs and MFs.

The kaolinite-illite ratio is relatively stable except at two levels: the medium-scale SB Ox6+ and the

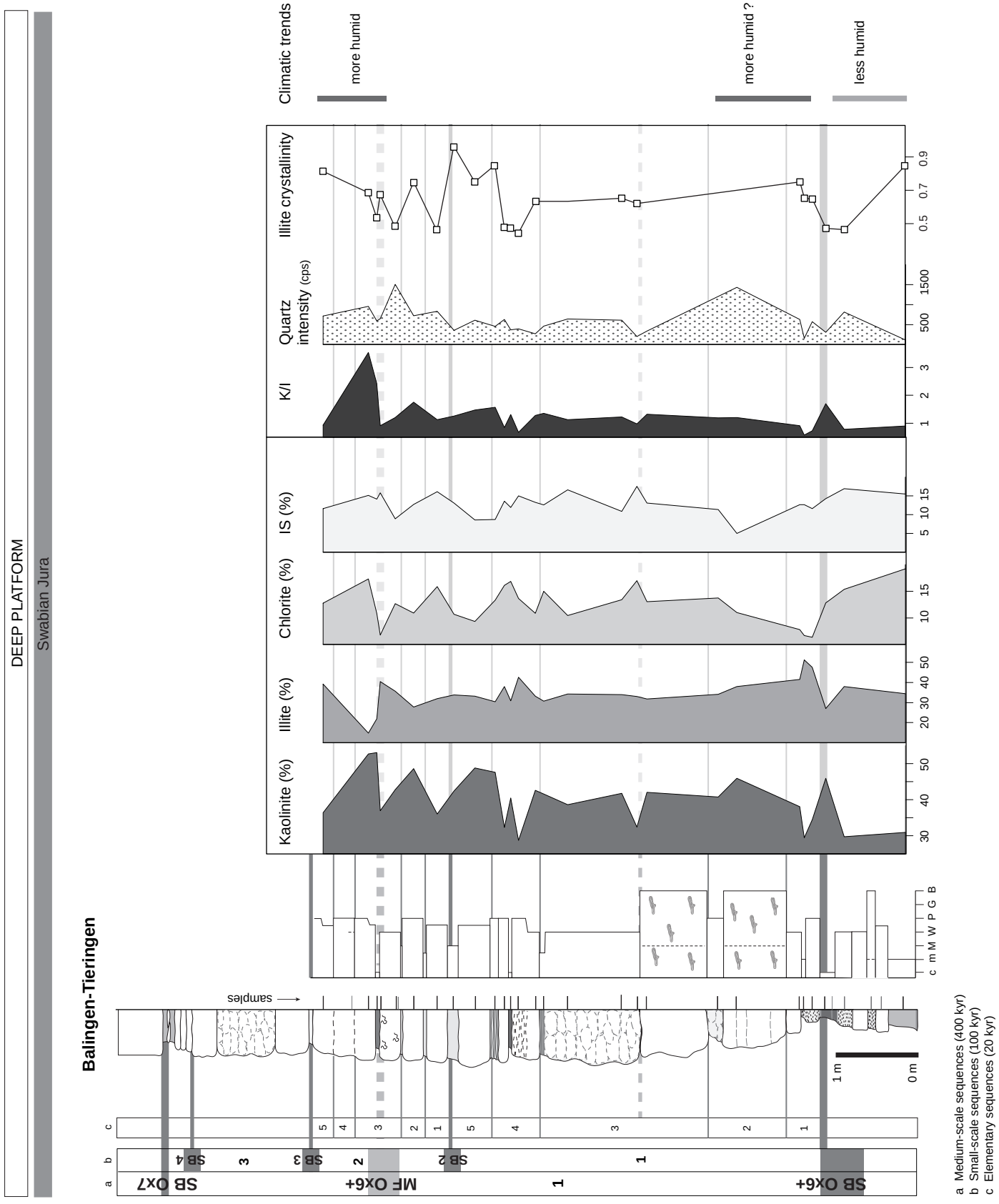
DEEP PLATFORM
Swabian Jura
Balingen-Tieringen
Climatic trends
more humid
more humid ?
less humid
Illite crystallinity
Quartz intensity (cps)
K/I
IS (%)
Chlorite (%)
Illite (%)
Kaolinite (%)
samples
SB Ox7
SB 4
SB 3
SB 2
SB Ox6+
MF Ox6+
1 m
0 m
a Medium-scale sequences (400 kyr)
b Small-scale sequences (100 kyr)
c Elementary sequences (20 kyr)

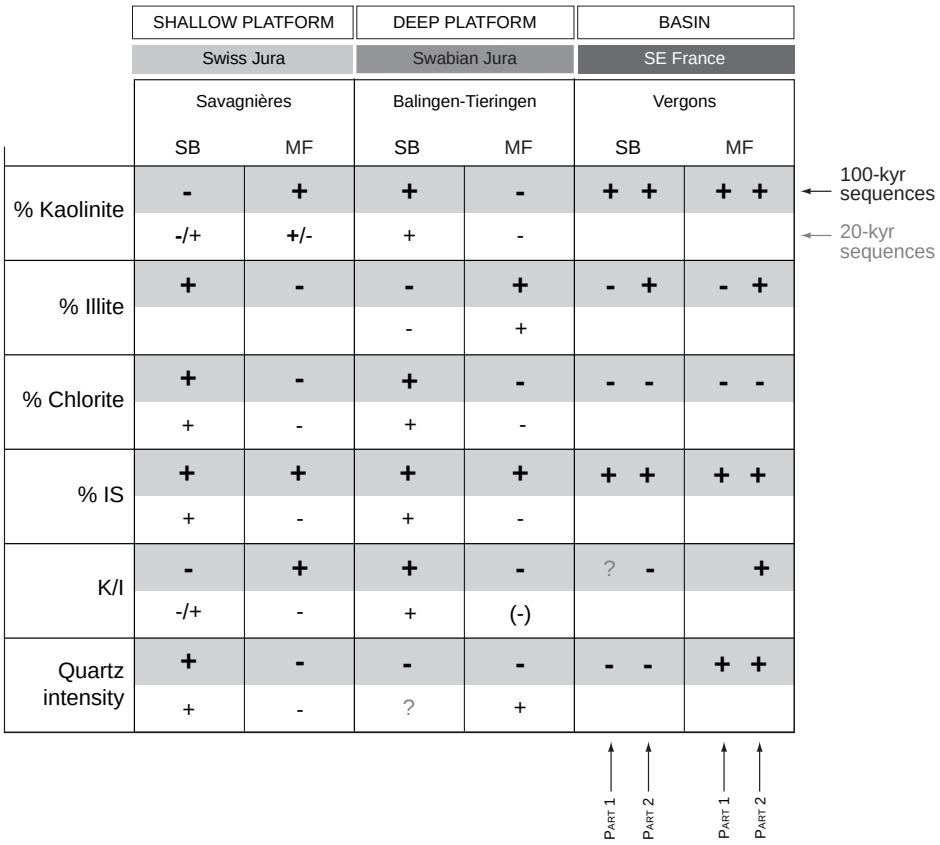

Fig. 8.8 - Minima (-) and maxima (+) in the abundance of clay-minerals (kaolinite, illite, chlorite and mixed illite-smectite minerals), K/I ratio, quartz intensity, and illite crystallinity for the three studied sections (from shallow platform to basin) around the sequence boundaries and maximum floodings of 100- and 20-kyr sequences.

medium-scale MF Ox6+. These levels of high values correlate with those of the Swiss Jura section (Fig. 8.5).

The quartz content and the sequence stratigraphy do not show any clear correlation. The IC values (0.4°-0.9° Δ2θ CuKα) are representative of poorly crystallized illites. No correlation exists with the Savagnières section. As the Swiss Jura, the Swabian Jura has a low burial depth.

The trend in clay-mineral distribution of the Balingen-Tieringen section is comparable to the one of the Savagnières section. Discrepancies, particularly concerning the relative abundances of kaolinite and illite, are explained by the different palaeogeographic positions that imply different source areas and different transport distances (Fig. 8. 3).

Fig. 8.7 - (facing page) Distribution of clay minerals, K/I ratio, quartz intensity and illite crystallinity within the first two small-scale sequences 1 and 2 of the Balingen-Tieringen section. Interpretations on climate evolution are proposed (on the right side).

SE France (basin)

Clay mineral assemblages of the Vergons section section are mainly composed of illite (40-80%), chlorite (10-40%), mixed-layer illite-smectite (5-40%), and kaolinite (0-30%). In this sedimentation area, terrigenous particles probably come from the Central Massif (Fig. 8.3).

In the Vergons section, the kaolinite trend is mainly parallel to the mixed-layer illite-smectite trend (Fig. 8.9). The illite percentage shows an increase towards the top part of the section. The kaolinite trend shows a negative correlation with the chlorite trend except in the transgressive part of the second small-scale sequence where the kaolinite trend is parallel to the illite trend. According to these trends, the section can be subdivided into three parts (cf. Fig. 8.9). The first two parts correspond to studied interval in the Swiss and Swabian Jura sections.

The comparison between clay-mineral assemblages and sequence stratigraphy (Figs 8.8 and 8.9) shows that in part 1 kaolinite and mixed-layer illite-smectite contents are relatively high around small-scale (100-kyr) MFs while the illite and chlorite contents are

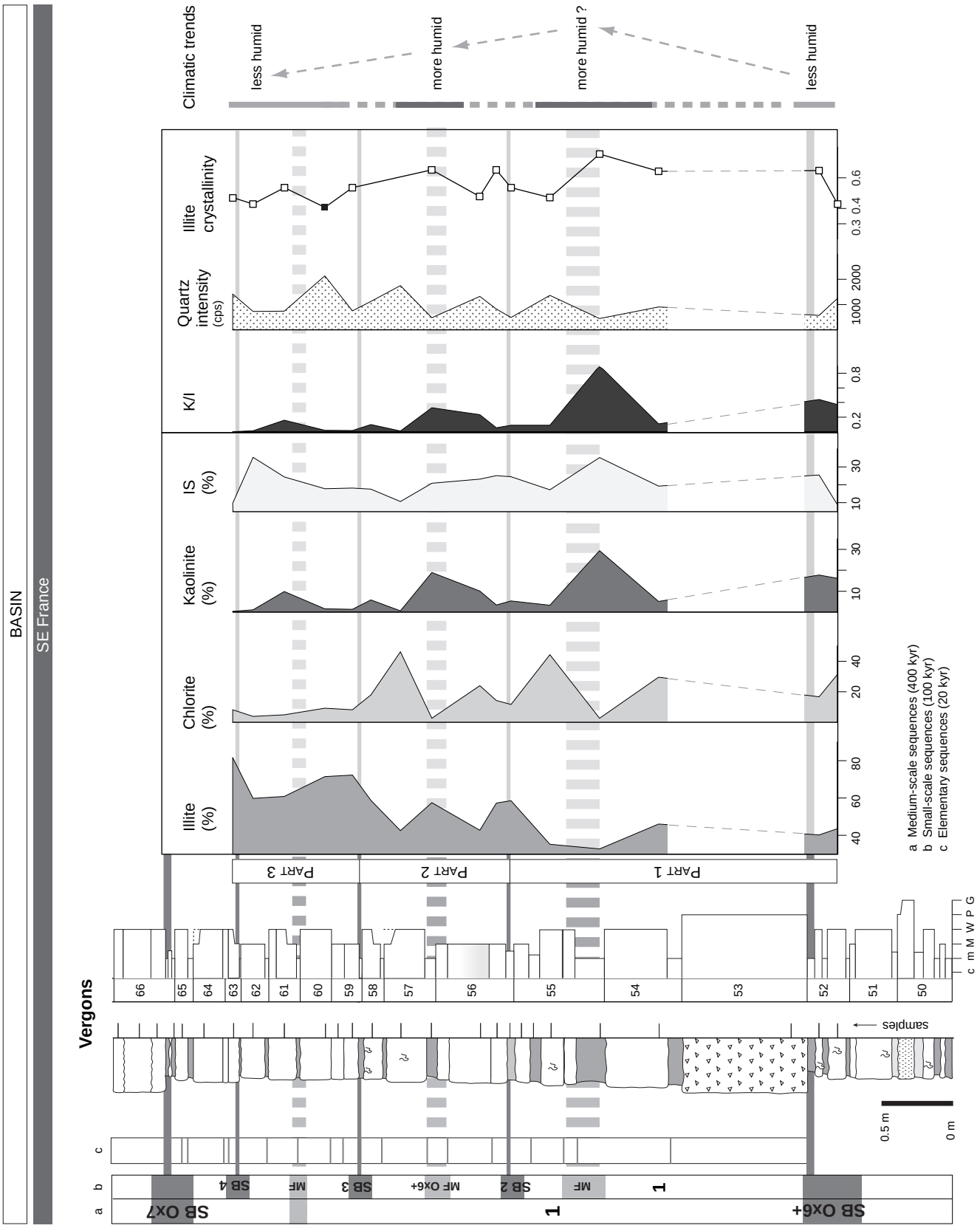
BASIN
SE France
Climatic trends
less humid
more humid
more humid ?
less humid
Illite crystallinity
Quartz intensity (cps)
K/I
IS (%)
Kaolinite (%)
Chlorite (%)
Illite (%)
PART 3
PART 2
PART 1
a Medium-scale sequences (400 kyr)
b Small-scale sequences (100 kyr)
c Elementary sequences (20 kyr)
Vergons
samples
0.5 m
0 m
SB Ox7
SB 4
MF
SB 3
MF Ox6+
SB 2
MF
SB Ox6+

Fig. 8.9 - (facing page) Distribution of clay minerals, K/I ratio, quartz intensity, illite crystallinity, and bulk mineralogy within the four small-scale sequences 1 to 4 of the Vergons section. Interpretations on climate evolution are proposed (on the right side).

relatively low. In part 2, kaolinite and illite contents are relatively high around small-scale SBs and MFs while chlorite content is low. In part 3, illite content is relatively high around small-scale SBs and low around small-scale MFs. Additionally, the highest contents in chlorite mainly occur in the highstand deposits (45%) and in the transgressive deposits (30%) of the small-scale sequences. The K/I ratio presents the highest values around the three small-scale (100-kyr) maximum floodings (Fig. 8.9). In the basin, an increase of kaolinite is commonly related to a transgression and a high value to a maximum flooding (Jan du Chêne et al. 1993; Deconinck 1993; Pittet 1996).

The quartz content and the sequence stratigraphy do not show any clear correlation. As for the Balingen-Tieringen section, the IC values of 0.4°-0.9° Δ2θ CuKα) indicate poorly crystallized illites, although burial depth was relatively high (>2000 m; Deconinck & Debrabant 1985).

Comparison from shallow platform to basin: discussion

A similar medium-scale evolution of the kaolinite content and the kaolinite/illite ratio is noticed between the Swiss and Swabian Jura sections. Low values are observed at the base of the sections, around the medium-scale SB Ox6+ and are followed by an increase of values. This trend is in agreement with the one of the Pichoux section, which shows an increase of the kaolinite content and K/I ratio at the base of the Hauptmumienbank Member (Fig. 8.1) around medium-scale SB Ox6+. Generally, high K/I values indicate more humid conditions. However, the change from siliciclastic-dominated to more carbonate facies at the base of the Hauptmumienbank/Steinebach members points to inverse conditions. Consequently, the obtained trends in the shallow and deep platform sections suggest that the distribution of clay minerals is not only controlled by climate changes but also by relative sea-level changes and platform morphology. Indeed, the base of the Hauptmumienbank/Steinebach members corresponds to a major transgressive surface, and facies distribution was influenced by the platform morphology, controlled by local/regional tectonics.

In addition, high kaolinite values and high K/I are recorded in the top part of the sections, around the medium-scale MF Ox6+. This level coincides with the marl or marly limestone interval, correlated over long distances, within the massive Hauptmumienbank limestones (cf. Chap. 5). It can be interpreted as a period of more humid conditions or more remobilization of kaolinite during the maximum flooding (Figs 8.11 and 8.6). This study allows to discuss the link between the kaolinite distribution and sea level (Fig. 8.6).

In the basin section, the trends of kaolinite content and K/I ratio are relatively similar to those of the other

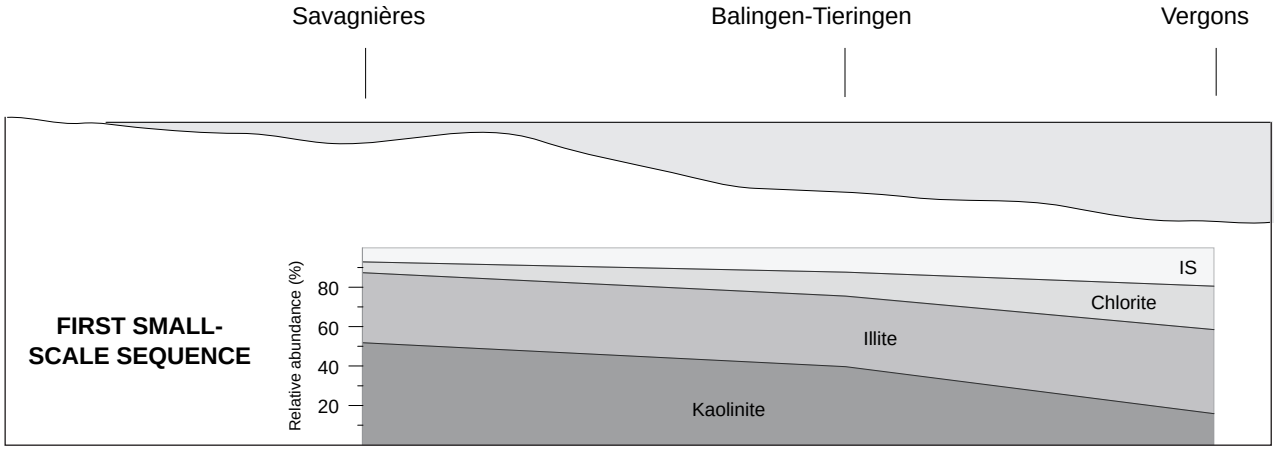

Fig. 8.10 - Schematic profile showing the differential settling of clay minerals from shallow platform to basin calculated for the first small-scale sequence. Relative abundance averaged over the whole small-scale sequence. For discussion refer to text.

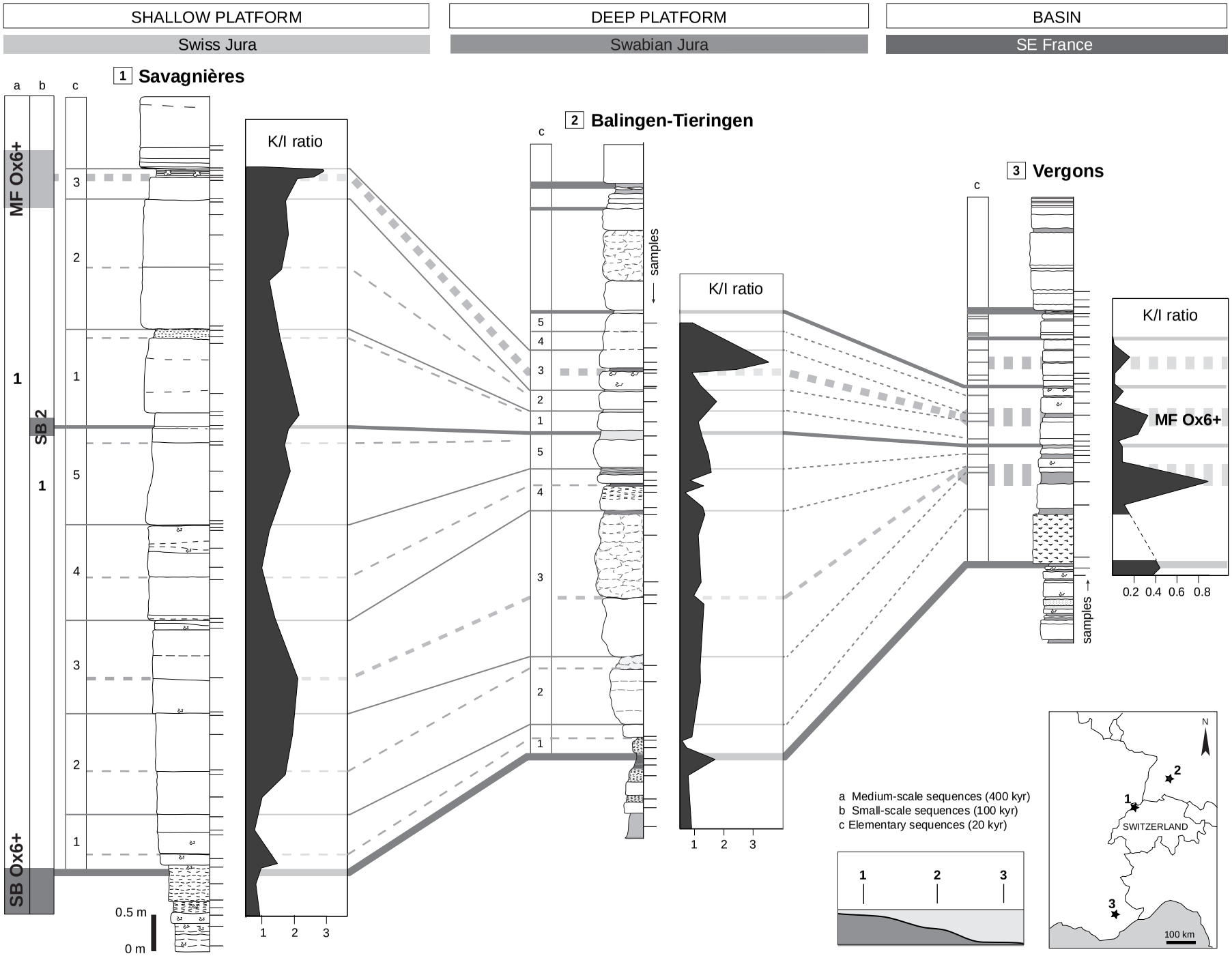
SHALLOW PLATFORM
Swiss Jura
DEEP PLATFORM
Swabian Jura
BASIN
SE France
1 Savagnières
2 Balingen-Tieringen
3 Vergons
a b c
MF Ox6+
SB 2
SB Ox6+
K/I ratio
samples
0.5 m
0 m
0.2 0.4 0.6 0.8
a Medium-scale sequences (400 kyr)
b Small-scale sequences (100 kyr)
c Elementary sequences (20 kyr)
N
SWITZERLAND
100 km

Fig. 8.11 - (facing page) Correlation of the K/I ratios from the shallow platform to the basin. A generally higher K/I ratio is observed at the medium-scale MF Ox6+.

sections around medium-scale SB Ox6+ (low values) and medium-scale MF Ox6+ (high values). However, because of diagenetic transformations of clay minerals (cf. above), palaeoclimate interpretations are not reliable.

The comparison of the coeval clay-mineral assemblages from platform to basin shows that kaolinite- and illite-dominated assemblages on the platform evolve into illite- and chlorite-dominated assemblages in the basin (Fig. 8.10). One explanation for this trend is differential settling of clay particles due to the platform morphology (i.e., epeiric platform; presence of a barrier or a reef that separated the platform from the basin; GODET et al. submitted). Moreover, this process probably was enhanced by relative sea-level changes. For example, during sea-level rise, platform area increases and the distance between the continent, where kaolinite is formed, and the basin becomes more important. Hence, this platform configuration during periods of high sea level favours trapping of kaolinite in the proximal part of the platform rather than in hemipelagic environments (Fig. 8.6).

At the scale of 100- and 20-kyr depositional sequences, the interpretation of clay-mineral distribution is more difficult. Maxima and minima of the different clay minerals occur differently between the sections and around the SBs and MFs (Fig. 8.8). For the shallow platform section, these discrepancies probably result from the complex dynamics of mixed carbonate-siliciclastic platform systems (e.g., platform morphology, facies mosaics). For the deep platform and basin sections, the potential diagenetic transformation of kaolinite in seawater (REX & MARTIN 1966), the lag time through remobilization, or the effects of burial diagenesis (CHAMLEY 1989) make the interpretation difficult.

The analysis of additional sections with a higher sampling density, especially towards the hinterland, would be helpful in order to clearly identify the role of climate, sea level, and regional/local tectonics as well as local factors in the clay-mineral distribution.

8.3 CARBON AND OXYGEN ISOTOPES

8.3.1 Introduction

Carbon and oxygen isotopes are commonly used for palaeoceanographic and palaeoclimatic interpretations (e.g., WEISSERT & ERBA 2004; WIERZBOWSKI 2002; MALCHUS & STEUBER 2002; BUONOCUNTO et al. 2002). Stable isotope data viewed in a stratigraphic context may also give useful information for interpreting depositional and diagenetic histories of limestones (e.g., JOACHIMSKI 1994; VINCENT 2001; VINCENT et al. 2004; PEARCE et al. 2005).

In shallow-marine carbonates, carbon and oxygen stable isotopes have been extensively studied (e.g., SCHOLLE & ARTHUR 1980; ALLAN & MATTHEWS 1982; JOACHIMSKI 1991, 1994; JIMENEZ DE CISNEROS & VERA 1993; VEIZER et al. 1999; RASSER & FENNINGER 2002; BARTOLINI et al. 2003; PARENTE et al. 2007). However, the complexity of sedimentological and early diagenetic phenomena in shallow environments complicates the interpretation of the isotopic record. Controlling factors include fractionation by the carbonate-producing organisms, porosity and permeability of the sediment, type and extent of vegetation cover, duration of subaerial exposure, and diagenetic alteration (JOACHIMSKI 1994).

Correlated on a global scale, $\delta^{13}C$ variations have been explained mainly in terms of changes in the rate of production and accumulation of organic and inorganic carbon (WEISSERT & MOHR 1996). Generally, positive excursions in $\delta^{13}C_{carb}$ are attributed to enhanced burial of organic carbon in sediments, leading to depletion of ^{12}C in the ocean carbon reservoir (e.g., KUMP & ARTHUR 1999). The Late Jurassic carbon isotope stratigraphy is marked by a positive carbon excursion of up to 3‰, dated of the early Transversarium zone in the Middle Oxfordian (e.g., BARTOLINI et al. 1996) and a distinct short-lived negative excursion in the middle Transversarium zone (PADDEN et al. 2001; Fig. 8.1). For the Middle Oxfordian positive excursion, LOUIS-SCHMID (2006) and LOUIS-SCHMID et al. (2007) propose an ocean-intrinsic process triggered by plate tectonic movements. This increased pCO_2 and thus modified the carbon cycle. Associated were a sea-level rise and a decrease in latitudinal temperature gradient caused by the opening of the North Atlantic. The short-lived negative excursion has been interpreted as reflecting

a sudden release of methane hydrate along the continental margins (Padden et al. 2001).

Platform carbonates are frequently exposed to meteoric fluids that may alter their original $\delta^{13}C$ as well as $\delta^{18}O$ (e.g., Dickson & Coleman 1980; Allan & Matthews 1982; Lohmann 1988; Marshall 1992; Joachimski 1994). Carbonates, which have undergone subaerial diagenesis, may be depleted in $\delta^{13}C$ due to the influence of organic ^{12}C (soil gas). Below the subaerial exposure surface, there commonly is a $\delta^{13}C$ decrease (Allan & Matthews 1977; Videtich & Matthews 1980). The intensity of the $\delta^{13}C$ isotopic signature thus is a function of the subaerial exposure time and degree of pedogenetic alteration (Joachimski 1994). Moreover, it has been shown that oxidation of organic matter, photosynthesis, and respiration can cause semi-restricted water masses on carbonate platforms to develop $\delta^{13}C$ values significantly different from those of the open ocean (Patterson & Walter 1994; Immenhauser et al. 2003).

$\delta^{18}O$ values depend on temperature, salinity, taxon-specific fractionation, and diagenetic alteration (e.g., Podlaha et al. 1998; Rosales et al. 2001). In carbonate sediments, depleted $\delta^{18}O$ either results from an increase in temperature or reflects a salinity decrease due to the interaction with isotopically depleted meteoric subsurface waters (Hudson 1977; Lohmann 1988). The oxygen-isotope record is commonly used for the calculation of seawater palaeotemperatures (e.g., Ditchfield 1997; Malchus & Steuber 2002; Weissert & Erba 2004). Frakes et al. (1992) indicate up to 27°C for the Late Oxfordian ocean surface temperatures according to oxygen isotopes measured on planktonic foraminifera and belemnites. Plunkett (1997) calculated palaeotemperatures of 26-27°C from (modified whole rock) Middle Oxfordian samples from the Swiss Jura platform. Several studies show a strong temperature increase during the Oxfordian (e.g., Fritz 1965; Hoffman et al. 1991; Podlaha et al. 1998; Abbink et al. 2001; Poulsen & Riding 2003; Fig. 8.1). This change coincides with a southwestward drift of the West European crustal plate, but a causal relationship remains to be demonstrated (Malchus & Steuber 2002).

Carbonates may also become enriched in ^{18}O during subaerial exposure due to the removal of ^{16}O by surface evaporation at the sediment-air interface (Allan & Matthews 1982). Accordingly, relatively low $\delta^{18}O$ values (meteoric diagenesis) as well as high $\delta^{18}O$ values (evaporation) in a carbonate succession may point to exposure and are commonly related to sequence boundaries (e.g., Pasquier 1995; Hillgärtner 1999).

Strong variations in $\delta^{13}C$ associated with low variations in $\delta^{18}O$ are typical for meteoric diagenesis, whereas a parallel evolution of $\delta^{13}C$ and $\delta^{18}O$ curves indicates the zone of mixed, meteoric-marine diagenesis (Allan & Matthews 1982; Plunkett 1997).

8.3.2 Material and analytical methods

For the stable isotope analysis, 77 samples from the Vorbourg, Savagnières, and Latrecey-Ormoy sections have been used (Annex 7). The analyses were performed on whole-rock samples, preferentially on micrite (homogenization of the signal) but also on grainstones. The measurements were carried out in the stable isotope laboratory of the University of Lausanne (Switzerland). The isotopes were measured with a Finnigan Delta Plus XL mass spectrometer with an attached GasBench II and a PAL autosampler. Rock powders were reacted with 100 % phosphoric acid at 90° C. The produced CO_2 was introduced into the GasBench II, which separates CO_2 from water and other possible impurities. The treated gas was then sent in a continuous flow mode into the mass spectrometer. During the continuous flow, 10 measurements are made for each sample. The obtained raw results are regularly corrected by comparison to an internal standard (Carrara Marble: 2.05 ‰ $\delta^{13}C$ and -1.75 ‰ $\delta^{18}O$) in between two samples. The internal standard is calibrated to the international standard NBS19 (1.95 ‰ $\delta^{13}C$ and -2.20 ‰ $\delta^{18}O$). The mean value of the 10 corrected raw results is calculated and represents the C and O isotope values for a given sample. The error margin includes the measurement and reproducibility error and is of ± 0.5 ‰.

8.3.3 Results and interpretations

In this work, the carbon and oxygen isotopic records from two shallow platform sections and one deep platform section are investigated at the scale of

Fig. 8.12 - (facing page) Trends of stables isotopes ($\delta^{18}O$ and $\delta^{13}C$) in the transgressive part of medium-scale sequence 1 of the Latrecey (Haute-Marne, deep platform), Vorbourg, and Savagnières (Swiss Jura, shallow platform) sections. Cross-plot of the $\delta^{18}O$ and $\delta^{13}C$ values.

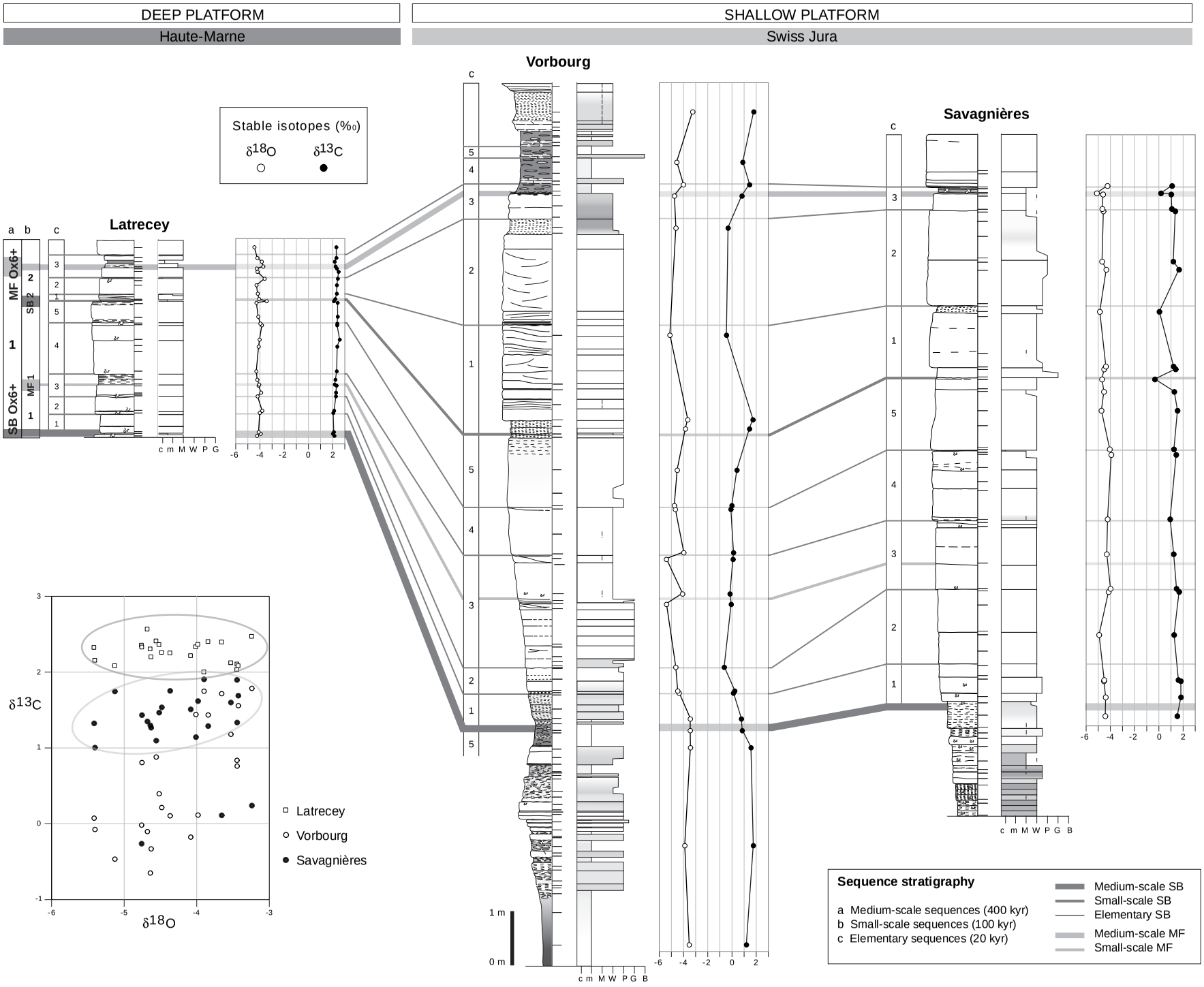
DEEP PLATFORM
Haute-Marne
SHALLOW PLATFORM
Swiss Jura
Stable isotopes (‰)
δ18O
δ13C
Latrecey
Vorbourg
Savagnières
a b c
MF Ox6+
SB 2
MF 1
SB Ox6+
c m M W P G
c m M W P G B
-6 -4 -2 0 2
1 m
0 m
δ13C
δ18O
Latrecey
Vorbourg
Savagnières
Sequence stratigraphy
a Medium-scale sequences (400 kyr)
b Small-scale sequences (100 kyr)
c Elementary sequences (20 kyr)
Medium-scale SB
Small-scale SB
Elementary SB
Medium-scale MF
Small-scale MF

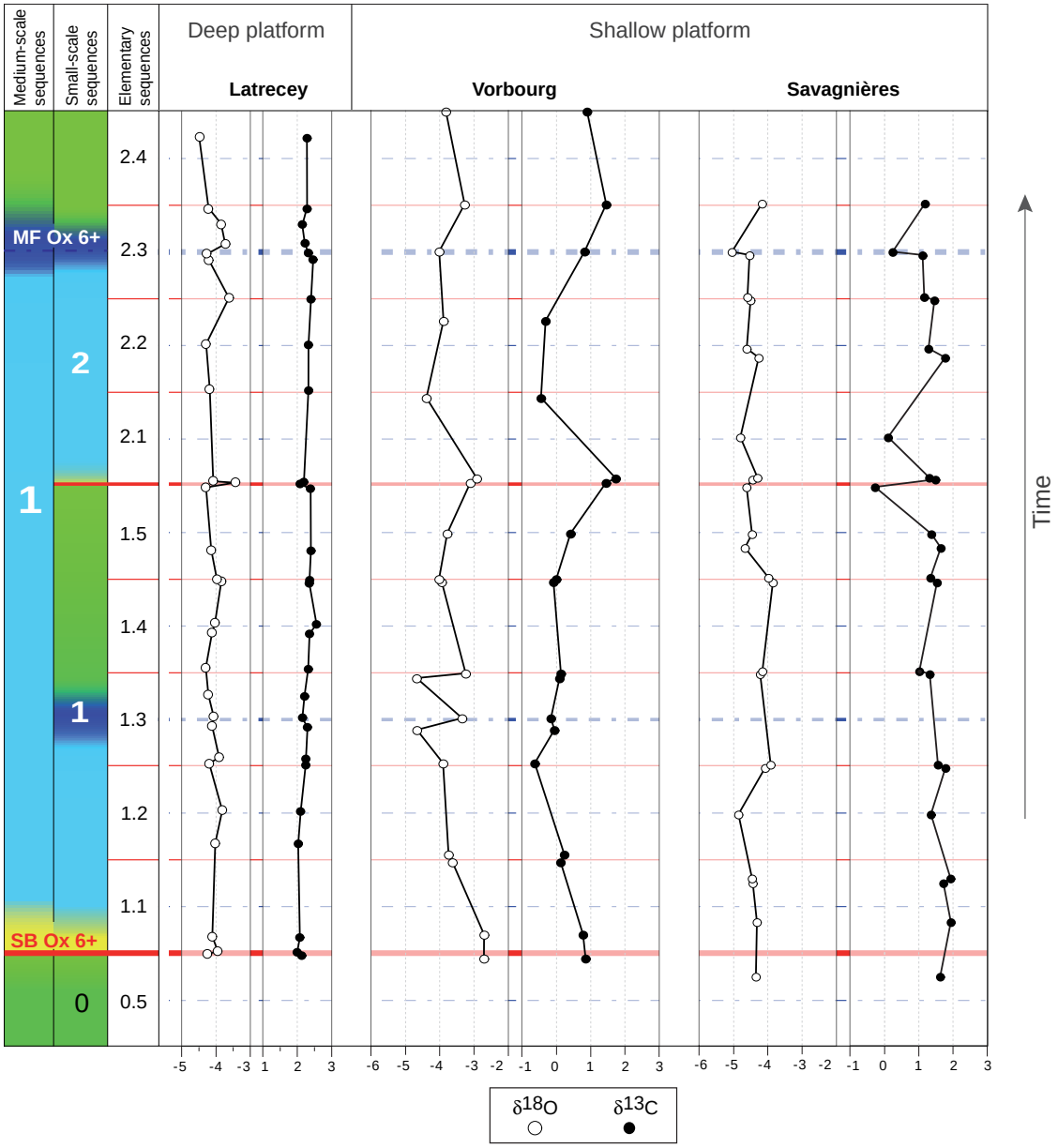

Fig. 8.13 - Trends of stables isotopes ($\delta^{18}O$ and $\delta^{13}C$) of the three studied sections placed in the high-resolution time-space diagram.

elementary sequences (20 kyr). Due to the absence of features indicating emersion or meteoric diagenesis in the studied sections (cf. Chap. 4), the measured values probably reflect the original sea-water composition.

Swiss Jura (shallow platform)

In the Swiss Jura sections, the $\delta^{13}C$ and $\delta^{18}O$ curves are relatively steady with only minor fluctuations (Fig. 8.12). The $\delta^{13}C$ values vary between –0.5 and +2 ‰ (Δ 2.5‰) in both studied sections, while the $\delta^{18}O$ values vary between –5 and –4 ‰ (Δ 1‰) in the Savagnières section and between –5.5 and –3.5 ‰ (Δ 2‰) in the Vorbourg section. The comparison of $\delta^{18}O$ and $\delta^{13}C$ values shows no significant correlation and hence suggests the preservation of the original isotopic signal (Fig. 8.12). In fact, the measured values fall well into the range indicated by Hudson (1977) for average marine limestones.

Compared with the values of Joachimski (1994), the $\delta^{13}C$ values of the Vorbourg section may be associated to more open marine environments than those in the Savagnières section.

Haute-Marne (deep platform)

In the Haute-Marne section (Latrecey), isotopic values are very homogeneous. The $\delta^{13}C$ values vary between +2.0 and +2.5 ‰ (Δ 0.5‰) and the $\delta^{18}O$ values vary between –4.5 and –3.5 ‰ (Δ 1‰). No correlation between the $\delta^{13}C$ and $\delta^{18}O$ values exists, suggesting an original signal. The steady curves are mainly explained by the equilibration of the carbonates in an open, water-buffered oxygen system (Allan & Matthews 1982), in agreement with the palaeogeographic position on the margin of the Paris Basin.

In the studied sections, no trends have been identified within the 100- and 20-kyr sequences. The minor isotopic fluctuations of ± 1‰, particularly around the small-scale SB 2 and the medium-scale MF Ox6+, probably reflect variations of local environmental conditions (e.g., salinity, temperature, trophic level). This is related to the variability of depositional environments, evidenced by the facies mosaics on the Swiss Jura carbonate platform **(**cf. Figs 7.3 and 7.4; Strasser & Védrine in press). The slight variations of less than 0.5‰ at the scale of the 20-kyr elementary sequences are interpreted as noise and cannot be related to environmental changes.

8.4 Conclusions

On the northern Tethys margin, the studied interval corresponds to less humid conditions with a global cooling and concurs with a long-term sea-level rise (Fig. 8.1). This study on platform and basin deposits shows the large potential of a high-resolution analysis.

Clay minerals show similar medium-scale trends between the sections from shallow platform to basin particularly around the medium-scale SB Ox6+and MF Ox6+. These patterns have not only been controlled by climate changes but also by relative sea-level changes and platform morphology. For example, at the medium-scale MF Ox6+, a remobilization of clay particles by the long-term transgression may be involved (cf. Fig. 8.6). At the scale of 100- and 20-kyr sequences, the interpretation of clay-mineral distribution is more difficult. The discrepancies probably result from the complex dynamics on the shallow platform or diagenetic transformations in seawater or during burial diagenesis.

The carbon and oxygen isotopic fluctuations are minor (±1‰) and probably reflect variations of local environmental conditions (e.g., salinity, temperature, trophic level). The oxygen isotopes do not allow to demonstrate temperature changes.

Additional sections and an increased sampling density would potentially improve the interpretation of both clay minerals and stable isotopes. This would help to answer questions on the composition of source areas, clay-mineral distribution and/or diagenetic transformation.

This study shows that clay-mineral assemblages and stable isotopes can give palaeoenvironmental information on the scale of 400 kyr and 100 kyr but that at higher time resolution is difficult to obtain. This is probably due to time-averaging by sedimentological and/or diagenetic processes.

* * *

9 - CONTROLLING FACTORS OF MIXED CARBONATE-SILICICLASTIC PLATFORMS

This chapter aims to identify the controlling factors that act on carbonate platform systems. From sedimentological, geochemical, and mineralogical data obtained in this work, the main factors that controlled the hydrodynamics, the carbonate ecosystem, and the formation of depositional sequences on the Swiss Jura shallow platform are discussed.

9.1 THE INTERPLAY OF TECTONICS, EUSTASY, AND CLIMATE

The sedimentary record results from a large number of local, regional, and global parameters, which are interrelated to different degrees (Fig. 9.1). In the studied mixed carbonate-siliciclastic systems, the sedimentary record results from relative sea-level fluctuations, carbonate production and accumulation, and terrigenous input. On shallow platforms, the potential of carbonate production is controlled by variations of factors intrinsic to the ecosystem (e.g., water depth, turbidity, hydrodynamism, nutrient availability, oxygenation, salinity, and temperature), which depend of sea-level variations, tectonics, and climate.

9.1.1 Tectonics

Tectonic activity is mainly linked to plate tectonics (VAIL et al. 1991). Phases of increased tectonic activity on a global scale (duration corresponding to 1st-order of VAIL et al. 1991) are responsible for widespread orogeny and the formation of sedimentary basins. Regional tectonics (2nd-order of VAIL et al. 1991) control variations in the subsidence rate of sedimentary basins. Local tectonics induce the small-scale structural changes.

Plate tectonics influence eustatic sea-level through variations of the volume of basins. Global climate is influenced by increased CO_2 released from ocean-floor spreading and/or volcanism or by decreased CO_2 due to continental weathering of silicates. Regional climate is furthermore controlled by the position of the continents and orogeny. Tectonics also influence platform morphology and the distribution of depositional environments through bathymetric and hydrodynamic variations. Tectonics together with climate control the production, transport, and distribution of terrigenous sediments and nutrients onto the shallow platform (MATTHEWS & PERLMUTTER 1994; VAIL et al. 1991).

9.1.2 Eustasy

Long-term eustatic sea-level variations (tectono-eustasy, 1st- and 2nd-order of VAIL et al. 1991) are linked to variations of the volume of oceans, which mainly depend of mid-oceanic ridge activity. The volume of oceans are also modified by the collision of continents, subduction, sub-marine magmatism, and sedimentary filling (VAIL et al. 1991). Short-term eustatic sea level fluctuations (glacio-eustasy, from 3rd- to 6th-order of VAIL et al. 1991) are linked to orbital parameters. Precession, obliquity and eccentricity variations create climate changes, which act on the volume of water masses, and consequently, on sea level. Sea-level changes were created by glaciation/deglaciation cycles of polar ice-caps and mountain glaciers, by thermal expansion and retraction of the uppermost layer of the ocean water, by thermally induced volume changes in deep-water circulation, and/or by water retention and release in lakes and aquifers (cf. Chap. 6.1).

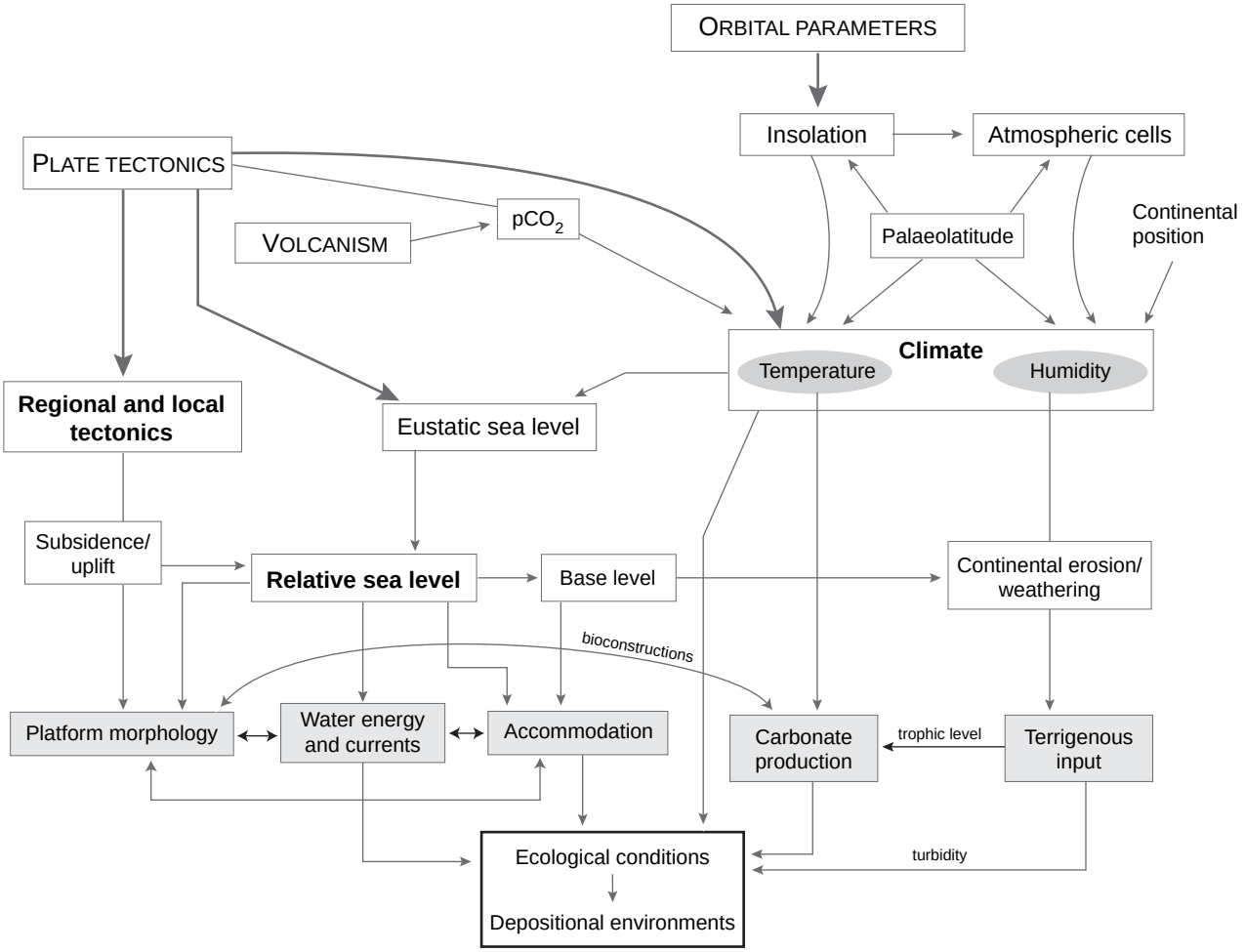

Fig. 9.1 - Control of orbital parameters and plate tectonics on climate, eustatic sea level, and regional tectonics modifying the ecological parameters of depositional environments. The three main controlling factors are in bold. The controlling factors evidenced by the facies, oncoid, and benthic foraminifer distribution (cf. Chap. 7) are in grey. Scale, amplitudes, and frequencies may strongly vary. Refer to text for discussion.

Sea-level variations directly influence bathymetry, hydrodynamism, nutrient availability, and temperature (e.g., HALLOCK & SCHLAGER 1986; JAMES 1997). A relative sea-level fall accentuates the platform morphology and favours the formation of restricted lagoons. Variations of base level are linked to the relative sea-level fluctuations and thus control the continental erosion and terrigenous input. Long-term eustatic sea-level variations are partly responsible of the geometry of system tracts (sensu VAIL et al. 1991; progradation, retrogradation, aggradation) and of the formation of long-term depositional sequences while short-term variations preferentially influence the formation of elementary, small-scale, and medium-scale sequences.

9.1.3 Climate

Global climate partly depends on orbital variations, which affect the insolation and the atmospheric circulation (MÖRNER 1994; MATTHEWS & PERLMUTTER 1994). Global climate is also controlled by greenhouse gases. Increased activity of the mid-oceanic ridges engenders an increase of atmospheric pCO_2 followed by an increase of temperature and rainfall (WEISSERT & MOHR 1996). Continental weathering of silicate minerals leads to a drop in pCO_2 and thus to a cooling. Gas hydrate dissociation releases CH_4, which acts as a greenhouse gas. Land-ocean distribution and elevation of mountain chains control the regional climate.

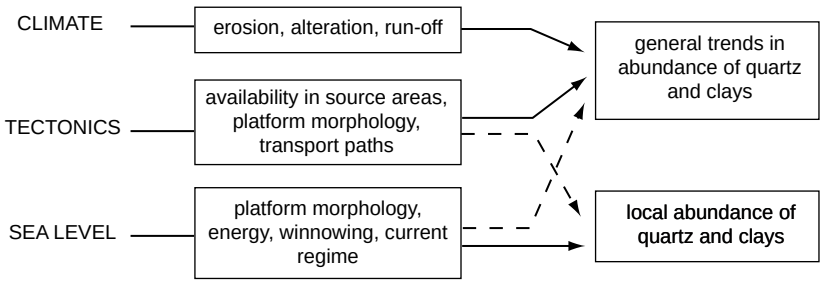

Fig. 9.2 - Main controlling factors acting on the siliciclastic distribution. Modified from HILLGÄRTNER (1999).

Rainfall and temperature strongly influence the ecosystems of shallow carbonate platforms and hence the potential of carbonate production. High precipitation favours the terrigenous sediment transport and distribution. The terrigenous sediment distribution thus may be related to orbital cycles defining the humidity conditions. These vary according to palaeolatitude and/or palaeoposition of the continents (MATTHEWS & PERLMUTTER 1994).

Continent-derived nutrients stimulate primary productivity, which may lead to eutrophication and turbidity increase on the shallow platform (HALLOCK & SCHLAGER 1986; DUPRAZ & STRASSER 1999). After abundant rainfalls, salinity decreases. Eutrophication, high turbidity, and low salinity are responsible for a decrease of the potential of carbonate production. Similarly, high aridity engenders, by evaporation, an increase of salinity, and hence a decrease of the carbonate production (HALLOCK & SCHLAGER 1986). Eustasy and climate are linked, through complex processes and feedback mechanisms, to variations of the orbital parameters (Fig. 9.1).

9.2 FACTORS CONTROLLING THE SEDIMENTATION OF THE SWISS JURA PLATFORM

Based on the study of the Swiss Jura sections (cf. Chap. 7), the facies distribution on the Swiss Jura platform is best described by a mosaic of juxtaposed depositional environments. Platform morphology, related to local and regional tectonics, was an important factor influencing the facies distribution (Fig. 9.1). The oncoid and benthic foraminifer distribution illustrates the influence of water energy and water depth (cf. Chap. 7 and Fig. 7.8), linked to relative sea-level fluctuations as well as the carbonate production and terrigenous input controlled by climate (humidity and temperature) and platform morphology (Figs 7.9 and 9.1).

The siliciclastic distribution in the Hauptmumienbank Member is variable. Trends in abundance of quartz and clays controlled by global factors (i.e., humidity changes, tectonics) and by local factors (i.e., platform morphology, water energy; Fig. 9.2) are observed. From the study of the marly Röschenz Member deposits, PITTET (1996) proposed more humid conditions during low sea-level periods at the scale of 100-kyr sequences. This can be explained by the palaeolatitudinal variations of the atmospheric cells (MATTHEWS & PERLMUTTER 1994; PITTET & STRASSER 1998b; PITTET et al. 2000; STRASSER et al. 2005; MARTIN-GARIN 2005). However, in the overlying Hauptmumienbank Member, siliciclastics occur not only around sequence boundaries but also around maximum floodings of the 100-kyr sequences. This is related to the long-term transgressive trend initiated at the base of the Hauptmumienbank Member, which modifies the continental erosion and allows the remobilization of siliciclastics formerly stored in the proximal part of the platform. The latter process is also proposed for the clay-mineral distribution (i.e., kaolinite; cf. Chap. 8).

The observed hierarchical stacking pattern of the depositional sequences is interpreted to be related to eustatic sea-level fluctuations driven by the Earth's orbital perturbation in the Milankovitch frequency band (cf. Chap. 3 and 6). The good correlation across the platform of small-scale and medium-scale sequences implies a common external controlling factor such as eustatic sea-level changes. However, the variability of facies and discontinuity surfaces (cf. Chap. 7) points to additional local controlling factors such as platform morphology and terrigenous input, acting on the carbonate productivity and accumulation.

The complex interaction of factors is evidenced particularly at the scale of elementary sequences. These sequences present a high facies variability (cf. Chaps 3 and 7). They are related to the precession cycles, which increase the seasonal contrast. These cycles acted on variations in precipitation and run-off on a regional scale, dependent on latitude (WATERHOUSE 1999; MALLINSON et al. 2003).

* * *

10 - CONCLUSIONS AND OUTLOOK

Based on a well-established bio- and sequence-stratigraphic framework, a high-resolution sedimentological study has been performed on a narrow time window in the Late Oxfordian (early Bimammatum zone). Seven shallow platform sections (Swiss Jura, Lorraine), two deep platform sections (Haute-Marne, Swabian Jura), and one basin section (SE France) have been logged and analysed in great detail. Based on a facies and microfacies analysis, the deposits are interpreted in terms of palaeoenvironments and sequence- and cyclostratigraphy.

The main results of this study are:

- Due to their high sensitivity to sea-level and climate changes, the shallow carbonate platform deposits from the Swiss Jura sections provide a high-resolution record of palaeoenvironmental changes occurring during a marine transgression, which is a favourable period for sediment preservation due to a high accommodation gain.

- The detailed facies and microfacies analysis allows to propose depositional models for the Swiss Jura platform and the other studied areas.

- The high-resolution sequence- and cyclostratigraphic analysis allows to define hierarchically stacked depositional sequences: medium-scale, small-scale, and elementary sequences, formed through orbitally controlled sea-level changes with periodicities of 400, 100, and 20 kyr, respectively.

- In this study, the first half of a medium-scale sequence is examined. It corresponds to two small-scale sequences, each composed of five elementary sequences. In the shallow platform sections, an elementary sequence generally consists of one to four beds including more or less developed marl intervals. In the deep platform sections, an elementary sequence generally consists of one or two limestone beds with a more or less developed marl interval. In the basin section, an elementary sequence is commonly defined by one marl-limestone couplet.

- This study provides a "*best-fit solution*" of high-resolution sequence-stratigraphical correlation from shallow-water platform (Jura, Lorraine platform) to deeper platform (Haute-Marne, Swabian Jura) and to basin sections (SE France). The good correlation of depositional sequences over long distances between the seven shallow platform sections and the similar number of elementary sequences in all sections are valuable arguments that allocyclic processes (i.e., eustatic sea-level fluctuations) must have been involved in the formation of these depositional sequences.

- A pre-existing morphology determined the geometry of the coast line and the distribution of depocenters on the platform. The relief also modified the hydrodynamic setting (current and/or wave directions and intensity), the pattern of sediment production and deposition, and the ecological conditions (e.g., water depth, salinity, turbidity, nutrient distribution). Carbonate production and accumulation, i.e. the preferential growth of reefs and the initiation of ooid shoals on tectonic highs further enhanced the relief on the platform. Climate changes also played a role in the facies distribution on the shallow platform. The terrigenous input, controlled by humidity changes in the hinterland and by sea level influenced carbonate production.

- Thickness variations at the scale of small-scale and elementary sequences reveals variations in the sediment accumulation rates. This is interpreted as resulting mainly from differential subsidence due to the activity of tectonic blocks. The relief created by tectonics therefore contributed significantly to the general facies distribution.

- The vertical and lateral distribution of facies, oncoids, and benthic foraminifera is investigated within elementary and small-scale sequences related to 20-kyr precession cycle and to the 100-kyr short-eccentricity cycle, respectively. When comparing the facies of time-equivalent small-scale and elementary sequences between the Swiss Jura sections, significant lateral facies changes appear (facies mosaic).

- The distribution of siliciclastics in the shallow platform sections shows a similar pattern with more or less developed marl intervals around the medium-scale SB Ox6+ and MF Ox6+ and the small-scale SB 2. Discrepancies in this distribution is explained by localized depressions, which were created by differential subsidence and served as channels, and by the remobilization of siliciclastics formerly stored in more proximal areas of the platform.

- Four types of oncoids are defined in the Hauptmumienbank Member from the Swiss Jura based on surface morphology, configuration and composition of the cortex, and the encasing sediment. Type 1 is sub-elliptical, micritic, and has a homogeneous cortex; Type 2 is elliptical, smooth, and displays micritic laminations with serpulid worm tubes and *Bullopora*; Type 3 is elliptical, lobate, and shows alternating laminae of *Bacinella-Lithocodium* and micrite; Type 4 is lobate and consists mainly of a *Bacinella-Lithocodium* meshwork.

- The stratigraphic and spatial distribution of oncoids in the six studied sections shows that each oncoid type can be attributed to a specific depositional environment. Type 1 oncoids characterize moderate-energy conditions in protected lagoons; Type 2 oncoids are related to higher energy conditions in open lagoons; Type 3 and 4 oncoids dominate in low- to very low-energy settings in open lagoons.

- Oncoid distribution is linked to relative sea-level changes. Micrite-dominated oncoids (types 1 and 2) are preferentially found around sequence boundaries and in transgressive deposits, whereas oncoids containing *Bacinella-Lithocodium* (types 3 and 4) are found rather around maximum floodings and in highstand deposits. This implies that changes in water energy and water depth were direct controlling factors. The heterogeneous oncoid distribution through space and time implies that the variable morphology of the Swiss Jura platform was also a controlling factor. Type 1 and 2 oncoids grew under meso- to eutrophic conditions, while type 3 and 4 oncoids, rich in light-dependent microencrusters (i.e., *Bacinella* and *Lithocodium*), flourished in oligotrophic waters. This study demonstrates that oncoids are valuable proxies for high-resolution palaeoenvironmental and palaeoecological studies.

- The distribution of the total abundance of benthic foraminifera shows a relatively patchy distribution without any "proximal-distal" trend. Contrary to the agglutinated foraminifera, the porcelaneous and hyaline foraminifera show a correlation with the sequence-stratigraphic evolution. Miliolids are preferentially found in the highstand deposits of some elementary and/or small-scale sequences. The hyaline foraminifera, rare in the studied sections, are preferentially found in the transgressive deposits of some elementary sequences. Consequently, the benthic foraminifera are indirectly linked to relative sea-level (accommodation changes) and to climate changes (sediment and nutrient input).

- The distribution of *Mohlerina basiliensis* and *Bacinella-Lithocodium* oncoids shows a strong correlation. *M. basiliensis* preferentially occurs when *Bacinella-Lithocodium* oncoids are present. The co-occurrence of *Bacinella-Lithocodium* oncoids and *M. basiliensis* suggests that they required similar ecological conditions.

- The successively later occurrence of *M. basiliensis* from "distal" to "proximal" sections illustrates the stepwise flooding of the platform and thus implies a dependence on normal-marine conditions.

- Clay mineral analyses have been performed on three sections from shallow platform, deep

platform, and basin. The medium-scale trends of the kaolinite content and K/I ratio between all three sections are comparable, particularly around the medium-scale SB Ox6+ and MF Ox6+. These patterns have been controlled not only by climate changes but also by relative sea-level changes and platform morphology.

- Performed on sections from the Swiss Jura and Haute-Marne, the carbon and oxygen isotope analyses show minor fluctuations (±1‰), particularly around the small-scale SB 2 and the medium-scale MF Ox6+ that probably reflect variations of local environmental conditions (e.g., salinity, temperature, trophic level). The oxygen isotopes do not allow to demonstrate temperature changes at the scale of small-scale or elementary sequences.

This study has led to several interesting results that may be used as starting points for further research:

The sequence- and cyclostratigraphic time frame obtained in this study may be used for performing facies analysis within an elementary sequence in order to interpret palaeoecological changes with a resolution higher than 20 kyr.

The methodology coupling high-resolution facies analysis with sequence- and cyclostratigraphic stratigraphic interpretation is an excellent tool for monitoring high-frequency palaeoenvironmental changes. This methodology may thus be applied to platform deposits from other stratigraphic periods and palaeogeographic areas, if a bio- and sequence-stratigraphic framework is already well defined.

The vertical and lateral distribution of marine oncoids may be investigated also in other sections from other palaeogeographic areas, following the same methodology than in the present study. For example, oncoids commonly occur in the Pagny-sur-Meuse section (Lorraine), in the two small-scale sequences following the interval of this study. It would be interesting to define the different types and to relate them to specific depositional environments as well as sequential positions. Similar studies could also be performed on deposits containing lacustrine and/or fluvial oncoids. In Switzerland and neighboring countries, some Tertiary deposits are rich in non-marine oncoids (e.g., Upper Palaeocene-Eocene, eastern Ebro Basin, NE Spain, Zamarreño et al. 1997; Oligocene, Rhineland, W Germany, Leinfelder & Hartkopf-Fröder 1990; Miocene, Digne foreland basin, SE France, Bauer 2006). Their distribution according to the sequence-stratigraphic framework and their micromorphology could be analysed.

The identification and quantification of additional genera and/or species of benthic foraminifera, particularly among the agglutinated foraminifera (Textularids), could give more precise indications on their palaeoecology.

More research on the benthic foraminifer *Mohlerina basiliensis* would be interesting for solving the problem of taxonomy. The wall microstructure of *M. basiliensis* (Middle-Late Bathonian to Early Valanginian) presents similarities to the one of Fusulinina. Most fusulinides became extinct in the Late Permian. *Tetrataxis* is one of the genera persisting until the Late Triassic (Groves & Altiner 2005). Consequently, the comparison of wall microstructures between *M. basiliensis* and *Tetrataxis* sp., e.g., with SEM analyses, could allow to link *Mohlerina basiliensis* to the Fusulinina suborder.

* * *

REFERENCES

ABBINK, O., TARAGONA, J., BRINKHUIS, H. & VISSCHER, H. (2001) Late Jurassic to earliest Cretaceous palaeoclimatic evolution of the southern North Sea. Global Planet. Change, 30, 231-256.

ADATTE, T. (1988) Etude sédimentologique, minéralogique, micropaléontologique et stratigraphique du Berriasien-Valanginien du Jura central. Parties I et II, Thèse Université de Neuchâtel, 480pp.

ALLAN, J.R. & MATTHEWS, R.K. (1977) Carbon and oxygen isotopes as diagenetic and stratigraphic tools: surface and subsurface data, Barbados, West Indies. Geology, 5, 16-20.

ALLAN, J.R. & MATTHEWS, R.K. (1982) Isotope signatures associated with early meteoric diagenesis. Sedimentology, 29, 797-817.

ALLENBACH, R.P. (2001) Synsedimentary tectonics in an epicontinental sea: a new interpretation of the Oxfordian basins of Northern Switzerland. Eclogae Geol. Helv., 94, 265-287.

ALLENBACH, R.P. (2002) The ups and downs of "Tectonic Quiescence" recognizing differential subsidence in the epicontinental sea of the Oxfordian in the Swiss Jura Mountains. Sedimentary Geology, 150, 323-342.

ANDERSON, E.J. & GOODWIN, P.W. (1990) The significance of metre-scale allocycles in the quest for a fundamental stratigraphic unit. J. Geol. Soc. London, 147, 507-518.

ARNAUD, H. (1988) Subsidence in certain domains of southeastern France during the Ligurian Tethys opening and spreading rates. Bull. Soc. Géol. France, 5, 725-732.

ARNAUD-VANNEAU, A. (1994) Benthic foraminifer distribution and sequence stratigraphy. Géologie Méditerranéenne, XXI, 3-4, 13-15.

ATROPS, F. (1982), La sous-famille des Ataxioceratinae (Ammonitina) dans le Kimméridgien inférieur du Sud-Est de la France. Docum. Lab. Géol., Lyon, 83, 453pp., 45 pls.

ATROPS, F. (1984), Genres et sous-genres chez les Ataxioceratinae (Ammonitina, Perisphinctidae) de l'Oxfordien supérieur - Kimméridgien inférieur. Bull. Soc. Géol. France, série 7, 26, 4, 633-644.

BARTOLINI, A., BAUMGARTNER, P.O. & GUEX, J. (1999) Middle and Late Jurassic radiolarian palaeoecology versus carbon-isotope stratigraphy. Palaeogeogr. Palaeoclimatol. Palaeoecol., 145, 43–60.

BARTOLINI, A., BAUMGARTNER, P.O. & HUNZIKER, J. (1996) Middle and Late Jurassic carbon stable-isotope stratigraphy and radiolarite sedimentation of the Umbria-Marche Basin (Central Italy). Eclogae geol. Helv., 89, 811-844.

BARTOLINI, A., PITTET, B., MATTIOLI, E. & HUNZIKER, J.C. (2003) Shallow-platform palaeoenvironmental conditions recorded in deep-shelf sediments: C and O stable isotopes in Upper Jurassic sections of southern Germany (Oxfordian - Kimmeridgian). Sedimentary Geology, 160, 1-3, 107-130.

BASSANT, P. (1999) The high-resolution stratigraphic architecture and evolution of the Burdigalian carbonate-siliciclastic sedimentary systems of the Mut Basin, Turkey. GeoFocus, 3, Fribourg, 278pp.

BAUER, H. (2006) Infuence du climat, de l'eustatisme et de la tectonique dans l'architecture des séries continentales. Cas du Miocène inférieur et moyen du bassin de Digne-Valensole (SE, France). Unpublished PhD thesis, Ecole des Mines de Paris, 311pp, 1 Pl.

BAUSCH, W.M., BIRKENMAJER, K., GRUNENBERG, T., KRAJEWSKI, K.P. & KUTYBA, J. (1998) Clay mineralogy of Jurassic marine shales in Spitsbergen: a possible evidence for climate cooling during Oxfordian. Bulletin of the Polish Academy of Sciences, Earth Sciences, 46, 211–221.

BEAUDOIN, B. (1977) Méthodes d'analyse sédimentaire et reconstitution du bassin: le Jurassique terminal – Berriasien des chaînes subalpines méridionale. PhD Thesis, Caen University.

BERGER, A. (1978) Long-term variations of caloric insolation resulting form the Earth's orbital elements. Quaternary

Research, 9, 139-167.

Berger, A. & Loutre, M.F. (2004) Théorie astronomique des paléoclimats. C. R. Geosciences, 336, 701-709.

Berger, A., Loutre, M.F. & Dehant, V. (1989) Astronomical frequencies for pre-Quaternary paleoclimate studies. Terra Nova, 1, 474-479.

Berner, R.A. (1989) Biogeochemical cycles of carbon and sulfur and their effect on atmospheric oxygen over phanerozoic time. Global & Planetary Change, 1, 97-122.

Bernier, P. (1984) Les formations carbonatées du Kimméridgien et du Portlandien dans le Jura méridional. Stratigraphie, micropaléontologie, sédimentologie. Document du Laboratoire de Géologie de l'Université de Lyon 1, 92, 1-2, 803pp.

Betzler, C. , Reijmer, J.J.G., Bernet, K., Eberli, G.P., Anselmetti, F.S. (1999) Sedimentary patterns and geometries of the Bahamian outer carbonate ramp (Miocene - Lower Pliocene, Great Bahama Bank). Sedimentology, 46, 1127-1143.

Blanc-Vernet, L., Clairefond, P. & Orsolini, P. (1979) Les foraminifères. Géologie Méditerranéenne, 6, 1, 171-209.

Blondel, T.J.A., Gorin, G.E. & Jan du Chêne, R. (1993) Sequence stratigraphy on coastal environments: sedimentology and palynofacies of the Miocene in central Tunisia. IAS Spec. Publ., 18, 161-179.

Boardman, M.R. & Neumann, A.C. (1984) Source of periplatform carbonates: Northwest Providence Channel, Bahamas. J. Sed. Petrol., 54, 4, 1110-1123.

Böhm, F. (2003) Required but disguised: environmental signals in limestone-marl alternations. Palaeogeogr. Palaeoclimatol. Palaeoecol., 189, 161-178.

Bolliger, W. & Burri, P. (1967) Versuch einer Zeitkorrelation zwischen Plattformcarbonaten und tiefermarinen Sedimenten mit Hilfe von Quarz-Feldspat-Schüttungen (mittlerer Malm des Schweizer Jura). Eclogae geol. Helv., 60, 491-507.

Bolliger, W. & Burri, P. (1970) Sedimentologie von Schelf-Carbonaten und Beckenablagerungen im Oxfordien des zentralen Schweizer Jura. Beitr Geol Karte Schweiz, NF 140, 96pp.

Bombardière, L. (1998) Distribution of sedimentary organic matter and sequence stratigraphy in Upper Jurassic carbonates of southeast France. Terre & Environnement, Université de Genève, 14, 145pp.

Brachert, T.C. (1992) Late Jurassic sponge buildups: environmental interpretation by comparison with microfabrics of modern hardgrounds. Eclogae geol. Helv., 85, 1, 45-58.

Brasier, M.D. (1995) Fossil indicators of nutrient level 1: Eutrophication and climate. Marine palaeoenvironmental analysis from fossils. Geol. Soc. London, Spec. Publ., 83, 113-132.

Bucur, I.I., Săsăran, L., Săsăran, E. & Schuller, V. (2004) Micropaleontological study of the Limestone olistoliths within Upper Cretaceous Wildflysch from Hasdate (Eastern border of the Gulau Mountains). Acta Paleontologica Romaniae, 4, 55-67.

Bucur, I.I., Senowbari-Daryan, B. & Abate, B. (1996) Remarks on some foraminifera from the Upper Jurassic (Tithonian) reef limestone of Madonie Mountains (Sicily). Bolletino della Società Paleontologica Italiana, 35, 1, 65-80.

Budd, D.A., Saller, A.H. & Harris, P.M. (1995) Foreword. In: Budd, D.A., Saller, A.H. & Harris, P.M (eds) Unconformities and porosity in carbonate strata. AAPG Memoir, 63, vii-xii.

Buonocunto, F.P., Sprovieri, M., Bellanca, A., D'Argenio, B., Ferreri, V., Neri, C. & Ferruzza, G. (2002) Cyclostratigraphy and high-frequency carbon isotope fluctuations in Upper Cretaceous shallow-water carbonates, southern Italy. Sedimentology, 49, 1321-1337.

Burkhalter, RM (1996) Die Passwang-Alloformation (unteres Aalénien bis unteres Bajocien) im zentralen und nördlichen Schweizer Jura. Eclogae Geol. Helv., 89, 875–934.

Cannariato, K.G., Kennett, J.P. & Behl, R.J. (1999) Biotic response to late Quaternary rapid climate switches in Santa Barbara Basin: Ecological and evolutionary implications. Geology, 27, 63-66.

Carpentier, C. (2004) Géométries et environnements de dépôt de l'Oxfordien de l'Est du Bassin de Paris. Doctoral thesis, University Henri Poincaré, Nancy, 470pp.

Carpentier, C. Martin-Garin, B. Lathuilière, B., Ferry S. (2006) Correlation of reefal Oxfordian episodes and climatic implications in the eastern Paris Basin (France). Terra Nova, 18, 3, 191–201.

Cecca, F. (2002) Palaeobiogeography of marine fossil invertebrates. Concepts and methods. Taylor & Francis, London & New York. 273pp.

Cecca, F., Azéma, J., Fourcade, E., Baudin, F., Guiraud, R., Ricou, L.-E., De Wever, P. (1993) Early Kimmeridgian palaeoenvironments (146 to 144 Ma). In: Dercourt, J., Ricou, L.E., Vrielynck, B. (eds), Atlas Tethys Palaeoenvironmental Maps. BEICIP-FRANLAB, Rueil-Malmaison.

Cecca, F., Martin-Garin, B., Marchand, D., Lathuillière, B., & Bartolini, A. (2005) Paleoclimatic control of biogeographic and sedimentary events in Tethyan and peri-Tethyan areas during the Oxfordian (Late Jurassic). Palaeogeogr. Palaeoclimatol. Palaeoecol., 222, 10-32.

Chamley, H. (1989) Clay sedimentology. Springer-Verlag, 623pp.

Cherchi, A. & Schroeder, R. (2006) Remarks on the systematic position of Lithocodium (Elliott) a problematic microorganism from the Mesozoic carbonate platforms of the Tethyan realm. Facies, 52, 435-440.

Claps, M., Erba, E., Masetti, D. & Melchiorri, F. (1995) Milankovitch-type cycles recorded in Toarcian black

shales from the Belluno Trough (Southern Alps Italy). Memorie Scienze Geologiche, Padova, 47, 179-188.

Cloetingh, S. (1988) Intraplate stresses: A tectonic cause for third-order cycles in apparent sea level? In: Wilgus, C.E., Hastings, B.S., Kendall, C.G.S.C., Posamentier, H.W., Ross, C.A. & Van Wagoner, J.C. (eds) Sea-level changes - an integrated approach. SEPM Special Publ., 42, 19-29.

Cogne, J.P. & Humler, E. (2004) Temporal variation of oceanic spreading and crustal production rates during the last 180 My. *Earth and Planetary Science Letters*, 227, 427-439.

Collin, P.Y. & Courville, P. (2000) Paléoenvironnements et biostratigraphie d'une série oxfordienne non condensée de référence (Saint-Blin - Semolly, Haute-Marne). Géologie de la France, 1, 59-63.

Collin, P.Y., Loreau, J.P. & Courville, P. (2005) Depositional environments and iron ooid formation in condensed sections (Callovian–Oxfordian, south-eastern Paris basin, France). *Sedimentology*, 52, 969–985.

Colombié, C. (2002) Sédimentologie, stratigraphie séquentielle et cyclostratigraphie du Kimméridgien du Jura suisse et Bassin vocontien (France): Relations plat-forme - bassin et facteurs déterminants. GeoFocus, 4, 198pp.

Colombié, C. & Strasser, A. (2003) Depositional sequences in the Kimmeridgian of the Vocontian Basin (France) controlled by carbonate export from shallow-water platforms. Geobios, 36 (6), 675-683.

Colombié, C. & Strasser, A. (2005) Facies, cycles, and controls on the evolution of a keep-up carbonate platform (Kimmeridgian, Swiss Jura). Sedimentology, 52 (6), 1207-1227.

Cotillon, P. (1991) Varves, beds, and bundles in pelagic sequences and their correlation (Mesozoic of SE France and Atlantic). In: Einsele, G., Ricken, W. & Seilacher, A. (eds) Cycles and Events in Stratigraphy, Springer-Verlag, Berlin, 820-839.

Courville, P. & Villier, L. (2003) L'Oxfordien moyen et supérieur de l'est du Bassin Parisien (France). L'exemple de Latrecey (Haute-Marne): aspects fauniques, paléoenvironnementaux et stratigraphiques. Revue de Paléobiologie, 22, 175-196.

Cross, T.A. (1991) High-resolution stratigraphic correlation from the perspectives of base-level cycles and sediment accommodation. In: Dolson, J. (ed.) Unconformity related hydrocarbon exploration and accumulation in clastic and carbonate settings. Rocky Mountain Assoc. Geol. Short Course Notes, 28-41.

Cross, T.A. & Lessenger, M.A. (1998) Sediment volume partitioning: rationale for stratigraphic model evaluation and high-resolution stratigraphic correlation. Sequence stratigraphy - concepts and applications, 8, 171-195.

Curtis, C.D. (1990) Aspects of climate influence on the clay mineralogy and geochemistry of soils, paleosols and clastic sedimentary rocks. J. geol. Soc. London, 147, 351-357.

Dahanayake, K. (1977) Classification of oncoids from the Upper Jurassic carbonates of the French Jura. Sedimentary Geology, 18, 337-353.

Dahanayake K (1978) Sequential position and environmental significance of different types of oncoids. Sedimentary Geology, 20, 301-316.

Dahanayake, K. (1983) Depositional environments of some Upper Jurassic oncoids. In: Peryt, T.M. (ed) Coated Grains, Springer, 377-385.

Darga, R. & Schlagintweit, F. (1991) Mikrofazies, Paläontologie und Stratigraphie der Lerchkogelkalke (Tithon-Berrias) des Dietrichshorns (Salzburger Land, Nördliche Kalkalpen). Jb. Geol. B.-A., 134, 2, 205-226.

D'Argenio, B., Ferreri, V., Weissert, H., Amodio, S., Buonocunto, F.P. & Wissler, L. (2004) A multidisciplinary approach to global correlation and geochronology, the Cretaceous shallow-water carbonates of southern Appennines, Italy. In: D'Argenio, B., Fischer, A.G., Premoli Silva, I., Weissert, H. & Ferreri, V. (eds) Cyclostratigraphy: Approaches and case histories. SEPM Spec. Publ., 81, 103-122.

Davaud, E. & Lombard, A. (1973) Statistical approach to the problem of alternating beds of limestone and marls (Upper Oxfordian of the French Jura). Eclogae geol. Helv., **68,** 491-509.

Davies, P.J., Bubela, B. & Ferguson, J. (1978) The formation of ooids. Sedimentology, 25, 703-730.

De Boer, P.L. & Smith D., G. (1994) Orbital forcing and cyclic sequences. IAS Spec. Publ., 19, 559pp.

Debrand-Passart, S., Courbouleix, S. & Lienhardt, M.-J. (eds) (1984) Synthèse géologique du Sud-Est de la France. Mémoire BRGM France. 125, 1, Stratigraphie et paléontologie and 126 (2) Atlas.

Deconinck, J.-F. (1993) Clay mineralogy of the Late Tithonian - Berriasian deep-sea carbonates of the Vocontian Trough (SE France): relationships with sequence stratigraphy. Bull. Centre Rech. Explor.-Prod. Elf Aquitaine, 17(1), 223-234.

Deconinck, J.-F., Beaudoin, B., Chamley, H., Joseph, P. & Raoult, J.-F. (1985) Contrôles tectonique, eustatique et climatique de la sédimentation argileuse du domaine subalpin français au Malm-Crétacé. Rev. Géol. Dyn. Géogr. Phys., 26, 5, 311-320.

Deconinck, J.-F. & Debrabant, P. (1985) Diagenèse des argiles dans le domaine subalpin: Rôles respectifs de la lithologie, de l'enfouissement et de la surcharge tectonique. Rev. de Géol. Dynamique et de Géograph. Physique, 26, 5, 321-330.

Deconinck, J.-F., Gillot, P.-Y., Steinberg, M. & Strasser, A. (2001) Syn-depositional, low temperature illite formation at the Jurassic-Cretaceous boundary (Purbeckian) in the Jura mountains (Switzerland and France): K/Ar and $\delta^{18}O$ evidence. Bull. Soc. géol. France, 173, 343-348.

Deconinck, J.-F., Strasser, A. & Debrabant, P. (1988) Formation of illitic minerals at surface temperatures in Purbeckian sediments (Lower Berriasian, Swiss and French Jura). Clay Minerals, 2, 91-103.

Delage, Y. & Hérouard, E. (1896) La cellule et les Protozoaires. Traité de Zoologie Concrète. Vol. 1, Paris, Schleicher Frères.

Dercourt, J., Ricou, L.E. & Vrielynck, B. (eds) (1993) Atlas: Tethys Palaeoenvironmental Maps. CCGM, Paris.

Dickson, J.A.D., Coleman, M.L. (1980) Changes in carbon and oxygen isotope composition during limestone diagenesis. Sedimentology, 27, 1, 107–118.

Dieni, I. & Radoičić, R. (1999) Clypeina dragastani sp. nov., Salpingoporella granieri sp. nov. and other dasycladalean algae from the Berriasian of Eastern Sardinia. Acta Palaeont. Romaniae, 2, 105-123.

Ditchfield, P.W. (1997) High northern palaeolatitude Jurassic-Cretaceous palaotemperature variation: new data from Kong Karls Land, Svalbard. Palaeogeogr., Palaeoclim., Palaeoecol., 130, 163-175.

Dromart, G., Allemand, P., Garcia J.P. & C., R. (1996) Variation cyclique de la production carbonatée au Jurassique le long d'un transect Bourgogne-Ardèche, Est-France. Bull. Soc. Géol. France, 167, 423-433.

Dromart, G., Garcia, J.-P., Gaumet, F., Picard, S., Rousseau, M., Atrops, F., Lecuyer, C. & Sheppard, S.M.F. (2003a) Perturbation of the carbon cycle at the Middle/Late Jurassic transition: geological and geochemical evidence. Amer. J. Sci., 303, 667-707.

Dromart, G., Garcia, J.-P., Picard, S., Atrops, F., Lecuyer, C. & Sheppard, S.M.F. (2003b) Ice age at the Middle-Late Jurassic transition ? Earth and Planetary Science Letters, 213, 205-220.

Dupraz, C. & Strasser, A. (1999) Microbialites and micro-encrusters in shallow coral bioherms (Middle to Late Oxfordian, Swiss Jura Mountains). Facies, 40, 101-130.

Dupraz, C. (1999) Paléontologie, paléoécologie et évolution des faciés récifaux de l'Oxfordien Moyen-Supérieur (Jura suisse et français). GeoFocus, 2, 200pp.

Dupraz, C. & Strasser, A. (2002) Nutritional modes in coral-microbialite reefs (Jurassic, Oxfordian, Switzerland): evolution of trophic structure as a response to environmental change. Palaios, 17, 449-471.

Dya, M. (1992) Mikropaläontologische und fazielle Untersuchungen im Oberjura zwischen Salzburg und Lofer. Dissertation TU, Berlin, 137pp.

Eder, W. (1982) Diagenetic redistribution of carbonate, a process in forming limestone-marl alternations (Devonian and Carboniferous, Rheinisches Schiefergebirge, W. Germany). In: Einsele, G. & Seilacher, A. (eds) Cyclic and event stratification. Springer, Berlin Heidelberg New York, 98-112.

Einsele, G. & Ricken, W. (1991) Limestone-marl alternation - an overview. In: Einsele, G., Ricken, W. & Seilacher, A. (eds) Cycles and events in stratigraphy, Springer, 24-47.

El Albani, A., Meunier, A. & Fürsich, F. (2005) Unusual occurrence of glauconite in a shallow lagoonal environment (Lower Cretaceous, northern Aquitaine Basin, SW France). Terra Nova, 17(5), 537-544.

Elliott, G.F. (1956) Further records of fossil calcareous algae from the Middle East. Micropaleontology, 2, 327-334.

Embry, A.F. (1993) Transgressive–regressive (T–R) sequence analysis of the Jurassic succession of the Sverdrup Basin, Canadian Arctic Archipelago. Can. J. Earth Sci., **30,** 301–320.

Embry, A.F. (1995) Sequence boundaries and sequence hierarchies: problems and proposals. In: Steel, R.J., Felt, V.L., Johannessen, E.P. & Mathieu, C. (eds) Sequence Stratigraphy on the Northwest European Margin. Norwegian Petroleum Society (NPF), **5**, Spec. Publ. 1-11.

Emmanuel, L. & Renard, M. (1993) Carbonate geochemistry (Mn, $\delta^{13}C$, $\delta^{18}O$) of the Late Tithonian-Berriasian pelagic limestones of the Vocontian Trough (SE France). Bull. Centre Rech. Explor.-Prod. Elf Aquitaine, 17(1), 205-221.

Enay, R (coord) (1984) Jurassique supérieur - Malm. In : Debrand-Passart, S., Courbouleix, S. & Lienhardt, M.-J. (eds) Synthèse géologique du Sud-Est de la France. Mém. BRGM, 125, 223-286.

Enay, R., Contini, D., & Boullier, A. (1988) Le séquanien-type de Franche-Comté (Oxfordien supérieur): datations et corrélations nouvelles, conséquences sur la paléogéographie et l'évolution du Jura et régions voisines. Eclogae geol. Helv., 81, 2, 295-363.

Eslinger, E. & Pevear, D. (1988) Clay minerals for petroleum geologists and engineers. SEPM short course, Tulsa, 22, 413pp.

Fischer, A.G., De Boer, P.L. & Premoli Silva, I. (1990) Cyclostratigraphy. In: Ginsburg, R.N. & Beaudoin, B. (eds) Cretaceous resources, events and rhythms, Kluwer, 139-172.

Flügel, E. & Steiger, T. (1981) An Upper Jurassic sponge-algal-buildup from north-eastern Frankenalb (West Germany). In: Tommey, D.F. (ed) European fossil reef models. SEPM Spec. Publ., 30, 371–397.

Flügel, E. (2004) Microfacies of carbonate rocks: Analysis, interpretation and application. Springer, 976pp.

Frakes, L.A., (1979) Climates throughout geologic time. Elsevier, Amsterdam, 310pp.

Frakes, L.A., Francis, J.E. & Syktus, J.I. (1992) Climate modes of the Phanerozoic. Cambridge University Press, 270pp.

Fritz, O.K. (1958) Schwammstotzen, Tuberolithe und Schuttbrekzien im Weissen Jura der Schwábischen Alb. Arb. Geol.-Paläont. Inst. TH Stuttgart, N.F. 13, 1-118.

Fritz, P. (1965) O^{18}/O^{16}-Isotopenanalysen und Paleotemperaturbestimmungen an Belemniten aus dem

schwäb. Jura. Geologische Rundschau, 54, 261–269.

Fugagnoli, A (2004) Trophic regimes of benthic foraminiferal assemblages in Lower Jurassic shallow water carbonates from northeastern Italy (Calcari Grigi, Trento Platform, Venetian Prealps). Palaeogeogr, Palaeoclim, Palaeoecol, 205, 111-130.

Gaillard, C. (1983) Les biohermes à spongiaires et leur environnement dans l'Oxfordien du Jura Méridional. Docum. Lab. Géol. Lyon, 90, 515pp.

Galloway, W.E. (1989) Genetic stratigraphic sequences in basin analysis: I. Architecture and genesis of flooding-surface bounded depositional units. AAPG. Bulletin, 73, 125-142.

Gawenda, P. (1999) Climatic and tectonic controls on turbiditic and pelagic sedimentation in the deep sea. The Paleocene Lower Eocene Zumaia Series (northern Spain). PhD thesis, ETH-Zurich.

Gawlick, H.J., Schlagintweit F. & Lein, R. (2003) Das Höherstein-Plateau südlich Bad Ischl – Neue Daten zur Stratigraphie, Fazies und Sedimentologie: Implikationen zur palägeographischen Rekonstruktion im Jura des zentralen Salzkammergutes. In: Weidinger J.T., Lobitzer, H. & Spitzbart, I. (eds), Beiträge zur Geologie des Salzkammerguts. Gmundner Geo-Studien, 2, 107–114.

Geel, T. (2000) Recognition of stratigraphic sequences in carbonate platform and slope deposits: empirical models based on microfacies analysis of Palaeogene deposits in southeastern Spain. Palaeogeogr., Palaeoclim., Palaeoecol., 155, 211-238.

Geister, J. & Lathuiliere, B. (1991) Jurassic coral reefs of the Northeastern Paris Basin (Luxembourg and Lorraine). Excursion Guidebook of VI International Symposium on fossil Cnidaria, Münster, 112pp.

Ginsburg, R.N. (1971) Landward movement of carbonate mud: new model for regressive cycles in carbonates. Bull. Amer. Ass. Petrol. Geol. (abstract), 55, 340.

Gischler, E. & Lomando, A.J. (1999) Recent sedimentary facies of isolated carbonate platforms, Belize-Yucatan system, Central America. J. Sed. Res., 69 (3), 747-763.

Godet, A., Bodin, S., Adatte, T. & Föllmi, K.B. Platform-induced clay-mineral fractionation along a northern Tethyan basin-platform transect: implications for the interpretation of Early Cretaceous climate change (Late Hauterivian-Early Aptian) (submitted)

Goldhammer, R.K., Dunn, P.A. & Hardie, L.A. (1990) Depositional cycles, composite sea-level changes, cylce stacking patterns, and the hierarchy of stratigraphic forcing: Examples from Alpine Triassic platform carbonates. GSA Bull., 102, 535-562.

Gornitz, V., Lebedeff, S. & Hansen, J. (1982) Global sea level trend in the past century. Science, 215, 1611-1614.

Graciansky, de, P.C., Dardeau G., Bodeur Y., Elmi S., Fortwengler D., Jacquin T., Marchand D. & Thierry J. (1999) Les Terres Noires du Sud-Est de la France (Jurassique moyen et supérieur) : interprétation en termes de stratigraphie séquentielle. Bull. Centre Rech. Elf Explor. Prod., 22, 1, 35-69.

Gradstein, F.M., Agterberg, F.P., Ogg, J.G., Hardenbol, J., van Veen, P., Thierry, J. & Huang, Z. (1995) A Triassic, Jurassic and Cretaceous time scale. Geochronology time scales and global stratigraphic correlations. SEPM Spec. Publ., 54, 95-126.

Greiner, G.O.G. (1969) Recent benthonic foraminifera environmental factors controlling their distribution. Nature, 223, 168-170.

Gröcke, D.R., Price, G.D., Baraboshkin, E., Mutterlose, J. & Ruffell, A.H. (2003) The Valanginian terrestrial carbon-isotope record. Geophysical Research Abstracts, 5, 13644.

Groves, J.R. & Altiner, D. (2005) Survival and recovery of calcareous foraminifera pursuant to the end-Permian mass extinction. C.R. Palevol, 4, 487-500.

Gwinner, M.P. (1976) Origin of the Upper Jurassic of the Swabian Alb. Contrib. Sedimentol., 5, 1-75.

Gygi, R.A. (1969) Zur Stratigraphie der Oxford-Stufe (oberes Jura-System) der Nordschweiz und des süddeutschen Grenzgebietes. Beitr Geol Karte Schweiz N.F., 136, 123 pp.

Gygi, R.A. (1986) Eustatic sea-level changes of the Oxfordian (Late Jurassic) and their effect documented in sediments and fossil assemblages of an epicontinental sea. Eclogae geol. Helv., 79, 455-491.

Gygi, R.A. (1990) Die Paläogeographie im Oxfordium und frühestem Kimmeridgium in der Nordschweiz. Jahreshefte des Geologischen Landesamts Baden-Württemberg, B. 32.

Gygi, R.A. (1992) Structure, pattern of distribution and paleobathymetry of late Jurassic microbialites (stromatolites and oncoids) in northern Switzerland. Eclogae geol. Helv., 85, 799-824.

Gygi, R.A. (1995) Datierung von Seichtwassersedimenten des Späten Jura in der Nordwestschweiz mit Ammoniten. Eclogae geol. Helv., 88, 1-58.

Gygi, R.A. (2000a) Annotated index of lithostratigraphic units currently used in the Upper Jurassic of northern Switzerland. Eclogae geol Helv 93:125-146

Gygi, R.A. (2000b) Integrated stratigraphy of the Oxfordian and Kimmeridgian (Late Jurassic) in northern Switzerland and adjacent southern Germany. Mém. de l'Académie Suisse des Sciences Naturelles, 104, 151pp.

Gygi, R.A., Coe, A.L. & Vail, P.R. (1998) Sequence stratigraphy of the Oxfordian and Kimmeridgian stages (Late Jurassic) in Northern Switzerland. In : de Graciansky, P.C, Hardenbol, J., Jacquin, T & Vail, P.R (eds), Mesozoic and Cenozoic Sequence Stratigraphy of European Basins. SEPM Spec. publ., 60, 527-544.

Gygi, R.A. & Persoz, F. (1986) Mineralostratigraphy, litho- and biostratigraphy combined in correlation of the Oxfordian (Late Jurassic) formations of the Swiss Jura range. Eclogae geol. Helv., 79, 385-454.

Hallam, A. (1975) Evolutionary size increase and longevity in Jurassic bivalves and ammonites. Nature, 258, 493-496.

Hallam, A. (1984) Continental humid and arid zones during the Jurassic and Cretaceous. Palaeogeogr., Palaeoclim., Palaeoecol., 47, 195-223.

Hallam, A. (1985) A review of Mesozoic climates. J. Geol. Soc. London, 142, 433-445.

Hallam, A. (1986) Role of climate in affecting late Jurassic and early Cretaceous sedimentation in the North Atlantic. In: Summerhayes, C.P. & Shackleton, N.J. (eds) North Atlantic Palaeoceanography. GSA. Spec. Publ., 21, 277-281.

Hallam, A. (1988) A reevaluation of Jurassic eustasy in the light of new data and the revised EXXON curve. SEPM Spec. Publ., 42, 261-273.

Hallam, A. (1993) Jurassic climates as inferred from the sedimentology and fossil record. Philosophical Transactions of the Royal Society (London), B341, 287-296.

Hallam, A. (1994) Jurassic climates as inferred from the sedimentary and fossil record. In: Allen, J.R.L., Holskins, B.J., Sellwood, B.W., Spicer, R.A. & Valdes, P.J. (eds) Palaeoclimates and their modelling. Chapman and Hall, London, 79-88.

Hallam, A. (2001) A review of the broad pattern of Jurassic sea-level changes and their possible causes in the light of current knowledge. Palaeogeogr., Palaeoclim., Palaeoecol., 167, 23-37.

Hallam, A., Grose, J.A. & Ruffell, A.H. (1991) Palaeoclimatic significance of changes in clay mineralogy across the Jurassic-Cretaceous boundary in England and France. Palaeogeogr., Palaeoclim., Palaeoecol., 81, 173-187.

Hallock, P. (1988) The role of nutrient availability in bioerosion: consequences to carbonate build-ups. Palaeogeogr., Palaeoclim., Palaeoecol., 63, 275-291.

Hallock, P. & Schlager, W. (1986) Nutrient excess and the demise of coral reefs and carbonate platforms. Palaios, 1, 389-398.

Haq, B.U., Hardenbol, J. & Vail, P.R. (1987) Chronology of fluctuating sea levels since the Triassic (250 million years ago to present). Science, 235, 1156-1167.

Haq, B.U., Hardenbol, J. and Vail, P.R. (1988) Mesozoic and Cenozoic chronostratigraphy and cycles of sea-level change. In: Wilgus C.K. et al. (eds), Sea-level changes: an integrated approach. SEPM Spec. Publ., 42, 71-108.

Hardenbol, J., Thierry, J., Farley, M.B., Jacquin, T., de Graciansky, P.-C. & Vail, P.R. (1998) Mesozoic and Cenozoic sequence chronostratigraphic framework of European basins. In: de Graciansky, P.-C., Hardenbol, J., Jacquin, T. & Vail, P.R. (eds) Mesozoic and Cenozoic sequence stratigraphy of European Basins. SEPM Spec. Publ., 60, 3-13.

Heim, A (1916) Monographie der Churfirsten-Mattstock-Gruppe (3. Teil). Beitr Geol Karte Schweiz N.F., 20, 369-573.

Helm, C. & Schülke, I. (1998) A coral-microbialite patch reef from the Late Jurassic (Florigemma-bank, Oxfordian) of NW Germany (Süntel Mountains). Facies, 39, 75-104.

Hemleben, C., Spindler, M. & Anderson, O. R. (1988) Modern planktonic foraminifera. Springer, New York. 363pp.

Hilgen, F., Schwarzacher, W. & Strasser, A. (2004) Concept and definitions in cyclostratigraphy (second report of the cyclostratigraphy working group). In: D'Argenio, B., Fischer, A. G., Premoli Silva, I., Weissert H. & Ferreri, V. (eds) Cyclostratigraphy: Approaches and case histories. SEPM Spec. Publ., 81, 303-305.

Hillgärtner, H. (1999) The evolution of the French Jura platform during the Late Berriasian to Early Valanginian: Controlling factors and timing. GeoFocus, 1, 203pp.

Hillgärtner, H. & Strasser, A. (2003). Quantification of high-frequency sea-level fluctuations in shallow-water carbonates: an example from the Berriasian-Valanginian (French Jura). Palaeogeogr., Palaeoclim., Palaeoecol., 200, 43-63.

Hoffman, A., Gruszczyński, M., Małkowski, K., Hałas, S., Matyja, B.A. & Wierzbowski, A. (1991) Carbon and oxygen isotope curves for the Oxfordian of Central Poland. Acta Geol Polonica, 41, 157–164.

Hohenegger, J. & Piller, W. (1975) Diagenetische Veränderungen bei obertriadischen Involutinidae (Foraminifera). Neues Jahrbuch für Geologie und Paläontologie, 1, 26-39.

Hubbard, R.J. (1988) Age and significance of sequence boundaries on Jurassic and Early Cretaceous rifted continental margins. AAPG Bull., 72, 1, 49-72.

Hudson, J.D. (1977) Stable isotopes and limestone lithification. J. geol. Soc. London, 133, 637-660.

Hug, W. (2003) Sequenzielle Faziesentwicklung der Karbonatplattform des Schweizer Jura im Späten Oxford und frühesten Kimmeridge. GeoFocus, 7, 156pp.

Humbert, L. (1971) Recherche méthodologique pour la restitution de l'histoire biosédimentaire d'un bassin. L'ensemble carbonaté Oxfordien de la partie orientale du Bassin de Paris. Thèse d'Etat Univ. Nancy, n°AO 5096, 364 pp.

Hunt, D. & Tucker, M.E. (1992) Stranded parasequences and the forced regressive wedge systems tract: Deposition during base-level fall. Sedimentary Geology, 81, 1-9.

Hunt, D. & Tucker, M.E. (1995) Stranded parasequences and the forced regressive wedge systems tract: Deposition during base-level fall - reply. Sedimentary Geology, 95 (1-2), 147-160.

Immenhauser, A., Della Porta, G. & Kenter, J.A.M. (2003) An alternative model for positive shifts in shallow-marine

carbonate $\delta^{13}C$ and $\delta^{18}O$. Sedimentology, 50, 953-959.

Immenhauser, A., Hillgärtner, H. & Van Betum, E. (2005) Microbial-foraminiferal episodes in the Early Aptian of the southern Tethyan margin: ecological significance and possible relation to Oceanic Anoxic Event 1a. Sedimentology, 52, 77-99.

IPCC (2001) Third Assessment Report - Climate Change 2001. http://www.ipcc.ch/pub/online.htm

Jacobs, D.K. & Sahagian, D.L. (1993) Climate-induced fluctuations in sea level during non-glacial times. Nature, 361, 710–712.

Jacquin, T., Dardeau, G., Durlet, C., de Graciansky, P.-C. & Hantzpergue, P. (1998) The North Sea cycle: An overview of 2nd-order transgressive/regressive facies cycles in Western Europe. In: de Graciansky, P.-C., Hardenbol, J., Jacquin, T. &Vail, P. R. (eds) Mesozoic and Cenozoic sequence stratigraphy of European Basins. SEPM Spec. Publ., 60, 445-466.

Jan du Chêne, R., Busnardo, R., Charollais, J., Clavel, B., Deconinck, J.-F., Emmanuel, L., Gardin, S., Gorin, G., Manivit, H., Monteil, E., Raynaud, J.-F., Renard, M., Steffen, D., Steinhauser, N., Strasser, A., Strohmenger, C. & Vail, P.R. (1993) Sequence-stratigraphic interpretation of Upper Tithonian-Berriasian reference sections in South-est France: A multidisciplinary approach. Bull. Centre Rech. Explor.-Prod. Elf Aquitaine, 17, 151-183.

Jenkyns, H.C. (1996) Relative sea-level change and carbon isotopes data from the Upper Jurassic (Oxfordian) of central and southern Europe. Terra Nova, 8, 75–85.

Jenkyns, H.C., Jones, C.E., Gröcke, D.R., Hesselbo, S.P. & Parkinson, D.N. (2002) Chemostratigraphy of the Jurassic System: applications, limitations and implications for palaeoceanography. J. geol. Soc. London, 159, 351-378.

Jimenez de Cisneros, C. & Vera, J.A. (1993) Milankovitch cyclicity in Purbeck peritidal limestones of the Prebetic (Berriasian, southern Spain). Sedimentology, 40, 513-537.

Joachimski, M.M. (1991) Stable Isotope (C,O) und Geochemie der Purbeck-Mikrite in Abhängigkeit von Fazies und Diagenese (Berriasian/Schweizer und Französischer Jura, Südengland). Erlanger geologische Abhandlung, 119, 1-114.

Joachimski, M.M. (1994) Subaerial exposure and deposition of shallowing upward sequences: Evidence from stable isotopes of Purbeckian peritidal carbonates (basal Cretaceous), Swiss and French Jura Mountains. Sedimentology, 41, 805-824.

Jones, B. & Desrochers, A. (1992) Shallow platform carbonates. In: Walker, R.G. & James, N.P. (eds) Facies models, response to sea-level change. Geol. Assoc. Can., 277-301.

Jones, C.E., Jenkyns, H.C., Coe, A.L. & Hesselbo, S.P. (1994) Strontium isotopic variations in Jurassic and Cretaceous seawater. Geochim. Cosmochim. Acta, 58, 3061-3074.

Jorissen, F.J., de Stiger, H.C. & Widmark, J.G.V. (1995) A conceptual model explaining benthic foraminiferal microhabitats. Marine Micropaleontology, 19, 3-15.

Kendall, G.S.C. & Schlager, W. (1981) Carbonates and relative changes in sea level. Marine Geology 44, 181-212.

Keupp, H. (1991) Fossil calcareous dinoflagellate cysts. In: Riding, R. (ed) Calcareous algae and stromatolites, Springer. 267-286.

Keupp, H., Koch, R. & Leinfelder, R. (1990) Steuerungsprozesse der Entwicklung von Oberjura-Spongiolithen Süddeutschlands: Kenntnisstand, Probleme und Perspektiven. Facies, 23, 141-174.

Killian, W. (1889) Description géologique de la Montagne de Lure (Basses-Alpes). Masson, 458pp.

Kindler, P., Davaud, E. & Strasser, A. (1997) Tyrrhenian coastal deposits from Sardinia (Italy): A petrographic record of high sea levels and shifting climate belts during the last interglacial (isotopic substage 5e). Palaeogeogr., Palaeoclim., Palaeoecol., 133, 1-25.

Kolla, V., Posamentier, H.W. & Eichenseer, H. (1995) Stranded parasequences and the forced regressive wedge systems tract: Deposition during base-level fall - discussion. Sedimentary Geology, 95, 139-145.

Kübler, B. & Jaboyedoff, M. (2000) Illite crystallinity. Comptes rendus de l'Académie des sciences, Série 2, Sciences de la terre et des planètes, 331, 75-89.

Kübler, B. (1987) "Cristallinité" de l'illite et mixed-layers: brève révision. Schweiz. Mineral. Petrogr. Mitt., 70.

Kump, L.R. & Arthur, M.A. 1999. Interpreting carbon-isotope excursions: carbonates and organic matter. Chemical Geology, 161, 181-198.

Kuss, J. (1990) Middle Jurassic calcareous algae from the Circum-Arabian area. Facies, 22, 59-86.

Lamy, F., Hebbeln, D. & Wefer, G. (1998) Late Quarternary precessional cycles od terrigenous sediment input off the Norte Chico, Chile (275° S) and palaeoclimatic implications. Palaeogeogr., Palaeoclim., Palaeoecol., 141, 233-251.

Lehrmann, D.J. & Goldhammer, R.K. (1999) Secular variation in parasequence and facies stacking patterns of platform carbonates: A guide to application of stacking-pattern analysis in strata of diverse ages and settings. In: Harris, P.M., Saller, A.H. & Simo, J.A. (eds) Advances in carbonate sequence stratigraphy: Application to reservoirs, outcroups and models. SEPM Spec. Publ., 63,187-225.

Leinfelder, R.R. & Hartkopf-Fröder, C. (1990) In situ accretion mechanism of concavo-convex lacustrine oncoids ("swallow-nests") from the Oligocene of the Mainz Basin (Rhineland, West Germany). Sedimentology, 37, 287-301.

Leinfelder, R.R., Krautter, M., Laternser, R., Nose, M., Schmid, D.U., Schweigert, G., M., Werner, W., Keupp,

H., Brugger, H., Herrmann, R., Rehfeld-Kiefer, U., Schroeder, J.H., Reinhold, C., Koch, R., Zeiss, A., Schweizer, V., Christmann, H., Menges, G. & Luterbacher, H. (1994) The origin of Jurassic reefs: current research developments and results. Facies, 31, 1-56.

Leinfelder, R.R., Nose, M., Schmid, D.U. & Werner, W. (1993) Microbial crusts of the Late Jurassic: composition, palaeoecological significance and importance in reef construction. Facies, 29, 195-230.

Lohmann, K.C. (1988) Geochemical patterns of meteoric diagenetic systems and their application to studies of paleokarst. In: James N.P. & Philip W.C. (eds), Paleokarst, Springer. 58-80.

Lombard, A. (1945) Attribution de microfossiles du Jurassique supérieur alpin à des Chlorophycées (Proto- et Pleurococcales). Eclogae geol. Helv., 38, 163-173.

Lorin, S., Courville, P., Collin, P.-Y., Thierry, J., & Tort, A. (2004) Modalités de réinstallation d'une plate-forme carbonatée après une crise sédimentaire: exemple de la limite Oxfordien moyen-Oxfordien supérieur dans le Sud-Est du Basin de Paris. Bull. Soc. Géol. France, 175, 3, 289-302.

Louis-Schmid, B. (2006) Feedback mechanisms between carbon cycling, climate and oceanography. Diss., Naturwissenschaften, Eidgenössische Technische Hochschule ETH Zürich, Nr. 16824, 132pp.

Louis-Schmid, B., Rais, P., Bernasconi, S.M., Pellenard, P., Collin, P.-Y. & Weissert, H. (2007) Detailed record of the mid-Oxfordian (Late Jurassic) positive carbon-isotope excursion in two hemipelagic sections (France and Switzerland): A plate tectonic trigger? Palaeogeogr., Palaeoclimatol., Palaeoecol., 248(3), 459-472.

Loutit, T. S., Hardenbol, J., Vail, P. R., & Baum, G. R., (1988) Condensed sections: The key to age dating and correlation of continental margin sequences. In: Wilgus, C. K., et al. (eds), Sea-level changes: An integrated approach. SEPM Spec. Publ., 42, 183–213.

MacLeod, K.G. & Hoppe, K.A. (1992) Evidence that inoceramid bivalves were benthic and harbored chemosynthetic symbionts. Geology, 20, 2, 117-120.

Malchus, N. & Steuber, T. (2002) Stable isotope records (O, C) of Jurassic aragonitic shells from England and NW Poland: palaeoecologic and environmental implications. Géobios, 35, 29-39.

Mallinson, D., Flower, B., Hine, A., Brooks, G. & Garza, R. (2003) Paleoclimate implications of high latitude precession-scale mineralogic fluctuations during early Oligocene Antarctic glaciation: The Great Australian Bight record. Global and Planetary Change, 39, 257-269.

Marchand, D. & Menot, J.C. (1980) Ardennes et Lorraine in : Synthèse géologique du bassin de Paris. Publ. Mém. B.R.G.M., 101, 204-206.

Marshall, J.D. (1992) Climatic and oceanographic isotopic signals from the carbonate rock record and their preservation. Geol Mag, 129, 149–160

Martin, R.E. (1988) Benthic foraminiferal zonation in deep-water carbonate platform margin environments, northern Little Bahama Bank. Journal of Paleontology, 62, 1, 1-8.

Martin-Garin, B. (2005) Climatic control of oxfordian coral reef distribution in the Tethys Ocean, including a comparative survey of Recent coral communities (Indian Ocean) and a new method of coral morphometrics based on fractal dimension. Thèse sur publications, University of Bern and University of Nancy, 253pp.

Matthews, M.D. & Perlmutter, M.A. (1994) Global cyclostratigraphy: an application to the Eocene Green River Basin. In : Boer, de, P.L., Smith, D.G. (eds) Orbital forcing and cyclic sequences. IAS Spec. Publ., 19, 459-481.

Mattioli, E. (1997) Nannoplankton productivity and diagenesis in the rhytmically bedded Toarcian-Aalenian Fiuminata section (Umbria-Marche Apennine, central Italy). Palaeogeogr., Palaeoclimatol., Palaeoecol., 130, 113-133.

Meyer, R.K.F. & Schmidt-Kaler, H. (1989) Paläogeographischer Atlas des süddeutschen Oberjura (Malm). Geol. Jb., A/115, 3-77.

Meyer, R.K.F. & Schmidt-Kaler, H. (1990) Palaögeographie und Schwammriffentwicklung des süddeutschen Malm - ein Überblick. Facies, 23, 175-184.

Miall, A.D. (1986) Eustatic sea-level changes interpreted from seismic stratigraphy: A critique of the methology with particular reference to the North Sea Jurassic record. AAPG Bull., 70(2), 131-137.

Miall, A.D. (1991) Stratigraphic sequences and their chronostratigraphic correlation. J. Sed. Petrol., 61, 4, 497-505.

Miall, A.D. (1992) EXXON global cycle chart: an event for every occasion? Geology, 20, 787-790.

Miall, A.D. (1997) The geology of stratigraphic sequences. Springer, 421pp.

Miall, A.D. & Miall, C.E. (2001) Sequence stratigraphy as a scientific enterprise: The evolution and persistence of conflicting paradigms. Earth Sci. Rev., 54, 321-348.

Milankovitch, M. (1941) Kanon der Erdbestrahlung und seine Anwendung auf das Eiszeitenproblem. Akad. Royal Serbe Spec. Publ., 132, Sect. Math. Nat. Sci., 33, 633pp.

Milliman, J.D., Freile, D., Steinen, R.P. & Wilber, R.J. (1993) Great Bahama Bank aragonitic muds: mostly inorganically precipitated, mostly exported. J. Sed. Petrol., 63, 589–595.

Mitchell, S.F. (1996) Foraminiferal assemblages from the late Lower and Middle Cenomanian of Speeton (North Yorkshire, U.K.): relationships with sea-level fluctuations and watermass distribution. Journal of Micropaleontology, 15, 37-54.

Mitchum, R.M. & Van Wagoner, J.C. (1991) High-frequency

seqeunces and their stacking patterns: Sequence-stratigraphic evidence of high-frequency eustatic cycles. Sedimentary Geology, 70, 131-160.

Mohler, W. (1938) Mikropaläontologische Untersuchungen in der nordschweizerischen Juraformation. Abh. Schweiz. Pal. Ges., 60, 1-53.

Montañez, I.P. & Osleger, D.A. (1993) Parasequence stacking patterns, third-order accommodation events, and sequence stratigraphy of Middle to Upper Cambrian platform carbonates, Bonanza King Formation, southern Great Basin. In: Loucks, R.G. & Sarg, J.F. (eds) Carbonate Sequence Stratigraphy/Recent developments and applications. AAPG Mem., 57, 305-326.

Moore, G.T., Hayashida, D.N., Ross, C.A. & Jacobson, S.R. (1992) Paleoclimate of the Kimmeridgian/Tithonian (Late Jurassic) world: I. Results using a general circulation model. Palaeogeogr., Palaeoclim., Palaeoecol., 93, 113-150.

Mörner, N.-A. (1994) Internal response to orbital forcing and external cyclic sedimentary sequences. In: Boer, De, P.L. & Smith, D.G. (eds) Orbital forcing and cyclic sequences. IAS Spec. Publ., 19, 25-33.

Munnecke, A. & Samtleben, C. (1996) The formation of micritic limestones and the development of limestone-marl alternations in the Silurian of Gotland, Sweden. Facies, 34, 159-176.

Munnecke, A., Westphal, H., Reijmer, J.J.G. & Samtleben, C. (1997) Microspar development during early marine burial diagenesis: a comparison of Pliocene carbonates from the Bahamas with Silurian limestones from Gotland (Sweden). Sedimentology, 44, 977–990.

Murray, J.W. (1991) Ecology and palaeoecology of benthic foraminifera. Logman Scientific and Technical, UK/New York, 397pp.

Nummedal, D. & Swift, D.J.P. (1987) Transgressive stratigraphy at sequence-bounding unconformities: some principles derived from Holocene and Cretaceous examples. In: Nummedal, D., Pilkey, O.H. & Howard, J.D. (eds) Sea-level fluctuation and coastal evolution. SEPM Spec. Publ., 41, 241-260.

Nystuen, J.P. (1998) History and development of sequence stratigraphy. In: Gradstein, F.M., Sandvik, K.O. & Milton, N.J. (eds.), Sequence stratigraphy - concepts and applications, 8, Amsterdam, 31-116.

O'Dogherty, L., Sandoval, J. & Vera, J.A. (2000) Ammonite faunal turnover tracing sea-level changes during the Jurassic (Betic Cordillera, southern Spain). Journal of the Geological Society, London, 157, 723-736.

Olivier, N., Carpentier, C., Martin-Garin, B., Lathuilière, B., Gaillard, C., Ferry, S., Hantzpergue, P. & Geister, J. (2004a) Coral-microbialite reefs in pure carbonate versus mixed carbonate-silicliclastic depositional environments: the example of the Pagny-sur-Meuse section (Upper Jurassic, northeastern France). Facies, 50, 229-255.

Olivier, N., Pittet, B. & Mattioli, E. (2004b) Palaeoenvironmental control on sponge-microbialite reefs and contemporaneous deep-shelf marl-limestone deposition (Late Oxfordian, southern Germany). Palaeogeogr., Palaeoclimatol., Palaeoecol., 212, 181-197.

Osleger, D. (1991) Subtidal carbonate cycles: Implications for allocyclic vs. autocyclic controls. Geology, 19, 917-920.

Osleger, D.A. & Read, J.F. (1991) Relation of eustacy to stacking patterns of meter-scale carbonate cycles, Late Cambrian, U.S.A. J. Sed. Res., 61, 7, 1225-1252.

Padden, M., Weissert, H. & de Rafélis, M. (2001) Evidence for Late Jurassic release of methane from gas hydrate. Geology, 29, 223-226.

Parente, M., Frijia, G. & Di Lucia, M. (2007) Carbon-isotope stratigraphy of Cenomanian-Turonian platform carbonates from the southern Apennines (Italy): a chemostratigraphic approach to the problem of correlation between shallow-water and deep-water successions. Journal of the Geological Society, 164, 3, 609-620.

Parrish, J.T. (1992) Jurassic climate and oceanography of the Pacific region. In: Westermann, G.E.G. (ed), The Jurassic of the Circum-Pacific. Cambridge University Press, 365–379.

Parrish, J.T. (1993) Climate of the supercontinent Pangea. J. Geol., 101, 215-233.

Pasquier, J.-B. (1995) Sédimentologie, stratigraphie séquentielle et cyclostratigraphie de la marge nord-téthysienne au Berriasien en Suisse occidentale (Jura, Helvétique et Ultrahelvétique; comparaison avec les séries de bassin des domaines Vocontien et Subbrianconnais). PhD thesis, University of Fribourg, Switzerland, 274pp.

Pasquier, J.-B. & Strasser, A. (1997) Platform-to-basin correlation by high-resolution sequence stratigraphy and cyclostratigraphy (Berriasian, Switzerland and France). Sedimentology, 44, 1071-1092.

Patterson, W.P. & Walter, L.M. (1994) Depletion of ^{13}C in seawater ΣCO_2 on modern carbonate platforms: significance for the carbon isotopic record of carbonates. Geology, 22, 885-888.

Pawellek, T. & Aigner, T. (2003) Stratigraphic architecture and gamma ray logs of deeper ramp carbonates (Upper Jurassic, SW Germany). Sedimentary Geology, 159, 203-240.

Pearce, C.R., Hesselbo, S.P. & Coe, A.L. (2005) The mid-Oxfordian (Late Jurassic) positive carbon-isotope excursion recognised from fossil wood in the British Isles. Palaeogeogr., Palaeoclimatol., Palaeoecol., 221, 343-357.

Pellaton, C. & Ullrich, S. (1997) Etude multidisciplinaire du Jurassique supérieur de la région de Castellane (SE France). Unpubl. Diploma Thesis, University of Geneva, 190pp.

Pellenard, P., Deconinck, J.-F., Huff, W.D., Thierry, J.,

Marchand, D., Fortwengler, D. & Trouillier, A. (2003) Characterization and correlation of Upper Jurassic (Oxfordian) bentonite deposits in the Paris Basin and the Subalpine Basin, France. Sedimentology, 50, 1035-1060.

Pemberton, S.G., Maceachern, J.A. & Frey, R.W. (1992) Trace fossils facies models: Environmental and allostratigraphic significance. In: Walker, R.G. & James, N.P. (eds), Facies Models, Response to Sea Level Change. Geol. Assoc. Can., 47-72.

Perlmutter, M.A. & Matthews, M.D. (1989) Global cyclostratigraphy - a model. In: Cross, T.A. (ed) Quantitative Dynamic Stratigraphy. Prentice-Hall, 233-260.

Perlmutter, M.A. & Matthews, M.D. (1992) Global cyclostratigraphy. Encyclopedia of Earth System Science, 2, 379-393.

Persoz, F. & Remane, J. (1976) Minéralogie et géochimie des formations à la limite Jurassique-Crétacé dans le Jura et le Basin vocontien. Eclogae geol. Helv., 69 (1), 1-38.

Peryt, T.M. (1981) Phanerozoic oncoids – an overview. Facies, 4, 197-214.

Peryt, T.M. (1983) Oncoids: a comment to recent developments. In: Peryt, T.M. (ed.) Coated Grains. Springer Verlag, Berlin, 273-275.

Pittet, B. (1994) Modèle d'estimation de la subsidence et des variations du niveau marin: un exemple de l'Oxfordien du Jura suisse. Eclogae geol. Helv., 87, 513-543.

Pittet, B. (1996) Contrôles climatiques, eustatiques et tectoniques sur des systèmes mixtes carbonates-siliciclastiques de plateforme: exemples de l'Oxfordien (Jura suisse, Normandie, Espagne). PhD thesis, University of Fribourg, Switzerland, 258pp.

Pittet, B. & Gorin, G. (1997) Distribution of sedimentary organic matter in a mixed carbonate-siliciclastic platform environment: Oxfordian of the Swiss Jura Mountains. Sedimentology, 44, 5, 915-937.

Pittet, B. & Mattioli, E. (2002) The carbonate signal and calcareous nannofossil distribution in an Upper Jurassic section (Balingen-Tieringen, Late Oxfordian, southern Germany). Palaeogeogr., Palaeoclim., Palaeoecol., 179, 71-96.

Pittet, B. & Strasser, A. (1998a) Depositional sequences in deep-shelf environments formed through carbonate-mud import from the shallow platform (Late Oxfordian, German Swabian Alps and eastern Swiss Jura). Eclogae geol. Helv., 91, 149-169.

Pittet, B. & Strasser, A. (1998b) Long-distance correlations by sequence stratigraphy and cyclostratigraphy: Examples and implications (Oxfordian from the Swiss Jura, Spain, and Normandy). Geol. Rundsch., 86, 852-874.

Pittet, B., Strasser, A. & Mattioli, E. (2000) Depositional sequences in deep-shelf environments: A response to sea-level changes and shallow-platform carbonate productivity (Oxfordian, Germany and Spain). J. Sed. Res., 70, 2, 392-407.

Plunkett, J.M. (1997) Early diagenesis of shallow platform carbonates in the Oxfordian of the Swiss Jura Mountains. PhD Thesis, University of Fribourg, Switzerland. 155pp.

Podlaha, O.G., Mutterlose, J. & Veizer, J. (1998) Preservation of $\delta^{18}O$ and $\delta^{13}C$ in belemnite rostra from the Jutassic/Early Cretaceous successions. Amer. J. Sci., 298, 324-347.

Pop, G. & Bucur, I.I. (2001) Upper Jurassic and Lower Cretaceous sedimentary formations from the Vâlcan Mountains (South Carpathians). Studia Universitatis Babes-Bolyai, Geologia, XLVI, 2, 77-94.

Posamentier, H.W. & James, D.P. (1993) An overview of sequence-stratigraphic concepts: Uses and abuses. In: Posamentier, H. W., Summerhayes, C. P., Haq, B. U. & Allen, G. P. (eds) IAS Spec. Publ., 18, 3-18.

Posamentier, H.W., Allen, G.P., James, D.P. & Tesson, M. (1992) Forced regressions in a sequence stratigraphic framework: concepts, examples and exploration significance. AAPG Bull., 76, 1687-1709.

Posamentier, H.W., Jervey, M.T. & Vail, P.R. (1988) Eustatic controls on clastic deposition I - conceptual framework. In: Wilgus, C.E., Hastings, B.S., Kendall, C.G.S.C., Posamentier, H.W., Ross, C.A. & Van Wagoner, J.C. (eds) Sea-level changes - an integrated approach. SEPM Spec. Publ., 42, 109-124.

Poulsen, N.E. & Riding, J.B. (2003) The Jurassic dinoflagellate cyst zonation of Subboreal Northwest Europe. In: Ineson, J.R. & Surlyk, F. (Eds) The Jurassic of Denmark and Greenland, Geol. Survey Denmark Greenland Bull., 1, 115-144.

Pratt, B.R. & James, N.P. (1986) The St George Group (Lower Ordovician) of western Newfoundland: Tidal flat island model for carbonate sedimentation in shallow epeiric seas. Sedimentology, 33, 313-343.

Pratt, B.R., James, N.P. & Covan, C.A. (1992) Peritidal carbonates. In: Walker, R.G. & James, N.P. (eds) Facies models: a response to sea-level change, Geol. Assoc. Can., 303-322.

Price, G.D. (1999) The evidence and implications of polar ice during the Mesozoic. Earth Sci. Rev., 48, 183-210.

Pümpin, V.F. (1965) Riffsedimentologische Untersuchungen im Rauracien von St Ursanne und Umgebung (Zentraler Schweizer Jura). Eclogae geol. HeIv., 58, 799-876.

Quenstedt, F.A. (1843) Das Flözgebirge Würtembergs. Mit besonderer Rücksicht auf den Jura. Laupp, Tübingen, 558pp.

Quenstedt, F.A. (1856) Der Jura Laupp Tübingen, 842pp, Atlas, 100 pls.

Radoicic, R. (1959) Some problematic microfossils from the Dinarian Cretaceous. Bull. Serv. Geol. Geophys. R.P. Serbie, 17, 87-92.

Rafélis Saint-Sauveur, de, M. (1996) Géochimie des

carbonates pélagiques et stratigraphie séquentielle : le contrôle des séquences de troisième ordre au cours du Jurassique supérieur (exemple du Domaine Vocontien). DEA, Univ. Pierre & Marie Curie – Paris VI, 30pp.

Rais, P., Louis, B., Bernasconi, S. & Weissert, H. (2005) Evidence for changes in intermediate-water currents in the Alpine Tethys during the Late Jurassic. EGU05, Geophysical Research Abstracts 7, 06583.

Rameil, N. (2005) Carbonate sedimentology, sequence stratigraphy, and cyclostratigraphy of the Tithonian in the Swiss and French Jura mountains: a high-resolution record in sea-level and climate. GeoFocus, 13, 246pp.

Rameil, N., Götz, A.E. & Feist-Burkhardt, S. (2000) High-resolution sequence interpretation of epeiric shelf carbonates by means of palynofacies analysis: An example from the Germanic Triassic (Lower Muschelkalk, Anisian) of East Thuringia, Germany. Facies, 43, 123-144.

Rankey, E.C. (2002) Spatial patterns of sediment accumulation on a Holocene carbonate tidal flat, Northwest Andros Island, Bahamas. J. Sed. Res., 72, 591-601.

Rasser, M.W. & Fenninger, A. (2002) Paleoenvironmental and diagenetic implications of $\delta^{18}O$ and $\delta^{13}C$ isotope ratios from the Upper Jurassic Plassen limestone (Northern Clacareous Alps, Austria). Géobios, 35, 41-49.

Read, J.F. (1995) Overview of carbonate platform sequences, cycle stratigraphy and reservoirs in greenhouse and icehouse worlds. In: Read, J.F., Kerans, C., Weber, L.J., Sarg, J.F., & Wright F.W., Milankovitch sea level changes, cycles and reservoirs on carbonate platforms in greenhouse and icehouse worlds. SEPM Short Course Notes No. 35, 1-102.

Reboulet, S. & Atrops, F. (1997) Quantitative variations of the valanginian ammonite fauna of the Vocontian Basin (southeastern France) between limestones-marls and within parasequence sets. Palaeogeogr., Palaeoclimatol., Palaeoecol, 135, 145-155.

Rees, P.M., Noto, C.R., Parrish, J.M. & Parrish, J.T. (2004) Late Jurassic climates, vegetation, and dinosaur distributions. The Journal of Geology, 112, 643-653.

Reineck, H.E. & Singh, I.B. (1975) Depositional Sedimentary Environments. Springer-Verlag, Berlin, 439pp.

Retallack, G.J. (2001) A 300 million year record of atmospheric carbon dioxide from fossil plant cuticles. Nature, 411, 287-290.

Rex, R.W & Martin, B.D. (1966) Clay mineral formation in sea water by submarine weathering of K-feldspar. Clays and Clay Minerals, 14(1), 235-240. DOI: 10.1346/CCMN.1966.0140120

Riegl, B. & Piller, W. E. (1999) Coral framework revisited – reefs and coral carpets in the northern Red Sea. Coral Reefs, 18, 241-253.

Robert, C. & Kennett, J.P. (1994) Antarctic subtropical humid episode at the Paleocene-Eocene boundary: clay mineral evidence. Geology 22, 211-214.

Rosales, I., Queseda, S. & Robles, S. (2001) Primary and diagenetic isotopic signals in fossils and hemipelagic carbonates: the Lower Jurassic of northern Spain. Sedimentology, 48, 1149-1169.

Ruf, M., Link, E., Pross, J. & Aigner, T. (2005) Integrated sequence stratigraphy: Facies, stable isotope and palynofacies analysis in a deeper epicontinental carbonate ramp (Late Jurassic, SW Germany). Sedimentary Geology, 175, 391-414.

Ruffell, A.H. & Batten, D.J. (1990) The Barremian–Aptian arid phase in Western Europe. Palaeogeogr., Palaeoclimatol., Palaeoecol., 80, 197–212.

Ruffell, A.H., Price, G.D., Mutterlose, J., Kessels, K., Baraboshkin, E. & Gröcke, D.R. (2002) Palaeoclimate indicators (clay minerals, calcareous nannofossils, stable isotopes) compared from two successions in the Late Jurassic of the Volga Basin (SE Russia). Geol. J., 37, 17-33.

Ruffell, A.H. & Rawson, P.F. (1994) Palaeoclimate controls on sequence stratigraphic patterns on the Late Jurassic to Mid-Cretaceous, with a case study from Eastern England. Palaeogeogr., Palaeoclim., Palaeoecol., 110, 43-54.

Samankassou, E., Strasser, A., Di Gioia, E., Rauber, G. & Dupraz, C. (2003) High-resolution record of lateral facies variations on a shallow carbonate platform (Upper Oxfordian, Swiss Jura Mountains). Eclogae geol. Helv., 96, 425-440.

Samankassou, E., Tresch, J. & Strasser, A. (2005) Origin of peloids in Early Cretaceous deposits, Dorset, South England. Facies, 51, 275-284.

Sandulli, R. & Raspini, A. (2004) Regional to global correlation of lower Cretaceous (Hauterivian-Barremian) shallow-water carbonates of the southern Apennines (Italy) and Dinarides (Montenegro), southern Tethyan Margin. Sedimentary Geology, 165, 1-2, 117-153.

Sasaran, E., Hosu, A., Spalnacan, R. & Bucur, I.I. (1999) Microfacies, microfossils and sedimentary evolution of the Sandulesti Limestone Formation in Cheile Turzii (Apuseni Mountains, Romania). Acta Paleontologica Romaniae, 2, 453-462.

Satterley, A.K. (1996) The interpretation of cyclic successions of the Middle and Upper Triassic of the Northern and Southern Alps. Earth Sci. Rev., 40, 181-207.

Schlager, W. (1989) Drowning unconformities on carbonate platforms. In: Crevello, P.D. et al. (eds), Controls on carbonate platform and basin development. SEPM Spec. Publ., 44, 15-25.

Schlager, W. (1991) Depositional bias and environmental change - important factors in sequence stratigraphy. Sedimentary Geology, 70, 109-130.

Schlager, W. (1993) Accommodation and supply - a dual control on stratigraphic sequences. Sedimentary Geology,

86, 111-136.

Schlager, W. (2005) Carbonate sedimentology and sequence stratigraphy. SEPM concepts in sedimentology and paleontology, 8, 200pp.

Schlager, W., Reijmer, J.J.G. & Droxler, A. (1994) Highstand shedding of carbonate platforms. J. Sed. Res., B64, 3, 270-281.

Schlagintweit, F. & Ebli, O. (1999) New results on microfacies, biostratigraphy and sedimentology of Late Jurassic-Early Cretaceous platform carbonates of the Northern Calcareous Alps, Part I: Tressenstein Limestone, Plassen Formation. Abh. Geol. B.-A., 56, 379-418.

Schlagintweit, F., Gawlick, H.-J. & Lein, R. (2005) Micropaleontology and biostratigraphy of the Plassen carbonate platform of the type locality (Upper Jurassic to Lower Cretaceous, Salzkammergut, Austria). Journal of Alpine Geology, 47, 11-102.

Schmid, D.U. (1996) Marine Mikrobolithe und Mikroinkrustierer aus dem Oberjura. Profil, 9, 101-251.

Schmid, D.U. & Leinfelder, R.R. (1996) The Jurassic Lithocodium aggregatum-Troglotella incrustans foraminiferal consortium. Palaeontology, 39, 1, 21-52.

Scholle, P.A. & Arthur, M.A. (1980) Carbon isotope fluctuations in Cretaceous pelagic limestones: potential stratigraphic and petroleum exploration tool. Am. Assoc. Petrol. Geol. Bull., 64, 1, 67-87.

Schulz, M. & Schäfer-Neth, C. (1998) Translating Milankovitch climate forcing into eustatic fluctuations via thermal deep water expansion: a conceptual link. Terra Nova, 9, 228–231.

Schwarzacher, W. (2000) Repetitions and cycles in stratigaphy. Earth Sci. Rev., 50, 51-75.

Schweigert, G. (1995a) Amoebopeltoceras n.g., eine neue Ammonitengattung aus dem Oberjura (Ober-Oxfordium bis Unter-Kimmeridgium) von Sqdwestdeutschland und Spanien. Stuttg. Beitr. Naturkd., B, 227, 1–12.

Schweigert, G. (1995b) Zum Auftreten der Ammonitenarten Amoeboceras bauhini (Oppel) und Amoeboceras schulginae Mesetzhnikov im Oberjura der Schwäbischen Alb. Jahresh. Ges. Naturkd. Württemb., 151, 171-184.

Schweigert, G. & Callomon, J.H. (1997) Der bauhini-Faunenhorizont und seine Bedeutung für die Korrelation zwischen tethyalem und subborealem Oberjura. Stuttg. Beitr. Naturkd., B, 247, 1-69.

Sellwood, B.W. & Price, G.D. (1993) Sedimentary facies as indicators of Mesozoic palaeoclimate. Philosophical Transactions: Biological Sciences, 341, 1297, 225-233.

Sellwood, B.W., Valdes, P.J. & Price, G.D. (2000) Geological evaluation of multiple general circulation model simulations of Late Jurassic palaeoclimate. Palaeogeogr., Palaeoclim., Palaeoecol., 156, 147-160.

Septfontaine, M. (1981) Les foraminifères imperforés des milieux de plate-forme au Mésozoïque: Détermination pratique, interprétation phylogénétique et utilisation biostratigraphique. Revue de Micropaléontologie, 23, 3-4, 169-203.

Serban, D., Bucur, I.I. & Sasaran, E. (2004) Micropaleontological assemblages and microfacies characteristics of the Upper Jurassic limestones from Căprioara-Pojoga (Mureş Trough). In: Codrea, V.A., Petrescu, I. & Dica, E.P. (eds), Acta Paleontologica Romaniae, Bukarest, 4, 475-484.

Shinn, E.A. & Robbin, D.M. (1983) Mechanical and chemical compaction in fine-grained shallow-water limestones. J. Sed. Res., 53, 2, 595-618.

Shiraishi, F. & Kano, A. (2004) Composition and spatial distribution of microencrusters and microbial crusts in upper Jurassic-lowermost Cretaceous reef limestone (Torinosu Limestone, southwest Japan). Facies, 50, 217-227.

Singer, A. (1980) The paleoclimatic interpretation of clay minerals in soils and weathering profiles. Earth Sci. Rev., 15, 303–326.

Singer, A. (1984) The paleoclimatic interpretation of clay minerals in sediments - a review. Earth Sci. Rev., 21, 251-293.

Sladen, C.P. (1983) Trends in Early Cretaceous clay mineralogy in Europe. Zitteliana, 10, 349–357.

Smith, D.G. (1989) Milankovitch cyclicity and the stratigraphic record - a review. Terra Nova, 1, 402-404.

Smith, F.D. (1955) Planktonic foraminifera as indicators of depositional environment. Micropal., 1, 2, 147-151.

Steinmann, G. (1880) Die Mumien des Hauptrogensteins. N. Jb. Min. Geol. Paläont., 1, 151-154.

Strasser, A. (1984) Black-pebble occurence and genesis in Holocene carbonate sediments (Florida Keys, Bahamas, and Tunisia). J. Sed. Petrol., 54, 4, 1097-1109.

Strasser, A. (1986) Ooids in Purbeck limestones (lowermost Cretaceous) of the Swiss and French Jura. Sedimentology, 33, 711-727.

Strasser, A. (1988) Shallowing-upward sequences in Purbeckian peritidal carbonates (lowermost Cretaceous, Swiss and French Jura Mountains). Sedimentology, 35, 369-383.

Strasser, A. (1991) Lagoonal-peritidal sequences in carbonate environments: Autocyclic and allocyclic processes. In: Einsele, G., Ricken, W. & Seilacher, A. (eds) Cycles and events in stratigraphy. Springer, 709-721.

Strasser, A. (1994) Milankovitch cyclicity and high-resolution sequence stratigraphy in lagoonal-peritidal carbonates (Upper Tithonian-Lower Berriasian, French Jura Mountains). In: de Boer, P. L. & Smith, D. G. Orbital forcing and cyclic sequences. IAS Spec. Publ., 19, 285-301.

Strasser, A. (2007) Astronomical time scale for the Swiss and French Jura Mountains (Middle Oxfordian to Late Kimmeridgian) Eclog. geol. Helv. (in press).

Strasser, A., Aurell, M., Badenas, B., Melendez, G. & Tomas, S. (2005) From platform to basin to swell: orbital control on sedimentary sequences in the Oxfordian, Spain. Terra Nova, 17, 407-413.

Strasser, A., Hilgen, F. & Heckel, P.H. (2006) Cyclostratigraphy – concepts, definitions, and applications. Newsletters on Stratigraphy, 42, 75-114.

Strasser, A. & Hillgärtner, H. (1998) High-frequency sea-level fluctuations recorded on a shallow carbonate platform (Berriasian and Lower Valanginian of Mount Salève, French Jura). Eclogae geol. Helv., 91, 375-390.

Strasser, A., Hillgärtner, H., Hug, W. & Pittet, B. (2000) Third-order depositional sequences reflecting Milankovitch cyclicity. Terra Nova, 12, 303-311.

Strasser, A., Hillgärtner, H. & Pasquier, J.-B. (2004) Cyclostratigraphic timing of sedimentary processes: An example from the Berriasian of the Swiss and French Jura Mountains. In: D'Argenio, B., Fischer, A.G., Premoli Silva, I., Weissert, H. & Ferreri, V. (eds) Cyclostratigraphy: Approaches and case histories. SEPM Spec. Publ., 81, 135-151.

Strasser, A., Pittet, B., Hillgärtner, H. & Pasquier, J.B. (1999) Depositional sequences in shallow carbonate-dominated sedimentary systems: concepts for a high-resolution analysis. Sedimentary Geology, 128, 201-221.

Strasser, A. & Samankassou, E. (2003) Carbonate sedimentation rates today and in the past: Holocene of Florida Bay, Bahamas, and Bermuda vs. Upper Jurassic and Lower Cretaceous of the Jura Mountains (Switzerland and France). Geologia Croatica, 56, 1, 1-18.

Strasser, A. & Védrine, S. Controls on facies mosaics of carbonate platforms: a case of study from the Oxfordian of the Swiss Jura. IAS Spec. Publ. (in press)

Strohmenger, C. & Strasser, A. (1993) Eustatic controls on the depositional evolution of Upper Tithonian and Berriasian deep-water carbonates (Vocontian Trough, SE France). Bull. Centre Rech. Explor.-Prod. Elf Aquitaine, 17(1), 183-203.

Surlyk, F. (1991) Sequence stratigraphy of the Jurassic-Lowermost Cretaceous of East Greenland. AAGP Bull., 75, 9, 1468-1488.

Swift, D.J.P. (1968) Coastal erosion and transgressive stratigraphy. J. Geol., 76, 444-456.

Tasli, K. (1993) Micropaléontologie, stratigraphie et environnement de depot des séries jurassiques à facies de plate-forme de la region de Kale-Gümüshane (Pontides Orientales, Turquie). Revue de Micropaléontologie, 36, 1, 44-65.

Thierry, J. et al. (41 co-authors) (2000) Map 10, Early Kimmeridgian. In: Dercourt J., Gaetani M. et al. (eds) Atlas Peri-Tethys, Palaeogeographical Maps. CCGM/CGMW, Paris.

Thiry, M. (1982) Les kaolinites des argiles de Provins: géologie et cristallinité. Bull. Minéral., 105, 521-526.

Thiry, M. (2000) Palaeoclimatic interpretation of clay minerals in marine deposits: an outlook from the continental origin. Earth Sci. Rev., 49, 201-221.

Thorne, J.A. & Swift, D.J.P. (1991a) Sedimentation on continental margins, II. Application of the regime concept. In: Swift, D.J.P. et al. (eds) Shelf sand and sandstone bodies. IAS Spec. Publ., 14, 33-58.

Thorne, J.A. & Swift, D.J.P. (1991b) Sedimentation on continental margins, VI. A regime model for depositional sequences, their component systems tracts, and bounding surfaces. In: Swift, D.J.P. et al. (eds) Shelf sand and sandstone bodies. IAS Spec. Publ., 14, 189-255.

Tomašových, A. (2004) Microfacies and depositional environment of an Upper Triassic intra-platform carbonate basin: the Fatric Unit of the West Carpathians (Slovakia). Facies, 50, 77-105.

Tresch, J. (2007) History of a Middle Berriasian transgression (France, Switzerland, and southern England). GeoFocus, 16, 271pp.

Trümpy, R. (1980) Geology of Switzerland - A guidebook. Part A: An outline of the geology of Switzerland. 104pp.

Tucker, M.E. (1993) Carbonate diagenesis and sequence stratigraphy. In: Wright, V.P. (ed) Sedimentology Review 1, 51-72.

Tucker, M.E. & Bathurst, R.G.C. (eds) (1990) Carbonate Diagenesis. Int. Assoc. Sediment. Reprint Series, 1, Blackwell Scientific, Oxford, 312pp.

Tucker, M.E. & Wright, V.P. (1990) Carbonate Sedimentology. Blackwell, 482pp.

Vail, P.R. (1987) Seismic stratigraphy interpretation using sequence stratigraphy; Part 1, Seismic stratigraphy interpretation procedure. In: Bally, A.W. (ed) Atlas of seismic stratigraphy. AAPG Studies in Geology, 27, 1, 1-10.

Vail, P.R., Audemard, F., Bowman, S.A., Eisner, P.N. & Perez-Cruz, C. (1991) The stratigraphic signatures of tectonics, eustacy and sedimentology - an overview. In: Einsele, G., Ricken, W. & Seilacher, A. (eds) Cycles and events in stratigraphy. Springer, 617-659.

Vail, P.R., Mitchum, R.M. & Thompson, D.B. (1977) Seismic stratigraphy and global changes of sea level, part 3: Relative changes of sea level from coastal onlap. In: Payton, C.E. (ed) Seismic stratigraphy - applications to hydrocarbon exploration. AAPG Mem., 26, 63-81.

Vakhrameev, V.A. (1981) Pollen Classopollis, indicator of Jurassic and Cretaceous climates. Palaeobotanist, 28, 301-307.

Vakhrameev, V.A. (1991) Jurassic and Cretaceous floras and c1imates of the Earth. Cambridge University Press, 318pp.

van Aarssen, B.G., Alexander, R. & Kagi, R.I. (2000) Palaeovegetation changes during Jurassic times. as

determined from higher plant-derived biomarkers. In: Skilbeck, C.G. & Hubble, T.C.T. (eds) Understanding Planet Earth; searching for a sustainable future; abstracts of the 15th Australian geological convention. Geological Society of Australia, 59, 505.

van der Zwaan, G.J., Duijnstee, I.A.P., den Dulk, M., Ernst, S.R., Jannink, N.T., & Kouwenhoven, T.J. (1999) Benthic foraminifers: Proxies or problems? A review of paleoecological concepts. Earth Sci. Rev., 46, 213–236.

Van Houten, F.B. & Purucker, M.E. (1984) Glauconitic peloids and chamositic ooids – favourable factors, constraints, and problems. Earth Sci. Rev., 20, 211-243.

Van Wagoner, J.C., Mitchum, R.M., Campion, K.M. & Rahamanian, V.D. (1990) Siliciclastic sequence stratigraphy in well logs, cores, and outcrops. AAPG Methods in Exploration, 7, 55pp.

Védrine, S. (2005) Reconstruction of high-frequency sea-level fluctuations of a transgressive interval on shallow carbonate platform (Late Oxfordian, Switzerland and France). 10ème Congrès Français de Sédimentologie - Livre des résumés, Publ. ASF, Paris, 51, 301.

Védrine, S. (2008) Co-occurrence of the foraminifer *Mohlerina basiliensis* with *Bacinella-Lithocodium* oncoids: palaeoenvironmental and palaeoecological implications (Late Oxfordian, Swiss Jura) (accepted in Journal of Micropalaeontology).

Védrine, S. & Spezzaferri, S. (2007) *Mohlerina basiliensis* (benthic foraminifer) and *Bacinella-Lithocodium* oncoids: palaeoenvironmental and palaeoecological implications (Late Oxfordian, Swiss Jura). EGU07, Geophysical Research Abstracts 9, 02957.

Védrine, S. & Strasser, A. (2005) High-frequency palaeoenvironmental and sea-level changes on the Jura and Lorraine shallow carbonate platforms (Late Oxforidan, Switzerland and France). 10ème Congrès Français de Sédimentologie - Livre des résumés, Publ. ASF, Paris, 51, 302.

Védrine, S., Strasser, A. & Hug, W. (2007) Oncoid growth and distribution controlled by sea level and climate. Facies, DOI 10.1007/s10347-007-0114-4.

Veizer, J., Ala, D., Azmy, K., Bruckschen, P., Buhl, D., Bruhn, F., Carden, G.A.F., Diener, A., Ebneth, S., Godderis, Y., Jasper, T., Korte, C., Pawellek, F., Podlaha, O.G. & Strauss, H. (1999) $^{87}Sr/^{86}Sr$, $\delta^{13}C$ and $\delta^{18}O$ evolution of Phanerozoic seawater. Chemical Geology, 161, 59-88.

Velde, B.C. (1995) Compaction and diagenesis. In: Velde, B.C. (ed) Origin and mineralogy of clays – Clays and the environment. Springer, 220-246.

Velić, I., Tišljar, J., Vlahović, I., Velić, J., Koch, G. & Matičec, D. (2002) Palaeogeographic variability and depositional environments of the Upper Jurassic carbonate rocks of Velica Kapela Mt. (Gorski Kotar Area, Adriatic carbonate platform, Croatia). Geologica Croatica, 55, 2, 121-138.

Videtich, P.E. & Mattews, R.K. (1980) Origin of discontinuity surfaces in limestones: isotopic and petrographic data, Pleistocene of Barbados, West Indies. J. Sed. Petrol., 50, 3, 971-980.

Vincent, B. 2001. Sédimentologie et géochimie de la diagenèse des carbonates. Application au Malm de la bordure Est du Bassin de Paris. PhD Thesis, Université de Dijon, 308pp.

Vincent, B., Emmanuel, L. & Loreau J.P. (2004) Signification du signal isotopique ($\delta^{18}O$, $\delta^{13}C$) des carbonates néritiques: composante diagénétique et composante originelle (Jurassique supérieur de l'Est du Bassin de Paris, France). CR Géosciences 336, 29-39.

Vincent, B., Rambeau, C., Emmanuel, L. & Loreau, J.P. (2006) Sedimentology and trace element geochemistry of shallow-marine carbonates: an approach to paleoenvironmental analysis along the Pagny-sur-Meuse Section (Upper Jurassic, France). Facies, 52(1), 69-84

Wagenplast, P., (1972) Ökologische untersuchung der fauna aus bank-und schwammfazies des weiβen Jura der Schwäbischen alb. Arb. Inst. Geol. Palöntol., 67, 1-99.

Walker, R.G. (1995) Sedimentary and tectonic origin of a transgressive surface of erosion: Viking Formation, Alberta, Canada. J. Sed. Res., B65, 2, 209-221.

Waterhouse, H.K. (1999) Orbital forcing of palynofacies in the Jurassic of France and the United Kingdom. Geology, 27, 6, 511-514.

Weaver, C.E. (1989) Clays, muds and shales. Elsevier, 819pp.

Weedon, G.P., Jenkyns, H.C., Coe, A.L. & Hesselbo, S.P. (1999) Astronomical calibration of the Jurassic time-scale from cyclostratigraphy in British mudrock formations. Phil. Trans. R. Soc. London., A 357, 1787-1813.

Weissert, H. & Erba, E. (2004) Volcanism, CO2 and palaeoclimate: a Late Jurassic-Early Cretaceous carbon and oxygen isotope record. Journal of the Geological Society, London, 161, 695-702.

Weissert, H. & Mohr, H. (1996) Late Jurassic climate and its impact on carbon cycling. Palaeogeogr., Palaeoclim., Palaeoecol., 122, 27-43.

Wernli, R. & Fookes, E. (1992) Troglotella incrustans n. gen., n. sp., un étrange et nouveau foraminifère calcicavicole du complexe récifal kimméridgien de Saint-Germain-de-Joux (Ain, France). Boll. Soc. Paleont. Ital., 31, 95-103.

Westphal, H., Böhm, F. & Bornholdt, S. (2004a) Orbital frequencies in the carbonate sedimentary record: Distorted by diagenesis? Facies, 50, 1, 3-11.

Westphal, H., Munnecke, A., Pross, J. & Herrle, J.O. (2004b) Multiproxy approach to understanding the origin of Cretaceous pelagic limestone-marl alternations (DSDP site 391, Blake-Bahama Basin). Sedimentology, 51, 1, 109-126.

Wetzel, A. & Allia, V. (2000) The significance of hiatus beds in shallow-water mudstones: an example from the Middle

Jurassic of Switzerland. J. Sed. Res., 70, 170-180.

Wetzel, A. (1991) Ecologic interpretation of deep-sea trace fossil communities. Palaeogeogr., Palaeoclimatol., Palaeoecol., 85, 47-69.

Wetzel, A., Allenbach, R. & Allia, V. (2003) Reactivated basement structures affecting the sedimentary facies in a tectonically ''quiescent'' epicontinental basin: an example from NW Switzerland. Sed. Geol. 157, 153-172.

Wierzbowski, H., (2002) Detailed oxygen and carbon isotope stratigraphy of the Oxfordian in Central Poland. International Journal of Earth Sciences (Geologische Rundschau), 91, 304–314.

Wignall, P.B. & Ruffell, A.H. (1990) The influence of a sudden climatic change on marine deposition in the Kimmeridgian of northwest Europe. J. Geol. Soc. London, 147, 365-371.

Wignall, P.B. (1993) The stratigraphy of the Upper Kimmeridge Clay (Late Jurassic) of Golden Hill, Vale of Pickering, North Yorkshire. Proceedings of the Yorkshire Geological Society, 49, 207-214.

Wing, S.L. & Boucher, L.D. (1998) Ecological aspects of the Cretaceous flowering plant radiation. Annu. Rev. Earth Planet. Sci., 26, 379–421.

Wright, V.P. & Burgess, P.M. (2005) The carbonate factory continuum, facies mosaics and microfacies: An appraisal of some of the key concepts unterpinning carbonate sedimentology. Facies, 51, 17-23.

Wright, V.P. (1994) Paleosols in shallow marine carbonate sequences. Earth Sci. Rev., 35, 367-395.

Zamarreno, I., Anadon, P. & Utrilla, R. (1997) Sedimentology and isotopic composition of Upper Palaeocene to Eocene non-marine stromatolites, eastern Ebro Basin, NE Spain. Sedimentology, 44,159-176.

Ziegler, M.A. (1962) Beiträge zur Kenntnis des unteren Malm im zentralen Schweizer Jura. Unpubl. PhD thesis, University of Zürich, 51pp.

Ziegler, P.A. (1988) Evolution of the Arctic-North Atlantic and the western Tethys. AAPG Mem., 43, 198pp.

Ziegler, P.A. (1990) Geological atlas of Western and Central Europe. – Shell Internationale Petroleum Maatshappij B.V., The Hague, 233pp.

* * *

PLATES

PLATE 1 – MACROSCOPIC SAMPLES

1 – Bioturbated oncoid-rich packstone/wackestone. Voyeboeuf section, Vy-8A.

2 – Clusters of serpulids (arrow). Savagnières section, Sa-22A.

3 – Ferrugineous ooid wackestone. Vorbourg section, Vo-32A.

4 – Type 3 oncoid floatstone. Vorbourg section, Vo-24A.

5 – Nodule of limestone rich in ferrugineous type 2 oncoids. Vorbourg section, Vo-K.

6 – Irregular type 2 oncoids dispersed in marly deposits. Top of Vorbourg section, Vo-34.


1
1 cm

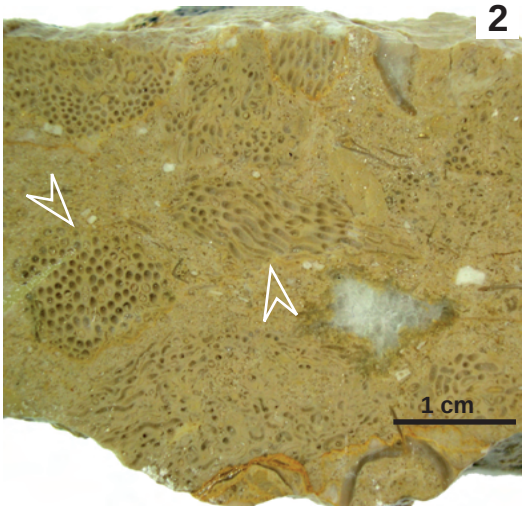
2
1 cm

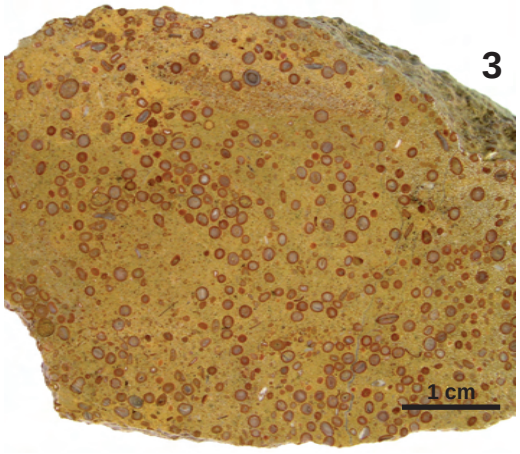
3
1 cm


4
1 cm

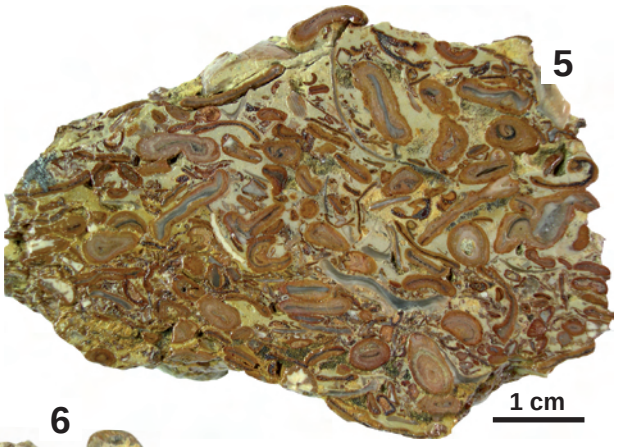
5
1 cm


6
1.5 cm

PLATE 2 - MACROSCOPIC SAMPLES

1 – Oyster-rich tempestites showing an alternation of high-energy (H) and lower energy (L) deposits. Black arrow points upwards. Pagny-sur-Meuse section, Pg-4.

2 – Dish-shaped siliceous sponges carrying thrombolitic microbial crusts floating in a wackestone (floatstone) with tuberoids and microbialite fragments. Balingen-Tieringen section, Bt-22.

3 – Lithoclastic rudstone. Vergons section, Vg-22.

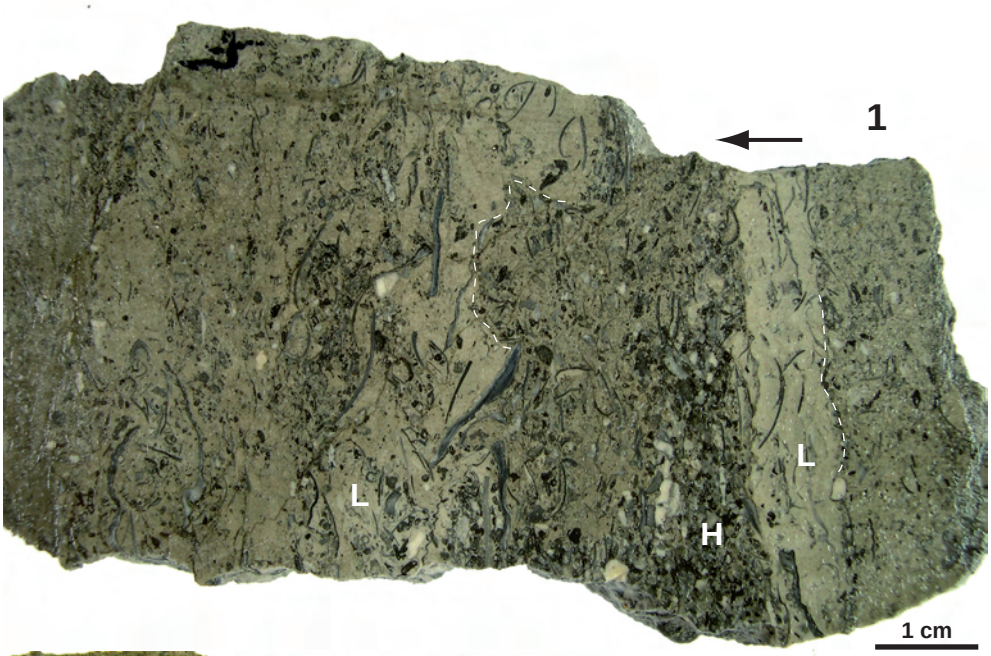
1
L
L
H
1 cm

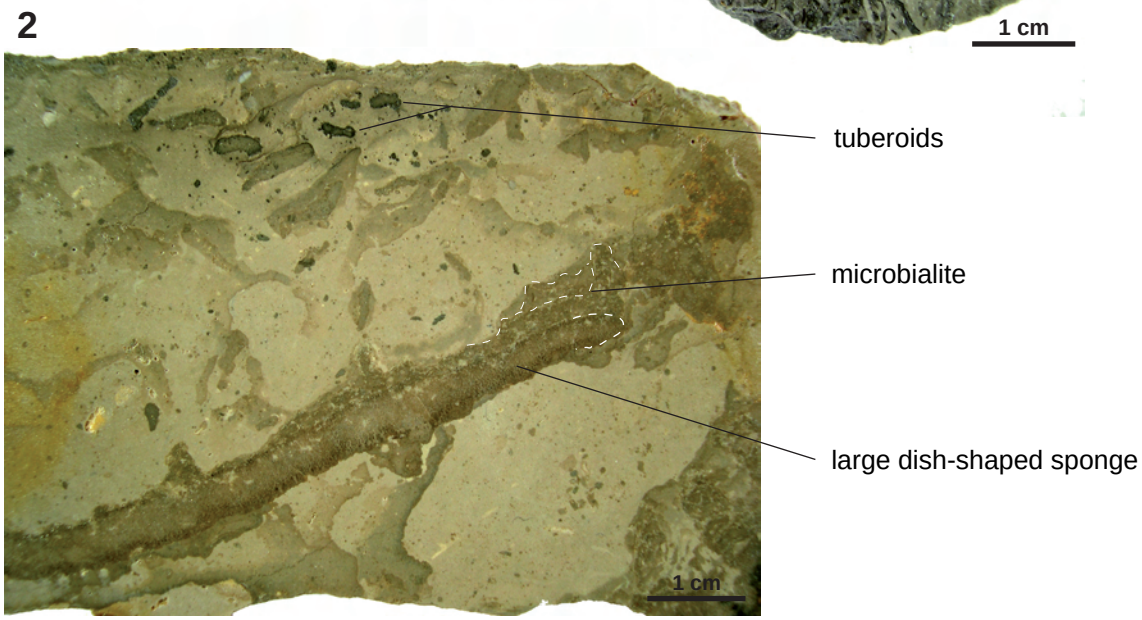
2
tuberoids
microbialite
large dish-shaped sponge
1 cm

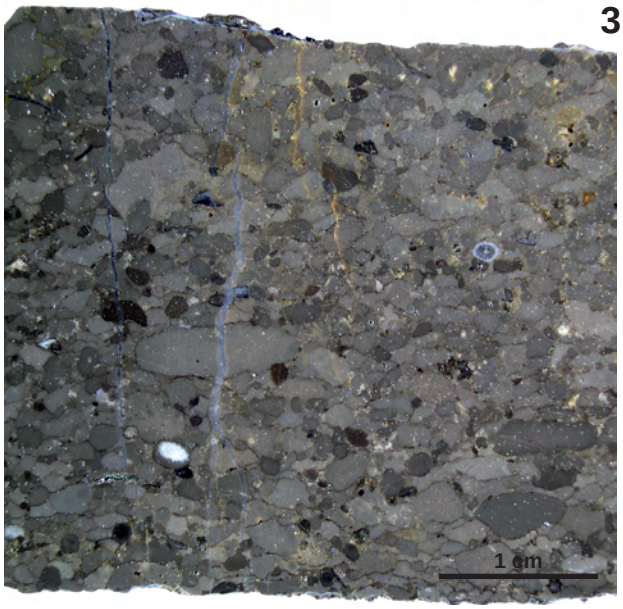
3
1 cm

PLATE 3 - HARDGROUNDS

1 – Oyster-encrusted hardground. Note the clay seam at the transition between ferrugineous ooids and oyster accumulation and the important dolomitization areas. Black arrow points upwards. Vorbourg section, Vo-32B.

2 – Highly perforated oyster accumulation. The bioperforations (arrows) correspond to *Gastrochaenolites* trace fossils. Vorbourg section, Vo32B.

3 – Thin section of a hardground with abundant oyster shells, a terebratulid brachiopod shell (top), and an echinoderm fragment (base). Note the dark impregnation of matrix by iron oxides (arrow). Vorbourg section, Vo-32B.

4 – Oyster-rich hardground at the top of an ooid packstone, slightly bioturbated (probably *Thalassinoides*). Pagny-sur-Meuse section, Pg-39A.

5 – Hardground surface rich in large oyster shells. Pagny-sur-Meuse section, Pg-39C.

6 – Thin section of the transitional zone between ooids and oysters. Pagny-sur-Meuse section, Pg-39A.

7 – Enlargement of the Fig. 6. Note the dark impregnation of matrix by iron oxides. Pagny-sur-Meuse section, Pg-39A.

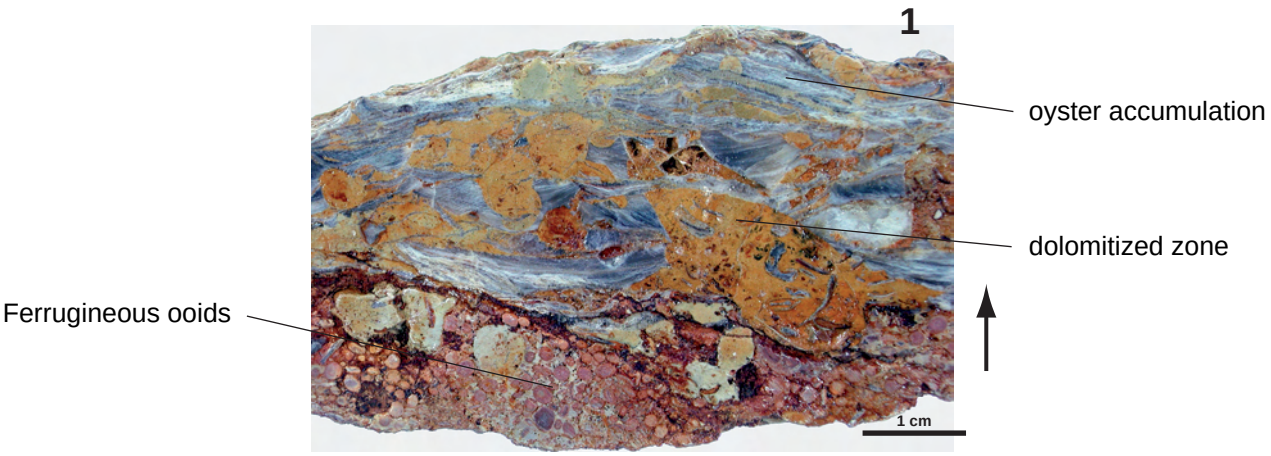
1
oyster accumulation
dolomitized zone
Ferrugineous ooids
1 cm

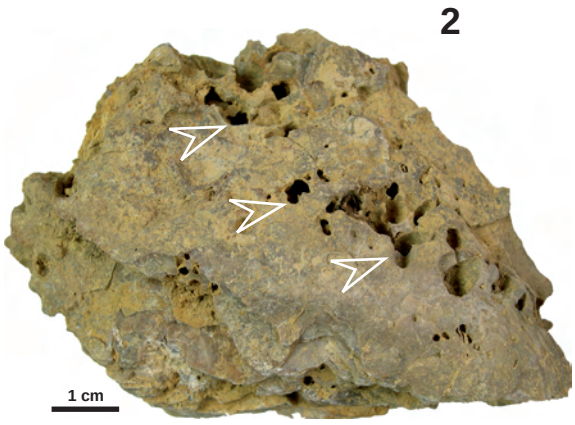
2
1 cm

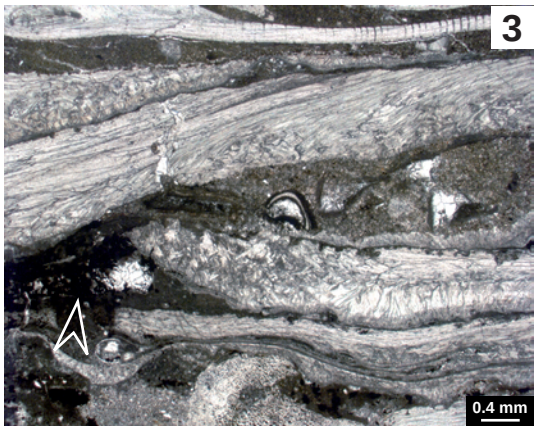
3
0.4 mm

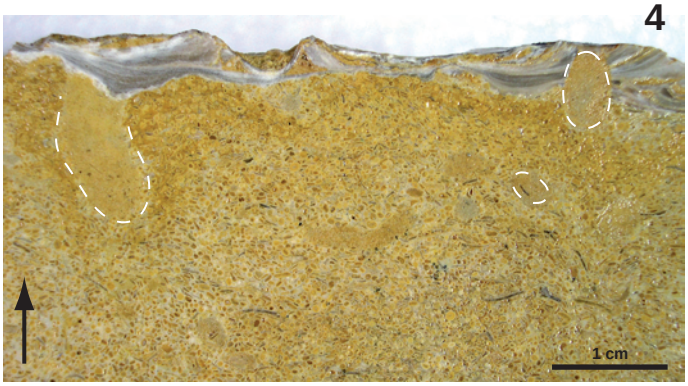
4
1 cm

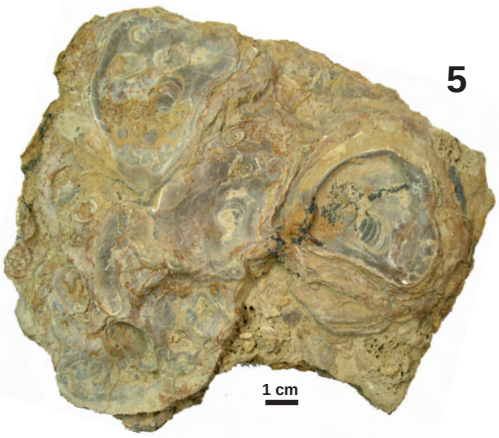
5
1 cm

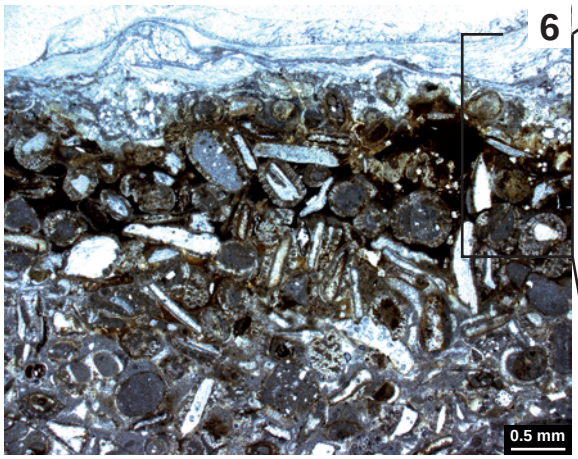
6
0.5 mm

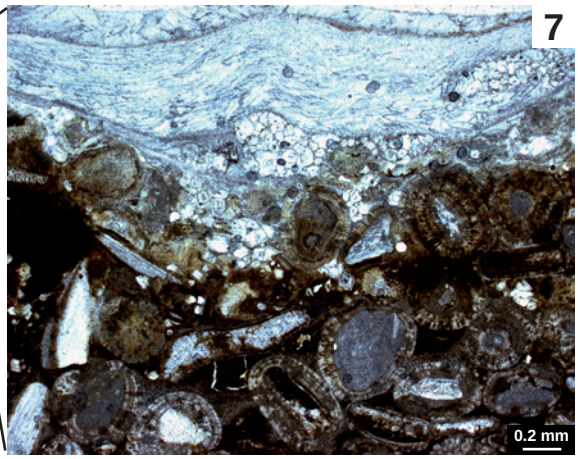
7
0.2 mm

PLATE 4 – NON-SKELETAL ELEMENTS (1)

1 – Type 1 oncoid with echinoderm fragment as nucleus and homogeneous, micritic cortex with barely visible laminations, found in a bioclastic wackestone. Savagnières section, Sa-32C.

2 – Elliptical type 2 oncoid with a large echinoderm fragment as nucleus and smooth contours. Micritic laminations of a first growth phase are onlapped by those of a second phase (arrow). Court section, BPCo-81.

3 – Elongate type 2 oncoid with a radial ooid trapped in the cortex. Court section, BPCo-81.

4 – Type 2 oncoid formed by several phases of growth. Serpulid worms encrusted at different growth stages. Voyeboeuf section, Vy-8a.

5 – Type 2 oncoid with a cortex encrusted by the foraminifer *Placopsilina* (arrow). Vorbourg section, Vo-11B.

6 – Type 3 oncoid with a cortex composed of irregular organism-bearing *Bacinella-Lithocodium* laminations and thinner micritic laminations. The contours are lobate. Note the *Troglotella incrustans* (arrow), which perforates the cortex. Pertuis section, Pe-81A.

7 – Detail of type 3 oncoid with *Bacinella-Lithocodium* meshwork and thin micritic laminations. Pertuis section, Pe-82A.

8 – Type 4 oncoid with lobate and diffuse contours, entirely composed of *Bacinella irregularis*. Voyeboeuf section, Vy-20.

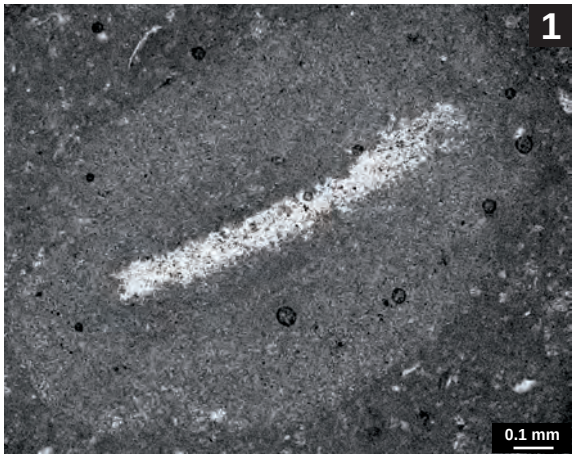
1
0.1 mm

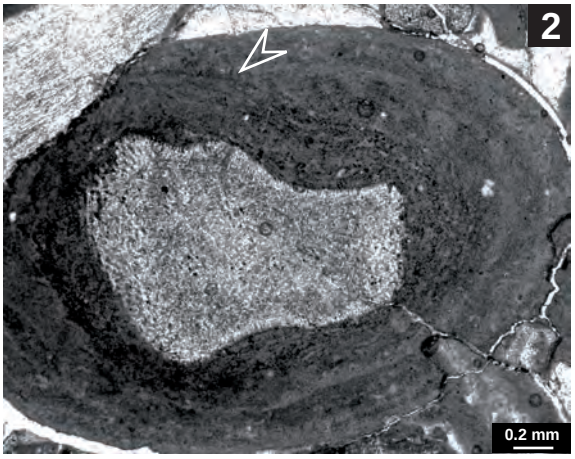
2
0.2 mm

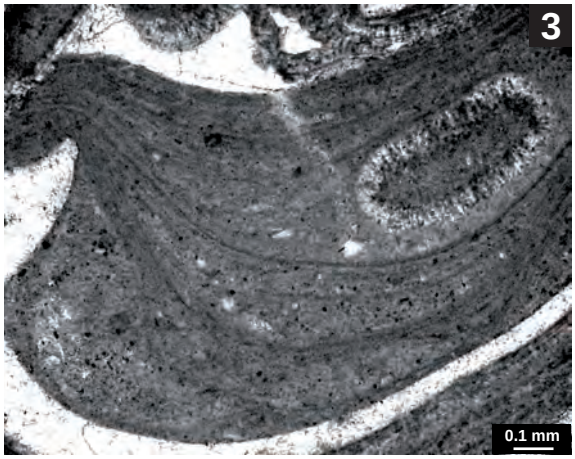
3
0.1 mm

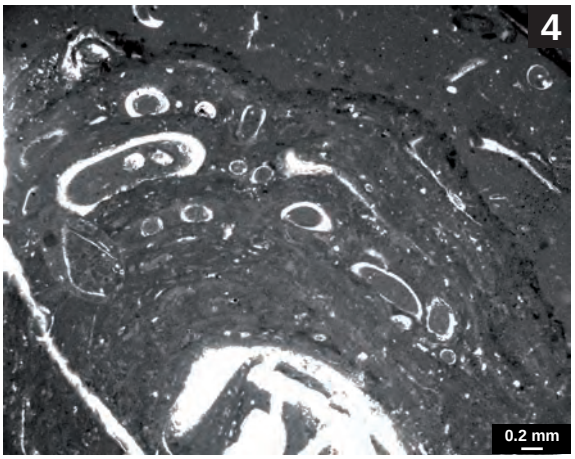
4
0.2 mm

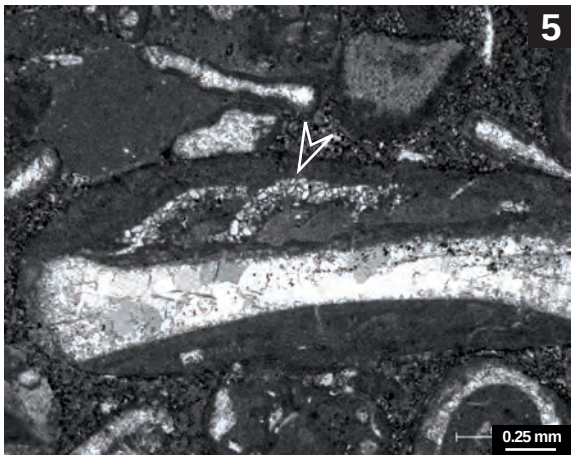
5
0.25 mm

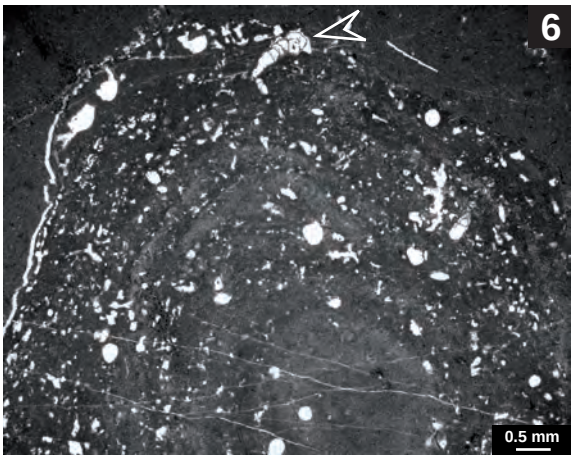
6
0.5 mm

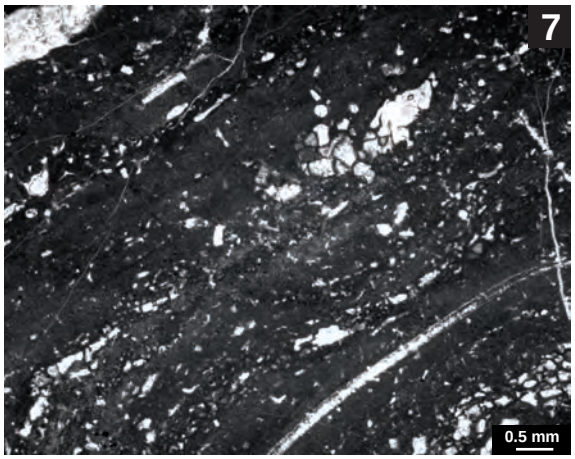
7
0.5 mm

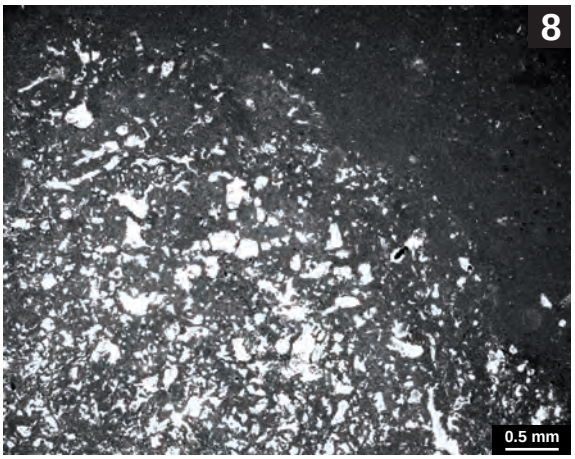
8
0.5 mm

PLATE 5 – NON-SKELETAL ELEMENTS (2)

1 – Ooid with thinly laminated fine radial cortices (type 3 of STRASSER 1986). Court section. JPC-29.

2 – Partially micritized radial ooid in a dolomitized matrix. Vorbourg section,Vo-32C.

3 – Partially micritized radial ooid with a gastropod as nucleus. Vorbourg section, Vo-31A.

4 – Oo-oncoid (type 2 ooid of STRASSER 1986) with a spherical radial ooid that evolves into an oncoid. Pagny-sur-Meuse section, Pg-21C2.

5 – Oo-oncoid. Voyeboeuf section, Vy-30

6 – Packstone rich in peloids and quartz. Pertuis section, Pe-F

7 – Well-rounded lithoclast rich in bioclastic fragments (i.e. echinoderms, bivalves, *Lenticulina*). Pagny-sur-Meuse section, Pg-21C1

8 – Lithoclast composed of ooids, which are bordered by an isopachous cement coat. Note truncated ooids. Pagny-sur-Meuse section, Pg-21C2

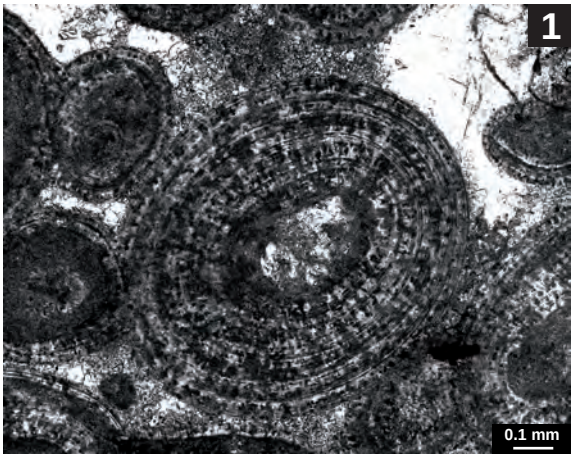
1
0.1 mm

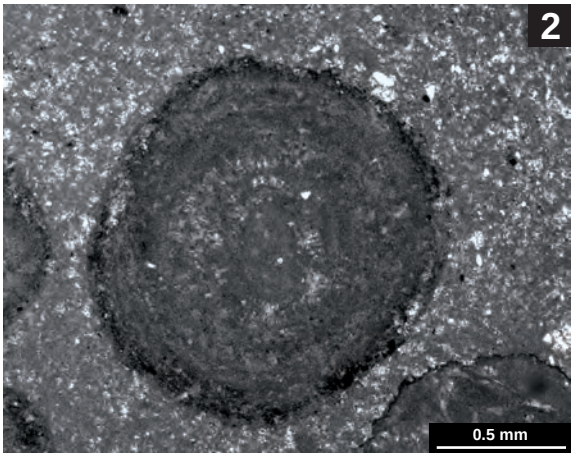
2
0.5 mm

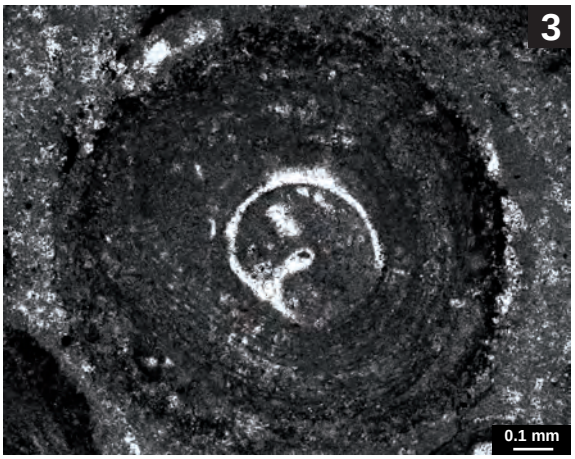
3
0.1 mm

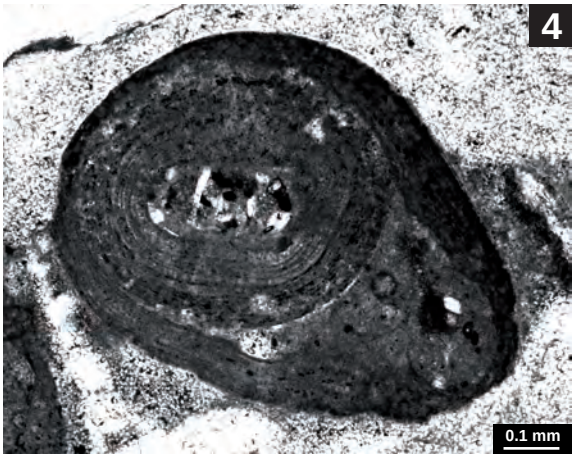
4
0.1 mm

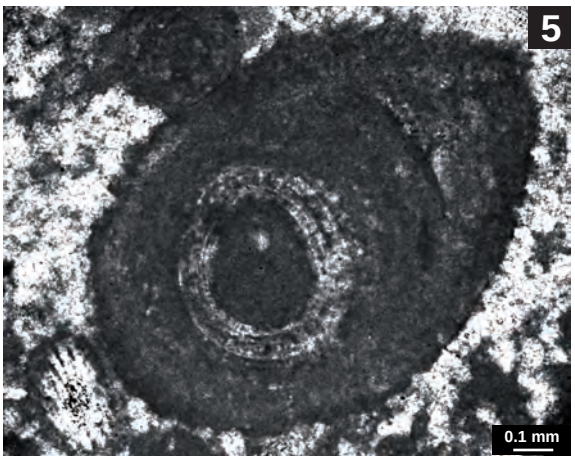
5
0.1 mm

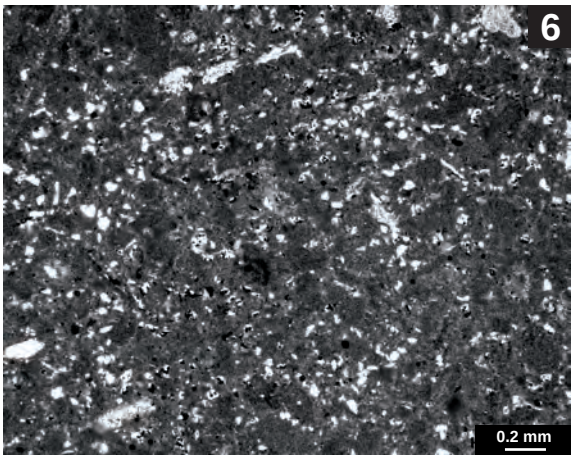
6
0.2 mm

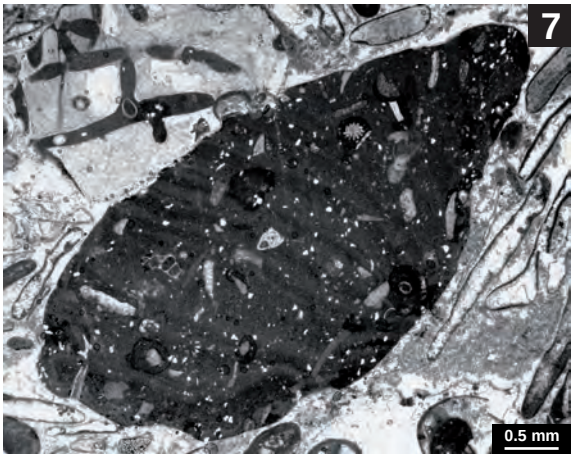
7
0.5 mm


8
0.1 mm

PLATE 6 – BIOCLASTS IN SHALLOW PLATFORM DEPOSITS

1 – Internal microstructure of an oyster shell. Voyeboeuf section, Vy-30.

2 – Fragment of inoceram shell. Vorbourg section, Vo-13.

3 – Well-preserved valve of ostracode. Vergons section, Vg-1.

4 – Perforated (Terebratulid) brachiopod shell. Pagny-sur-Meuse section, Pg-4.1.

5 – Echinoid plate fragment. Savagnières section, Sa-18.

6 – Partially micritized dasycladaceans. Vorbourg section, Vo-10C.

7 – Cluster of serpulids showing compaction structures (arrow). Savagnières section, Sa-22.

8 – Coral perforated by lithophages. Hautes-Roches section, Hr-4.

9 – Longitudinal section through microsolenid coral. Hautes-Roches section, Hr-5B.

10 – *Stylina*, transversal section. Court section, BPCo-67.

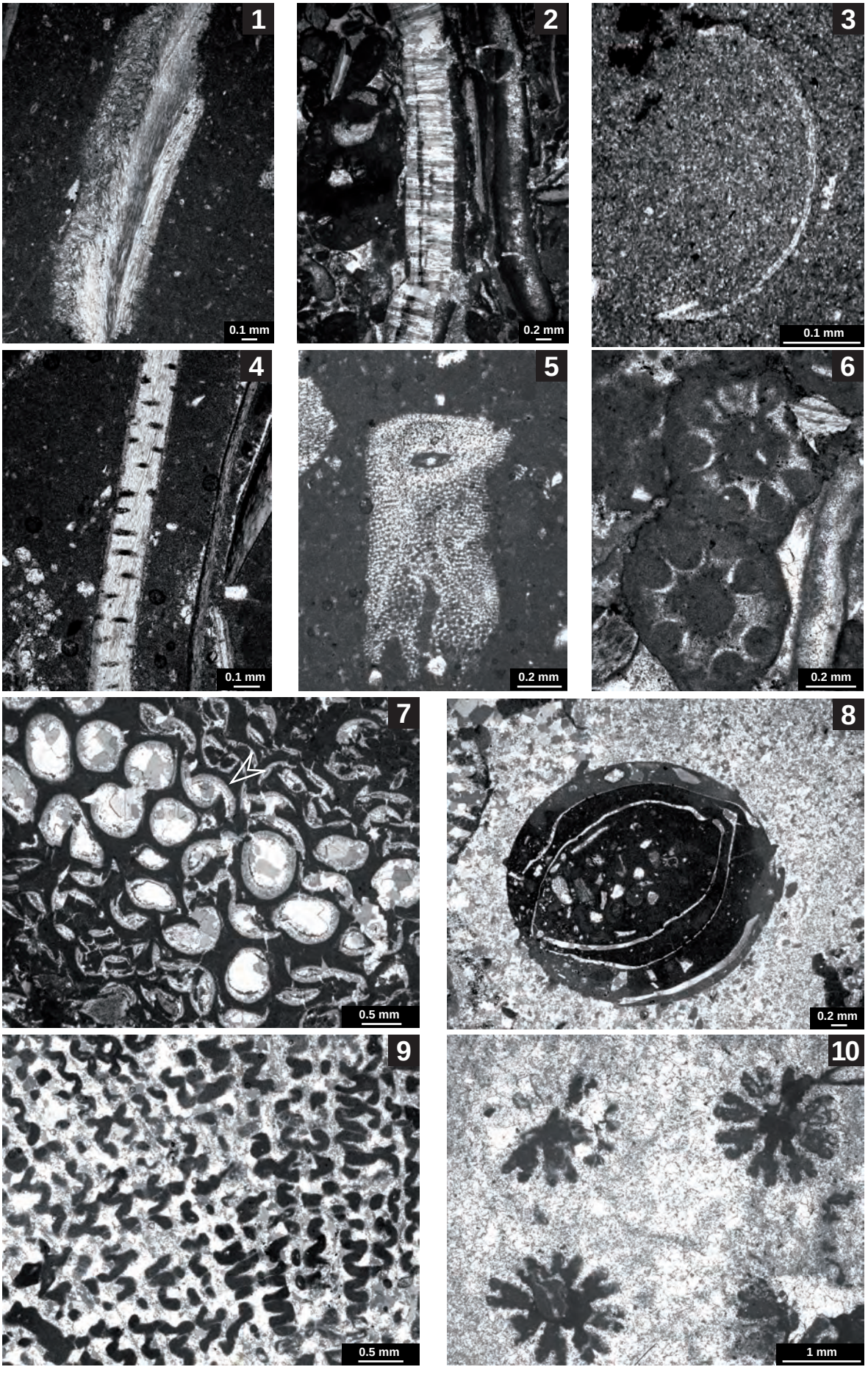
1
0.1 mm
2
0.2 mm
3
0.1 mm
4
0.1 mm
5
0.2 mm
6
0.2 mm
7
0.5 mm
8
0.2 mm
9
0.5 mm
10
1 mm

PLATE 7 – BIOCLASTS IN DEEP PLATFORM AND BASIN DEPOSITS

1 – Ammonite fragments. Vergons section, Vg-42.

2 – Aptychus associated with Protoglobigerinids. Vergons section, Vg-17.2.

3 – *Globochaete* and filament. Vergons section, Vg-33.

4 – Radiolaria with the polar spine. Vergons section, Vg-31.

5 – Meshwork of hexactinellid siliceous sponge, characterized by cross-shaped spicules. Balingen-Tieringen section, Bt-30B.1.

6 – Radiolarian with the skeletal structure still preserved. Vergons section, Vg-36.2.

7 – Disintegration of sponge fragment leading to a tuberoid with micritic and peloidal microstructure. Balingen-Tieringen section, Bt-39B1.

8 – Tuberoid with sponge microstructure locally preserved. Balingen-Tieringen section, Bt-14B.

9 – Micritic and peloidal microstructure of a tuberoid. Balingen-Tieringen, Bt-21.2.

10 – Microencrusted micritic lithoclast. Balingen-Tieringen section, Bt-37.2.

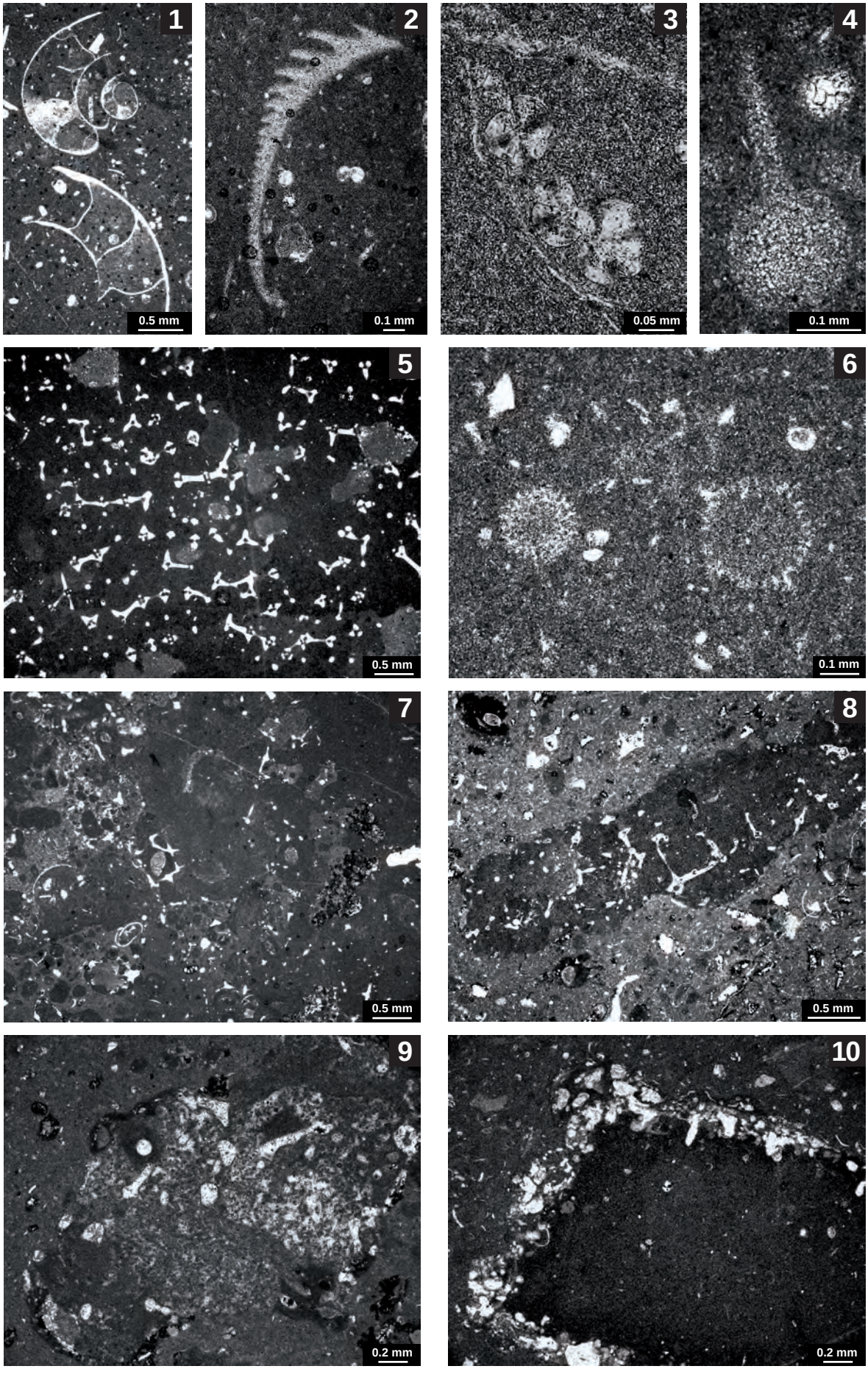
1
0.5 mm
2
0.1 mm
3
0.05 mm
4
0.1 mm
5
0.5 mm
6
0.1 mm
7
0.5 mm
8
0.5 mm
9
0.2 mm
10
0.2 mm

PLATE 8 – BENTHIC AND PLANKTONIC FORAMINIFERA

1 – Large agglutinated foraminifer (*Pseudocyclammina?)* agglutinating small *Pseudocyclammina* and bioclasts. Court section, BPCo-53.

2 – *Pseudocyclammina* sp. (subaxial section). Court section. SVCo-2.

3 – Enlargement of the Fig. 1. Court section, BPCo-53.

4 – Equatorial section of *Pseudocyclammina* sp. Vorbourg section, Vo-10.

5 – Subaxial section of *Nautiloculina* sp. Pertuis section, Pe-81B.

6 – Textularid with a simple wall microstructure. Vorbourg section, Vo-23.

7 – Miliolid foraminifer. Pertuis section, Pe-82A.

8 – Equatorial section of *Lenticulina* sp. Vorbourg section, Vo-O.

9 – Subaxial section of *Lenticulina* sp. Vorbourg section, Vo-4.

10 – Protoglobigerinid. Balingen-Tieringen section, Bt-39B.2.

11 – Protoglobigerinid. Balingen-Tieringen section, Vg-43.

12 – Protoglobigerinid. Balingen-Tieringen section, Vg-43.

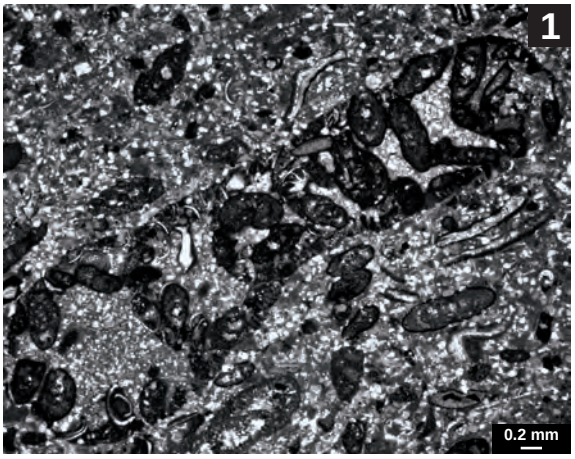
1
0.2 mm

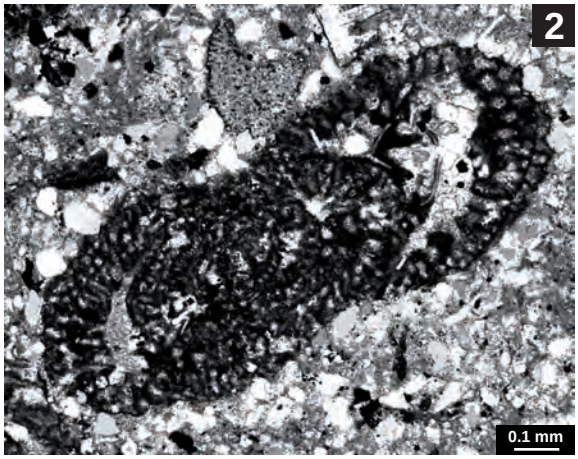
2
0.1 mm

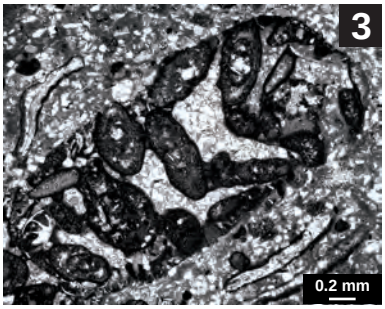
3
0.2 mm

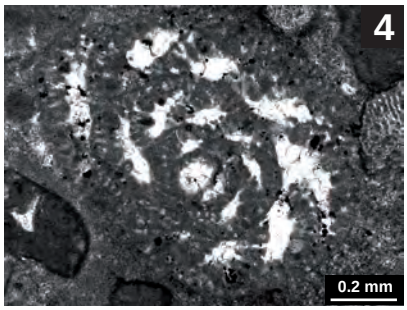
4
0.2 mm

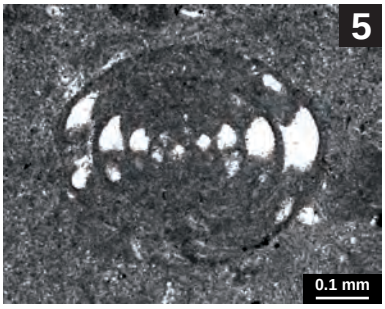
5
0.1 mm


6
0.2 mm

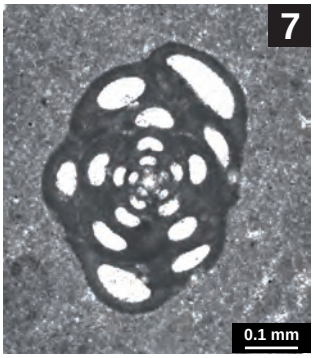
7
0.1 mm

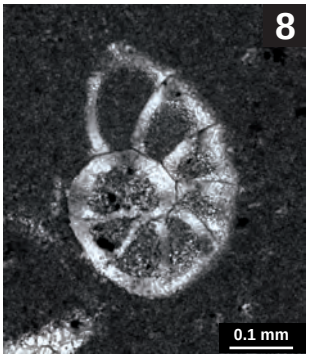
8
0.1 mm


9
0.1 mm

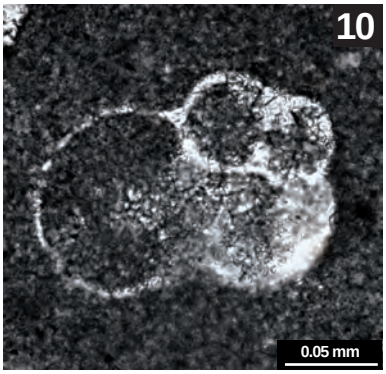
10
0.05 mm

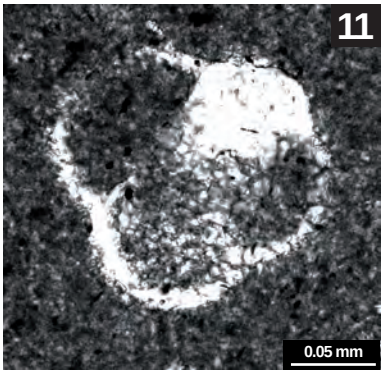
11
0.05 mm

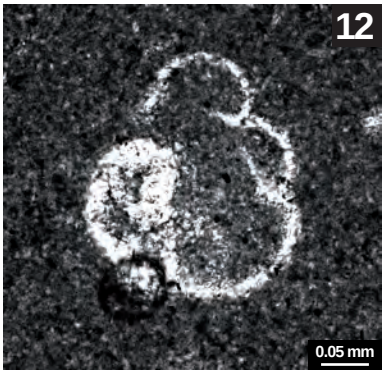
12
0.05 mm

PLATE 9 – *MOHLERINA BASILIENSIS*

1 – Subaxial section of *Mohlerina basiliensis*. Vorbourg section, Vo-20.

2 – Enlargement of specimen in Fig. 1 showing double-layered structure: thin dark micritic (M) and thick hyaline radial-fibrous calcite layers (R). Vorbourg section, Vo-20.

3 – Subaxial section of *Mohlerina basiliensis*. Pertuis section, Pe-81B.

4 – Axial section of *Mohlerina basiliensis*. Savagnières section, Sa-19A.

5 – Enlargement of specimen in Fig. 3. Pertuis section, Pe-81B.

6 – Subaxial section of *Mohlerina basiliensis*. Pertuis section, Pe-80B.

7 – Equatorial section of *Mohlerina basiliensis*. Pertuis section, Pe-86B.

8 – Equatorial section of *Mohlerina basiliensis*. Pertuis section, Pe-86B.

9 – Equatorial section of *Mohlerina basiliensis*. Pertuis section, Pe-84B.

10 – High-energy facies (packstone/grainstone) composed of oncoid, peloids, bivalves, *Mohlerina basiliensis*, and Miliolids. Vorbourg section, Vo-24A.

11 – *Bacinella-Lithocodium* oncoid wackestone associated with *Mohlerina basiliensis* (Mo), and a perforated brachiopod fragment (Br). Pertuis section, Pe-83A.

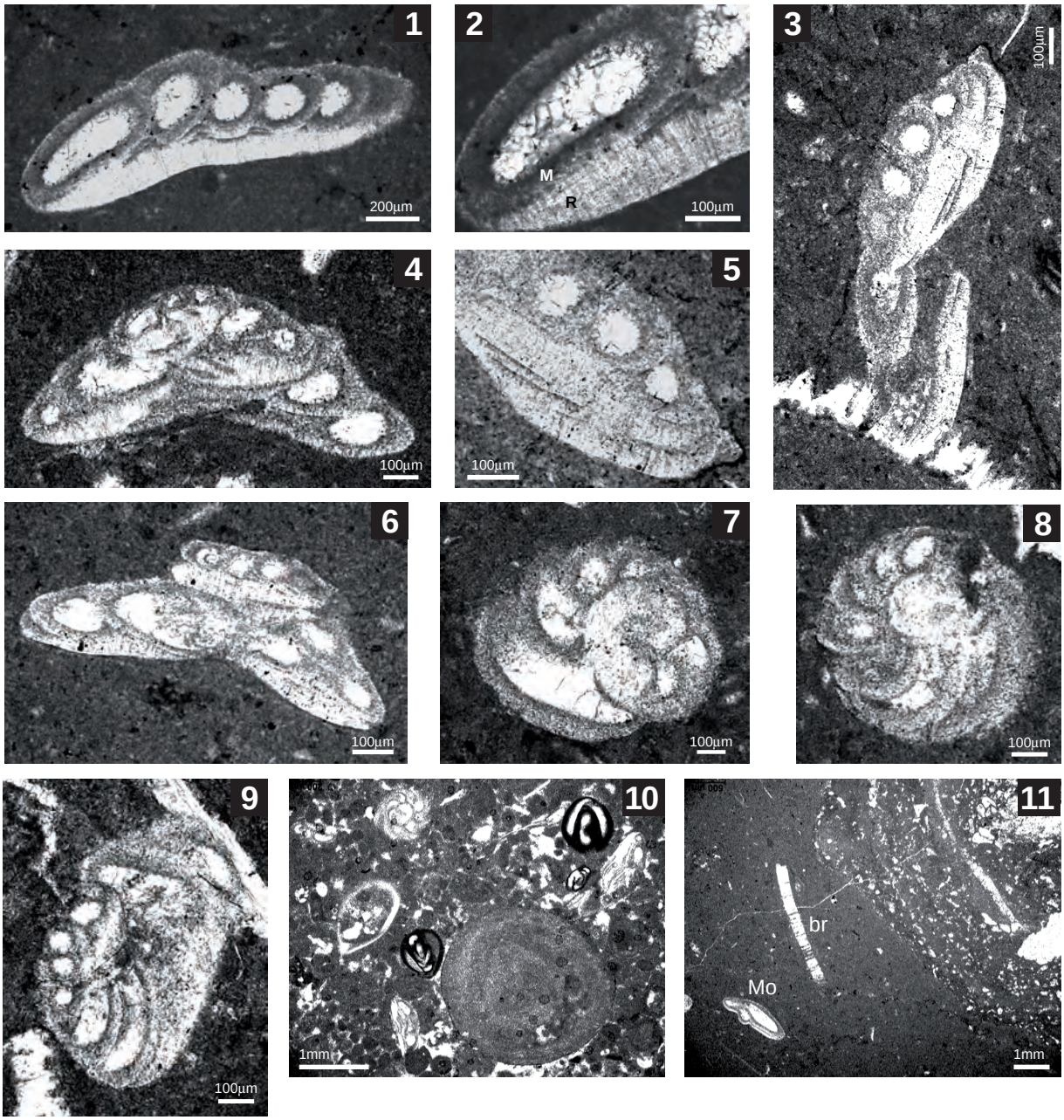
1
200µm
2
M
R
100µm
3
100µm
4
100µm
5
100µm
6
100µm
7
100µm
8
100µm
9
100µm
10
1mm
11
br
Mo
1mm

PLATE 10 – MICROENCRUSTERS AND MICROBIAL ENCRUSTATIONS

1 – *Bacinella irregularis* meshwork. Pertuis section, Pe-82A.

2 – *Lithocodium aggregatum* with *Troglotella incrustans* (arrow). Pertuis section, Pe-84A.

3 – *Bullopora tuberculata* with its typical spines. Balingen-Tieringen, Bt-26A.

4 – *Troglotella incrustans* (arrow) in micritic oncoid cortex. Vorbourg section, Vo-24.

5 – Two phases of encrustation by the agglutinating foraminifer *Placopsilina* sp. (arrow). Hautes-Roches section, Hr-5B.

6 – *Tubiphytes* sp. Vorbourg section, Vo-4.

7 – Common microencrusting foraminifera (nubeculariids). Balingen-Tieringen section, Bt-35.

8 – Microbial encrustation on coral with *Placopsilina*. Note the direction of growth to the top (orientated thin section). Hautes-Roches section, Hr-4.

9 – Oncoid cortex mainly composed of *Bacinella irregularis* meshwork in alternation with thin micritic laminations. Pertuis section, Pe-82A.

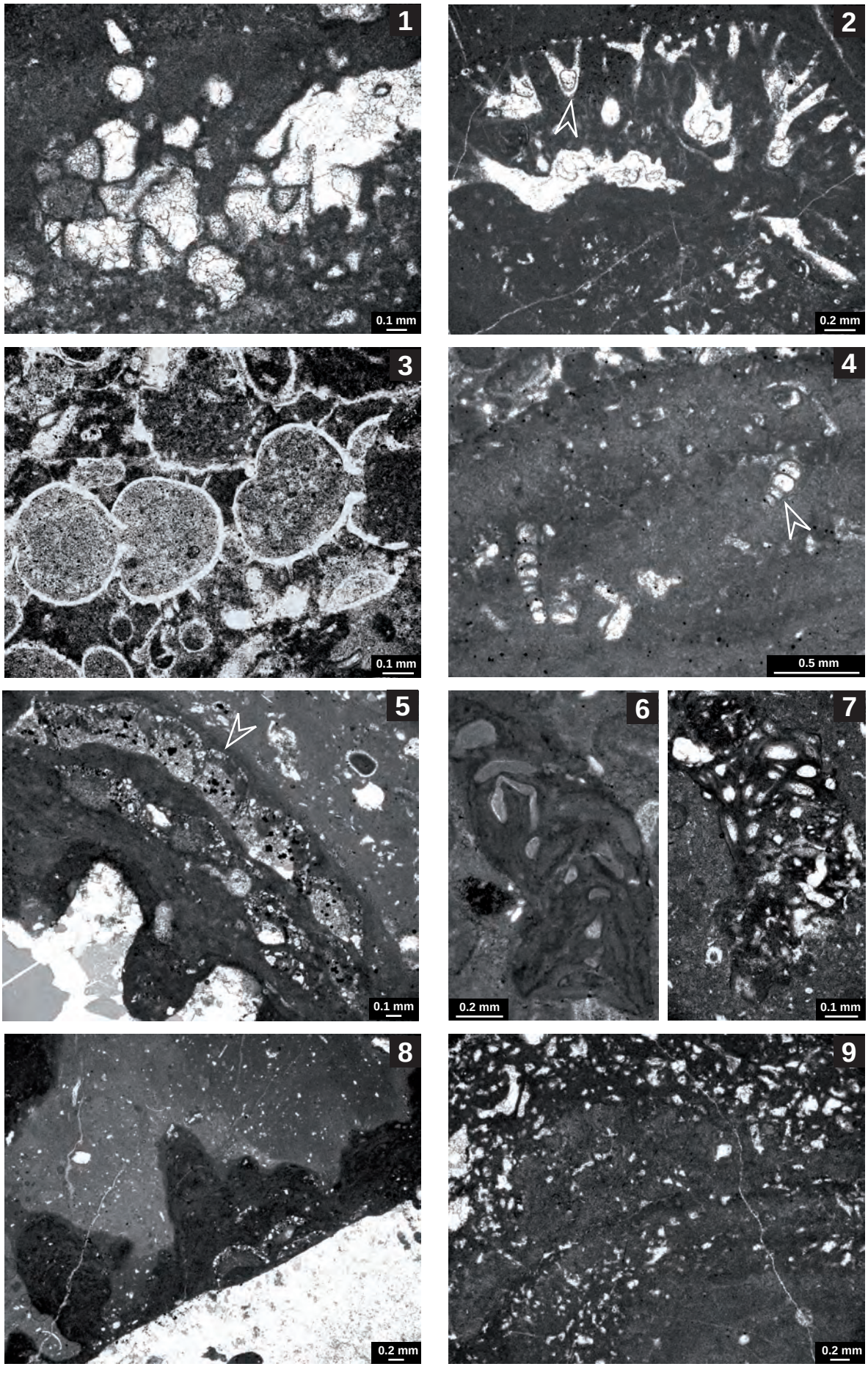
1
0.1 mm
2
0.2 mm
3
0.1 mm
4
0.5 mm
5
0.1 mm
6
0.2 mm
7
0.1 mm
8
0.2 mm
9
0.2 mm

PLATE 11 – SHALLOW CARBONATE PLATFORM MICROFACIES

1 – Mudstone with birdseyes. Microfacies tf1, Court section, BPCo-71.

2 – Peloidal and bioclastic packstone rich in quartz. Microfacies prl2, Savagnières section, Sa-1A.

3 – Packstone rich in Textularids (black grains), echinoderms, various bioclasts, and quartz grains. Microfacies sol7, Court section, SVCo-2.

4 – Peloidal packstone. Microfacies prl3, Pertuis section, Pe-F.

5 – Bioclastic packstone with bivalves, Textularids, and serpulids. Microfacies sol1, Pertuis section, BPPe-68.

6 – Wackestone rich in Terebratulid brachiopods. Microfacies ol1, Vorbourg section, Vo-N.

7 – Peloidal and ooidal packstone-grainstone. Microfacies sol6, Vorbourg section, Vo-14.

8 – Bioclastic and peloidal packstone-grainstone. Microfacies sol7, Vorbourg section, Vo-10C.

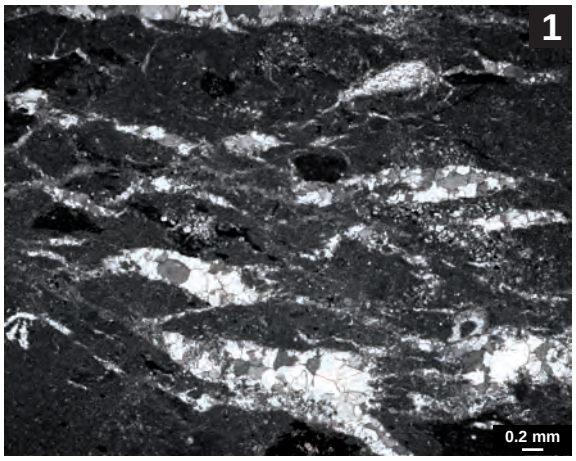
1
0.2 mm

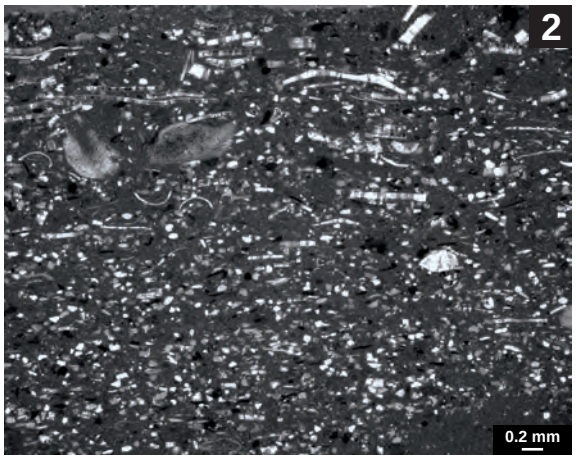
2
0.2 mm

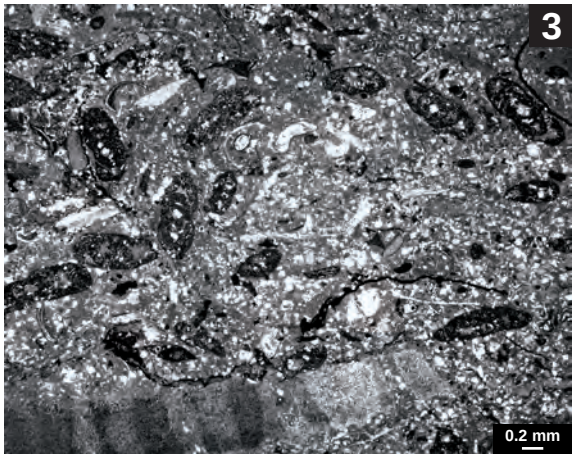
3
0.2 mm

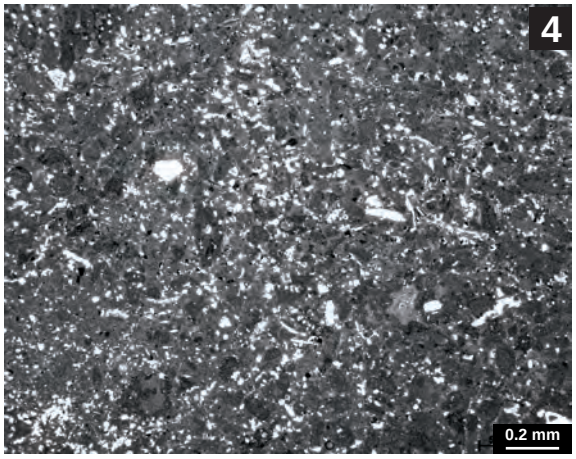
4
0.2 mm

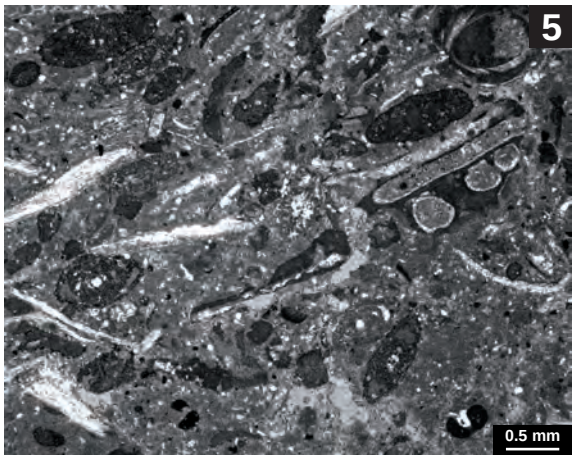
5
0.5 mm

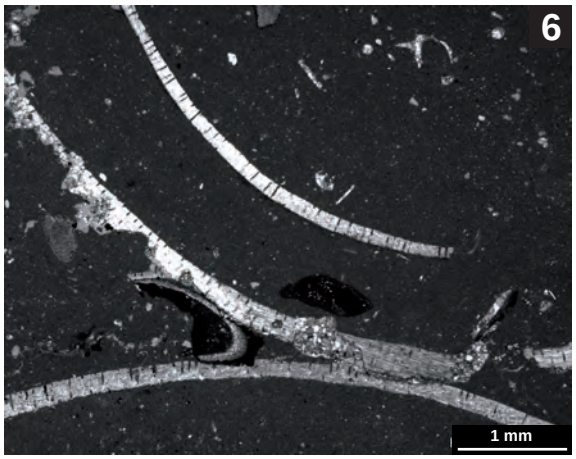
6
1 mm

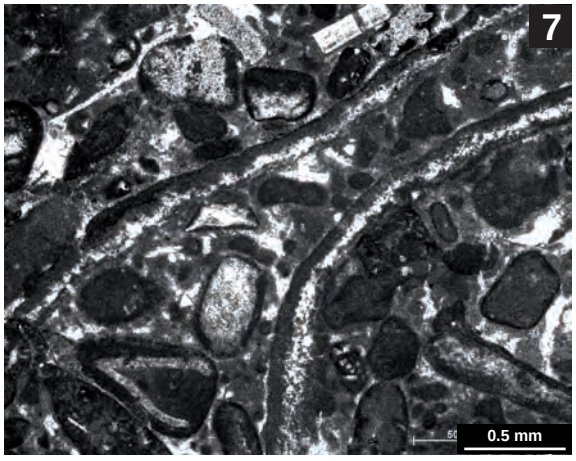
7
0.5 mm

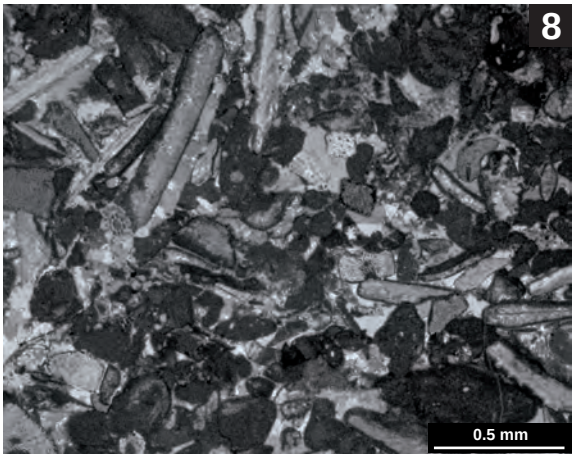
8
0.5 mm

PLATE 12 - SHALLOW CARBONATE PLATFORM MICROFACIES

1 – Type 2 oncoid packstone with a dolomitzed matrix. Microfacies sol5, Vorbourg section, Vo-12.

2 – Type 3 oncoid wackestone/floatstone with *Mohlerina basiliensis*. Microfacies ol2, Vorbourg section, Vo-22.

3 – Micritic ooid wackestone in a partially dolomitized matrix. Microfacies bar4, Vorbourg section, Vo-32.

4 – Type 3 ooid grainstone with isopachous cement around grains. Note the important compaction following the first phase of cementation. Microfacies bar5, Hautes-Roches section, Hr-25.

5 – Type 3 ooid grainstone with large type 2 oncoids. Microfacies bar5, Hautes-Roches section, Hr-10.

6 – Ooid and bioclastic packstone. Microfacies bar8, Pagny-sur-Meuse section, Pg-34.2.

7 – Bioclastic (oysters) packstone. Microfacies bar8, Pagny-sur-Meuse section, Pg-21C.2.

8 – Bioclastic packstone/grainstone with a few type 3 ooids. Microfacies bar12, Pagny-sur-Meuse section, Pg-19.

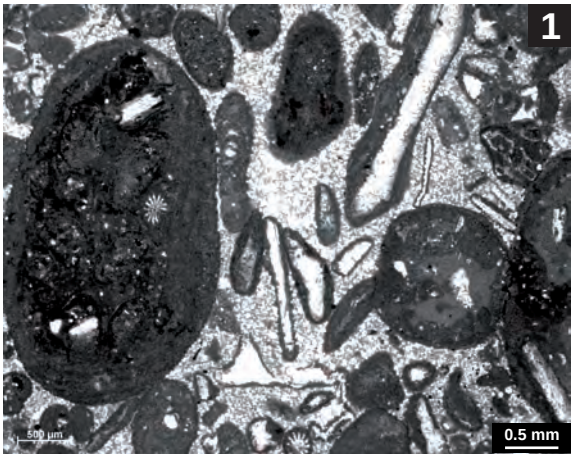
1
500 µm
0.5 mm

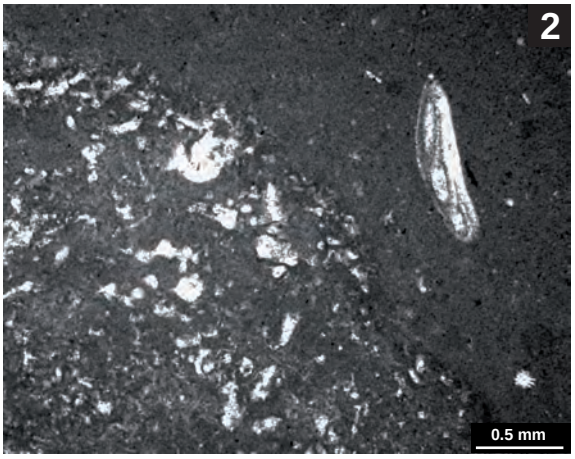
2
0.5 mm

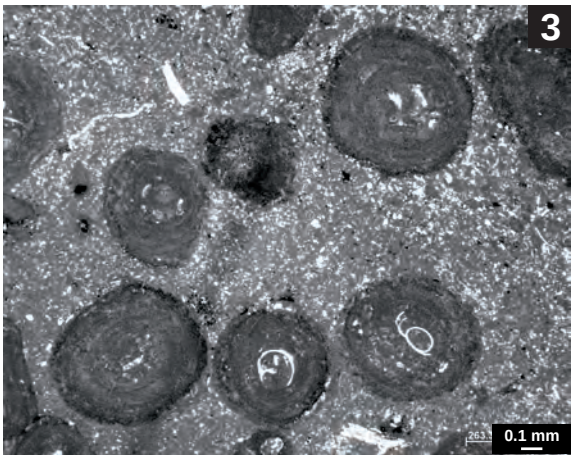
3
0.1 mm

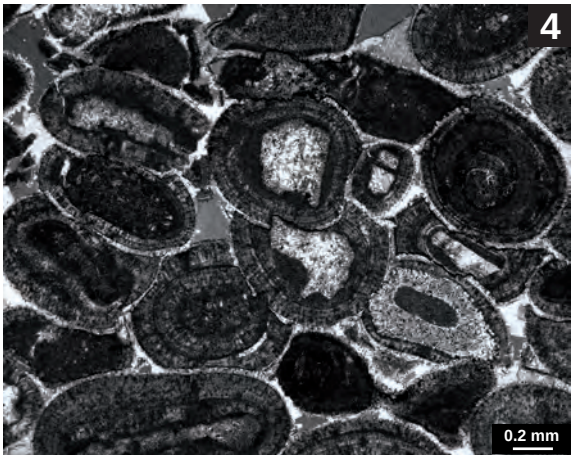
4
0.2 mm

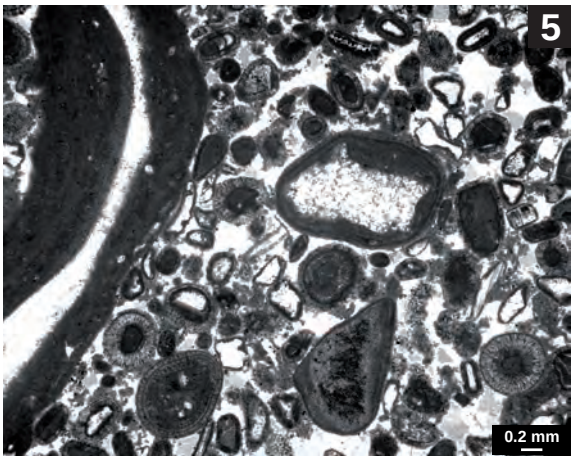
5
0.2 mm

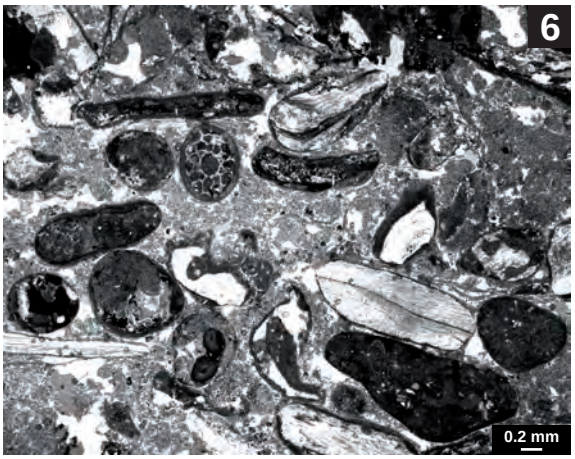
6
0.2 mm

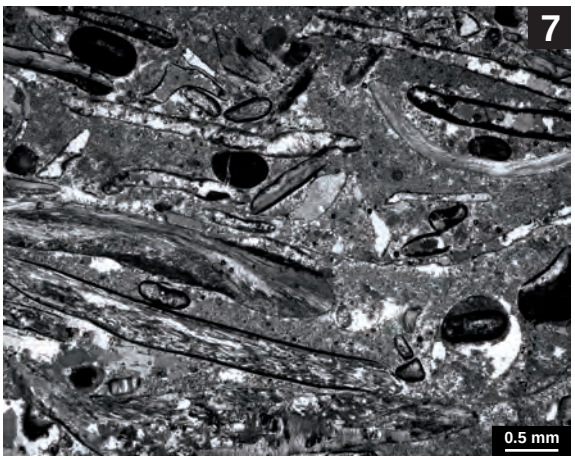
7
0.5 mm

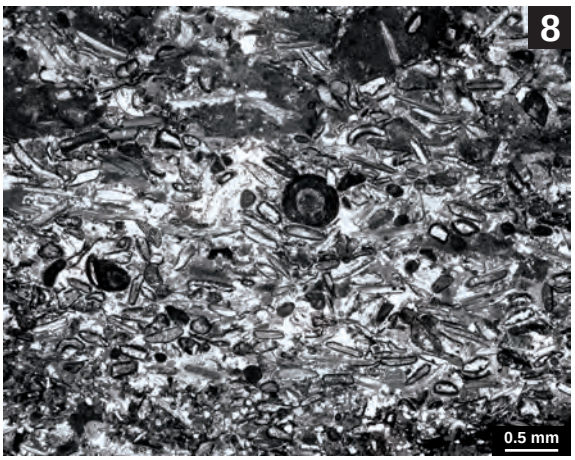
8
0.5 mm

PLATE 13 – DEEP PLATFORM AND BASIN MICROFACIES

1 – Bioclastic wackestone with radiolarians, Protoglobigerinids, and ammonites. Microfacies b5, Vergons section, Vg-43.1.

2 – Bioclastic wackestone with abundant radiolarians. Microfacies b5, Vergons section, Vg-46.

3 – Tuberoid with the internal structure of desmosponge and microencrusted by, e.g., *Tolypammina* sp. (arrow). Microfacies ds6, Balingen-Tieringen section, Bt-28

4 – Formation of peloids from a large tuberoid. Microfacies ds8, Balingen-Tieringen section, Bt-30B.1.

5 – Sponge covered by microbialite. Microfacies ds5, Balingen-Tieringen section, Bt-22.1.

6 – Peloidal packstone with subrounded lithoclasts. Microfacies ds9, Balingen-Tieringen section, Bt-45.

7 – Lithoclastic-peloidal grainstone. Microfacies b7, Vergons section, Vg-12A.2.

8 – Lithoclastic grainstone with micrite mud infiltrated at a later stage. Note the allochthonous elements such as ooids (arrow). Microfacies b7, Vergons section, Vg-18.2.

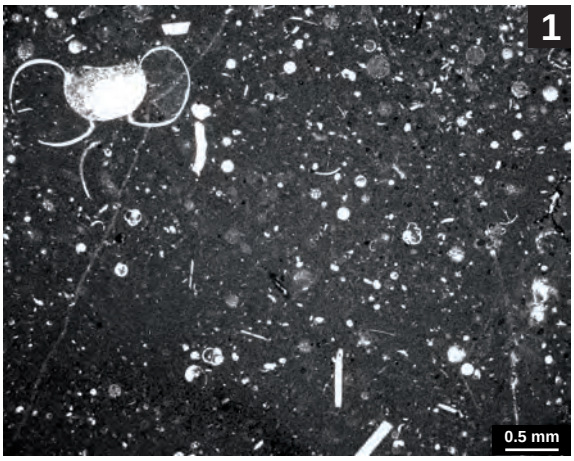
1
0.5 mm

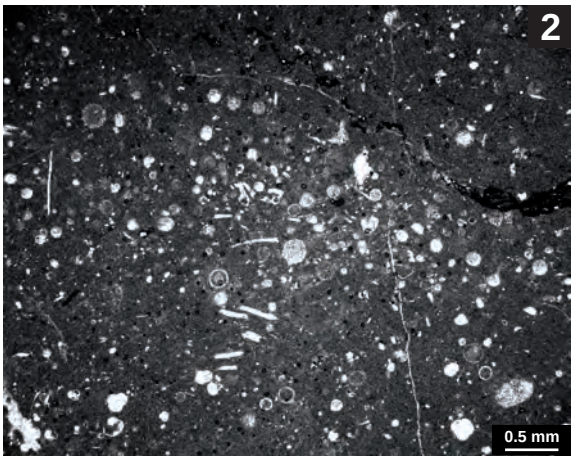
2
0.5 mm

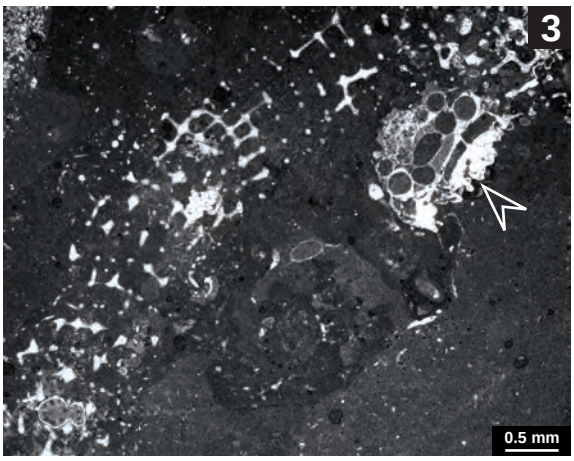
3
0.5 mm

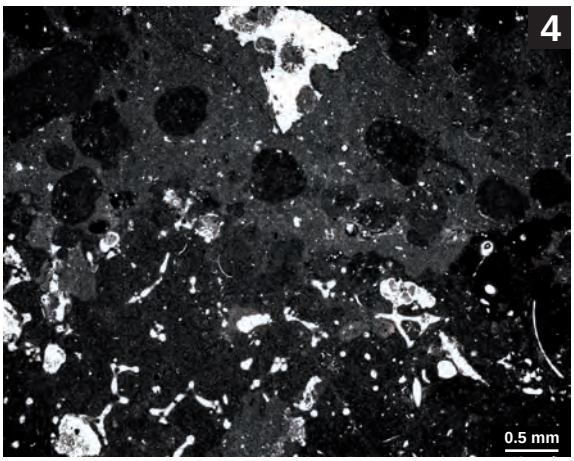
4
0.5 mm

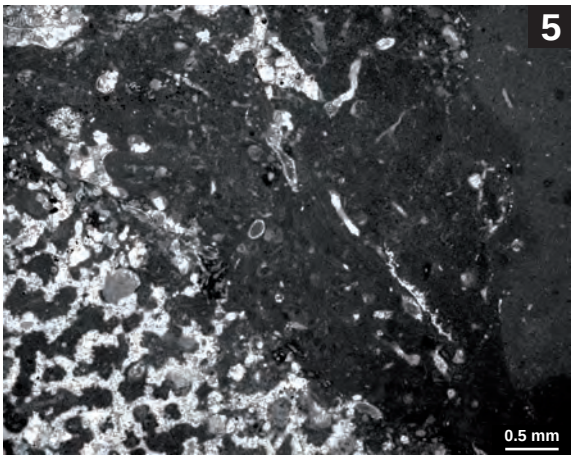
5
0.5 mm

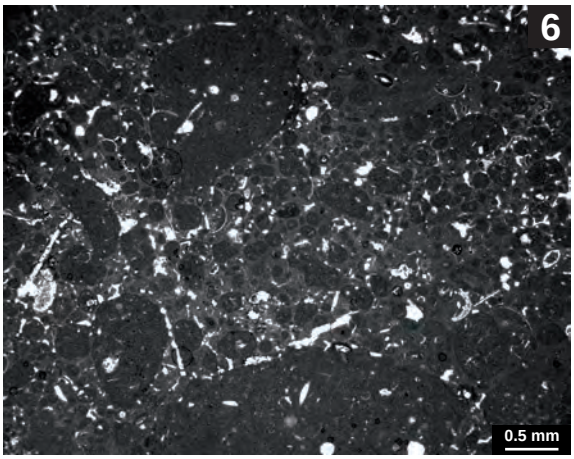
6
0.5 mm

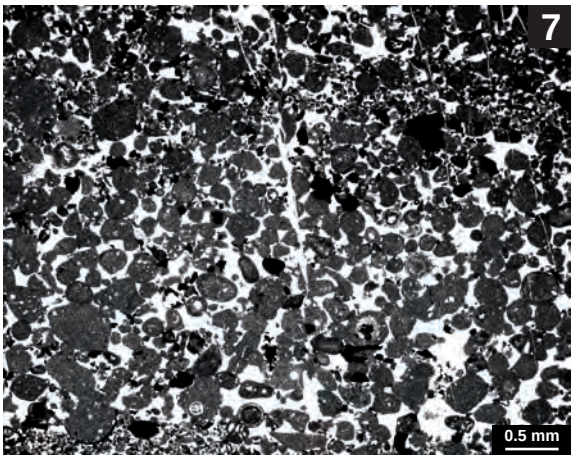
7
0.5 mm

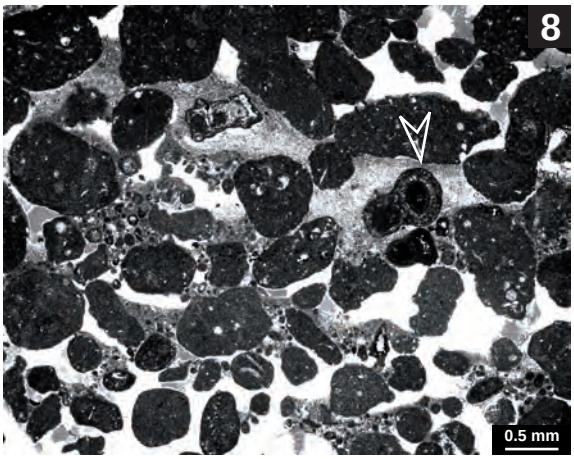
8
0.5 mm

PLATE 14 – SWISS JURA PLATFORM SECTIONS

1 – Voyeboeuf section from SB Ox6+ to MFS Ox6+.

2 – Savagnières section from SB Ox6+ to MFS Ox6+.

3 – Pertuis section from SB Ox6+ to MFS Ox6+.

4 – Top part of the Vorbourg section around MFS Ox6+.

5 – Base of the Vorbourg section around the SB Ox6+.

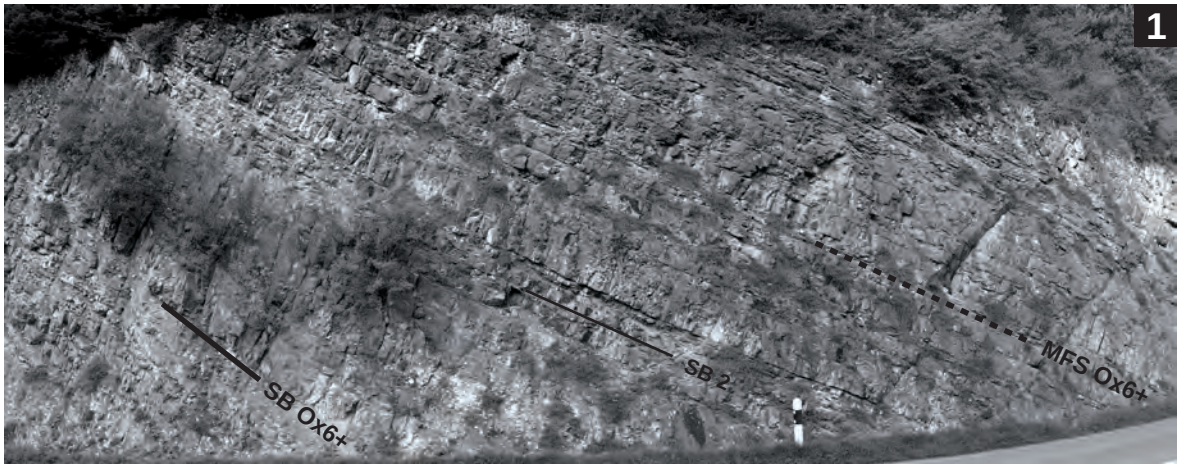
1
SB Ox6+
SB 2
MFS Ox6+

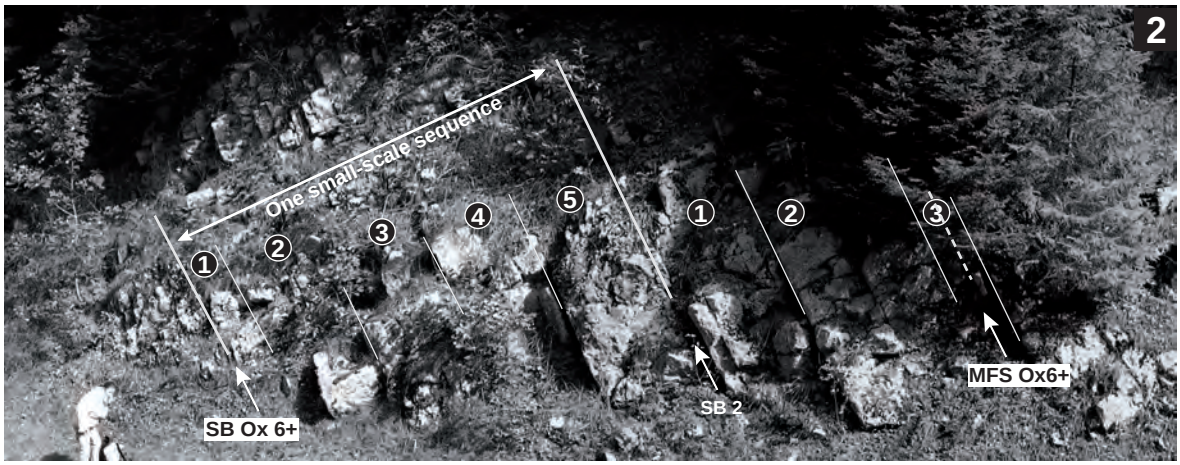
2
One small-scale sequence
1
2
3
4
5
1
2
3
SB Ox 6+
SB 2
MFS Ox6+


3
fault zone
SB Ox 6+
1
2
3
4
5
SB 2
marly
deposits
MFS Ox6+

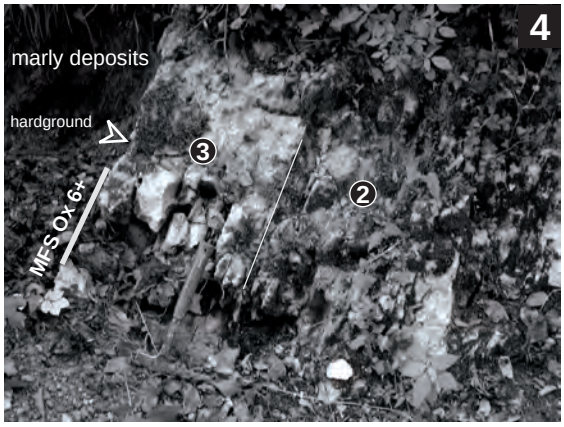
4
marly deposits
hardground
3
2
MFS Ox 6+

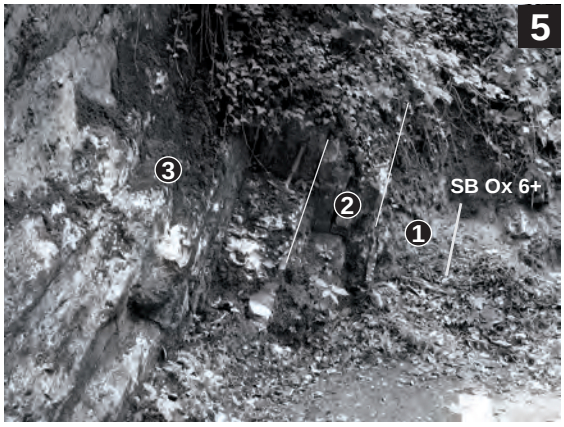
5
3
2
1
SB Ox 6+

PLATE 15 – LORRAINE PLATFORM SECTIONS

1 – Upper part of the Pagny-sur-Meuse quarry exposing the “Calcaires à polypiers de Pagny”, the “Oolithe de Saucourt inférieure”, and the “Marnes à huîtres de Pagny”.

2 – Base of the Pagny-sur-Meuse section around the SB Ox6+ showing an evolution from marly deposits to tidally influenced carbonate deposits, LB = lenticular bedding.

3 – First part of the Pagny-sur-Meuse section characterized by thick dark bioclastic marly limestones.

4 – Enlargement of a bioclastic bed showing important shell accumulations (arrow) probably caused by storms.

5 – Second part of the Pagny-sur-Meuse section dominated by thick bioclastic limestones. Medium-scale, small-scale and elementary sequence boundaries are identified. This part is interpreted as one 100-kyr sequence.

6 – Top part of the Pagny-sur-Meuse section exposing dune crests (arrow). This level is interpreted as the maximum-flooding surface MF Ox6+.

7 – Detail of the maximum-flooding surface MF Ox6+ locally encrusted by oysters.

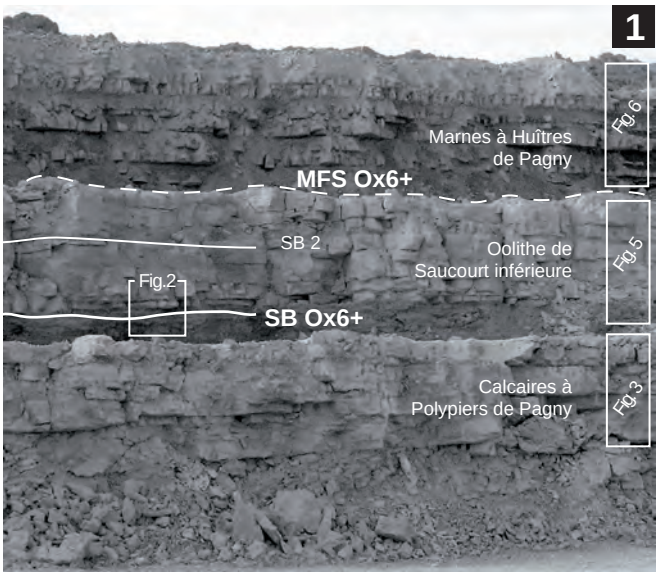
1
Marnes à Huîtres
de Pagny
MFS Ox6+
SB 2
Oolithe de
Saucourt inférieure
Fig.2
SB Ox6+
Calcaires à
Polypiers de Pagny
Fig.6
Fig.5
Fig.3

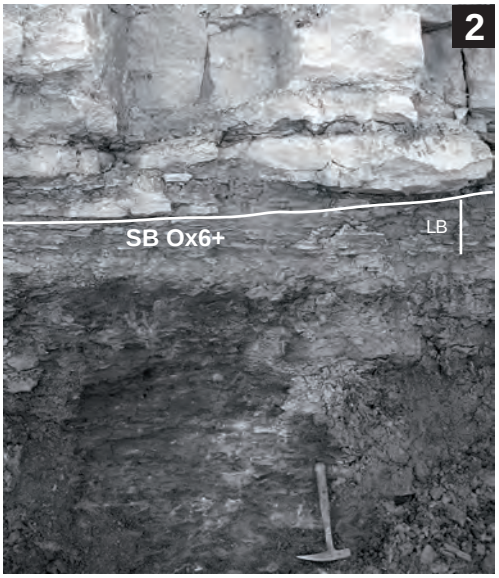
2
SB Ox6+
LB

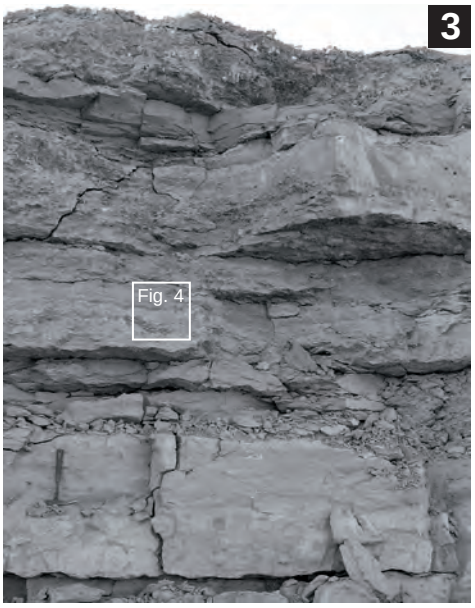
3
Fig. 4

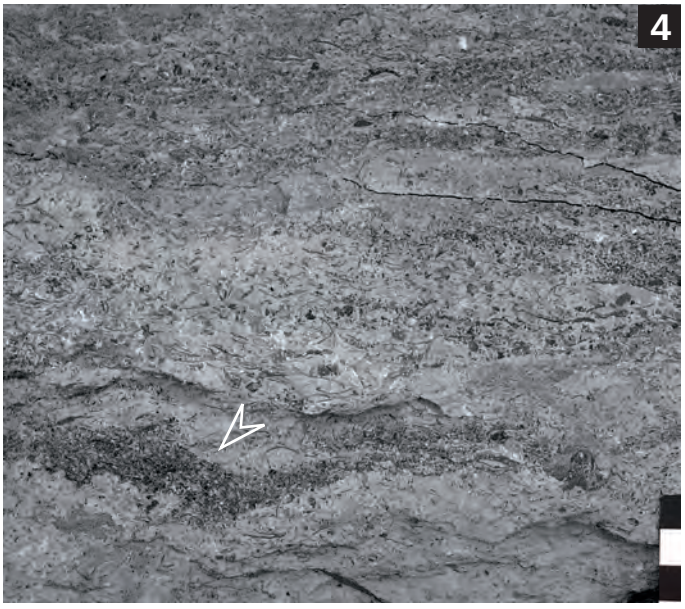
4

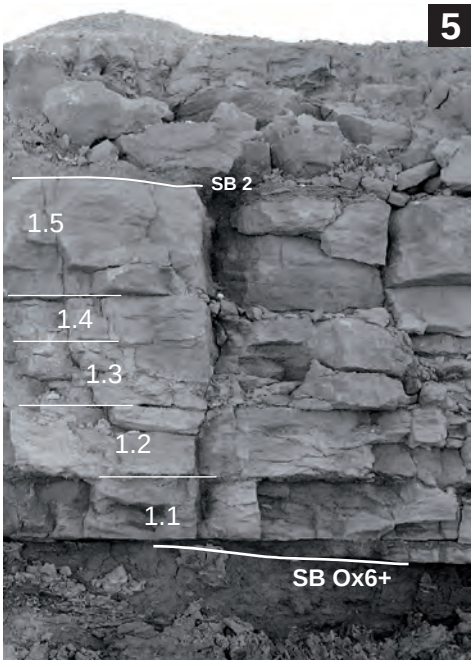
5
SB 2
1.5
1.4
1.3
1.2
1.1
SB Ox6+


6

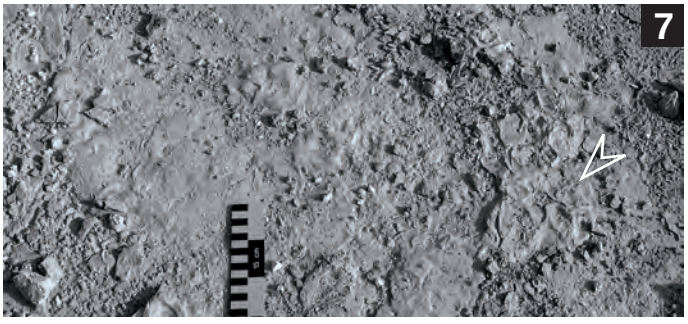
7

PLATE 16 - LORRAINE AND HAUTE-MARNE PLATFORM SECTIONS

1 – Important lateral facies variations in the second part of the Pagny-sur-Meuse section. The base of the outcrop exposes the upper part of a coral bioherm overlain by thin marls on the left side and marl-dominated deposits on the right side. OSI : Oolithe de Saucourt Inférieure ; CPP : Calcaires à Polypiers de Pagny.

2 – Detail of the upper part of the coral bioherm showing karstification (ferrugineous color).

3 – Top part of the Latrecey-sur-Ormoy section exposing thin laminated mudstones. Diagnostic surfaces of different orders are placed according to facies and microfacies analysis, A facies change from relatively thick to thinly laminated limestones marks the MFS Ox6+.

4 – The complete Latrecey-sur-Ormoy section. Mudstone texture and relatively low thicknesses of beds make the recognition of stacking pattern difficult.

5 – Base of the Latrecey-sur-Ormoy section showing massive beds.

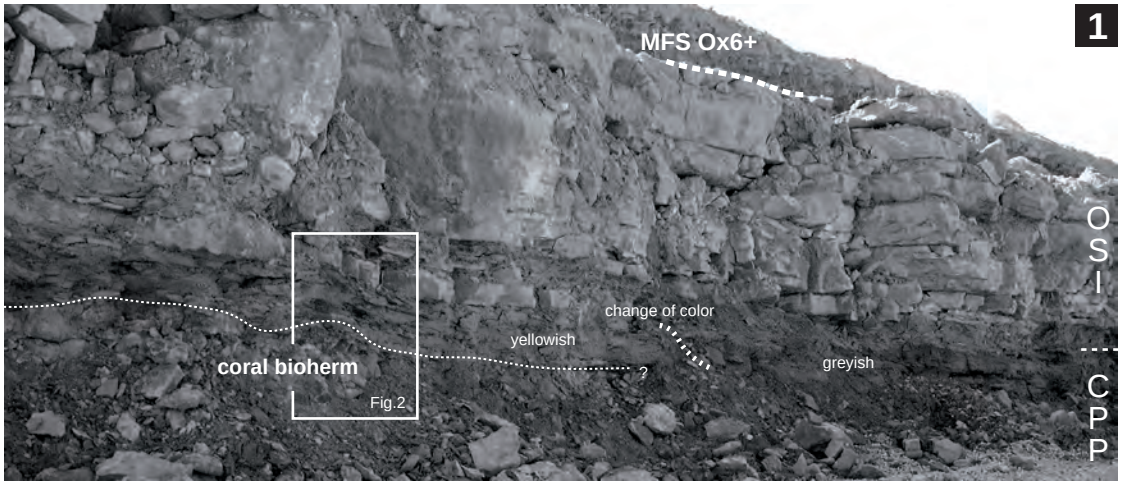
1
MFS Ox6+
O
S
I
C
P
P
change of color
yellowish
greyish
coral bioherm
?
Fig.2

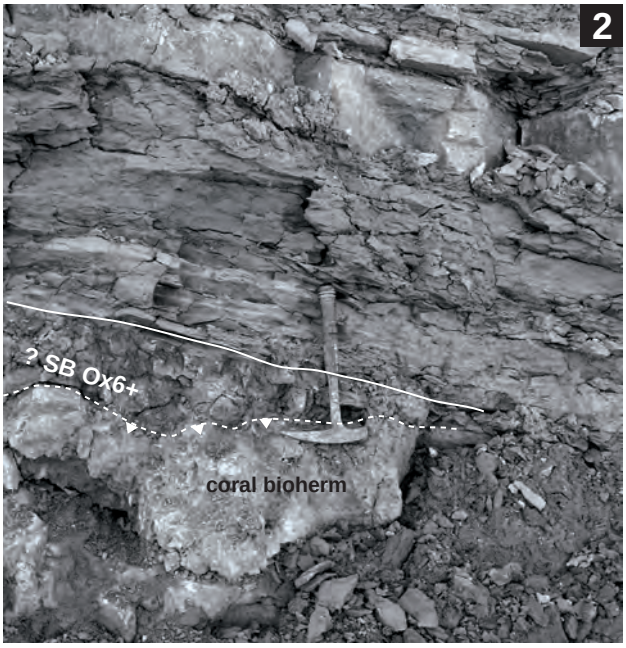
2
? SB Ox6+
coral bioherm

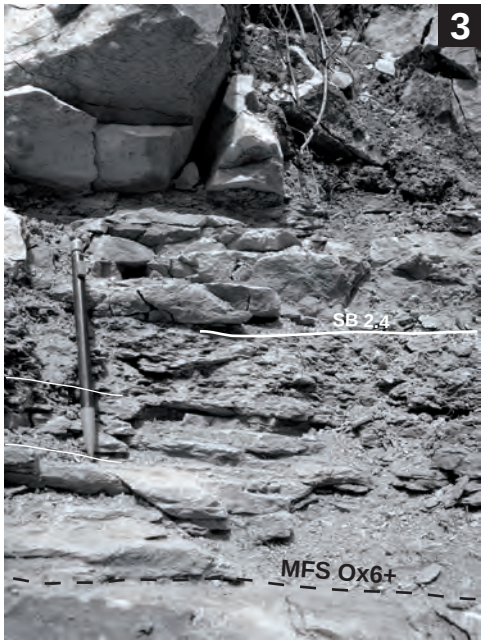
3
SB 2.4
MFS Ox6+


4
Fig.5


5
SB 1.2
SB Ox6+

PLATE 17 – SWABIAN JURA AND SE FRANCE SECTIONS

1 – Base of the Balingen-Tieringen section characterized by marly deposits followed by sponge bioherms.

2 – Balingen-Tieringen section: bioherms are overlain by relatively thick beds.

3 – Panorama of the Vergons section. The numbers of several key beds are indicated. The arrow points to an undulated bed (bed 48), which presents a slump (c.f. Fig. 4).

4 – Enlargement of the mid-part of the Vergons section between bed 45 and 53. Note that bed 48 deforms bed 47 (arrow).

5 – Top part of the Vergons section containing MF Ox6+. The identification of this MF is based on facies and microfacies analysis.

6 – Bed succession in the top part of the Vergons section presenting nodular surfaces, interpreted as the result of intense bioturbation.

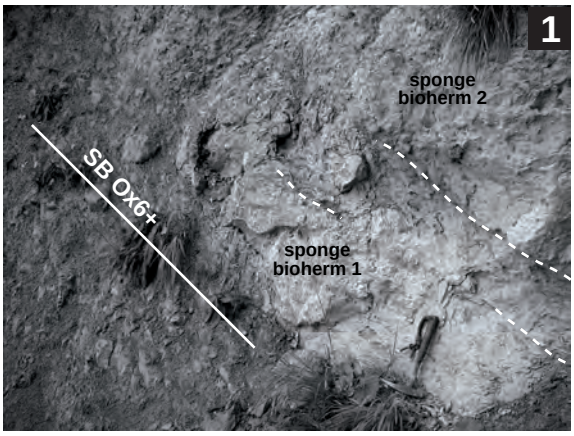
1
sponge bioherm 2
SB Ox6+
sponge bioherm 1

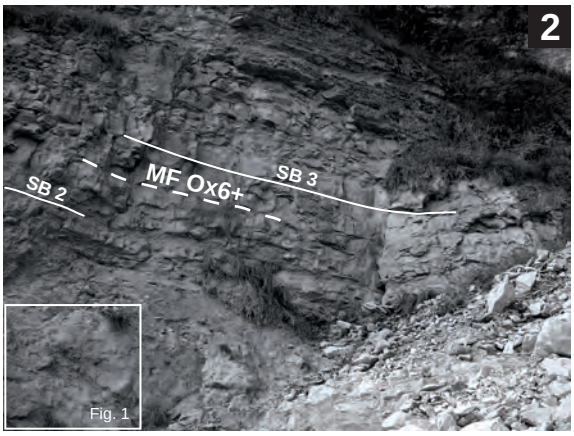
2
SB 2
MF Ox6+
SB 3
Fig. 1

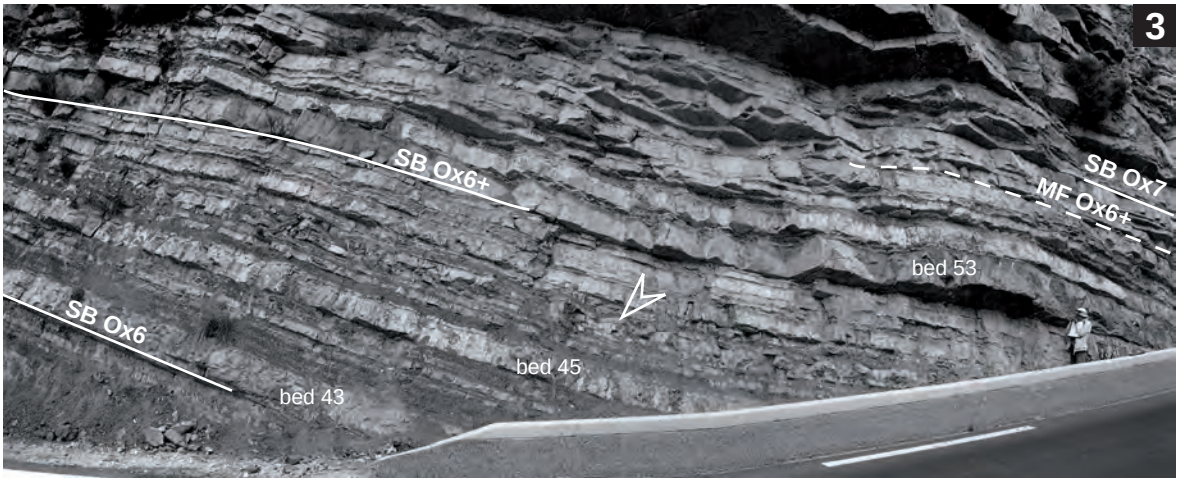
3
SB Ox6+
SB Ox7
MF Ox6+
bed 53
SB Ox6
bed 45
bed 43

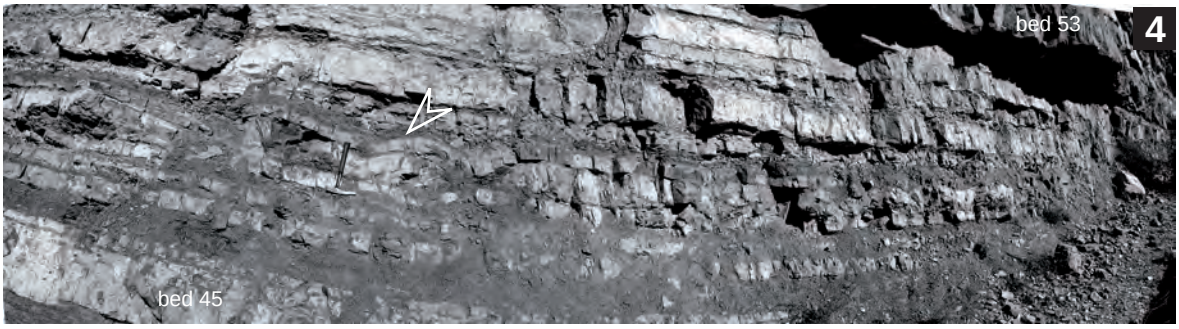
4
bed 53
bed 45

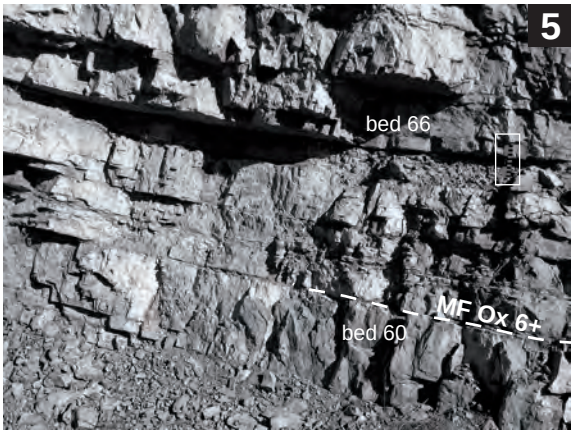
5
bed 66
MF Ox 6+
bed 60

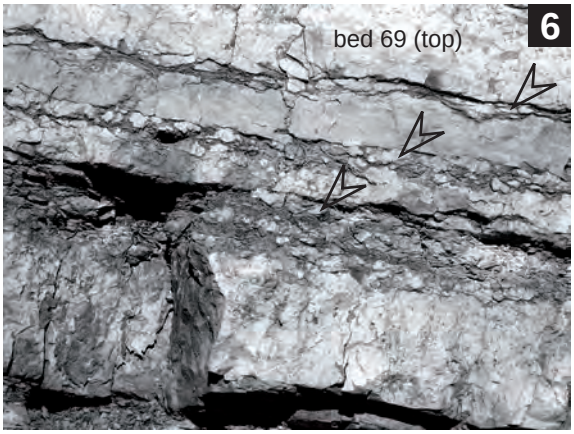
6
bed 69 (top)

ANNEX

Suborder **Rotaliina** DELAGE & HÉROUARD, 1896
Family **Discorbidae** EHRENBERG, 1838
Genus *Mohlerina* BUCUR, SENOWBARI-DARYAN & ABATE, 1996

Mohlerina basiliensis (MOHLER, 1938) pl. 9, figs. 1-11

1938 *Conicospirillina basiliensis* MOHLER n. sp.: MOHLER: 27, pl. 4, fig. 5.

1991 *Conicospirillina basiliensis* MOHLER: DARGA & SCHLAGINTWEIT: 214, pl. 2, fig. 5.

1992 *Conicospirillina basiliensis* MOHLER: DYA: 63, pl. 11, figs. 9-10.

1993 *Archaeosepta basiliensis* (Mohler) nov. comb.: Tasli : 60, pl. 3, figs. 6-7.

1996 *Mohlerina basiliensis* (MOHLER) nov. comb. : BUCUR et al. : 70, pl. 3, figs. 3-6, pl. 4, figs. 2-3, 5-9.

1999 *Mohlerina basiliensis* (MOHLER) : SCHLAGINTWEIT & EBLI : 400, pl. 6, figs. 1-2, ? pl. 4, fig. 10.

2000 *Mohlerina basiliensis* (MOHLER) : DIENI & RADOICIC: figs. 6a-d.

2001 *Mohlerina basiliensis* (MOHLER) : POP & BUCUR: pl. 4, figs. 6-7, 9.

2003 *Mohlerina basiliensis* (MOHLER): GAWLICK et al.: pl. 2, figs. 6-7.

2004 *Conicospirillina basiliensis* Mohler: FLÜGEL: pl. 69, fig. 6.

2004 *Mohlerina basiliensis* (MOHLER): BUCUR et al.: pl. 3, figs 23-24.

2004 *Mohlerina basiliensis* (MOHLER): SERBAN et al.: pl. 4, figs. 14-15.

Annex 1 - Taxonomy of *Mohlerina basiliensis*.

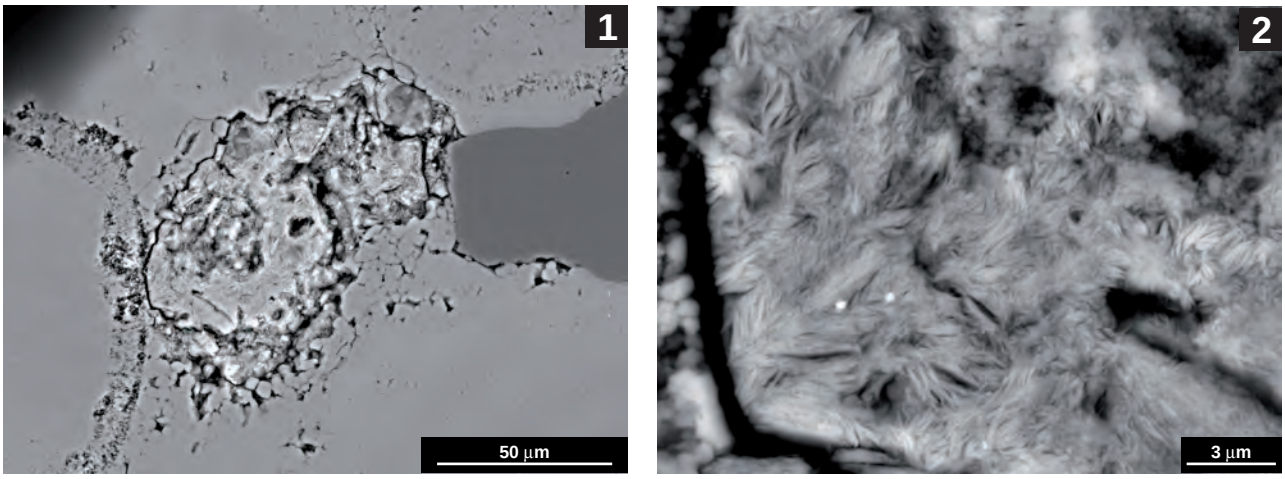

Annex 2a - SEM backscatter photomicrographs of a green grain, sample PG-19. .

Sample PG-19

$Ca_{0.13}\ P_{0.05}\ K_{0.53}\ Na_{0.05}\ Fe_{1.05}\ Mg_{0.28}\ Al_{0.71}\ Si_{3.53}\ O_{10}$ Glauconite composition

Sample BT-16

$K_{0.55}\ Na_{0.04}\ Fe_{1}\ Mg_{0.34}\ Al_{0.83}\ Si_{3.56}\ O_{10}$ Glauconite composition

GLAUCONITE $K_{0.6}\ Na_{0.05}\ Fe^{3+}_{1.3}\ Mg_{0.4}\ Fe^{2+}_{0.2}\ Al_{0.3}\ Si_{3.8}\ O_{10}\ (OH)_2$

CHAMOSITE $Fe^{2+}_{3}\ Mg_{1.5}\ Al_{1}\ Fe^{3+}_{0.5}\ Si_{3}\ Al_{2}\ O_{12}\ (OH)_6$

Annex 2b - Stoechiometric formula obtained by EDX analyses of green grains. These formulae indicate a glauconite composition by comparison with the empirical stoechiometric formulae of glauconite and chamosite.

Code	Section	Samples
si1	PG	20
si2	HR	1,2,3
	VO	1,9,11,33
	VY	16C,16,17C
si3	HR	31,32
	VO	A,B,C,L,34
	VY	23A,25,
	PE	93,G,BPPe76B
si4	HR	6,18
si5	PG	8,15,16,17,18,18A
tf1	PG	19
tf2	CO	BP70
prl1	VY	1,1A,2A,2B,28C
	SA	29,29A,29B,30A,30,31B,32C,32,32B
	CO	BP44,45,46,47
	CO	BP49,50,51
	VY	6A,6C,15C,16As,28,5A,5,5B,6,6B,16B,17,17B,23,23C,24A2,24,26C,27,27As,28A,28B,29
	PE	91,92
	SA	1,1A,1B,1Bbis,2,1C,3,3A,3B,4D,4C,5A
	PE	87B,87C,88,88A
	PE	A,B
	VY	8,9B,9A,13,13A,14A,15A,15B,17D,23A
prl2	PE	F,94,H
	PE	E
	SA	9B,9,13,14,21A20A,22A,22B
	CO	BP58
sol1	PE	68,70,72,73,74
sol2	CO	BP73, Sam2
	VY	34
sol3	CO	SV2,BP53,BP55,BP57
sol4	VO	12A,13
sol5	VO	11B,12
	VY	8A,12,12Cs,24B
	SA	24A,25,25A
	SA	6A,6,6B
	VO	K
sol6	VO	14,A9,15
sol7	VO	7A,7,8,A5,10B,10
	CO	BP74,BP75
	VY	10,10C,11,22B,22,24C,24A1,26A,26B,31,33
	PE	76.1,76
	PE	90,D
	VY	3,3A,4,7,7A,10A,22A
ol1	VO	24A,25,26
ol2	VO	N,O,Q,R,R1,S
	VO	M
	VY	30,32
	CO	JP80,JP81,BP85
	PE	89,C
ol3	SA	4A,4,4B,5
	VY	20C,21,21A,21B,22A,24bis,26
	SA	10,11,12,12A
	SA	18,19
	PE	BP77,BP78,78A,78B,80A
ol4	VO	24A,25,26
	VO	20, 20B,21,22A,22,23,24
	PE	BP80,81A,BP81,81B,82A,BP82,83A,BP83,84A,BP84,84B,BP85
ol5	SA	19A,19B,20
	VY	9,18,19,20,20A,20B
	SA	7,8,9A
ol6	PE	86,86B,87A,87
bar1	CO	BP82,JP78
bar2	PE	66, 67
	VY	10B,11A,11B,11C,12B,12A,13B,14,14B,20A
	VO	27,28,29,30
bar3	VO	31A,31
bar4	VO	32A,32,32B
bar5	CO	JP29
	HR	8,9A,9B,10,11,12,13,14,15,16,22,23,24,25
bar6	VO	F,E,G,A4,6CB,6B,6C
	VO	2,J,3
	SA	15,16A,16B,16C
	SA	23,24,26
	SA	26A,27
	CO	BP83,JP79, Sam1
	CO	BP79,BP80,SV6,BP81,JP77
bar7	CO	BP59,BP60,BP61,JP18,JP13,BP62,BP77,BP78
	VO	18A,18,19A,19,19B,20A
	VO	16,17A,17,17B
	PE	BP79
bar8	PG	21C,23,24A,B,26,27,28,29,30,31,33,34,35,36A,36B,37A,38
bar9	PG	21A,B
bar10	PG	39B
bar11	PG	32
c1	HR	29,30
c2	HR	4,5A,5B,6,17A,17B
	CO	BP63,JP10,BP64,JP4,BP65,BP66,BP67,BP68,BP69,BP70,JP108,BP72,BP76
c3	HR	7A,7B,19,20,21,28
c4	HR	26,27
dp1	BT	1,2,4,36
dp2	BT	8,9,13,18,20,2729,41,47
dp3	BT	3,5,6,7
dp4	LA	all samples
dp5	BT	39A,B,40
dp6	BT	22,23,25
dp7	BT	26,28
dp8	BT	10,15
dp9	BT	11,12,14,16,19,21,24,30,31,33,34,35,37,38,46
dp10	BT	42,43,44,45
b1	VG	21,24,25A
b2	VG	13
b3	VG	1,2,5,8,11,15,16,19,26,28,29,33,34,37,39.2,47,49
b4	VG	17,20,21
b5	VG	7A,C,9,10,17,20,23,25,31,32,35,36,38,39.1,40,42,43,44,45,46
b6	VG	22
b7	VG	12A,B,18,48

Annex 3 - List of samples for each microfacies types (cf. Tab. 2.1, 2.2, 2.3).

VOYEBOEUF									
Samples	**Position (m)**	**Seq. position**	**Nb total**	**Aggl**	**Hyal**	**Porc**	**% Aggl**	**% Hyal**	**% Porc**
3	0.895	0.1	5	1	4	0	20	80	0
3A	1.09	2.9	10	3	7	0	30	70	0
4	1.16	4.5	5	2	3	0	40	60	0
5A	1.24	5.6	4	2	2	0	50	50	0
5	1.32	5.9	8	6	2	0	75	25	0
5B	1.39	0.1	8	7	1	0	88	13	0
6	1.43	0.2	9	7	2	0	78	22	0
6A	1.54	2.9	2	1	1	0	50	50	0
6C	1.6	3.25	1	1	0	0	100	0	0
6B	1.81	4	1	1	0	0	100	0	0
7	2.03	4.75	8	5	3	0	63	38	0
7A	2.32	5.8	20	8	12	0	40	60	0
8A	2.38	0.2	12	11	1	0	92	8	0
8	2.545	1.8	10	10	0	0	100	0	0
9	2.63	2.25	18	15	3	0	83	17	0
9B	2.85	5	15	9	6	0	60	40	0
9A	2.94	5.9	1	1	0	0	100	0	0
10A	2.97	0.1	12	8	4	0	67	33	0
10	3.02	0.2	43	38	3	2	88	7	5
10C	3.55	1.5	48	45	0	3	94	0	6
10B	4.1	2.9	39	36	0	3	92	0	8
11	4.33	3.4	14	7	5	2	50	36	14
11A	4.38	3.5	40	33	5	2	83	13	5
11B	4.58	4	28	21	4	3	75	14	11
11C	4.75	4.4	18	12	1	5	67	6	28
12B	4.79	4.5	42	26	3	13	62	7	31
12A	5.02	5	25	12	3	10	48	12	40
12	5.33	5.9	8	3	4	1	38	50	13
12Cs	5.36	6	4	4	0	0	100	0	0
13	5.42	0.1	14	14	0	0	100	0	0
13B	5.67	2	13	10	3	0	77	23	0
13A	5.81	2.9	15	13	2	0	87	13	0
14A	5.84	3.1	17	14	0	3	82	0	18
14	5.92	5	32	22	8	2	69	25	6
15A	6.12	1.4	22	21	0	1	95	0	5
15B	6.32	2.9	5	5	0	0	100	0	0
15C	6.35	3.1	3	3	0	0	100	0	0
16B	6.51	0.1	5	5	0	0	100	0	0
16As	6.59	1	1	1	0	0	100	0	0
17D	6.65	1	6	6	0	0	100	0	0
17	6.72	1.8	6	6	0	0	100	0	0
17B	6.78	2.25	5	4	1	0	80	20	0
18	6.84	3.1	11	8	1	2	73	9	18
19	6.87	3.2	13	11	2	0	85	15	0
20	7.06	3.9	17	12	1	4	71	6	24
20A	7.22	4.1	22	10	3	9	45	14	41
20B	7.8	5.8	30	8	2	20	27	7	67
20C	7.82	5.9	26	12	1	13	46	4	50
21	7.87	0.1	42	28	4	10	67	10	24
21A	8.01	0.8	46	28	10	8	61	22	17
21B	8.04	0.9	43	32	2	9	74	5	21
22A	8.09	1.1	35	31	1	3	89	3	9
22B	8.2	1.9	38	34	1	3	89	3	8
22	8.43	2.8	35	23	3	9	66	9	26
23	8.57	4.5	11	9	2	0	82	18	0
23A	8.66	5.5	13	12	1	0	92	8	0
23C	8.72	0.1	13	13	0	0	100	0	0
24A2	8.77	0.5	9	9	0	0	100	0	0
24	8.84	0.9	19	18	1	0	95	5	0
24B	9	1.5	23	21	2	0	91	9	0
24C	9.14	2	31	28	3	0	90	10	0
24bis	9.29	2.8	27	26	1	0	96	4	0
24A1	9.33	2.9	21	19	2	0	90	10	0
26	9.49	0.1	52	47	5	0	90	10	0
26A	9.6	0.9	33	31	2	0	94	6	0
26B	9.8	1.9	44	36	8	0	82	18	0
26C	9.94	2.5	10	8	2	0	80	20	0
27	10	2.9	9	9	0	0	100	0	0
27As	10.02	3	5	5	0	0	100	0	0
28A	10.08	5	2	1	1	0	50	50	0
28B	10.14	6	8	7	1	0	88	13	0
28C	10.19	0.2	1	0	0	1	0	0	100
28	10.22	0.25	5	4	0	1	80	0	20
29	10.32	0.6	2	2	0	0	100	0	0
30	10.46	1.25	6	6	0	0	100	0	0
31	10.71	2	25	17	1	7	68	4	28
32	10.96	2.9	28	10	3	15	36	11	54
33	11.04	3	32	21	4	7	66	13	22
34	11.4	0.1	19	16	3	0	84	16	0

VORBOURG									
Samples	**Position (m)**	**Seq. position**	**Nb total**	**Aggl**	**Hyal**	**Porc**	**% Aggl**	**% Hyal**	**% Porc**
F	1.51		15	15	0	0	100	0	0
E	1.8		17	17	0	0	100	0	0
G	1.87		11	9	2	0	82	18	0
H	2.06		28	18	10	0	64	36	0
I	2.24		20	18	2	0	90	10	0
2	2.4		10	5	5	0	50	50	0
J	2.43		9	9	0	0	100	0	0
3	2.55		29	26	3	0	90	10	0
4	2.7		24	19	5	0	79	21	0
5	2.84		16	13	3	0	81	19	0
6CB	2.89		25	22	3	0	88	12	0
6B	2.93		24	23	1	0	96	4	0
6	3.02		23	23	0	0	100	0	0
6C	3.15		13	13	0	0	100	0	0
7A	3.25		29	26	3	0	90	10	0
7	3.5		42	37	5	0	88	12	0
8	3.57		51	46	5	0	90	10	0
A5	3.77	0.1	39	36	3	0	92	8	0
10B	3.9	1.5	47	43	4	0	91	9	0
10	4.05	2.9	77	77	0	0	100	0	0
11B	4.53	0.1	55	54	1	0	98	2	0
12	4.62	1.5	59	59	0	0	100	0	0
12A	4.8	3.2	32	32	0	0	100	0	0
13	5.06	5.9	51	51	0	0	100	0	0
14	5.1	0.1	56	56	0	0	100	0	0
A9	5.14	0.5	19	18	1	0	95	5	0
15	5.35	3.1	29	28	0	1	97	0	3
16	5.55	5.9	17	13	4	0	76	24	0
17A	5.58	0.1	19	18	1	0	95	5	0
17	5.6	0.15	20	20	0	0	100	0	0
17B	5.68	0.4	12	10	2	0	83	17	0
18A	5.77	0.5	10	10	0	0	100	0	0
18	5.95	1	17	16	0	1	94	0	6
19A	6.03	1.1	31	31	0	0	100	0	0
19	6.67	2.6	16	10	3	3	63	19	19
19B	6.76	2.9	20	18	1	1	90	5	5
20A	6.81	3.1	32	20	0	12	63	0	38
20	6.95	3.5	35	17	4	14	49	11	40
21	7.6	5.8	23	11	4	8	48	17	35
22A	7.72	0.1	12	10	2	0	83	17	0
22	8.06	2.5	37	26	4	7	70	11	19
23	8.82	2.5	47	37	1	9	79	2	19
24	9.26	4.5	5	3	0	2	60	0	40
24A	9.87	5.9	40	1	7	32	3	18	80
25	9.93	6	23	2	1	20	9	4	87
26	10.07	0.5	16	12	0	4	75	0	25
27A	10.2	1	3	3	0	0	100	0	0
27	10.48	1.5	3	3	0	0	100	0	0
28	10.76	2.8	4	4	0	0	100	0	0
29	10.86	3	1	0	1	0	0	100	0
30	11.78	5.8	3	2	1	0	67	33	0
31A	13.67	3	4	3	1	0	75	25	0
31	13.78	4.5	3	2	1	0	67	33	0
32A	13.98	0.1	24	24	0	0	100	0	0
32	14.18	2.5	10	9	1	0	90	10	0
32B	14.38	2.9	17	16	1	0	94	6	0
K	14.65	0.1	0	0	0	0	0	0	0
M	15.11	0.1	1	0	1	0	0	100	0
N	15.37	0.2	2	1	1	0	50	50	0
O	15.5		3	0	3	0	0	100	0
P	15.6		4	3	1	0	75	25	0
Q	15.67		32	27	5	0	84	16	0
R	15.76		27	20	7	0	74	26	0
R1-a	15.95		16	15	1	0	94	6	0
S	16.43		37	37	0	0	100	0	0

Annex 4a - Absolute abundance of benthic foraminifera in the Voyeboeuf and Vorbourg sections.

SAVAGNIERES									
Samples	Position (m)	Seq. position	Nb total	Aggl	Hyal	Porc	% Aggl	% Hyal	% Porc
1	0.025		2	1	1	0	50	50	0
1A	0.25		7	0	7	0	0	100	0
1Bbis	0.59		2	2	0	0	100	0	0
2	0.71		3	3	0	0	100	0	0
3A	1.04		1	1	0	0	100	0	0
3B	1.31		10	4	6	0	40	60	0
4A	1.46	1.5	41	1	40	0	2	98	0
4	1.56	2	9	3	6	0	33	67	0
4B	1.67	3.1	8	6	2	0	75	25	0
4D	1.89	4.5	6	4	2	0	67	33	0
4C	2.12	6	1	1	0	0	100	0	0
5	2.24	2	9	5	4	0	56	44	0
6A	2.565	4.5	12	5	7	0	42	58	0
6	2.63	4.8	7	5	2	0	71	29	0
6B	2.815	5.9	13	8	5	0	62	38	0
7	3.09	1.5	10	5	5	0	50	50	0
8	3.39	2.9	4	2	0	2	50	0	50
9A	3.46	3.1	16	5	5	6	31	31	38
9B	3.95	5	10	8	2	0	80	20	0
9	4.21	5.9	14	11	3	0	79	21	0
10	4.26	0.1	15	5	7	3	33	47	20
11	4.73	3.1	11	3	3	5	27	27	45
12	5.41	5.8	6	5	1	0	83	17	0
12A	5.485	5.9	6	4	2	0	67	33	0
13	5.545	0.1	10	3	3	4	30	30	40
14	6.08	2.9	13	4	6	3	31	46	23
15	6.35	3.2	13	9	2	2	69	15	15
16A	6.51	4.5	10	6	3	1	60	30	10
16B	6.755	5.8	12	10	2	0	83	17	0
16C	6.795	5.9	10	9	1	0	90	10	0
18	6.845	0.1	4	2	0	2	50	0	50
19	6.89	0.2	6	4	2	0	67	33	0
19A	7.29	1	16	6	10	0	38	63	0
19B	7.57	2	21	12	7	2	57	33	10
20	7.93	2.9	5	2	3	0	40	60	40
20A	7.98	3.1	25	11	2	12	44	8	0
21A	8.15	5.9	17	10	3	4	59	18	71
22A	8.2	0.1	13	13	0	0	100	0	31
22B	8.34	0.4	31	29	1	1	94	3	3
23	8.39	0.5	19	14	2	3	74	11	16
24	8.64	1.1	10	1	9	0	10	90	0
24A	9.33	2.75	4	3	1	0	75	25	0
25	9.42	3.1	11	6	3	2	55	27	18
25A	9.51	5.9	3	3	0	0	100	0	0
26	9.57	0.2	16	14	2	0	88	13	0
26A	10.19	2.2	5	2	2	1	40	40	20
27	10.34	2.8	9	9	0	0	100	0	0
29	10.82	4.5	7	3	3	1	43	43	14
29A	11.1	5.2	9	7	0	2	78	0	22
29B	11.275	5.9	6	6	0	0	100	0	0
30A	11.325	0.1	13	13	0	0	100	0	0
30	11.56	2.8	6	6	0	0	100	0	0
31Bbis	11.615	3	10	9	1	0	90	10	0
31B	11.71	5.9	11	10	1	0	91	9	0
32C	11.745	0.1	11	10	1	0	91	9	0
32	11.99	2.9	7	6	1	0	86	14	0
32B	12.05	3.1	9	8	1	0	89	11	0

PERTUIS									
Samples	Position (m)	Seq. position	Nb total	Aggl	Hyal	Porc	% Aggl	% Hyal	% Porc
66	1.25		29	28	1	0	97	3	0
67	1.65		24	23	1	0	96	4	0
68	1.94		172	169	3	0	98	2	0
70	2.43		55	54	1	0	98	2	0
72	2.75		2	2	0	0	100	0	0
73	3.03		35	35	0	0	100	0	0
74	3.21		71	70	1	0	99	1	0
76.1	3.57	2	40	26	14	0	65	35	0
77	3.92	1.5	1	1	0	0	100	0	0
78	4.15	3.5	13	8	4	1	62	31	8
78A	4.54	5	20	15	3	2	75	15	10
78B	4.81	5.9	7	3	3	1	43	43	14
80A	5.08	3.1	8	2	6	0	25	75	0
80	5.36	4	5	4	1	0	80	20	0
80B	5.47	4.5	22	14	4	4	64	18	18
81A	5.5	4.6	17	13	3	1	76	18	6
81	5.69	5	13	8	3	2	62	23	15
81B	5.92	5.9	33	14	11	8	42	33	24
82A	5.95	0.1	25	15	4	6	60	16	24
82	6.17	1.5	15	8	2	5	53	13	33
83A	6.45	3.1	10	1	8	1	10	80	10
83	7.34	4.5	11	6	2	3	55	18	27
84A	7.73	5	12	6	3	3	50	25	25
84	8.275	5.7	13	9	1	3	69	8	23
84B	8.41	5.9	36	6	2	28	17	6	78
85	8.77	1.5	28	8	2	18	29	7	64
86	9.47	4	35	12	1	22	34	3	63
86B	10.67	5.9	61	23	6	32	38	10	52
87A	10.71	0.1	69	28	13	28	41	19	41
87	10.9	1	28	13	2	13	46	7	46
87B	11.435	2.9	11	5	3	3	45	27	27
87C	11.48	3.1	4	3	1	0	75	25	0
88	11.81	4.5	12	8	1	3	67	8	25
88A	12	5.9	27	21	2	4	78	7	15
A	12.07	0.1	28	23	3	2	82	11	7
B	12.14	1	50	37	5	8	74	10	16
C	12.31	2.5	16	9	1	6	56	6	38
89	12.66	5.9	24	12	0	12	50	0	50
90	12.79	1.5	35	33	0	2	94	0	6
D	12.89	2.9	21	19	2	0	90	10	0
E	13	4.5	24	17	1	6	71	4	25
91	13.12	0.1	27	24	1	2	89	4	7
92	13.24	1.5	14	2	1	11	14	7	79
F	13.48	2.9	27	5	6	16	19	22	59
94	13.72	0.1	28	6	1	21	21	4	75
H	13.955	4	15	9	0	6	60	0	40

Annex 4b - Absolute abundance of benthic foraminifera in the Savagnières and Pertuis sections.

VOYEBOEUF	
Samples	**Nb *Mohlerina***
18	1
19	1
20A	2
20B	1
22	1

VORBOURG	
Samples	**Nb *Mohlerina***
20	3
21	4
22A	1
22	4
24A	7
25	1

SAVAGNIERES	
Samples	**Nb *Mohlerina***
6A	2
6B	3
7	4
14	1
19A	8
19B	5
20	3
20A	2

PERTUIS	
Samples	**Nb *Mohlerina***
78	4
78A	3
78B	3
80A	6
80	1
80B	4
81A	2
81	3
81B	11
82A	4
82	1
83A	7
83	2
84A	3
84	1
84B	1
85	2
86	1
86B	6
87A	12
87	2

Annex 5 - Absolute abundance of the benthic foraminifer *Mohlerina basiliensis* in the Voyeboeuf, Vorbourg, Savagnières, and Pertuis sections.

	Sample	N°GEA	Position (m)	Sequential		from the <2µm glycoled fraction								from the <16µm fraction			from the <2µm glycoled fraction						<2µm fraction
				elem. seq.	interval	M 001 8.8 - 8.9°	IS 9 - 9.3°	K001 / C002 12.2 - 12.4°	M 002 17.8 - 17.9°	K 002 24.8 - 24.9°	C 004 25.1 - 25.2°	K001 calc	C002calc	Quartz 20.85°	Feldspar 27.5 - 27.6°	Plagio. 27.9°	SUM	% Kaol	% Mica	% Chl	% Ill-Sm	K/I	K/IS	illite cristallinity in Δ2 θ Cu Kα
SAVAGNIERES SECTION	SA-4A	983	1.46	1	1	420	27	424	150	341	24	396	28	327	57		871	45	48	3	3	0.9	14.7	0.44
	SA-4D	984	1.89	4.5	4.5	463	35	410	113	317	28	377	33	206	141		908	41	51	4	4	0.8	10.8	0.33
	SA-4C	985	2.12	5.9	5.9	269	25	310	117	320	58	262	48	681	94		604	43	45	8	4	1.0	10.5	
	SA-5a		2.18	0.1	6.1	250	89	414	134	440	51	371	43	20	10		753	49	33	6	12	1.5	4.2	0.44
	SA-6		2.64	4.8	10.8	591	54	516	137	505	64	458	58	31	71		1161	39	51	5	5	0.8	8.5	0.24
	SA-7		3.09	1.25	13.25	456	39	523	136	454	63	459	64	87	10		1018	45	45	6	4	1.0	11.8	0.22
	SA-8	986	3.4	2.9	14.9	373	10	667	113	609	25	641	26	188	44		1050	61	36	3	1	1.7	64.1	0.22
	SA-9B		3.95	5	17	352	49	763	164	651	75	684	79	71	10		1164	59	30	7	4	1.9	14.0	0.22
	SA-10	987	4.26	0.1	18.1	160	43	355	66	282	30	321	34	336	111		558	58	29	6	8	2.0	7.5	0.22
	SA-11	402	4.725	3.1	21.1	165	67	357	92	439	11	348	9	33	25		589	59	28	1	11	2.1	5.2	0.22
	SA-13	988	5.55	0.1	24.1	312	45	484	120	405	44	437	47	116	143		841	52	37	6	5	1.4	9.7	0.44
	SA-15		6.24	3.5	27.5	301	34	350	133	332	57	299	51	305	76		685	44	44	7	5	1.0	8.8	0.67
	SA-16B	989	6.75	5.8	29.8	190	41	272	84	197	33	233	39	330	60		503	46	38	8	8	1.2	5.7	0.49
	SA-19B		7.57	2	32	306	45	597	106	505	20	574	23	91	10		948	61	32	2	5	1.9	12.8	0.22
	SA-20	990	7.93	2.9	32.9	287	56	541	96	438	48	488	53	174	44		884	55	32	6	6	1.7	8.7	0.22
	SA-21A	991	8.15	5.9	35.9	191	75	391	110	378	48	347	44	174	81		657	53	29	7	11	1.8	4.6	0.44
	SA-22B	992	8.34	0.4	36.4	212	149	484	136	436	28	455	29	266	71		845	54	25	3	18	2.1	3.1	0.33
	SA-25	993	9.41	3.1	39.1	228	47	389	234	649	63	355	34	181	98		664	53	34	5	7	1.6	7.5	0.78
	SA-26A	994	10.19	2.2	44.2	428	23	583	101	436	46	527	56	216	70		1034	51	41	5	2	1.2	22.9	0.27
	SA-27	995	10.34	2.8	44.8	481	84	822	219	831	54	772	50	135	53		1387	56	35	4	6	1.6	9.2	0.33
	SA-29		10.82	4.4	50.4	313	24	651	128	677	97	569	82	163	35		988	58	32	8	2	1.8	23.7	0.18
	SA-29B	996	11.28	5.9	47.9	245	68	485	130	427	61	424	61	196	76		798	53	31	8	9	1.7	6.2	0.27
	SA-30	997	11.59	2.8	50.8	229	35	521	145	573	49	480	41	128	71		785	61	29	5	4	2.1	13.7	0.33
	SA-31B BIS	998	11.61	3	51	313	110	863	174	842	56	809	54	79	48		1286	63	24	4	9	2.6	7.4	0.67
	SA-31 B	403	11.71	5.9	53.9	331	100	1062	190	1146	85	989	73	71	10		1493	66	22	5	7	3.0	9.9	0.33
	SA-32C	999	11.75	0.1	54.1	533	57	692	196	589	144	556	136	368	123		1282	43	42	11	4	1.0	9.8	0.24
BALINGEN-TIERINGEN SECTION	BT-13	404	5.42			120	54	175	94	140	87	108	67	117	68		349	31	34	19	15	0.9	2.0	0.85
	BT-16	405	6.15			189	84	224	109	223	115	148	76	812	87		497	30	38	15	17	0.8	1.8	0.46
	BT-18		6.37			183	97	399	207	462	129	312	87	303	221		679	46	27	13	14	1.7	3.2	0.47
	BT-19	406	6.53			246	60	211	84	162	30	178	33	571	107		517	34	48	6	12	0.7	3.0	0.65
	BT-20M	407	6.625			373	92	263	112	206	47	214	49	157	59		728	29	51	7	13	0.6	2.3	0.65
	BT-21	408	6.68			345	105	381	141	384	79	316	65	624	81		831	38	42	8	13	0.9	3.0	0.75
	BT-22	409	7.43			328	43	491	140	393	94	396	95	1429	195		862	46	38	11	5	1.2	9.2	
	BT-24	410	7.65			199	66	317	133	196	66	237	80				582	41	34	14	11	1.2	3.6	
	BT-25B	411	8.5			251	103	434	132	371	115	331	103	339	128		788	42	32	13	13	1.3	3.2	
	BT-26A	412	8.62			287	152	429	118	248	130	281	148	202	66		868	32	33	17	18	1.0	1.9	0.62
	BT-27M	413	8.8			226	72	367	139	370	119	278	89	609	164		665	42	34	13	11	1.2	3.9	0.65
	BT-28	414	9.445			420	203	600	220	407	110	472	128	641	146		1223	39	34	10	17	1.1	2.3	0.63
	BT-29	415	9.73			386	158	709	259	598	215	522	187	462	193		1253	42	31	15	13	1.4	3.3	
	BT-30B	416	9.83			225	90	362	126	282	72	288	74	270	89		677	43	33	11	13	1.3	3.2	0.63
	BT-31	417	10.03			347	122	345	89	196	93	234	111	394	118		814	29	43	14	15	0.7	1.9	0.44
	BT-32M	418	10.125			161	62	299	114	346	144	211	88	366	122		522	40	31	17	12	1.3	3.4	0.47
	BT-33	419	10.2			331	118	422	142	271	135	282	140	629	114		871	32	38	16	14	0.9	2.4	0.48
	BT-34	420	10.31			228	65	457	103	397	111	357	100	454	75		750	48	30	13	9	1.6	5.5	0.85
	BT-35	421	10.55			201	52	352	85	309	59	296	56	610	118		605	49	33	9	9	1.5	5.7	0.75
	BT-36M		10.8			344	133	539	143	437	110	431	108	355	107		1016	42	34	11	13	1.3	3.2	0.96
	BT-37		11			165	83	267	105	211	93	185	82	829	106		515	36	32	16	16	1.1	2.2	0.46
	BT-38		11.28			260	119	558	131	585	131	456	102	717	105		937	49	28	11	13	1.8	3.8	0.75
	BT-39B		11.5			413	103	642	129	398	118	495	147	1506	167		1158	43	36	13	9	1.2	4.8	0.48
	BT-40		11.68			474	185	513	158	371	68	434	79	648	115		1172	37	40	7	16	0.9	2.3	0.67
	BT-41M		11.72			221	143	646	191	759	155	536	110	593	147		1010	53	22	11	14	2.4	3.8	0.54
	BT-42		11.82			132	134	621	139	536	176	467	154	953	147		887	53	15	17	15	3.5	3.5	0.69
	BT-44		12.36			246	73	309	120	322	113	229	80	714	99		628	36	39	13	12	0.9	3.1	0.81
VERGONS SECTION	VG-20	422	6.85			165	34	180	112	55	106	61	119	1233		7013	379	16	44	31	9	0.4	1.8	0.43
	VG-21		6.95			169	107	145	138	67	63	75	70	570		996	421	18	40	17	25	0.4	0.7	0.65
	VG-22	423	7.1			239	33	297	108	185	99	193	104	2522		10176	569	34	42	18	6	0.8	5.9	0.26
	VG-23	424	7.82			136	57	102	88	18	105	15	87	900		5009	295	5	46	30	19	0.1	0.3	0.64
	VG-24M		8.14			171	184	168	145	108	10	154	14	447		182	523	29	33	3	35	0.9	0.8	0.76
	VG-25	425	8.41			218	106	294	188	12	164	20	274	1362		5664	618	3	35	44	17	0.1	0.2	0.47
	VG-27		8.62			210	88	61	62	24	53	19	42	483		2493	359	5	58	12	25	0.1	0.2	0.54
	VG-28	426	8.7			153	67	47	134	5	21	9	38	815		8257	267	3	57	14	25	0.1	0.1	0.65
	VG-29	427	8.79			113	61	90	115	27	64	27	63	1316		10296	264	10	43	24	23	0.2	0.4	0.48
	VG-30M		9.05			337	122	127	188	107	15	111	16	473		106	586	19	58	3	21	0.3	0.9	0.65
	VG-31	428	9.22			188	47	207	89	1	75	3	204	1749		8808	442	1	43	46	11	0.0	0.1	
	VG-32	429	9.38			294	88	119	90	19	58	29	90	1124		13083	501	6	59	18	18	0.1	0.3	
	VG-33	430	9.48			251	63	33	133	7	42	5	28	744		2949	347	1	72	8	18	0.0	0.1	0.54
	VG-35	431	9.63			153	38	23	106	6	35	3	20	2132		12273	214	2	71	9	18	0.0	0.1	0.41
	VG-36	432	9.85			170	68	41	112	16	8	27	14	738		6566	279	10	61	5	24	0.2	0.4	0.54
	VG-37	433	10.02			122	72	10	65	2	7	2	8	726		6203	204	1	60	4	35	0.0	0.0	0.43
	VG-38	434	10.13			237	28	25	81	1	20	1	24	1418		18453	290	0	82	8	10	0.0	0.0	0.47

Annex 6 - Clay-mineral analysis of the Savagnières, Balingen-Tieringen, and Vergons sections. The samples used for the Fig. 8.10 are in grey.

SAVAGNIERES				
Samples	**Position (m)**	**Seq. position**	**$\delta^{13}C$**	**$\delta^{18}O$**
SA-4D	1.89	4.5	1.60	-4.38
SA-5	2.24	2	1.91	-4.35
SA-6A	2.73	4.5	1.69	-4.47
SA-6	2.78	4.8	1.90	-4.49
SA-8	3.55	2.9	1.34	-4.89
SA-9	4.38	5.9	1.76	-4.11
SA-10	4.44	0.1	1.54	-3.94
SA-12A	5.55	5.9	1.30	-4.25
SA-13	5.61	0.1	1.01	-4.19
SA-16B	6.93	5.8	1.51	-3.88
SA-18	6.99	0.1	1.33	-4.01
SA-19B	7.72	2	1.62	-4.70
SA-20	8.08	2.9	1.35	-4.49
SA-21A	8.3	5.9	-0.26	-4.65
SA-22B	8.48	0.4	1.47	-4.47
SA-23	8.53	0.5	1.29	-4.33
SA-25	9.56	3.1	0.12	-4.84
SA-26A	10.34	2.2	1.75	-4.30
SA-27	10.49	2.8	1.27	-4.65
SA-29B	11.42	5.9	1.44	-4.53
SA-30A	11.47	0.1	1.15	-4.62
SA-30	11.72	2.8	1.10	-4.57
SA-31B bis	11.76	3	0.24	-5.08
SA-32C	11.89	0.1	1.17	-4.20

LATRECEY				
Samples	**Position (m)**	**Seq. position**	**$\delta^{13}C$**	**$\delta^{18}O$**
LA-1	0.03	5.9	2.12	-4.26
LA-2m	0.07	0.05	2.00	-3.96
LA-3	0.1	1	2.08	-4.12
LA-4	0.46	1	2.03	-4.03
LA-5	0.5	3.1	2.11	-3.83
LA-6A	0.77	0.1	2.25	-4.21
LA-6D	0.84	0.5	2.26	-3.92
LA-6E	0.97	2.5	2.31	-4.12
LA-6C	0.99	3.1	2.16	-4.08
LA-7	1.08	4.5	2.22	-4.23
LA-8	1.24	0.25	2.33	-4.31
LA-9A	1.7	2.5	2.37	-4.12
LA-10	1.83	0.1	2.57	-4.04
LA-11A	2.1	3.1	2.36	-3.85
LA-11B	2.13	5.9	2.36	-3.98
LA-12	2.26	1.8	2.40	-4.15
LA-12B	2.52	5.8	2.40	-4.30
LA-13m	2.55	0.1	2.09	-3.46
LA-14	2.59	0.2	2.20	-4.09
LA-15	2.69	0.1	2.33	-4.19
LA-15C	2.85	3	2.33	-4.30
LA-16m	2.97	0.1	2.41	-3.63
LA-17	3.1	1.5	2.47	-4.22
LA-17B	3.16	1.9	2.33	-4.28
LA-18m	3.2	2.1	2.23	-3.74
LA-19m	3.29	4	2.15	-3.86
LA-20	3.36	5	2.29	-4.23
LA-21	3.56	1.5	2.29	-4.47

VORBOURG				
Samples	**Position (m)**	**Seq. position**	**$\delta^{13}C$**	**$\delta^{18}O$**
VO-A	0.4		1.18	-3.53
VO-A3	2.25		1.75	-3.90
VO-A6	4.08		1.56	-3.43
VO-A7	4.4	0	0.84	-3.45
VO-A8	4.62	1.5	0.76	-3.45
VO-14	5.1	0.1	0.11	-4.37
VO-A9	5.14	0.5	0.22	-4.48
VO-A10	5.58	0.1	-0.65	-4.64
VO-A11	6.76	2.5	-0.07	-5.41
VO-20	6.95	3.25	-0.17	-4.09
VO-21	7.6	5.8	0.08	-5.42
VO-A12	7.72	0.1	0.12	-3.99
VO-A13	8.53	5.9	-0.10	-4.68
VO-A14	8.6	0.1	-0.01	-4.76
VO-A15	9.26	3	0.40	-4.52
VO-A16	10.03	0.2	1.44	-3.85
VO-A17	10.2	0.5	1.72	-3.66
VO-30	11.78	5.6	-0.46	-5.13
VO-A18	13.78	4.5	-0.33	-4.63
VO-A19	14.38	2.9	0.81	-4.76
VO-A20	14.59	5.9	1.44	-4.01
VO-L	15.01	5.8	0.88	-4.56
VO-A21	15.95	4	1.79	-3.24

Annex 7 - Stable isotope analyses.

CURRICULUM VITAE

Stéphanie VÉDRINE
Date of birth: 20/05/1980
Place of birth: Paris 14 (France)
Nationality: French

EDUCATIONAL BACKGROUND

Oct. 2003 – present	**PhD in carbonate sedimentology,** University of Fribourg (Switzerland) *High-frequency palaeoenvironmental changes in mixed carbonate-siliciclastic sedimentary systems (Late Oxfordian, Switzerland, France, and southern Germany)* University of Fribourg (Switzerland) Supervisor: Prof. André STRASSER
2001 –2003	**Diplôme d'Etudes Approfondies** in Dynamics of Sedimentary Environments (equivalent to Master's degree M2), University of Rouen (France)
1998 – 2001	**Licence** in Fundamental Geology (equivalent to Bachelor's degree), University of Paris VI (France)

PROFESSIONAL EXPERIENCE

Oct. 2003 - present	Research project at the Laboratory of Geology-Palaeontology (University of Fribourg, Switzerland) on "*High-frequency palaeoenvironmental changes in mixed carbonate-siliciclastic sedimentary systems (Late Oxfordian, Switzerland, France, and southern Germany)"* Supervisor: A. STRASSER
July-Sept. 2003	Research training period at the Departement of Structural and Sedimentary Interpretation at Total (Pau, France) on "*Late diagenesis of carbonates*". Supervisors: A. MEYER & F. WALGENWITZ (Total)
Jan. – July 2003	Research project at the Laboratory of Biogeosciences (University of Burgundy) and at the Laboratory of Geology of Sedimentary Basins (University of Paris VI) on "*Palaeoenvironmental and palaeoclimatic changes at the Lias-Dogger transition on the North-African margin (Central High Atlas, Morocco): contributions of brachiopod shell geochemistry* " Supervisors: C. DURLET (Univ. Burgundy) & L. LE CALLONNEC (Univ. Paris VI)
Jan. – June 2002	Research project at the Laboratory of Geology of Sedimentary Basins (University of Paris VI, France) on "*Chemostratigraphy of the Kimmeridgian from La Rochelle*" Supervisors : M. de RAFÉLIS & M. RENARD (Univ. Paris VI)
July 2000	Research training period at the Laboratory of Dynamic Meteorology (University of Paris VI, France) on "*Meteorological modelling*". Supervisor: H. LE TREUT (Univ. Paris VI)

TEACHING

2003 – present	Teaching assistant for practical courses (Sedimentary microscopy, Carbonate sedimentology) and field excursions for undergraduate students at the University of Fribourg (Switzerland)

POSTGRADUATE COURSES

October 2006	3rd cycle course CUSO on Coral reef ecosystems: past and present, a case study in the Red Sea (Egypt). Organisers: S. Spezzaferri, A. Strasser, E. Samankassou (University of Fribourg), D. Basso, and F. Benzoni (University of Milano-Bicocca)
April 2004	3rd cycle course CUSO on Pleistocene and Holocene carbonate environments on Eleuthera Island (Bahamas). Organisers: P. Kindler, C. de Bono (University of Geneva), and A. Strasser (University of Fribourg)

SKILLS

Languages	French: native; English: fluent; Spanish: basics
Technical	Fieldwork (logging sections, gamma-ray measurements), optical microscopy, cathodoluminescence, SEM analysis, clay mineralogy by X-ray diffraction

RECREATIONAL

Astronomy, scuba-diving (Open water PADI), skiing